AD-A036 355 ADVISORY GROUP FOR AEROSPACE RESEARCH AND DEVELOPMENT--ETC F/G 20/14
ARTIFICIAL MODIFICATION OF PROPAGATION MEDIA.(U)
JAN 77 H J ALBRECHT

UNCLASSIFIED AGARD-CP-192 NL

1 OF 3
ADA036355

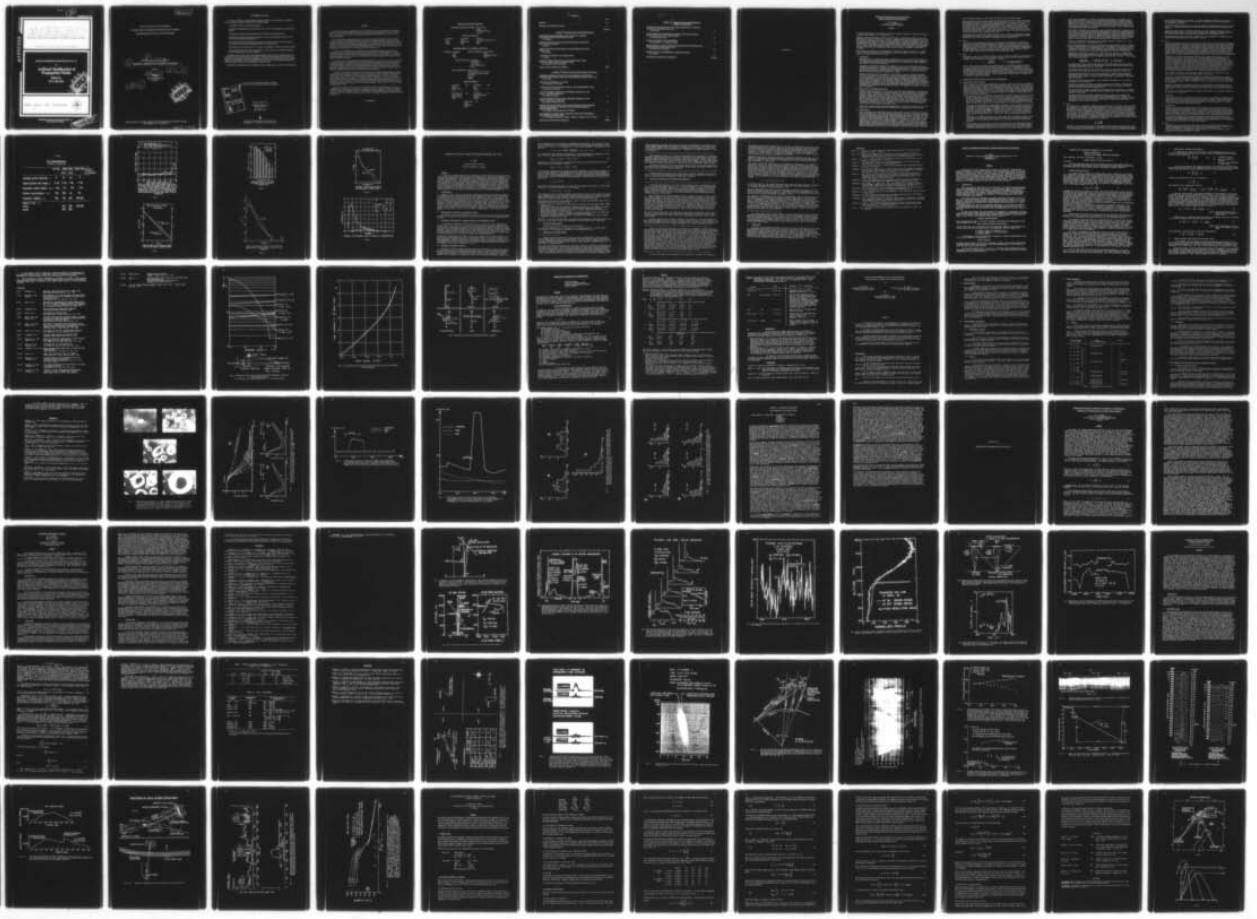

AGARD-CP-192

AGARD-CP-192

AGARD

ADVISORY GROUP FOR AEROSPACE RESEARCH & DEVELOPMENT

7 RUE ANCELLE 92200 NEUILLY SUR SEINE FRANCE

AGARD CONFERENCE PROCEEDINGS No. 192

on

Artificial Modification of Propagation Media

Edited by
H.J.Albrecht

NORTH ATLANTIC TREATY ORGANIZATION

DISTRIBUTION AND AVAILABILITY
ON BACK COVER

AGARD-CP-192

NORTH ATLANTIC TREATY ORGANIZATION

ADVISORY GROUP FOR AEROSPACE RESEARCH AND DEVELOPMENT

(ORGANISATION DU TRAITE DE L'ATLANTIQUE NORD)

AGARD Conference Proceedings No.192

ARTIFICIAL MODIFICATION OF PROPAGATION MEDIA

Edited by

H.J.Albrecht
FGAN
Wachtberg-Werthhoven
Germany

Jan 77

Last page

195 p.

Papers presented at the Electromagnetic Wave Propagation Panel Specialists' Meeting
held in Brussels, 26–29 April 1976.

THE MISSION OF AGARD

The mission of AGARD is to bring together the leading personalities of the NATO nations in the fields of science and technology relating to aerospace for the following purposes:

- Exchanging of scientific and technical information;
- Continuously stimulating advances in the aerospace sciences relevant to strengthening the common defence posture;
- Improving the co-operation among member nations in aerospace research and development;
- Providing scientific and technical advice and assistance to the North Atlantic Military Committee in the field of aerospace research and development;
- Rendering scientific and technical assistance, as requested, to other NATO bodies and to member nations in connection with research and development problems in the aerospace field;
- Providing assistance to member nations for the purpose of increasing their scientific and technical potential;
- Recommending effective ways for the member nations to use their research and development capabilities for the common benefit of the NATO community.

The highest authority within AGARD is the National Delegates Board consisting of officially appointed senior representatives from each member nation. The mission of AGARD is carried out through the Panels which are composed of experts appointed by the National Delegates, the Consultant and Exchange Program and the Aerospace Applications Studies Program. The results of AGARD work are reported to the member nations and the NATO Authorities through the AGARD series of publications of which this is one.

Participation in AGARD activities is by invitation only and is normally limited to citizens of the NATO nations.

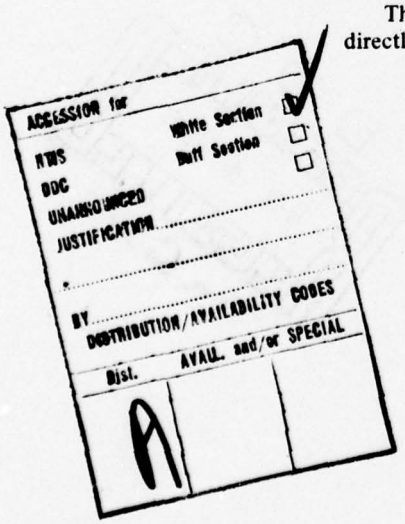

Published January 1977

ISBN 92-835-1234-1

Printed by Technical Editing and Reproduction Ltd
Harford House, 7–9 Charlotte St, London, W1P 1HD

PREFACE

The Electromagnetic Wave Propagation Panel of AGARD had selected "Artificial Modification of Propagation Media" as the topic of a Specialists' Meeting. The meeting took place at Brussels, Belgium, from 26th to 29th April 1976. These Conference Proceedings contain papers and contributions to discussions, as well as accounts of the round-table discussions.

Up to a certain extent, proposal and selection of the topic of a scientific meeting may represent an indirect method of steering current and planned work into a certain direction considered important; such activities might even be stimulated if relevant research is yet in an initial state. At the present this is fully applicable to the artificial modification of the tropospheric propagation medium, whereas man-made influences upon the ionosphere have been the subject of research for several years. The AGARD/EPP-Symposium on non-linear effects in electromagnetic wave propagation, held in November 1973, touched upon some of the related areas.

In studies on the modification of any atmospheric region as a propagation medium, the objectives aim at favourable effects upon communication circuits and other applications concerned with propagation. In general, chances of realization are mainly a question of available means with respect to the effects desired. The variation of tropospheric parameters, however, is still at its very beginning and will require appropriate basic research to ensure proper reproducibility and control.

The entire subject of "Artificial Modification of Propagation Media" was dealt with in three sessions, concerning anthropogeneous changes to non-ionized media, to ionized media by electromagnetic waves, and to ionized media by chemical substances. In addition to papers and their discussions, the present, yet dynamic state of research in this field was especially accounted for by round-table discussions at the end of each of the sessions. Each of the sessions was introduced by review papers on the present state of the art and possible future development; they were followed by contributed papers reporting on special projects and recent results.

In summary, this Specialists' Meeting concerned the recognition and definition of limiting propagation criteria, optimum methods of modification, and efficiency of changing propagation media as a function of means employed. It represented an early, if not the first scientific meeting actually addressing, with its main topic, the anthropogeneous changes to the earth's atmosphere as a propagation medium. In addition to a review of the state of the art and the predominant directions of progress, the stimulation of propagation-oriented modification projects may be mentioned as a major achievement of the meeting. Promising areas of future research were indicated as well. These Conference Proceedings give a full account of the three sessions mentioned; a separate report will cover proceedings of a supplementary session.

Appreciation is expressed to all who assisted in the organization of the Specialists' Meeting as well as in the compilation of these Proceedings, to members of the programme committee, authors and contributors to discussions, chairmen of sessions and round-table discussions, to AGARD staff and other collaborators. A special acknowledgement is expressed for the assistance rendered by Prof. W.E.Gordon in compiling and editing the round-table discussion of Session II.

H.J.ALBRECHT

PROGRAM AND MEETING OFFICIALS

PROGRAM CHAIRMAN and EDITOR: Dr H.J.Albrecht
FGAN
Wachtberg-Werthhoven
Germany

PROGRAM COMMITTEE

Dr J.Belrose	Dr T.J.Elkins	Dr I.Katz
CRC	AFCRL	John Hopkins Appl. Phys. Lab.
Ottawa	Bedford, Mass.	Laurel
Canada	USA	USA

ELECTROMAGNETIC WAVE PROPAGATION PANEL

CHAIRMAN: Mr P.Halley
CNET
Paris
France

DEPUTY CHAIRMAN: Dr H.J.Albrecht
FGAN
Wachtberg-Werthhoven
Germany

PANEL EXECUTIVE: Dr N.R.Ogg
AGARD-NATO
7, rue Ancelle
92200, Neuilly-sur-Seine
France

HOST COORDINATOR: Major F.Kennis
Chef de la Sous Section "Avionics"
Etat Major de la Force Aerienne
Place Dailly
Brussels
Belgium

SESSION CHAIRMEN

Dr J.Aarons (II)
AFCRL
Bedford, Mass.
USA

Dr J.Belrose (III)
CRC
Ottawa
Canada

Prof. W.E.Gordon (II)
Rice University
Houston, Texas
USA

Dr H.Jeske (I)
Universität Hamburg
Hamburg
Germany

Dr W.F.Utlaut (II)
NOAA
Boulder, Col.
USA

CONTENTS

SESSION III – MODIFICATION OF IONIZED MEDIA BY CHEMICAL SUBSTANCES

SESSION I

NON-IONISED PROPAGATION MEDIA WITH ARTIFICIALLY MODIFIED PRECIPITATION CHARACTERISTICS

E. Kleinjung
Schule für Wehrgeophysik
8080 Fürstenfeldbruck, Germany

SUMMARY

Artificial modification of precipitation and clouds is mainly orientated to enhance precipitation, to suppress hail formation, or to dissipate fog.

Changes of several precipitation parameters, such as rate, horizontal and temporal extent, size distribution and shape of drops, due to artificial influence upon them have been reported but they are within the range of their natural occurrence. Essential alterations of propagation conditions are therefore not assumed. In the case of hail suppression no conclusive experimental results of influencing the hail growth in a cloud are available. However, theoretical approaches show a diminution of hail size through artificial modification and thus suggesting changes in the propagation of e. m. waves. Several fog dispersal methods are in practical use, changes of the essential parameters in space and time are generally known therefore changes of propagation conditions are calculable.

Redistribution and suppression of precipitation by overseeding clouds are presented as possible fields of practical applicability of modification efforts on propagation conditions, though at present not investigated in the latter case.

1. INTRODUCTION

Hydrometeors such as cloud- and precipition particles have a more or less strong influence on the propagation of electromagnetic waves especially in the high-frequency range. Changes of the cloud and precipitation parameters caused by artificial modification, whether intended or inadvertent will alter these conditions.

The purpose of this paper therefore is an attempt to point out the deviations of the meteorological characteristics - important for propagation calculations - of artificially influenced precipitation and fog and to compare them with conditions as they occur in nature. This will then lead to an attempt of indicating promising areas of application. Propagation effects of natural tropospheric conditions are assumed to be known.

Because of the great natural variability of precipitation in space and time the evaluation of modification results is very difficult if not at the present time impossible especially in as much as some of the very specific precipitation parameters are concerned. Another difficulty in searching for artificially influenced changes in precipitation parameters is due to the fact that the primary aim of weather modification is to enhance or suppress the amount of precipitation. Investigations of the artificial modification of other precipitation parameters such as intensity, duration, or drop size distribution, are rare. Therefore some of the results presented later, showing a change of the precipitation characteristics caused by artificial influences, are statistically not significant. However, they suggest that research in this field will be worthwhile.

2. PHYSICAL BASIS OF WEATHER MODIFICATION

Artificial weather modification in the sense of this paper means enhancement of precipitation (rain and snow), suppression of hail, and dissipation of fog. The activities in this field are worldwide and meet with different success. In the last 25 years there have been attempts to release or enhance precipitation from nearly all modifiable cloud-types, mainly orographic stratiform clouds with most success (Grant and Kahan 1974), frontal clouds (Leskov 1971), stratiform clouds of little vertical depth (Serpolay and Andro 1973, Biswas and Dennis 1971) and all types of convective clouds (Simpson and Dennis 1974). The results partially contradict each other. Efforts have been made to dissipate fog of various types considering its origin - radiation or advection fog - or its composition - water or ice fog - or its temperature - above or below 0°C (Silverman and Weinstein, 1974).

A brief survey of the physical and meteorological basis of artificial precipitation and cloud modification seems to be indicated here to facilitate the interpretation of the results.

2.1 PRECIPITATION

Aside from dynamic and thermodynamic aspects 2 microphysical processes account for the formation of precipitation (1) the collision-coalescense process and (2) the ice-crystal (Bergeron) process for supercooled clouds. Altering these microphysical processes of formation and growth of cloud and precipitation particles by introducing seeding agents into the clouds - in order to change the size distribution or phase of the cloud particles - is the most commonly practised way of weather modification today. Dependent on the temperature of the cloud (1) giant hygroscopic salt nuclei in the size range 20-100µm or a spray of fine water and (2) solid carbon dioxide or crystals such as silver iodide are brought into the clouds, thus intensifying the various microphysical processes of droplet growth and with proper seeding causing the intended modification. Introduction of ice-crystals and following glaciation of a number of supercooled water drops may, in the case of convective clouds lead to an increase in vertical

motion through the release of latent heat of fusion. We speak of dynamic seeding.

Adding AgI-crystals to the clouds in order to overcome the normal lack of sufficient freezing nuclei active at relatively high freezing temperatures (about -5°C), will start or accelerate the glaciation process in the cloud if by contact-nucleation or sublimation, is still a controversial question in cloud physics (Alkezweeney 1971, Hitchfeld 1975, Young 1974). Further growth will occur by diffusion of water vapor to the crystal until it becomes large enough for riming to take place. Continued riming will lead to graupel (Gagin 1974) if the ice nucleus concentrations don't exceed a few tens per liter ($v \leq 3$ m/s). With nucleus concentrations of more than 100 l^{-1} a supercooled cloud glaciates rapidly and snowflake aggregation becomes the dominant growth mechanism (Jiusto 1971).

Summarizing, we can conclude that - except the time factor - there is no significant change in the formation and nature of precipitation elements. Only very high concentrations of seeding agents will lead to preferred snowflake development at subzero-temperatures.

2.2 HAIL

In the case of hail suppression the aim is to eliminate the possibility for the growth of individual large hailstones causing damage on the ground. So far this has been done by the injection of a number of crystallizing reagents (AgI) into the accumulation zone of liquid supercooled water (temperatures 0 - -20°C) of a thundercloud, where we assume the basic growth of large hailstones to occur. The introduction of many potential hailstones all competing for the same finite supply of supercooled water should be associated with a decrease in their ultimate diameter as theoretical calculations show (Sulakvelidze 1967).

2.3 FOG

Dissipation of fog or low stratiform clouds in order to improve the visibility in certain areas is based on an influence on cloud microphysics similar to that exerted in precipitation enhancement. From the equation of meteorological visibility

$$V = \frac{3{,}912}{\sum_{i=1}^{n} \pi K_i N_i r_i^2} \qquad (K = \text{Scattering efficiency of a fog particle})$$

it may be seen that fog dispersal can be attained either by decreasing the number concentration N_i of fog particles or by decreasing their radius r_i, or both. Decreasing the radii of fog droplets by their evaporation is the most promising approach to fog dissipation. This can be achieved either by the introduction of hygroscopic material and in the case of supercooled fog of crystallizing agents, or by increasing the water vapor capacity of the foggy air through heating the fog or mixing the fog with drier air from aloft. Although there are no distinctions in the physical properties of warm ($t \geq 0$°C) and supercooled fog modification, attempts with the latter have been most successful.

3. ARTIFICIALLY MODIFIED PRECIPITATION AND FOG CHARACTERISTICS

3.1 PRECIPITATION (RAIN AND SNOW)

Those precipitation characteristics which should be known in order to determine the propagation of e. m. waves, such as intensity, horizontal and temporal extent, drop size distribution, and shape of the drops are of a great natural variability, as already mentioned in the introduction, and present the greatest obstacle in the evaluation of a modification success. For example unmodified convective rainfall commonly varies by factors of 10 to 1000, while the largest seeding effects have never exceeded a factor of 2 to 3 (Simpson 1975). Changes of these characteristics due to an artificial influence on the modifiable clouds are therefore in general within these limits of the natural occurrence.

a) The precipitation rate for modified convective showers is in the range of naturally occuring rainfall-rates. Reported values are up to 100 mm hr^{-1}. Simpson and Wiggert (1971) found in Florida no significant difference in rainfall-rate between seeded and unseeded single tropical cumulus clouds, while Stantchev et al. (1973) in agreement with several Russian authors report a 5% increase on the average (i.e. 0.8 mm hr^{-1}) as the result of dynamic seeding in Eastern Europe, which seems to be of no great importance for the propagation of e. m. waves.

   In general the meteorological conditions typical for the occurrence of maximum precipitation intensities of convective origin rather suggest suppression than enhancement experiments. The results of the modification of orographic clouds are similar. There is a statistically significant increase in the amount of precipitation by 10-20% on the average in nearly all experiments with orographic clouds, if seeding is performed in the effective temperature range. This increase is always due to a longer life time of the precipitating clouds than to an increase in intensity as Fig. 1 shows for the Colorado experiments (Chappell at al. 1971).

   Experiments in the USSR with frontal type clouds (Leskov 1973) indicate that rainfall rates of artificial and natural precipitation are of the same order of magnitude, normally only a few mm hr^{-1}, and increasing natural intensity is correlated with increasing artificial intensity.

b) Data on changes of the horizontal, vertical and temporal extent of precipitating clouds due to artificial modification are sparse. In the already mentioned "Florida dynamic seeding experiments" randomized seeding of single convective cells resulted in an excess of 47% in area for the seeded echoes compared with the unseeded control echoes (Simpson and Wiggert

1971). This corresponds to an increase of roughly 20% in diameter. The duration of the seeded echoes exceeded those of the unseeded echoes by 39%, and in the vertical growth an increase of 3.5 km on the average of the seeded clouds was observed. Simpson and Wiggert stated that the longer life and greater extent of the clouds caused the increased precipitation amount by a factor of 2 - 3. Further investigations by other authors (Dennis et al. 1975) showed similar results of horizontal and vertical increase of seeded clouds although no quantitative data have been reported.

With respect to changes in the horizontal extent of precipitation areas of orographic origin we have to differentiate between a pure enhancement of naturally occurring precipitation and the release of precipitation by artificial modification. The latter happens especially in the higher temperature range, where seeding disrupts the stable cloud microstructure and initiates the precipitation process. In the former case no significant changes in precipitation areas are reported, while in the latter a remarkable increase will occur depending mainly on the size of the seeded cloud area. However, exact data cannot be given.

Changes in the duration of precipitation of orographic origin by a factor of 2 - 3 have already been mentioned in connection with Fig. 1.

c) Only a few measurements of drop size distributions for seeded convective clouds in comparison with unseeded control clouds have been reported. According to the theory of cloud modification the introduction of a seeding agent into a cloud leads to the formation of more precipitation particles with a shift to smaller drops. Some drop size distributions so far measured are in agreement with this seeding hypothesis while others are contradictory.

Measurements in Switzerland (Roesli et al. 1974) and Arizona (Jones et al. 1968) showed higher drop concentrations with smaller drops for seeded rainfall than for unseeded. The following size distributions given in a Marshall-Palmer form $N(D) = N_0 \exp(-\lambda D)$ by Roesli et al. confirm this result.

Seeded N(D)	=	20 000 exp (-3.16 D)	R = 10.2 mm hr^{-1}
Unseeded N(D)	=	3 000 exp (-2.10 D)	R = 10.2 mm hr^{-1}

The high value of N_0 and a steep slope indicate high concentrations of smaller drops for the seeded cases compared with the unseeded cases, where the distribution function shows a broad spectrum with few but rather large drops.

In contrast to this Miller and Eden (1972) found a number of larger drops falling out of seeded clouds than of unseeded clouds. Some of their results are shown in Fig. 2 and 3.

The mean drop size spectra in Fig. 2 show a small shift to larger drops for seeded air-mass showers. While in Fig. 3, obtained by summarizing the data for different depth of penetration through seeded and unseeded clouds, the increase of larger drops in the seeded cases is obvious.

The different modification mechanism - the microphysical and dynamic one - may offer an explanation of the differences.

Although in individual cases small differences in drop size distribution between seeded and unseeded rainfalls have been found, these differences are well within the limits of natural occurrences (Danielson and Huggins 1974).

No data concerning the shape of artificially influenced drops are available. It is assumed that there is no substantial difference between artificial and natural raindrops in their shape and canting angle.

The sparse quantitative information regarding changes of precipitation parameters by artificial modification which are important for the propagation of e. m. waves is not sufficient yet to provide any statistical data on the frequency of the occurrence of specific rainfall rates - even in areas with a large number of modification experiments - in comparison with their natural occurrence.

3.2 HAIL

Hail suppression is orientated to change the size distribution of hailstones, mainly to prevent the formation of the larger sizes. Size distributions of naturally occurring hailstones obey an exponential law as Douglas (1964) has shown (Fig. 4) or may be expressed by more complicated distribution functions (Sulakvelidze 1969, Rozenberg 1972). So far it has been impossible to meet the requirement for propagation calculations - that the size distribution of hailstones must be known - as measurements in artificially influenced hailstorms are lacking. Only theoretical advances have been made showing a considerable diminution of the diameters of hailstones after adding seeding agents in or beneath the accumulation zone of supercooled liquid water in the cloud. After calculations of Sulakvelidze (1969) the final rootmean-cubic radius $\bar{R}e$ obtained as a result of the artificial seeding can be expressed by

$$\bar{R}_e = \bar{R}_i \sqrt[3]{\frac{N_i}{N_e}}$$

where $\bar{R}_i$ is the root-mean-cubic radius of hailstones without seeding, N_i and N_e are the corresponding concentrations of hailstones. A concentration of $10^2 - 10^3$ m^{-3} introduced hail embryos of 1 mm size against a natural amount of $10^0 - 10^1$ m^{-3} would therefore be sufficient to reduce

the final hailstone size by a factor of 4 - 5. With a decrease in diameter by a factor of 4 - 5 and an increase in concentration by 10^2 there may be a possibility of calculating changes in the propagation parameters.

The shift to smaller hailstone sizes on seed days compared with no-seed days, as shown in Fig.5, points in the direction postulated by theory as do the model calculations by Young and Atlas (1974).

However the limited number of adequate experiments and their statistical evaluation, and a modification theory which is far from being conclusive and in agreement with observations made in hailstorms show that hail suppression is at present only at a beginning stage.

The theoretical approaches offer only a possible way of the modification of propagation parameters by artificial influencing of hail growth in clouds.

3.3 FOG

The physical properties of natural fog are given in Table 1 with the distinction of the various modes of formation and constitution. Warm and supercooled fog have the same physical properties. Radiation fogs tend to have high concentrations of smaller droplets, while advection fogs have lower concentrations of relatively large droplets, due to the origin of the aerosol particles on which they mainly form-maritime or continental. Vertical thickness and horizontal extent of fog vary appreciably, the depth between a few m and several 100 m, the area between 1 km^2 and several 1000 km^2 dependent on meteorological and geographical conditions. The afore-mentioned characteristics of fog are mean values, variability due to nature, age and density of fog is great in time and space. Therefore modification efforts have to take this fact into consideration.

Dissipation of fog means increasing the visibility in a certain area. Since $\Sigma N_i r_i^2$ is inversely proportional to the visibility, the size distribution of fog droplets has to be changed in such a manner that r_i, N_i or both are reduced. Introduction of hygroscopic or crystallizing agents of a proper concentration and size (between 20 -50μ) will lead to evaporation of the fog droplets below their critical radii and is followed by absorption and condensation or sublimation of the water vapor by the seeding particles, which grow to large particles and fall out. The result is fewer and larger drops and increased visibility. Side-effects are rain- or snow-out of the clouds, amount and intensity of precipitation are very small. By supplying sufficient thermal energy will also help to evaporate the fog droplets, thus continuously diminishing their size until they reach their critical radii. A typical example of the change in drop size distribution due to hygroscopic seeding is shown in Fig. 6.

The increase in diameter in connection with a marked decrease in concentration and liquid water content due to fall-out of the largest particles is obvious.

Since most of the fog dispersal efforts were made at airports, the horizontal and vertical extent of the region to be cleared is dependent on the needs of aviation. In most cases areas of less than 1 km^2 with a volume of fog approximately 50 - 100 Mill m^3 have to be dissipated. By more extensive seeding actions with respect to area even larger areas of fog or low stratus may be cleared.

Changes of the physical properties as well as of horizontal and vertical extent of fog due to artificial modification are generally known or may be calculated by an increasing number of fog dispersal models (Koenig 1971, Weinstein and Silverman 1974) at various stages of development.

With these data, possible alterations of propagation parameters by the artificial dissipation of fog have to be calculable.

4. CONCLUSIONS

Though large afforts have been made in the last ten years in the evaluation of weather modification experiments with an increasing number of modification models and highly sophisticated statistics we are in many fields in an early stage. But precipitation modification may offer some indications of promising applications with respect to the propagation of e. m. waves. An attempt in pointing out these should be made.

4.1 PRECIPITATION

Changes in precipitation intensity achievable with present technological means seems to be not significant for practical applications in wave propagation. On the other hand, the possibility of influencing the release or even a temporal shift of the precipitation process under certain conditions, a redistribution of precipitation by artifical influences, a diminution or prevention (Neiburger 1969) by overseeding of definite clouds, may become important in areas where communication links would not be affected at all or to a lesser extent by precipitation.

With the steady expansion of the frequency spectrum towards 50 and 100 GHz, and with the appropriate increasing susceptibility to precipitation, such applications will have an essential effect upon link reliability. This would also be of great importance for the optimization of link diversity conditions in satellite communications.

4.2 HAIL

The verification of the theoretical approaches by means of experimental results would be a positive development in this field. As a result, the unpredictable propagation effects of hail could in certain cases be "watered down" to rain which is better understood.
Summarizing, there is a large amount of research work still to be done. It seems, in some fields, to be promising but difficult to solve.

REFERENCES

1. Alkezweeney, A. J., 1971, "A contact nucleation model for seeded clouds", J. Appl. Meteorol. 10, 732-738

2. Biswas, K. R. and Dennis, A. S., 1971, "Formation of a rainshower by salt seeding", J. Appl. Meteorol. 10, 780-784

3. Chappell, C. F.; Grant, L. O. and Mielke, P. W., 1971, "Cloud seeding effects on precipitation intensity and duration of wintertime orographic clouds", J. Appl. Meteorol. 10, 1006-1010

4. Danielson, K. and Huggins, A. W., 1974, "Raindrop size distribution measurement of high elevation continental cumuli" in Conference on Cloud Physics, Tuscon, A.M.S., pp 305-310

5. Dennis, A. S. et al., 1975, "Analysis of radar observations of a randomized cloud seeding experiment", J. Appl. Meteorol. 14, 897-908

6. Douglas, R. H., 1964, "Hail size distributions", in 11th Weather Radar Conference, A.M.S. Boston, pp 147-149

7. Gagin, A. and Neumann, J., 1974, "Rain stimulation and cloud physics" in Weather and Climate Modification, pp 454-494 edited by W. N. Hess, John Wiley & Sons, New York

8. Grant, L. O. and Kahan, A. M., 1974, "Weather modification for augmenting orographic precipitation" in Weather and Climate Modification pp 282-317 edited by W. N. Hess, John Wiley & Sons, New York

9. Hitchfeld, W. F., 1971, "Hail suppression - evaluation and other problems" in 4th Conference on Weather Modification, Fort Lauderdale, A.M.S., pp 97-98

10. Jiusto, J. E., 1971, "Crystal development and glaciation of a supercooled cloud", J. Rech. Atmos. 5, 69-85

11. Jones, D. M., Stout, G. E. and Mueller, E., 1968, "Raindrop spectra for seeded and unseeded showers" in Preprints First National Conf. Weather Modification, Albany, A.M.S. Boston, pp 99-106

12. Kocmond, W. C., Pilié, R. J. et al., 1970, "Valley fog clearance" in Preprints Second Conf. Weather Modification, Santa Barbara, A.M.S. Boston

13. Koenig, L. R., 1971, "Numerical experiments pertaining to warm-fog clearing", Monthly Weather Rev. 99, 227-241

14. Leskov, B. N., 1971, "Change in the intensity of artificial precipitation in time with frontal cloud modifications", NTIS-AD 783743
Transl. from Russ. Trudy Ukr NIGMI 99, 44-51

15. Leskov, B. N., 1973, "The experimental seeding of frontal clouds in winter in order to increase precipitation" in Proceedings of the WMO/IAMAP, Scientific Conference on Weather Modification, Tashkent, pp 143-148

16. Miller, A. H. and Eden, J. C., 1972, "Airborne and ground based drop size distribution in Florida summer showers and simultaneous radar reflectivity and rainfall data", in Preprints Third Conf. Weather Modification, Rapid City, A.M.S. Boston, pp 208-213

17. Miller, J. R., Boyd, E. I., Schleusener, R. A. and Dennis, A. S., 1975, "Hail suppression data from Western North Dakota, 1969-1972, J. Appl. Meteorol. 14, 755-762

18. Neiburger, M., 1969, "Artificial modification of clouds and precipitation", WMO-No. 249, TP 137, pp 33

19. Roesli, H. P., Joss, J. and Schüepp, M., 1974, "Possible influence of evaporation below cloud base on rain enhancement", J. Appl. Meteorol. 13, 783-787

20. Rozenberg, V. I., 1972, "Scattering and attenuation of electromagnetic radiation by atmospheric particles", Hydrometeorol. Press, Leningrad

21. Serpoley, R. and Andro, M., 1973, "Rapid inducement of precipitation by seeding stratified air layers" in Proceedings of the WMO/IAMAP Scientific Conference on Weather Modification, Tashkent, pp 63-67

22. Silverman, B. A. and Weinstein, A. I., 1974, "Fog" in Weather and Climate Modification, pp 355-383, edited by W.N. Hess, John Wiley & Sons, New York

23. Simpson, J., 1974, "Weather Modification - where are we now and where should we be going, convective cloud modification" in 4th conference on Weather Modification, A.M.S., pp 1-6

24. Simpson, J. and Wiggert, V., 1971, "1968 Florida cumulus seeding experiment: Numerical model results", Monthly Weather Rev. 99, 87-118

25. Simpson, J. and Dennis, A. S., 1974, "Cumulus clouds and their modification" in Weather and Climate Modification, pp 229-281, edited by W.N. Hess, John Wiley & Sons, New York

26. Stantchev, K., Boev, P. and Petrov, R., 1973, "On the thermodynamic criteria for the intensity of convective cloud development" in Proceedings of the WMO/IAMAP Scientific Conference on Weather Modification, Tashkent, pp 385-394

27. Sulakvelidze, G. K., 1969, "Rainstorms and hail", pp 230-233, Transl. from Russ., Israel Prog. f. Scientific Translations, Jerusalem

28. Weinstein, A. I. and Silverman, B. A., 1973, "A numerical analysis of some practical aspects of urea seeding for warm-fog dispersal at airports", J. Appl. Meteorol. 12, 771-780

29. Young, K. C., 1974, "The conversion of a supercooled cloud to ice via contact nucleation and direct injection of ice crystals" in Conference on Cloud Physics Tucson, A.M.S. Boston, pp 175-179

30. Young, K. G. and Atlas, D., 1974, "NHRE microphysics: An overview with emphasis on hail growth and suppression", in 4th Conference on Weather Modification, Fort Lauderdale, A.M.S. Boston, pp 119-124

TABLE 1

Fog Characteristics

(a. Silverman & Weinstein 1974)

	Ice Fog	Water Fogs		Valley Fog (Special case of radiation fog a. Kocmond et al. 1970)
		Radiation	Advection	
Average particle diameter (μ)	8	10	20	17
Typical particle size range (μ)	2-30	5-35	7-65	4-50
Equivalent water content (g/m^3)	0.10	0.11	0.17	0.15
Particle concentration (cm^{-3})	150	200	40	55
Horizontal visibility (m)	200	100	300	100-300
Depth of fog (m)				
mean		100	200	100-200
severe		300	600	

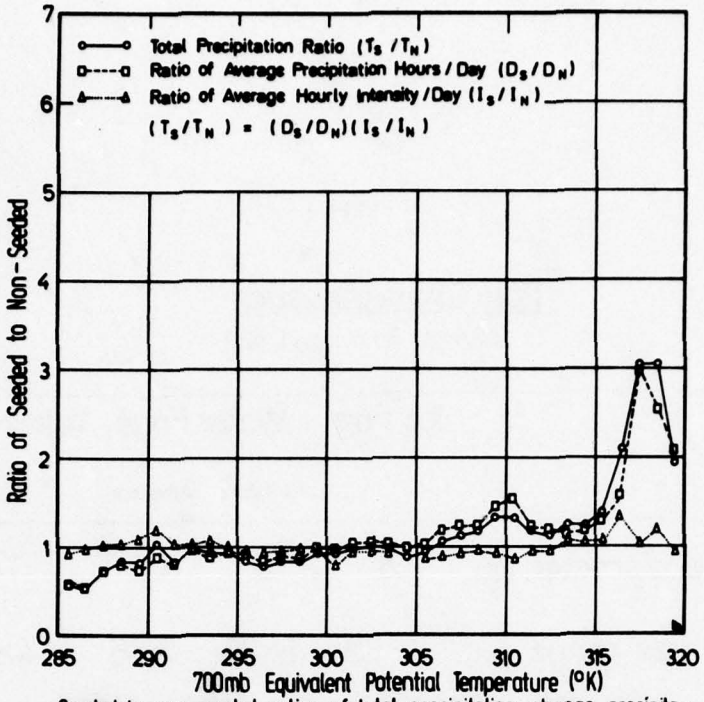

Seeded to non-seeded ratios of total precipitation change, precipitation duration change, and precipitation intensity change as a function of 700mb equivalent potential temperature. Plotted values are computed using a running mean over a 5K temperature interval. Precipitation data were measured at the High Altitude Observatory during experimental days of the total Climax sample (623 days) (a. Chappell 1971)

Figure 1

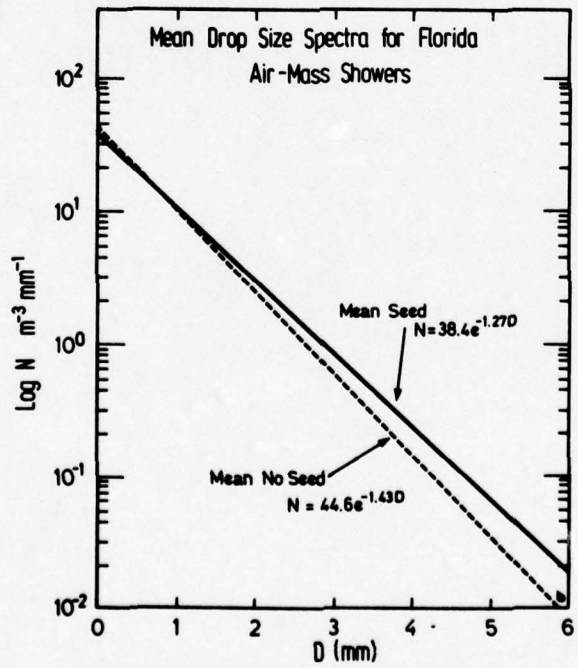

Mean drop spectra for both seeded and unseeded Florida air-mass showers a. Eden & Miller (1972).

Figure 2

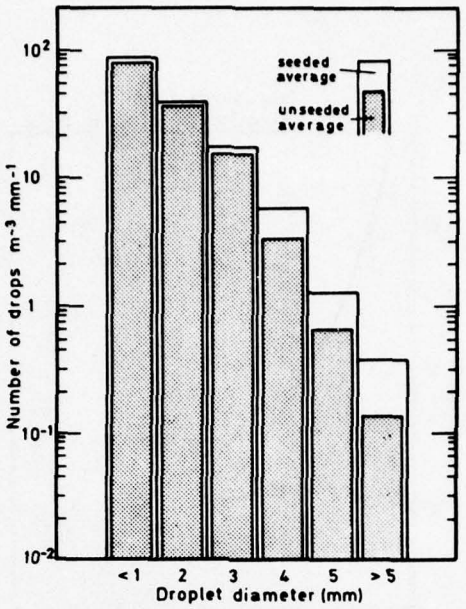

Average drop distributions for both seeded and unseeded Florida air-mass showers a. Eden & Miller (1972).

Figure 3

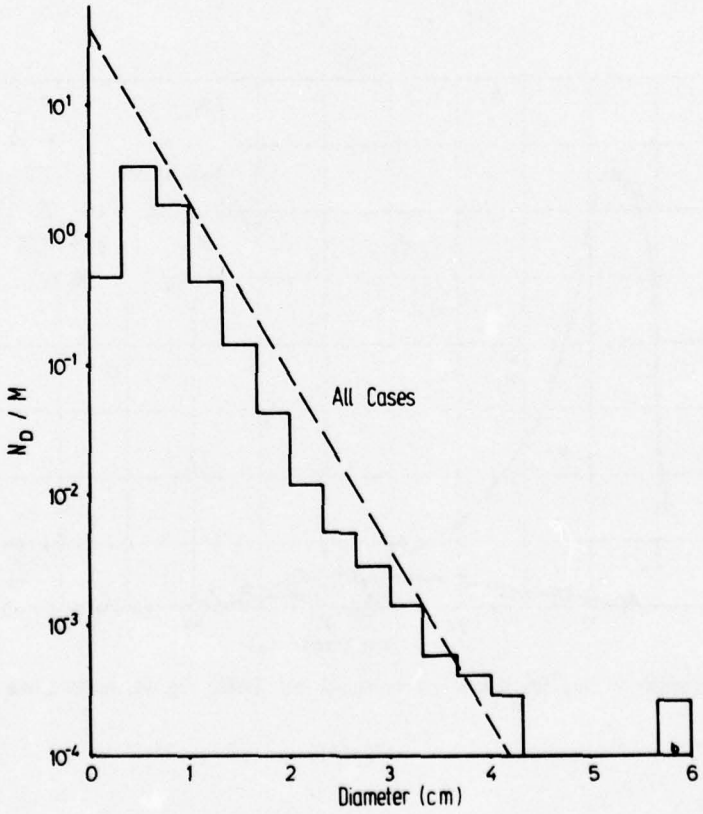

Composite size distribution, normalized to unit ice content for all samples. Dashed line show function $N_D = 32.2 \exp(-3.09 D)$ (a. Douglas 1964)

Figure 4

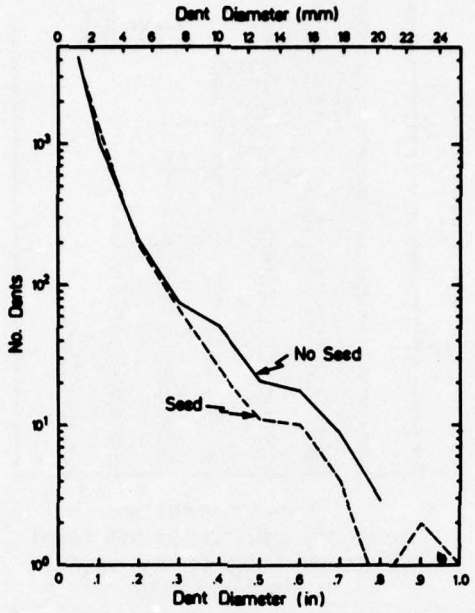

Distributions of seed day and no-seed day hail dent diameters (a. Miller et al. 1974).

Figure 5

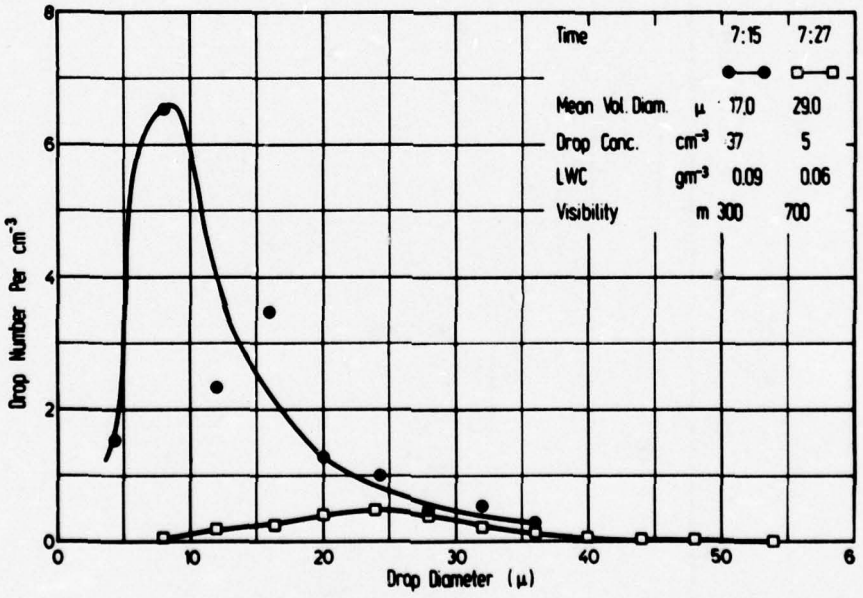

Comparison of Drop Size Distributions in Natural and Seeded Fog (a. Kocmond, Pielke et al 1970

Figure 6

MAN-MADE MODIFICATION OF CLEAR-AIR PROPAGATION CONDITIONS (VHF to EHF)

H. Jeske

Meteorologisches Institut

Universität Hamburg, Germany

Summary

In contrast to weather modification experiments in the hydrometeor-filled atmosphere (fog, clouds, precipation) there is only little experience in the clear atmosphere. Possible are dispersions of man-made media in the atmosphere (radar chaff, gases,aerosols) or direct modifications of the refractive-index field, especially characterized by its vertical gradiant, duct-, and reflecting layers.The use of radar chaff is well defined, other admixtures are less studied under operational conditions. As typical examples for an alteration of the environmental conditions the meteorological situation during large forest-fires and the suppression of evaporation by monomolecular films on water surfaces may be considered. Above a forest (or other) fire a subnormal refraction layer will be formed. The reduction of evaporation diminishes the thickness of the permanent-existing evaporation duct over sea and so its extensive influence on microwave propagation.

1. Introduction

Aerosol-, cloud-, fog-, precipitation - generally referred to as weather modification experiments are well known and successfully applied for practical use. The benefit or applicability for telecommunication or radar problems are almost insignificant - at least for wavelengths greater than some mm. For IR- and optical waves, fog modification has doubtlessly a certain importance (e.g. dissipation of fog on a regular basis at airports or fog production for masking effects). The modification possibilities in the clear atmosphere (without hydrometeors or effective aerosols) seems to be even more rare, especially if we are looking for modification under operational conditions. As with the general weather modification programs the decision wether to undertake such strains must be made in any specific situation on the basis of weighting the probabilities of benefit against the cost and the risk. In the following a rough sketch of this field will be given.

2. Parameters for describing propagation effects

At first let us briefly summarize the influence of the clear, non-ionized, atmosphere on radio wave propagation below some 100 GHz and introduce the relevant propagation parameters.

2.1 Attenuation by molecular resonant absorption of atmospheric gases

The essential parameters we need are the c o n c e n t r a t i o n (g/m^3) and the a b s o r p t i o n c o e f f i c i e n t over the interesting spectra (attenuation/length) under various physical or meteorological conditions. The major atmospheric gases that need to be discussed as absorbers in the frequency range under discussion are oxygen and water vapour. We know sufficiently well their natural concentration (also water vapour statistics could be made available) and the main features of their absorption spectra, although some characteristics within the minima of the absorption spectra of water vapour are under discussion (e.g. influence of dimere and polymere molecules).

In addition to oxygen and water vapour, there are a number of trace constituents or pollutants which have absorption lines in the microwave region as SO_2, CO_2, CO, N_2O or O_3. These "ppm-gases" normally constitute a negligible portion of the general composition of the atmosphere - also under unfavorable environmental conditions attenuation effects are negligible. Nevertheless, absorption in the microwave region ascribed to pollutants in the atmosphere is a field of research up to now.

2.2 Dielectric propagation effects

The field of the real radio refractive-index of the atmosphere is the central point of all theories of radio propagation mechanisms through the lower atmosphere. Indeed, it depends on the structure of the refractive-index field in space and time which propagation mechanism (refraction, ducting, reflection, scattering) is dominating. For wave lengths >1.5 cm (outside the absorption region also for shorter radio-wave lengths) the

lower atmosphere may be considered as a diamagnetical dielectric. The refractive index n or the refractivity N is a well known function of the meteorological parameters p (total pressure of the air), T (air temperature), e (water vapour pressure). With adequate accuracy is:

$$N = (n-1)\cdot 10^6 = \frac{77.6p}{T} + \frac{3.73\cdot 10^5 e}{T^2} \quad (p,e \text{ in mb, } T \text{ in K}) \tag{1}$$

The relation for small changes or gradients in N and small changes in temperature, pressure, and water vapour may be derived for mean ground conditions as:

$$\Delta N_{radio} = 0.27\Delta p - 1.27\Delta T + 4.5\Delta e \tag{2a}$$

There exists a large influence of water vapour contrary to optical waves which can be learned from the correspondent relation:

$$\Delta N_{opt} = 0.27\ \Delta p - 0.95\Delta T - 0.04\Delta e \tag{2b}$$

If we know the distribution of the meteorological parameters we may deduce relevant refractive-index models of the atmosphere. This has been done and we are well informed about the mean refractive-index field and its variation on a world-wide basis (Bean and Dutton, 1966). For the height dependence of n holds an exponentia law. For Middle-Europe one gets as a reference atmosphere from meteorological radio sondes the formula (Großkopf, 1970):

$$N = 325\cdot e^{-0.136z} \tag{3}$$

with 325 as the mean ground value of N and 0.136 as exponent. This yields a linear dependence within the lowest kilometer of the atmosphere

$$N = 325 - 40z \quad (z \text{ in km})$$

The gradients within the lowest kilometer vary between 0 and 105 N-units/km(95%-5%-value) with a median value of 40 N-units/km. In addition to this relation of a more or less well mixed atmosphere we can make available detailed inversion-statistics (important for propagation by reflection) and duct statistics in the stratified atmosphere.

The parameters to estimate the propagation effects on radio/radar systems (which must be modified artificially if required) are:

1) absolute value of refractivity N especially to determine the radio path length (phase, delay time),
2) vertical N-gradient for evaluating all refractive effects as, for example, elevation angel error, ray curvature, diffraction field strength beyond the horizon,
3) duct height statistics (gradient <-0.157/m) to predict super-refraction effects on amplitude and phase of a radio signal,
4) inversion-statistics (height, thickness, refractivity decrease within the inversion) to evaluate multipath effects connected with reflected fields,
5) spectra of refractive-index variations to estimate the transmission loss or usuable bandwidth of troposcatter links.

Generally, we may say that we control the dielectrical propagation mechanisms and are frequently in a position to predict the propagation effects under natural conditions.

3. Artificial modification

The possibilities are divided into two categories

a) artificial admixtures to the atmosphere, that means dispersion of man-made media
b) changing of the propagation parameters of the atmosphere itself.

3.1 Dispersion of man-made media

3.1.1 R a d a r C h a f f

Chaff has been used during war time as a mean of establishing a large reflecting area to radar waves in order to mask airplanes. The chaff was made from thin aluminium foil strips approximately one-half-wave lengths long ($\lambda/2$-dipol). Unquestionably, the use of radar chaff under operational conditions also today will be an effective tool for camouflage or jamming purposes.

During the last decade the possibility using chaff clouds for transhorizon communications for short time intervals (chaff scatter channels) was investigated with good theoretical and experimental success. In use are metallic dipols or aluminium coated glass chaffs (short or $\lambda/2$-dipols), placed at a modest altitude somewhere between transmitter and receiver. The dispersion may be carried through by aircraft or small rocket systems. Models of the scattering cross section of clouds of chaff dipols for different distribution of

dipol orientation (uniform, horizontal or vertical) are available now (s.Lampert 1976). The agreement between predicted and measured values of transmission loss,coherent band width, fading spectra among other things is promising (see e.g. Langelier et al.,1967), that means a temporal limited communication - independent of weather conditions - would be guaranteed.

3.1.2 S p e c i a l g a s e s, l a r g e r a e r o s o l p a r t i c l e s, f o g

The propagation effects of such additional admixtures are attenuation or refraction phenomena. The effective influence is mainly a function of the concentration and the physical and chemical properties of the material used, the size of the clouds or fog areas produced and the wave length under operation. Camonflage by smoke - or fog screens is well known for optical waves and could be of interest for mm- or submm-waves, too. The resulting propagation effects are evaluable if the details of the artificial cloud are known.

It should be mentioned that also biological matter may be an imaginable material as we learned from the discussion of the radar angle problem which was partly solved by considering the back scatter of insects and birds.

3.1.2 O b s t a c l e s w i t h i n t h e r a d i o t r a n s m i s s i o n p a t h

Shadowing effects for short line-of-sight links crossing a shipping route are well known. A very deep interference fading is possible, so that the operational security of a radio connection may be endangered for short time intervals.

3.2 Artificial modification of propagation parameters

3.2.1 C h a n g i n g o f t h e m e a n e n v i r o n m e n t a l c o n d i t i o n s

If the mean meteorological condition will be changed we have a correspondent reaction in the refractive-index (s.equ. 1 to 3). The whole problem is very close connected with the question of weather modification or climatic changes in consequence of environmental pollution (Neiburger, 1969). Within weather modification research in the first place the interest is concentrated to increase or decrease the precipitation rate, to suppress hail, to reduce lightning, to decrease destructive winds accompanying thunderstorms, tornadoes, or hurricans.

Modifications of the clear atmosphere on their different scales are widely unknown. For example, proposals to change on a global scale the radiational budget of the earth by the introduction of clouds of soot or ice crystals into the atmosphere at particular latitudes and heights, and coating with carbon black the snow and ice surface at high altitudes have remained the subject of vague speculation on climate modification. In the range of the microclimate of plants there have been attempts to alter the local radiational balance and improve crop growth by covering the ground with carbon black or by other means. Part of standard agricultural practice are - among other things - the protection of crops from wind damage through the use of rows of trees as wind breaks, and the protection of orchards and kitchen-gardens from frost by means of wind machines, heaters and sprinkling systems.

But also if there would exist such modification experiments the influence on the propagation of microwaves would be very limited and an operational application seems to be out of the question, because the natural variations of propagation conditions will overlap these effects.

In this connection the continuous changes of the climate by civilization should be mentioned,for example the local climate in and near larger cities or cooling towers or the well known problems connected with the enhancement of CO_2-concentration in the atmosphere. Also here the influence on the tropospheric propagation is only of academic interest.

3.2.2 C o n d i t i o n s d u r i n g f o r e s t - o r w i l d - f i r e s

Almost all forest fires are direct or indirect the consequence of human activities. Often large areas are burning.In connection with such fires a special instable (convective) meteorological field develops with very strong subnormal refractive-index gradients above the fire. That means the ray curvature (proportional to the vertical N-gradient) has a negative sign - curvature against the sense of the earth curvature as under the conditions for a mirage over a heated asphalt street. Within the surface layer a total internal reflection with strong multipath effects is possible, a radio connection crossing the fire may break down. Within the surface layer of the fire temperatures of 500°C and more have been measured (Mißbach, 1973). Typical values in a height of 500 m in the surroundings of the fire are 20 to 25°C as we know from aircraft ascents during large scale control fires in West Australia (R.J.Taylor et al., 1971). Above the 500 m level we have approximate near adiabatic gradients. No information is available about the humidity conditions - apart from the known facts that on days with forest fires typical values of the relative humidity are 30% (Geiger, 1948). But the temperature gradient alone is sufficient to form a strong subnormal refraction layer. Within the smoke plume a strong turbulence is observed. For effective ionization effects the temperatures are to low.

3.2.3 R e t a r d a t i o n o f e v a p o r a t i o n b y m o n o l a y e r s

In the recent decade there were above all two reasons to intensify the research on

the problem of evaporation suppression. a) In order to conserve water to meet the ever-increasing demand, it was tried to suppress the rate of evaporation from lakes and larger water reservoirs by the application of mono-molecular chemical films on the water surface (oil or fatty alcohol). b) From numerical studies about developing and maintaining of tropical storms it was found out (Rosenthal 1971) that the exchange of moisture is a crucial factor, so evaporation suppression research with regard to hurricane abatement was initiated (s. Mallinger et al.1973).

Evaporation also has an essential influence on microwave porpagation over sea. As a consequence of evaporation a permanent existing surface duct, the so-called evaporation duct, is formed. This duct controls the propagation over sea for wave lengths smaller some centimeters (s. Jeske,1973).

The results of detailed experiments on the suppression of evaporation, for example, at Lake Hefner (Bean et al, 1969; Grossman et al,1969) show that monomolecular films (a mixture of a 40 percent hexadecanol and 60 percent octadecanol, or ethoxylated alcohol), when spread on a water surface, reduce the evaporation by about 50-60%. The wind speed during these experiments was below 6 m/s. Higher wind speeds tend to break up the film cover. The reduction of evaporation has been attributed on the one hand to the chemical structure of the film that acts as a molecular barrier to evaporation. On the other hand the film on the water surface also suppresses ripples generated by wind and changes so the roughness parameter z_0 which is related with the turbulent fluxes (Mallinger et al,1973). For the evaporation E (flux of moisture) we may write the so-called bulk-formula:

$$E = -\bar{\rho}\, k^2\, \bar{u}_1\, \Delta\bar{q}_1 / (\ln z_1/z_0)^2 \qquad (4)$$

$\bar{\rho}$: density of wet air; $\Delta\bar{q}$: mean difference of the specific humidity between a reference level z_1 (say 10m) and immediately above the surface; $\bar{u}_1$: mean wind velocity at z_1; z_0: roughness parameter; k: Karman constant = 0.4.

The last mentioned effect may be the major mechanism responsible for evaporation retardation by monolayers under wind (Wu,1971). Furthermore, the wave suppression acts to diminish the area of the water surface in contact with the air. This mechanism will be effective also at greater wind velocities (Garrett, 1971).

The reduction of evaporation has of course an correspondent effect on the refractive-index gradient or the thickness of the evaporation duct. Under neutral stability conditions the thickness of the evaporation duct is direct proportional to the evaporation rate E. (Otherwise we get a smaller modification of this relation by consideration of the sensible heat flux and some stability functions.) So, for example, the annual median value of the evaporation duct thickness in the German Bight would be reduced from 7 m to 3.5 m or in the Mediteranien from 14 m to 7 m if we take into account a 50% suppression of evaporation. This would have essential effects on amplitude and phase of the electromagnetic field of radio or radar links. But - examine closely - also in this case an operational application has to be doubted.

3.2.4 Other possibilities

For completeness also two other subjects should be mentioned which were discussed recently and are partly under research. This is firstly an atmospheric modification by high-power microwave beams. So in the absorption line of water vapour an energy transfer into the atmosphere (for example inside clouds) may be of practical interest. Secondly the generation of shock waves by supersonic aircrafts should be enumerated. These may create inhomogeneities in the refractive-index field and so give rise to reflection or scattering of radio waves.

4. Conclusion

For most of the enumerated possibilities of an artificial modification of the clear-air propagation conditions of microwaves a practical application for communication or radar problems cannot be seen today. An exception is the use of radar chaff clouds for camouflage or jamming purposes and also as scatter-communication channel. Under extreme conditions the influence of large forest-(or other) fires on propagation should be noticed. Generally,the variation of propagation parameters due to normal weather changes will overlap artificial modification attemps. Merely for mm- or submm-waves within a locally limited area some operational applications may be imaginable in future.

References

Bean, B.R., Dutton, E.J., 1966, Radio Meteorology; National Bureau of Standards Monograph 92, Boulder, Colorado

Bean, B.R., McGavin R.E.,Emmanuel, C.B.,Krinks,R.W.,1969, Radio-Physical Studies of Evaporation at Lake Hefner, 1966 and 1967; Technical Report of Environmental Science Services Administration ERL 115-W PL7, Boulder, Colorado

Garrett, D.G., 1971, A novel approach to evaporation control with monomolecular films; Journal of Geophys. Res., Vol.76, No.21

Geiger, R., 1948, Neue Unterlagen für die Waldbrandbekämpfung (2.Teil); Mitteilungen Reichsinstitut f. Forst- und Holzwirtschaft, Nr.5

Großkopf, J.,1970, Wellenausbreitung I; Hochschultaschenbücher des Bibliographischen Instituts, Nr. 141/141a

Grossman, R.L., Bean, B.R., Marlatt, W.E., 1969, Airborne Infrared Radiometer Investigation of Water Surface Temperature with and without an Evaporation-Retarding Monomolecular Layer; Journal of Geophys.Res., Vol.74, No.10

Jeske, H., 1973, State and limits of prediction methods of radar wave propagation conditions over sea; in Modern Topics in Microwave Propagation and Air-Sea Interaction (ed. A.Zancla); Nato Advanced Study Institutes Series (C), D. Reidel Publ.Company, Dordrecht-Holland

Lampert, E., 1976, Chaff produced scatter propagation; AGARD Conference Proceeding on "Artificial Modification of Propagation Media", Brussels, April 1976

Langelier, R.M., Bauer, L.H., Bush, A.N., 1967, The Transmission of Digital Signals Trough Random, Time-Variant, Dispersive Channels with Application to Chaff Scatter; IEEE Transactions on Antennas and Propagation, Vol.AP-15, No.1

Mallinger, W.D., Mickelson, Th.P.,1973, Experiments with Monomolecular Films on the Surface of the Open Sea; Journal of Physical Oceanography, Vol.3

Mießbach, K., 1973, Waldbrand.Verhütung und Bekämpfung; 2.Aufl. Deutscher Landwirtschaftsverlag, Berlin

Neiburger, M., 1969, Artificial Modifications of Clouds and Precipitation; World Meteorolical Organization, Technical Note No.105

Rosenthal, S.L., 1971, The response of a tropical cyclone model to variations in boundary layer parameters, initial conditions, lateral boundary conditions, and domain size; *Monthly Weather Review, Vol.99, p 767-777*

Taylor, R.J. et al., 1971, Some Meteorological Aspects of Three Intense Forest Fires; Technical Paper No.21 of Commonwealth Scientific and Industrial Res.Org., Div. of Meteorological Physics, Australia

Wu, J., 1971, Evaporation retardation by monolayers: Another mechanism; Science, 174, p. 283-285

REVIEW ON COMMUNICATION ASPECTS OF CHAFF-PRODUCED SCATTER PROPAGATION

E. Lampert
Siemens AG, Zentrallaboratorium für Nachrichtentechnik Lab 710
Hofmannstr. 51
8000 München 70

SUMMARY

With chaff- a cloud of many dipoles released into the air - communication channels especially for over-the-horizon links can be established. This review paper attempts to summarize the means to describe such a channel with emphasis on the average scatter cross section of the cloud with respect to the length of the dipoles and their distribution in space. The lifetime, fading frequency and coherence bandwidth of this channel are estimated using aerodynamic data from literature. On this basis a comparison of the path loss of the chaff channel with that of a troposcatter channel leads to an advantage of at least 10 dB over the latter channel, however the mean lifetime of the chaff channel is restricted to less than one hour.

1. INTRODUCTION

Chaff was used for the first time in World War II to produce large reflecting areas for electromagnetic (EM) waves. So in a certain angle region the common range radars were saturated and the own combat aircraft could be masked by this chaff clouds. - Chaff consists of clouds of thin aluminum foil or metallized glass strips of approximately half a wave length. Packages of these dipoles - at least several hundred thousands - are released from aircrafts or rockets producing large dipole clouds floating slowly downward.

Now modern radars are equipped with doppler detection (MTI-radar) so the targets can be separated because of their different speed. However chaff is still an effective electronic counter measure as the apparent radar cross section of a target behind the cloud can be reduced. This results from the shielding effect of a thick chaff cloud [1].
In communications chaff can also be applied effectively. It can be used to generate a reliable propagation path for EM waves when transmitter and receiver don't have mutual visibility. This path can then be used for communication or to jam a radio relay link.

As each chaff dipole receives EM power and reradiates it according to its own radiation pattern the plane wave radiated from a transmitter is scattered by the chaff cloud to the receiver. The scattered power however varies randomly in amplitude and phase, so in a first step one has to deal with the methods of

CHANNEL CHARACTERIZATION

These considerations lead to the major problem in evaluating the transmission loss: the determination of the

MEAN BISTATIC SCATTER CROSS-SECTION

of the chaff cloud. The calculation has to be done with regard to the different statistical distributions of dipole axis in the atmosphere. The most common are:

a) equally random in a vertical cone
b) equally random in a horizontal plane
c) totally random

In the moment of chaff release from a airplane or rocket the dipoles are very close to one another so the question of

MUTUAL COUPLING

of chaff dipoles arises. As there is a decrease in scatter cross section when mutual coupling occurs, limits can be given on both the maximum density of the dipoles in space and the scatter cross-section.

As very long dipoles ($\lambda/2$ = 1,5 m for f = 100 MHz) behave differently from an aerodynamic point of view compared to short ones (< 10 cm) the cross-section of short dipoles has to be considered as well.

Regarding the important EM parameters of the channel

DOPPLER SPECTRUM and

COMMUNICATION CHANNEL CORRELATION BANDWIDTH

their behaviour can only be determined, if the

Descent Modes of Particular Dipoles

are known.

With all these data kept in mind and checked against experimental results reported in literature the effectivity of the artificially produced "Chaff Channel" can be compared with the always present natural "Tropospheric Scatter Channel".

2. CHANNEL CHARACTERIZATION

In a chaff scatter channel the incident power from a transmitter is scattered at a multitude of individual dipoles. These dipoles are more or less randomly oriented in the cloud and apart from a common descent velocity their motion can be considered random. So the signal at the receiver is the sum of many sinusoidal signals with mutually independent amplitude and phase. Because of the high number of scatterers this random process tends to become a wide sense stationary complex gaussian random process with time when the incident signal is a sinusoid. The amplitude of the received signal has a rayleigh-distribution, the Power P_2 is exponentially distributed: ($\langle P_2 \rangle$ is the time average of P_2) [2, 3]

$$p(P_2) = \exp\left(-\frac{P_2}{\langle P_2 \rangle}\right) \qquad (1)$$

Although the transmission channel is linear, the output signal has a nonzero spectral distribution when a sinusoidal signal is transmitted. This results from the time variability of the channel which originates from the random motion of the dipoles thereby causing signal fading. The statistical behaviour of the channel can be described by the time-frequency autocorrelation function [2]. As we deal with broad band systems and channels it is possible to calculate the effects at low modulation frequencies, resp. the time dependance, independently from those occuring at high frequencies, resp. the frequency selective fading or vice versa.
From the time-frequency autocorrelation function therefore usually two one dimensional correlation functions are derived:
The frequency correlation function which describes the frequency coherence of the channel and from which the coherence or correlation bandwidth of the channel is derived, i.e. the bandwidth up to which information transmission is reasonable. The time correlation function is a measure of the fading velocity at a fixed frequency. Frequently the Fourier transform of these two expressions are better understood or measurable.

Alternatively the channel may be described by the scattering function, see e.g. Kennedy [4], which is the fourier-transform of the time-frequency autocorrelation function. So all parameters can easily be related to the scattering function.

The frequency correlation function corresponds to the time delay distribution (delay scattering function) and the time correlation function to the doppler spectrum (frequency scattering function). From radar back scatter experiments there is quite a good knowledge of the different types of doppler spectra. As almost no measured values on the frequency correlation function of time-variable channels and chaff channels especially are known it is usually assumed as being gaussian with the correlation bandwidth as single parameter. This parameter is usually estimated in its order of magnitude from the path geometry.

The theory of information transmission over such a type of time-variable channel is rather developped because the chaff channel behaves rather similar to a troposcatter channel [5, 2]. Bello and Nelin considered analogue and digital systems [6, 7]. - To get an acceptable availability of a certain signal level at the receiver amplitude fading has to be countered by introducing enough system margin into the power balance. If the bandwidth of the modulated RF-signal comes into the order of the correlation bandwidth signal distortion occurs. In FDM/FM system this leads to excessive intermodulation in the baseband. In digital FSK and PSK transmission systems irreducible errors occur because of intersymbol interference. So usually the bit-rate should be kept below 0.1 of the correlation bandwidth, otherwise modulation methods comparatively insensitive to multipath have to be applied, e.g. fast frequency hopping [4, 8].

So far it has been shown that the most important parameters of the chaff channel are its mean value of the received power, the doppler spectrum, resp. mean fading frequency and the path delay distribution, resp. the correlation bandwidth.

3. MEAN BISTATIC SCATTER CROSS-SECTION

To determine the average received power P_2 the transmission equations of a bistatic radar system is used [9]. The chaff cloud is illuminated by the transmitter with a flux density ϕ_2

$$\phi_2 = \frac{P_1 \cdot G_1}{4\pi\, r_1^2} \qquad (2)$$

P_1 transmitter power
G_1 gain of transmitter antenna
r_1 distance from transmitter to chaff cloud

To get to the receiver the transmitted signal is scattered by the chaff cloud which can be characterized by its average cross section $\bar{\sigma}$. At the receiver the antenna with an effective area A_3 collects the mean power P_3 from the scattered field:

$$P_3 = \frac{\phi_2 \cdot \bar{\sigma}}{4\pi \cdot r_2^2} \cdot A_3 \qquad (3)$$

As gain G_3 and effective area A_3 are related via

$$A_3 = \frac{\lambda^2}{4\pi} \cdot G_3 \qquad (4)$$

this results in the transmission equation

$$\frac{P_3}{P_1} \cdot \frac{G_1 \cdot G_2}{4\pi} \cdot \frac{\bar{\sigma}}{(r_1 \cdot r_2)^2} \cdot \left(\frac{\lambda}{4\pi}\right)^2 = \frac{A_1 \cdot A_2}{4\pi} \cdot \frac{\bar{\sigma}}{\lambda^2} \cdot \frac{1}{(r_1 \cdot r_2)^2} \qquad (5)$$

The mean cross section $\bar{\sigma}$ is naturally dependent on the direction to both the transmitter and the receiver compared with the location of the dipole cloud and the kind of statistical distribution of the dipoles in the cloud. If these values are known, the average cross section can be calculated from the transmission equation when a single dipole is used as a scatterer. In a fixed spherical coordinate system G (φ, Θ) is the gain of the particular dipole in the direction φ, Θ. As the dipole is short circuited all the power collected from the incident field has to be reradiated and none will be dissipated in a matched load. Under this condition the dipole will collect the power P_d out of the incident field. The value of P_d is proportional to the effective area A (φ, Θ) of the dipole in this particular direction:

$$P_d = 4 \cdot A \cdot \phi = 4 \cdot \frac{\lambda^2}{4\pi} \cdot G(\varphi_T, \Theta_T) \cdot \phi \qquad (6)$$

$(\varphi_T, \Theta_T$ polar coordinates of the transmitter with respect to dipole axis)

The power P_d is reradiated again according to the antenna pattern of the dipole, so the power collected by the receiver has the value:

$$P_3 = \frac{\lambda^2}{4\pi} \cdot G_3 \cdot G(\varphi_R, \Theta_R) \cdot P_d \cdot \frac{1}{4\pi R_2^2} \qquad (7)$$

$(\varphi_R, \Theta_R$ polar coordinates of the receiver with respect to dipole axis)

For an individual scatter-dipole we get the cross-section

$$\sigma = \frac{\lambda^2}{\pi} \cdot G\,(\varphi_R, \Theta_R) \cdot G\,(\varphi_T, \Theta_T) \qquad (8)$$

4. AVERAGE SCATTER CROSS SECTION OF THE CHAFF CLOUD

It is assumed that the distance between two dipoles is large ($\gg \lambda/2$) so no mutual coupling occurs and the dipoles are considered as mutually independent. To get the average cross-section $\bar{\sigma}$ of the chaff cloud, Equ. (3), we have to calculate the average on all σ values, Equ. (8), over a given distribution of dipole axis in space.

Palermo and Bauer [10] calculated the average cross-section $\bar{\sigma}$ for $\lambda/2$ dipoles for uniform, horizontal and vertical distributions, Fig. 1. Hessemer [9] published also results for the average cross-section for a vertical cone distribution. His results differ slightly from the first mentioned as he used for reasons of simplification the gain pattern of a short dipole instead of that of a $\lambda/2$-dipole.

Fig. 1 shows the values computed by Palerno and Bauer. The assumption that only at one terminal azimuth and elevation angles differ considerably from zero originates from the discussion of Equ. (5). As the received power is inversely proportional to $(r_1 \cdot r_2)^2$ small values of attenuation are only reached when the chaff cloud is dispersed above one terminal.

When using purely random distributed chaff the mean scatter cross section has its maximum value:

$$\bar{\sigma}_{max} = 0.15 \cdot \lambda^2 \cdot N \qquad (9a)$$

when the azimuth and elevation angle is approximately zero. The scatter cross section however decreases to about:

$$\bar{\sigma}_{min} = 0.038 \cdot \lambda^2 \cdot N \qquad (9b)$$

when both azimuth and elevation angle approach $\frac{\pi}{2}$. When using horizontal polarization $\bar{\sigma}$ is independent on the elevation with vertical polarization $\bar{\sigma}$ in independent on the azimuth. This effect is easily understood when looking at the gain pattern of a single dipole.

If one succeeds in distributing the dipoles in a way that all axis are in a horizontal plane, values of $\bar{\sigma}$ ranging from $0{,}3\lambda^2 N$ down to $0.066\lambda^2 N$ may be attained.

Fig. 1 shows that chaff reacts differently on horizontally and vertically polarized waves. - As a dipole is an omnidirectional antenna in the plane perpendicular to its axis the polarization of the scattered wave differs from that of the incident wave. Therefore with uniformely distributed dipoles and high values of azimuth and elevation angle circular polarization yields better results compared to linear polarization. Mack and Reiffen [11] showed that in this case an improvement of about 2.5 dB is achieved. Better results can be attained if polarization tracking is used at the receiver. - (As the planning of radio relay networks usually relies on at least 20 dB of polarization decoupling the effect of altering polarization by chaff scatter can produce degradations.)

5. EFFECTIVITY OF SHORT DIPOLES

The discussion of the mean scatter cross section has shown that it is advantageous to distribute the chaff dipoles only in a horizontal plane. To achieve this distribution the dipoles have to be cut into pieces. The short dipoles however are less efficient in reradiating EM power than $\lambda/2$ dipoles. Therefore one has to look for an optimum between the dipole length and the possibility of horizontal chaff dispersion. This optimum is dependent on the diameter of the dipoles as the dipole can extract more power from the primary field when its reactance is low. A cloud consisting of thick wires however would fall down like a stone. For thin wires (diameter less than 1% of wave length) Hessemer [9] calculated the loss in average scatter cross section compared to $\lambda/2$-dipoles on the basis of equal total length. If this diagram, Fig. 2, is compared with the average cross section Fig. 1 it can be recognized that only under very unfavourable conditions, e.g. very high elevation angles short dipoles yield better results than $\lambda/2$-dipoles.
(A dipole with a length of 0.1 λ has already a loss of 41 dB.) To overcome this disadvantages there have been attempts to produce broadband chaff [12, 13].

6. MUTUAL COUPLING

As the average scatter cross section of the cloud is proportional to the number of particles N, it seems that the received power can be increased indefinitely. This however has limits because all dipoles have to be within the antenna beam of receiver and transmitter otherwise the familiar troposcatter phenomenon of antenna to medium coupling loss will occur [14]. If under this constraint N is increased, the density of dipoles in space will increase to a point where mutual coupling occurs. Wickliff and Garbacz [15, 16] have shown that this phenomenon decreases the average scatter cross section when the medium space between the elements is below 2 λ. When approaching $\lambda/2$ the decrease is about 3 dB.

Further it has to be appreciated that thick chaff clouds (corridore chaff) produce a considerable amount of shielding of the primary field and the scattered field [1]. Therefore in both directions to transmitter and receiver the cloud should look like a thin layer.

7. AERODYNAMIC PROPERTIES

For a complete description of the chaff channel under the aspect of the time available for useful wave propagation aerodynamic data are needed. Puskar et al [17]

have made extensive drop tests, Fig. 3, and found that for 2.5 cm dipoles the preferred descent mode is the spiral mode which actually does not produce a purely horizontal dipole axis. As it can be assumed that the rotation takes place with almost constant velocity the doppler spectrum of the received signal has distinct lines according to this rotation.

Usually the point of release of the dipoles is on the great circle between transmitter and receiver in the vicinity of one location. As long as the cloud is in between transmitter and receiver, the parameters of the link are only slightly altered when there is a horizontal drift. This drift however can cause the cloud to move off the great circle line and behind one of the stations. Even if the cloud is tracked by both antennas the attenuation can rise noticably as the distance to the nearby terminal will vary significanty. For estimation of this effect one has to take into account horizontal drift velocities of about 3 m/s to 25 m/s.

Several experiments show that in calm air the average descent speed $\bar{v}$ is between 0.5 and 1.5 m/s depending on the orientation of the dipoles in space [2, 3]. Katz [18] also calculated the descent velocity and the spread of the cloud using Reynold's number.

It seems feasible to disperse up to 30×10^6 dipoles (at 4.5 GHz) into a single cloud in starting heights of about 9000 m to 10000 m.

Considering a link of 150 km over smooth earth mutual visibility is achieved at a height of 440 m when the cloud is positioned at the middle in between the two stations and about 1800 m when the cloud is above one station. This leads to usable cloud life times of about 1 hour. These values can be shorter if there are downwinds and longer if there is an appropriate updrift.

8. FADING FREQUENCY AND COHERENCE BANDWIDTH

If we assume that the distribution of vertical speed among the individual dipoles ranges from zero to v_{max} with $\bar{v}$ as average ($\bar{v}$ = 0.5 to 1.5 m/s) and the cloud situated above one terminal, we get the following equation for the medium fading frequency $\bar{f}_s$ ($c = 3 \cdot 10^8$ m/s):

$$\bar{f}_s \approx \frac{\bar{v}}{c} \cdot f_r \qquad (10)$$

So at radio frequencies of about f_r = 4.5 GHz $\bar{f}_s$ will reach values of about 25 Hz. This value can be diminished when the chaff cloud is situated in the middle between the two terminals. With common values of the antenna beamwidths (2°) the fading frequency can be reduced by a factor of 10. This choice however will produce the highest value of attenuation.

The order of magnitude of the coherence bandwidth can also be determined as the power flow is restricted to the cones under which the terminals see the cloud. If ϕ_1 and ϕ_2 are the angles subtended by the cloud at the antennas the coherence bandwidth is given by [18]:

$$B_c = \frac{c}{\cot(\frac{\Theta}{2}) \cdot (r_1\phi_1 + r_2\phi_2)} \qquad (11a)$$

Θ being the crossing angle of the antenna beams. Equ. (11a) reduces to

$$B_c = \frac{c}{\Delta} \qquad (11b)$$

when the cloud is positioned above one terminal ($r_1 \gg r_2$) and Δ is the spread of the cloud in the direction of the far terminal. With a cloud spread of 300 m this results in a coherence bandwidth B_c = 1 MHz. So with basic modulation schemes [7] the information bandwidth is limited to about 100 kHz.

9. ATTENUATION OF CHAFF- AND TROPOSPHERIC-SCATTER CHANNELS

As both effects chaff-scatter and troposcatter are used to produce over-the-horizon communication links their path loss should be compared. For a troposcatter link working at 4.5 GHz over a distance of about 150 km and with antennas with about 37 dB gain (2° beamwidth) there will be only 4 dB antenna-to-medium coupling loss. With an optimally situated scatter volume the path attenuation will be less than 164 dB in 99% of the time in the worst month [19].

When using chaff scatter with a chaff cloud of about 10^6 dipoles released over one terminal at 10000 m above ground the mean path loss will be 137 dB. At shorter distances, e.g. 100 km the difference in path loss between the two transmission media reduces from 27 dB to 22 dB. However when looking at chaff experiments [2, 3] the measured loss was about 3 to 10 dB higher than theoretically predicted. On the other hand troposcatter behaves much better during longer periods of the year as illustrated by the high availability of that link.

In the present stage of technology it therefore seems to be advantageous to use chaff when there is only a short-time need for a communication channel and the geographical or meteorological situation is unfavourable for troposcatter.

This conclusion is almost independent on frequency (< 10 GHz). If the antenna areas are kept constant and also the total weight of the chaff the received power P_3 increases proportional to frequency in the chaff channel as well as in the troposcatter link.

LITERATURE

[1] Kownacki, S.: Screening (Shielding) Effect of a Chaff Cloud IEEE Trans AES July 1967 pp. 731 - 734

[2] Langelier, R.N. et al.: The Transmission of Digital Signals Through Random, Time-Variant, Dispersive Channels with Application to Chaff Scatter. IEEE Trans AP-15 Jan. 1967 pp. 172 - 183

[3] Bauer, L.H.: Experimental Investigation of Chaff-Transmission in the 1300 to 1800 MHz Frequency Range, Final Report vol. I, II Advanced Communications Group, Radiation Inc. Melbourne Florida, AD 283 318, AD 283 319

[4] Kennedy, R.S.: Fading Dispersive Communication Channels John Wiley and Sons, New York 1969

[5] Bello, P.A.: A Troposcatter Channel Model IEEE Trans COM-17, April 1969, pp. 130 - 137

[6] Bello, P.A. and Nelin, B.D.: The Effect of Frequency Selective Fading on Intermodulation Distortion and Subcarrier Phase Stability in Frequency Modulation Systems IEEE Trans CS-12, March 1964, pp. 84 - 101

[7] Bello, P.A. and Nelin, B.D.: The Effect of Frequency Selective Fading on the Binary Error Probabilities of Incoherent and Differentially Coherent Marched Filter Receivers IEEE Trans CS-11, June 1963, pp. 170 - 186

[8] Lebow, I.L. et al.: "The West Ford Belt as a Communications Medium" Proc IEEE vol. 52, May 1964, pp. 543 - 563

[9] Hessemer, R.A.: "Scatter Communications with Radar Chaff" IRE-Trans AP-9, March 1961, pp. 211 - 217

[10] Palermo, C.J. and Bauer, L.H.: Bistatic Scattering Cross Section of Chaff Dipoles with Application to Communications Proc IEEE, vol. 53, Aug. 1965, pp. 1119 - 2121

[11] Mack, C.L. and Reiffen, B.: RF Characteristics of Thin Dipoles Proc IEEE vol. 52, May 1964, pp. 533 - 542

[12] Richmond, J.H. et al: Tumble-Average Radar Backscatter of Some Thin-Wire Chaff Elements IEEE Trans AP 22, Jan 1974, pp. 124 - 126

[13] Thal, H.L.: Radar Cross Section of Arcs on V Shapes IEEE Trans AP 17, Sept. 1969, pp. 663 - 665

[14] Battesti, J. et Boithias, L.: Nouveaux Elements sur la Propagation par les Heterogeneites de l'Atmosphere Annales des Telecommunications 26 no 1-2, 1971, pp. 1/96 - 16/16

[15] Wickliff, R. and Garbacz, R.: The Average Backscattering Cross Section of Clouds of Randomized Dipoles IEEE Trans AP 22, pp. 503 - 505, 1974

[16] Wickliff, R. and Garbacz, R.: Addendum to "The Average Backscattering Cross Section of Clouds of Randomized Dipoles" IEEE Trans AP 22, pp. 842 - 843, Sept. 74

[17] Puskar et al: Radar Reflector Studies, NAECON '74 Record pp. 177 - 183

[18] Katz, L.: Forward Scatter Chaff System for Air-Ground Long-Haul Communications, National Telecommunication Conference record 72, pp. 10C-1 to 10C-7.

[19] C.C.I.R. XIIIth Plenary Assembly, Geneva 1974, vol. V, Report 238-2, pp. 209 - 229

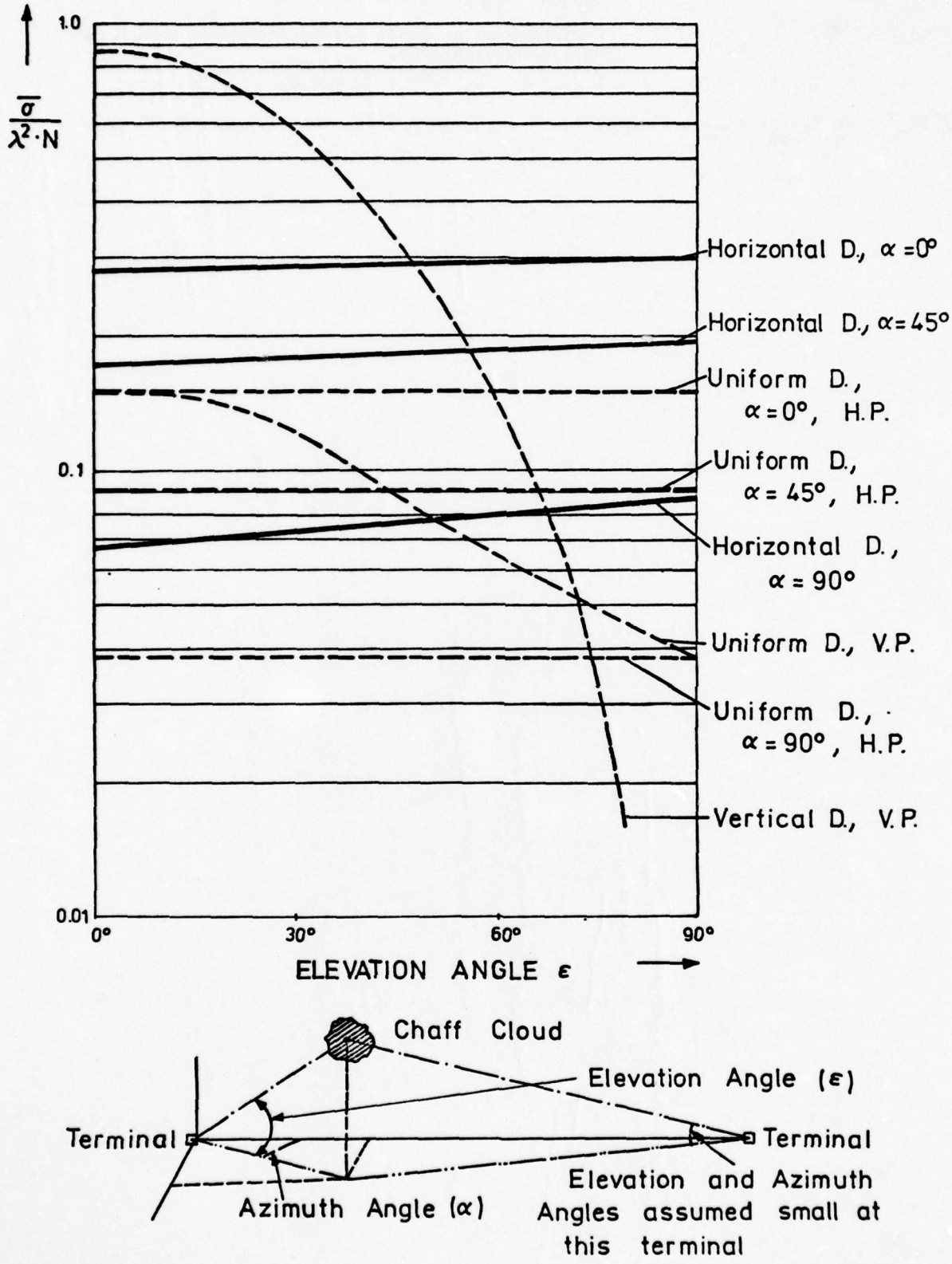

Fig.1 Average scatter cross-section of λ/2-dipole cloud for different distributions in space after Palermo and Bauer (Ref.10)
(D. = Distribution; H.P. = Horizontal Polarization; V.P. = Vertical Polarization)

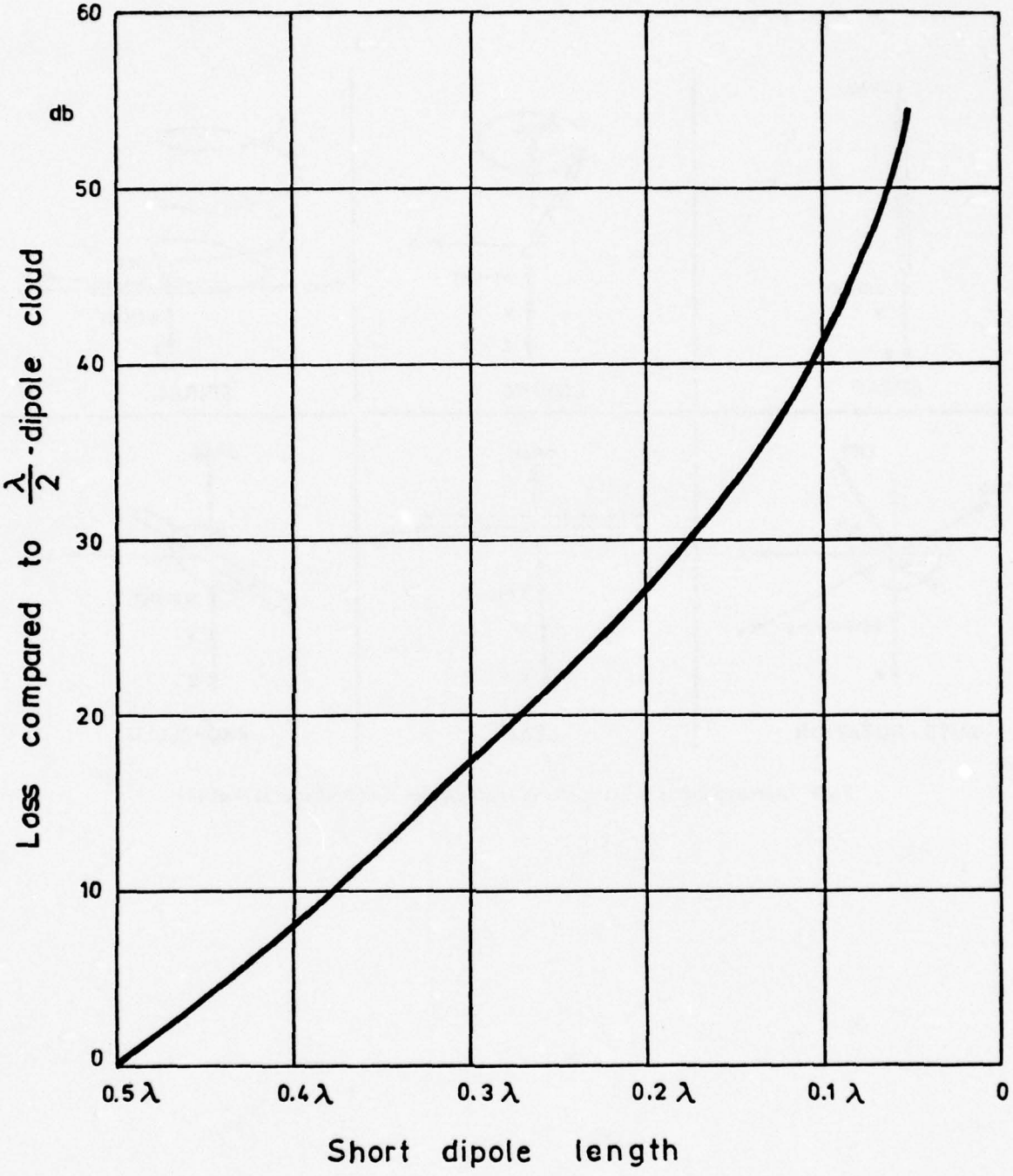

Fig.2 Loss in average scatter cross-section of a short dipole compared to one of half-a-wave-length after Hessemer (Ref.9)

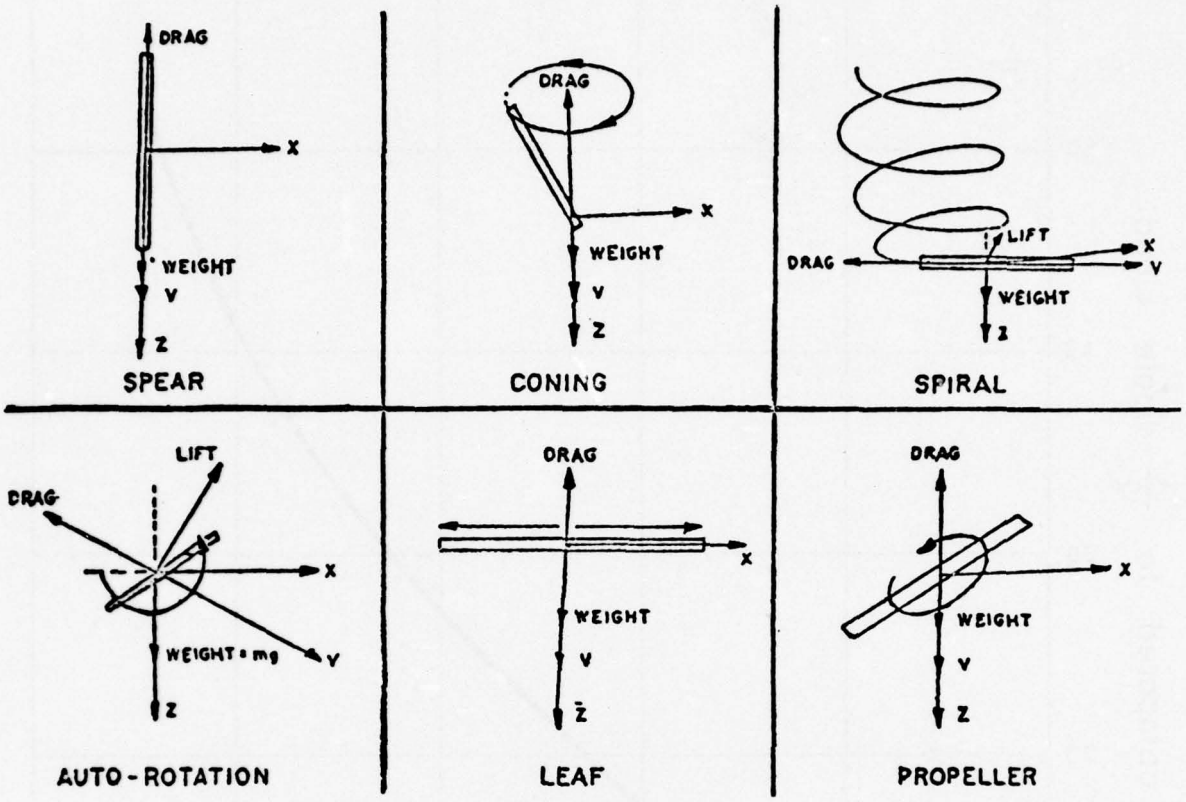

Fig.3 Aerodynamic descent modes of chaff-dipoles after Puskar et al (Ref.17)

DISCUSSION OF ARTIFICIAL FOG MODIFICATION

Gottfried Hänel
Institut für Meteorologie
Johannes Gutenberg-Universität
Mainz, Germany

SUMMARY

The importance of fog comes from its attenuation of electromagnetic radiation and its influence on the radiation budget of the atmosphere. Doing a first step into artificial fog modification it is necessary to discuss on the base of appropriate budget equations local changes with time of the extinction and absorption coefficients of fog particles. It comes out that small fog particles can be altered by small particles, and large fog particles can be influenced by large particles.

1. BASIC CONSIDERATIONS

In this discussion on artificial fog modification we regard microphysical effects alone on the basis of budget considerations. For this purpose we divide the fog particles into classes of particles of almost equal size in dry state as well as equal chemical composition and structure in dry state. The total extinction coefficient (additional subscript "E") or absorption coefficient (additional subscript "A") is given as the sum of the extinction or absorption coefficients of the classes

$$\sigma = \sum_i \sigma_i \tag{1}$$

For each class of particles a budget consideration is necessary. Thus we have to regard a set of budget equations when we look on the total extinction or absorption coefficient. This increases largely the difficulties inherent in our problem.

Each budget equation for σ_i includes the following processes:

(A) Atmospheric motion.
(B) Sedimention of particles.
(C) Brownian diffusion of particles.
(D) Influence of relative humidity.
(E) Sources and sinks by coagulation, coalescence, disintegration, and change of chemical composition and structure.

For evaluation of the influence of the relative humidity (D) it is assumed that the time of adaption of a particle to a new relative humidity is small compared to the period of humidity change. Thus with respect to relative humidity it can be assumed thermodynamic equilibrium. Therefore the results cannot applied to clouds. The budget equation reads

$$\frac{\partial \ln \sigma_i}{\partial t} = -\underbrace{\frac{\nabla \cdot (N_i \mathbf{V})}{N_i}}_{(A)} + \underbrace{w_i \frac{\partial \ln N_i}{\partial z}}_{(B)} + \underbrace{\frac{\nabla \cdot (D_i \nabla N_i)}{N_i}}_{(C)} + \underbrace{\left(2 \frac{\partial \ln r_i}{\partial f} + \frac{\partial \ln \varkappa_i}{\partial f}\right) \frac{\partial f}{\partial t}}_{(D)} + \underbrace{Q_i}_{(E)} \tag{2}$$

$\sigma_i = N_i \pi r_i^2 \varkappa_i$ = extinction or absorption coefficient of class i
N_i = particle number per unit volume of class i
r_i = equivalent radius = radius of a sphere with the same volume like the particle
$\varkappa_i$ = efficiency factor of extinction or absorption of a particle
w_i = settling velocity of a particle
D_i = diffusion coefficient of a particle
$\mathbf{V}$ = (microscale) barycentric velocity of the particle loaded air
f = relative humidity
t = time
z = height
∇ = nabla operator
Q_i = term describing sources and sinks

In this paper we cannot discuss the whole problem, therefore we will restrict to the following particles parameters: the settling velocity, the diffusion coefficient and the term (D) describing the influence of relative humidity on the extinction coefficient $\pi r_i^2 \varkappa_i$ of the single particle. The effect of atmospheric motion on the particles concentration (A), the change with height $\partial \ln N_i / \partial z$ of the logarithm of the particles concentration and the local change with time of relative humidity $\partial f / \partial t$ are known by solving the appertaining budget equation for a large atmospheric volume and by a quantitative humidity forecast.

2. RESULTS

The settling velocity, the diffusion coefficient, and the change with relative humidity of the logarithm $\ln(\pi r_i^2 \varkappa_i)$ of the extinction and absorption coefficient of a single particle are given for different sizes in dry state and different relative humidities. Two aerosol types, a maritime aerosol (model 3) and a continental aerosol from an "unpolluted" area (model 6) are regarded. The experimental data on the particles and basic theoretic considerations regarding the humidity influence on the particles properties are given in an earlier paper (HÄNEL 1976). The settling velocities and diffusion coefficients of the particles

Table 1: Settling velocity w_i, diffusion coefficient D_i and $2(\partial \ln r_i / \partial f)$ the twofold change with relative humidity of the logarithm of the equivalent radius (equal to the change with relative humidity of the logarithm $\ln(\pi r_i^2)$ of the particle's geometric cross section) for maritime aerosol (Model 3) and continental clean air aerosol (Model 6) for various equivalent radii r_{oi} in dry state and relative humidities f.

Model	r_{oi} (cm)	10^{-6}	10^{-5}	10^{-4}	10^{-3}
	f	Settling velocity w_i (cm/sec) at 20° C and 1013.25 mb			
3	0	$3.6 \cdot 10^{-5}$	$5.6 \cdot 10^{-4}$	0.032	2.9
	0.8	$3.2 \cdot 10^{-5}$	$6.5 \cdot 10^{-4}$	0.045	4.2
	0.995	$4.0 \cdot 10^{-5}$	0.0024	0.26	23
6	0	$2.7 \cdot 10^{-5}$	$4.3 \cdot 10^{-4}$	0.024	2.2
	0.8	$2.7 \cdot 10^{-5}$	$4.6 \cdot 10^{-4}$	0.029	2.7
	0.995	$2.9 \cdot 10^{-5}$	0.0014	0.16	14
	f	Diffusion coefficient D_i (cm^2/sec) at 20° C and 1013.25 mb			
	0	$1.5 \cdot 10^{-4}$	$2.3 \cdot 10^{-6}$	$1.3 \cdot 10^{-7}$	$1.2 \cdot 10^{-8}$
3	0.8	$7.5 \cdot 10^{-5}$	$1.1 \cdot 10^{-6}$	$7.6 \cdot 10^{-8}$	$7.2 \cdot 10^{-9}$
	0.995	$3.0 \cdot 10^{-5}$	$3.5 \cdot 10^{-7}$	$2.6 \cdot 10^{-8}$	$2.5 \cdot 10^{-9}$
6	0.8	$1.2 \cdot 10^{-4}$	$1.6 \cdot 10^{-6}$	$1.0 \cdot 10^{-7}$	$9.4 \cdot 10^{-9}$
	0.995	$6.0 \cdot 10^{-5}$	$5.1 \cdot 10^{-7}$	$3.4 \cdot 10^{-8}$	$3.3 \cdot 10^{-9}$
	f	Change with relative humidity of the logarithm of equivalent radius $2(\partial \ln r_i / \partial f)$			
3	0	0.07	0.07	0.07	0.07
	0.8	4.4	4.0	3.2	3.1
	0.995	13	130	220	240
6	0	0.04	0.04	0.04	0.04
	0.8	2.2	3.9	3.9	3.9
	0.995	4.9	120	230	250

have been computed with the formulae given by FUCHS (1964) assuming spherical shape. Results are compiled in Table 1 offering the following pecularities:

a. Settling velocity w_i:
Remains nearly constant with changing relative humidity, when the particles are small. Increases with relative humidity when the particles are large. Is different for different aerosol types.

b. Diffusion coefficient D_i:
Decreases with increasing size in dry state and with increasing relative humidity. Differences at large relative humidities for different aerosol types.

c. Twofold change with relative humidity of the logarithm of the equivalent radius $2(\partial \ln r_i / \partial f)$:
Its change with relative humidity is large, when the relative humidity itself is near unity. There are differences for different aerosol types. The computations are performed considering the vapor pressure increase over a curved surface. Thus smaller particles have a smaller radius increase with relative humidity than larger ones owing the same chemical composition and structure. In Table 2 the logarithmic changes with relative humidity $\partial \ln \varkappa_{Ei} / \partial f$ and $\partial \ln \varkappa_{Ai} / \partial f$ of the efficiency factors $\varkappa_{Ei}$ of extinction and $\varkappa_{Ai}$ of absorption are discussed qualitatively.

Table 2: Discussion of the changes with relative humidity of the logarithms of the efficiency factors $\varkappa_{Ei}$ of extinction and $\varkappa_{Ai}$ of absorption. λ is the wavelength of radiation. $\varkappa_{Ei}$ and $\varkappa_{Ai}$ are computed with the theory of MIE (1908) for homogeneous spheres.

r_{oi} (cm)	f	λ (μm)	$\partial \ln \varkappa_{Ei} / \partial f$ and $\partial \ln \varkappa_{Ai} / \partial f$
10^{-6} to 10^{-3}	0	0.3 to 12	Negligible like $2/r_i \cdot \partial n_i / \partial f$ Exception Model 6 at λ = 12 μm
10^{-6}	0.8 to 0.995	0.3 to 12	Both relative changes of $\varkappa_{Ei}$ and $\varkappa_{Ai}$ are almost equal. Their amount is of the same order like the relative change of ϱr_i^4 . Positive for increasing or constant imaginary part of refractive index, when the size increases. Negative in all the other cases. Humidity influence can be made small with specific materials.
10^{-5}	0.8	0.3 to 12	Amount usually of the same order like $2/r_i \cdot \partial r_i / \partial f$
10^{-4} to 10^{-3}	0.8	0.3 to 12	Usually small or negligible compared to $2/r_i \cdot \partial r_i / \partial f$ Exception Model 6 at λ = 12 μm and $r_{oi} = 10^{-4}$ cm.
10^{-5} to 10^{-3}	0.995	0.3 to 12	Small compared to $2/r_i \cdot \partial r_i / \partial f$ Exception for visible and near infrared: Strong negative values for $\partial \ln \varkappa_{Ai} / \partial f$.

3. DISCUSSION

From the present results combined with the knowledge on coagulation due to Brownian motion (e.g. FUCHS 1964) and coalescence of drops due to different velocities (e.g. MASON 1963) the following inferences can be drawn about artificial modification of extinction and absorption coefficients.

1. Small particles (10^{-6} - 10^{-5}cm): Using appropriate materials, the influence of relative humidity on the extinction or on the absorption coefficient can be made negligible. Since their diffusion coefficient, i.e. their mobility is large, the composition of small particles can be changed by coagulation. Doing this, small particles of another composition must be introduced into the air. Alternatively small particles can be formed in the air by condensation or chemical reactions.
2. Large particles (10^{-4} - 10^{-3} cm): When a large influence of relative humidity on the extinction or absorption coefficient is needed, large particles must be introduced into the atmosphere. However due to their large settling velocity the largest particles are removed fastest from the atmosphere. Moreover they can be gathered by large, rapidly falling drops or particles.

It comes out that the small particles can be changed by small particles, and the large particles can be influenced by large particles. Final conclusions including technical aspects cannot be given until detailed model computations are performed.

LITERATURE

Fuchs, N.A. (1964) The Mechanics of Aerosols. Pergamon Press, Oxford.

Hänel, G. (1976) The Properties of Atmospheric Aerosol Particles as Functions of the Relative Humidity at Thermodynamic Equilibrium With the Surrounding Moist Air. Advances in Geophysics 19, 73-188

Mason, B.J. (1963) The Physics of Clouds. Oxford Univ. Press (Clarendon), London and New York

Mie, G. (1908) Beitrag zur Optik trüber Medien. Annln. Phys. 25, 377-445

ARTIFICIAL MODIFICATION OF THE AIR MICROSTRUCTURE INSIDE CLOUDY OR SIMPLY MOIST STRATIFIED LAYERS

by

R. Serpolay
Observatoire du Puy de Dôme
Clermont-Ferrand, France

M. Andro
Université de Bretagne Occidentale
I.U.T. de Lorient, France

and

S. Godard
Observatoire du Puy de Dôme
Clermont-Ferrand, France

SUMMARY

I In laboratory conditions, the transparency of a fog can be artificially increased by dispersing an aerosol of sodium alginate (mean particulate size : 30 µm) with a result comparable to that obtained with an aerosol of sodium chloride (mean particulate size : 5 µm).

By means of a ground-based device of in-line sources bloving the chemicals inside natural fogs the above result has been confirmed only in part, sodium alginate acting more moderately and less quickly than sodium chloride.

II The same device has been used for seeding with sodium chloride particles clear but moist air layers, the relative humidity of which being above the critical hygroscopicity of the salt. Thus precipitations of briny drizzle have been induced, the droplet sizes of which reaching 100 to 300 µm.

On the basis of these results, the effects of such modifications upon the propagation of microwaves in the media are theoretically examined.

I - Introduction

At the joint Conference on Aeronautical Meteorology (Paris, 24-25 mai 1971), one of the authors of this paper presented a project for new attempts in the field of warm fog modification (SERPOLAY, R. 1971). The method proposed for this research combined two means :

1°) as seeding agent, a polyelectrolyte chemically extracted and prepared from seaweeds : sodium alginate ;

2°) for dispersing adequately this chemical finely grinded (mean particulate size : 30 µm), a ground based device about which no more detail will be given than in the previous paper of 1971.

In the course of three campaigns carried out in the 1971, 1972 and 1973 summer times, it seemed suitable to have to compare the efficiency of this chemical to that of more known one : sodium chloride.

The aim of this paper is to let knov all the results obtained in this work.

Several seeding experiments with sodium chloride were conducted not only in cloudy but also in clear -but moist- air layers : they led to induce drizzles.

Then, the results were examined not only with respect to the artificial modification of the visual range but also from the point of view of the artificial modification of the propagation media for microwaves.

II - Seeding agents

Alginates -the salts of the aginic acid extracted from seaweeds - exhibit an unquestionable affinity for water, particularly for liquid water. Among them, sodium alginate has been recognized as the most efficient under this respect (MAGUET, M. and SERPOLAY, R. 1973).

Finely grinded particles of such a chemical are suspended on spider's threads and observed under a microscope. If cloudy air is sucked in through the network, cloud droplets are picked up by the threads as well as by the alginate particles. Liquid water spreads over the surface of the latter and is soon absorbed in their mass : this process results in a swelling of the particles.

On the following set of pictures (Fig. 1) we can see the growth of a single particle of sodium alginate by such a coalescence-absorption process until it reaches the size of a drizzle drop. But for the viscosity forces exerted inside the drop and on its surface -forces which would have failed in the case of a drop of pure water or saline solution- it would have been extremely difficult to reach such a size because the drop would have been blown away from the threads by the air stream at the very early stage of its growth.

For comparing the efficiency of the chemical to that of sodium chloride, we chose for the latter a powdered material (mean particulate size : 5 µm) mixed with 5 % of an anti-motant powder, the purpose of which being to separate the particles from each others under storage conditions and to ensure a better dispersion in the atmosphere.

III - Cloud chamber experiments

On the base of these observations, we came to wonder if it would be possible to modify locally the structure of clouds and fogs by spraying sodium alginate powder inside them.

3.1. Experimental method

A 18 cubic meter cloud chamber was equiped in such a way that the variations of the light intensity transmitted through the artificial cloud could be recorded.

In a first series of tests, a given quantity of alginate powder was sprayed inside the chamber at the time when the cloudy air source was interrupted for a given level of optical density.

In a second series of tests, the cloud source was maintained in operation after the powder was dispersed, this operative way providing, in addition, a slight turbulence within the chamber.

Although hygroscopic sodium chloride particles display a different size distribution in the experiments carried out and behave differently from sodium alginate particles since their action results essentially in vapour transfer -by vapour pressure lowering on their surface- they were the subject of a similar study for comparison purposes.

3.2. Results

In the first series of tests (Fig. 2, a), curves 1, 2 and 3 are corresponding to growing masses of alginate : they are all above curve 4 which corresponds to sodium chloride.

In the second series of tests (Fig. 2, b and c), the curves relative to alginate evolve parallel with those relative to sodium chloride ; however, their effect on visibility is less marked and we can note that the quantities of alginate which are dispersed are markedly higher for a less important result. This may be due not only to the fact that the vapor pressure does not drop, or only slightly, in the vicinity of the alginate particles -for which only the coalescence- absorption process takes place- but also to the fact that, because of technical difficulties, it proved impossible to use alginate particles with a size similar to that of sodium chloride particles. This involves a smaller specific surface, on the one hand, and a shorter residence-time in the cloudy air, on the other hand.

IV - Field experiments

Sodium alginate powder being a substance less corrosive than sodium chloride, we thought it interesting to investigate whether the above laboratory results could be applied to natural fogs for improving the visibility on the runways.

4.1. For this purpose, field trials were undertaken on the Brest-Guipavas airport where a device for dispersing powdered substances in the atmosphere was developped and installed. An application to patent the principle on which this device is based in association with the use of sodium alginate to modify the structure of fogs was made in France in 1972 (French patent n° 72-32-687). Let us recall briefly the main features of this device.

On a portion of the airfield five dispensers of powder were arranged in-line over a distance of 220 m. Each dispenser is associated with a blowing device inducing an air stream which can raise the powder up to a height of 6 - 20 m above the ground, assuming that the wind velocity does not exceed 4 m/s.

4.2. To complete this presentation of the trials we carried out, we ought to mention that the choice of the test site was dictated by a frequent occurence of advection fogs in that area during the summer time.

The Guipavas airport is located inside the Brittany peninsula, approximately 25 km from the West and North coasts at an altitude of 90 m a. s. l. The presence of fogs on this area usually coincides with an anticyclonic situation associated with winds blowing from directions ranging from N-W to N-E. Due to the temperature lowering, the fogs which hang over the sea during the day are invading the inland during the night. However, while their thickness, off the shore, can be approximately 100 m, it decreases to 10 m or a few scores of meters at Guipavas, according to a diabatic rather than adiabatic process.

4.3. Results

As in the case of the cloud chamber experiments, the field trials were conducted with sodium chloride powder as a reference, the two chemicals being able to be used successively, after a break period, in the same fog conditions.

The results of these trials are outlined in the following table (Table 1). They are based on measurements generally made by night, in several locations of the air field, by visual means and by visibility recorders such as the S.A.P.E. -used by the French Meteorological Office- and the "Videograph"- built by Impuls Physik.

Date and number of the trial	Nature of the seeding agent	Result
9. 9. 1971	Sodium alginate	+
14. 9. 1971 (1)	"	+
" (2)	"	+
15. 9. 1971 (1)	"	0
" (2)	Sodium chloride	+
20. 9. 1971 (1)	"	+ (?)
" (2)	"	+
29. 9. 1971 (1)	"	+ (drizzle)
" (2)	Sodium alginate	+ (?)
18. 7. 1972 (1)	"	0
" (2)	"	0
6. 9. 1972	"	0
7. 9. 1972	"	+
7. 9. 1973 (1)	Sodium chloride	0 (drizzle)
" (2)	"	0 (drizzle)
" (3)	Sodium alginate	0
10. 9. 1973 (1)	"	0
" (2)	Sodium chloride	0 (drizzle)
7. 10. 1973 (1)	Sodium alginate	+
8. 10. 1973 (1)	Sodium chloride	+ (drizzle)

Table 1 - Summing up of the results

In the result column, the sign + indicates that the experiment led to a positive result as far as the improvement of visibility is concerned.

The sign + (?) indicates that the visibility improvement cannot be unquestionably ascribed to the seeding, but that the presumption is in favour of a correlation.

The sign 0 indicates that the results of the experiment are not significant, that is, did not enable us to conclude that the seeding has improved the visibility.

If we consider only the positive results obtained with sodium alginate, we can conclude that the technique used is likely to improve the visibility from initial levels of the order of 150 m or below. This way, the visual range could be increased to approximately twice the value of the initial visibility (Fig. 3). This increment factor might even exceed 2 in the case of an initial visibility ranging from 50 to 100 m. Although we are not in a position to confirm it, it appears that this result is also valid in the case of an initial visibility of the order of 300 m.

The visibility increasing effects are felt at distances ranging between 300 and 1 000 m, leeward of the device.

The visibility improvements achieved through sodium chloride seedings are still more spectacular : from an initial level of 300 m., the visual range can be increased up to over 1 000 m (Fig. 4). This improvement factor, which is slightly above 3, is also found for an initial visibility below 100 m.

These results are essentially valid in those areas where brine precipitations caused by the sodium chloride aerosol occur.

4.4. Discussion

There again, the divergences observed between the results obtained respectively with the two kinds of substance can easily be accounted for by their different granulometry and physico-chemical behaviour. In particular, the action of sodium chloride is quicker than that of sodium alginate.

Referring again to the table 1, we should point out that, although the two kinds of substance used differ by their physico-chemical activity, a similar percentage of operations not followed by visibility improvement is obtained (40%). Therefore, the nature and granulometry of the substances used are not the only factors involved, and we should try to trace other causes. A thorough analysis of the experimental conditions revealed two main causes :

a) the poor thickness of the fog layer above the airfield ; as a result, only a portion of the aerosol (plume) can remain in contact with the fog, while the upper part spreads into clear air ;

b) the presence of an area planted with 5-6 m high trees, windward of the device, between the North-West and North-East directions ; this tree-planted area makes up a shield against the motion of any cloudy air mass coming from these directions. The influence of this shield effect on the airflow was verified in conditions of clear weather. It is such that the wind velocities at a height of 10-12 m are markedly higher than those recorded at a height of 3 m., the corresponding directions being sometimes appreciably different.

The latter remark accounts for the fact that mobile observers and control devices may have been inadequately located by night and in foggy weather.

V - The change of the microstructure in the seeded air layers.

5.1. The case of fogs and clouds

The interest of fog and cloud modification by means of sodium alginate or sodium chloride aerosols does not seem to relate only to the transparency of these natural media to visible radiations.

As a matter of fact, if we try to trace the physical cause to which the improvement of visibility during these operations can be attributed, we note that due either to a condensation-coalescence process or to a coalescence-absorption process, a large number of cloud droplets are replaced by a small number of large drops.

This was observed, precisely, on several occasions, in the course of the field experiments conducted with sodium chloride : the areas where visibility improvements were the greatest coincided with those where brine precipitations occured. Brine drops collected on a Formvar solution film, as well as their dry residues, were examined a posteriori from the size distribution point of view.

The following histograms were obtained (Fig. 5). We notice that, as far as the 29 September 1971 experiment is concerned, the drop sizes range between 100 and 300 µm in diameter (A) while those of the dry residues range between 40 and 150 µm (B). It is noteworthy to compare the latter with the particle size distribution of the seeding chemical (C).

There is not doubt that larger precipitation elements would have been obtained if their time of residence within the cloud had exceeded 3 minutes, the time which elapsed from the moment the sodium chloride injection started to the moment the drops were collected.

There is not doubt either that large precipitation elements could be formed from sodium alginate particles staying a long while within cloudy layers.

Now, while clouds and fogs are transparent media for the micro-waves which travel through them, they may behave differently when the water which forms them is re-distributed by seeding in the shape of particles whose sizes exceed 300 or 400 µm.

This question will be considered in the end of the paper from a theoretical standpoint ; but it would also require to be studied further from an experimental standpoint.

5.2. The case of moist air layers

The presence of cloud droplets does not seem to be absolutely necessary to the artificial inducement of aqueous precipitation elements in the atmosphere.

As a matter of fact, brine precipitations were artificially initiated by means of the device set up at Guipavas by dispersing a sodium chloride aerosol inside air layers whose relative humidity ranged between 80 and 95 %.

Fig. 6 shows the sizes of the drops induced by this method are similar to those of the brine drops generated in the fogs with the same substance. This is all the more verifiable as the relative humidity of the air layer is closer to saturation.

VI - Microwaves propagation in the seeded air layers

The effect on electro-magnetic wave propagation of a population of spheres with a refractive index different from the medium (air) where they are located, is in fact twofold : one part of the incident electromagnetic energy is absorbed, while the other part is scattered. The resultant of these two phenomena represents the propagation loss (signal attenuation). The energy scattered in the opposite direction to the incident energy is sometimes non-negligible ; it is this "backscattering" which makes it possible to observe radar echoes on certain clouds or precipitations.

This physical characteristics of dielectric spheres have been calculated in the case of water (Herman, Browning and Battan, 1961). Their calculations give us directly the attenuation (Q_T) and backscattering (Q_B) cross-sections for various drop diameters in relation to the considered wavelengths. Besides, we know that when the drops are small enough with respect to the wavelength ($\frac{2\pi a}{\lambda} \leq 0.15$, where "a" is the radius of the drop and "λ" the wavelength), the calculations of Q_T and Q_B according to Mie's complete theory are simplified (Rayleigh's approximation) and we can write :

$$(1) \qquad Q_B = \frac{64\,\pi^5}{\lambda^4} \left| \frac{m^2 - 1}{m^2 + 2} \right| a^6$$

$$(2) \qquad Q_T = \frac{8\,\pi^2}{\lambda} \, IM \left\{ - \left[\frac{m^2 - 1}{m^2 + 2} \right] \right\} a^3$$

where $m = n - ik$, is the complex water index for the wavelength considered.

The results presented previously show that the radius of the drops obtained does not exceed 0.02 cm and that Rayleigh's approximation is applicable to the various usual radar wavelengths (0.86 cm ; 3.2 cm ; 10 cm) currently used.

The propagation attenuation is usually expressed in decibels/km. It is easily demonstrated (Battan, 1973 ; Godard, 1965 ; Waldteufel, 1973) that this

expression assumes the following form :

$$A\ (db:km) = 0{,}4343 \sum_{vol} n_i\ Q_{Ti}$$

As Q_T is proportionnal to a^3, the expression $\sum n_i\ Q_{Ti}$ is proportionnal to the liquid water content, whatever the granulometry of the drops may be. In other words, if a fog or a cloud is modified by the inducement of large elements (a = 200 µm) to the detriment of smaller ones, propagation is not affected. It may be improved if the large elements precipitate, thus reducing the water percentage. On the other hand, the generation of a population of drops in initially clear air may bring about a propagation loss which, anyway, will only be perceptible in the case of short wavelengths (λ < 1 cm).

For the sake of example, the production of a population of 7 000 drops/m^3 with a radius of 0.02 cm (which corresponds approximately to the same water contents as a rain of 1 $mm.h^{-1}$) will induce an attenuation of about 0.3 db/km (λ = 0,86 cm).

As regards radar reflectivity, which characterizes the intensity of the echo received and corresponds to the sum per volume unit of the drop backscattering cross-section (Q_B), the impact of the size of the drops is quite different, because reflectivity increases as the sixth power of the radius (formula (1)).

It is easy to show (Battan, 1973 ; Godard, 1970 and Waldteufel, 1973) that reflectivity η expressed in cm^{-1} is written in the following form :

$$\eta = n \times Q_B \times 10^{-6}$$

where n is the number of drops per m^3 with a cross section Q_B (cm^2).

In the example given above, it is easy to calculate that the population considered corresponds to a liquid water content of 0.234 g/m^3 and that the reflectivities are respectively given by the following table for different wavelenght considered (Table II).

λ (cm)	0,86	3,2	5,5	10
η (cm^{-1})	$7{,}0 \cdot 10^{-9}$	$8{,}4 \cdot 10^{-11}$	$7 \cdot 10^{-12}$	$1{,}1 \cdot 10^{-12}$

Table II

It appears from these figures that such a population will be detected by a medium performance radar from distances up to 10 km, whatever the wavelength may be.

If the same liquid water content results from a population of ten times smaller drops (radius : 20 µm), the reflectivities will be one thousand times lower and only a radar operating on short wavelength (0.86 cm) can detect such fog from a distance of 2-3 km.

These examples show that the modifications induced in rather thin fog or clouds can be detected by radioelectric means. In our calculations however, we did not take into account a possible salt solution effect on the refractive index of the drops.

Finally, the predicted reflectivities show that one should not expect to achieve a considerable "jamming" effect on eventual radar targets by using simple small size water drops.

ACKNOWLEDGMENTS

The experiments on Brest-Guipavas Airport were supported by contracts N° 71/001 and 73/215 from the Direction des Recherches et Moyens d'Essais and by grants from the Directions of Aéroport de Paris and Compagnie Air France. We wish more particularly to acknowledge the help of Colonel Guyaux, MM. J. Bachelez and P.-D. Cot, the respective responsibles of these Establishments and to thank them for their constant interest in our work.

We wish to express our best thanks to MM. J.-Y. Paugam, R. Mazé and P. Morizur for their direct assistance during the field experiments ; to Commandant Farion, from Brest-Guipavas Airport Authority, and M. E. Renaud, from Meteorological Service, for the kindness with which they placed many facilities at our disposal on the air field.

REFERENCES

BATTAN L. J., 1973, "Radar Observation of the Atmosphere", The University of Chicago Press.

GODARD S., 1965, "Propriétés de l'atténuation par la pluie des ondes radioélectriques dans la bande 0.86 cm", Journal de Recherches Atmosphériques, Vol. II, pp. 121-167.

GODARD S., 1970, "Propagation of centimeter and millimeter wavelengths through precipitations", I.E.E.E. Transactions on antennas and Propagation, Vol. AP 18 n° 4, pp. 530-535.

HERMAN B.M., BROWNING S.R., BATTAN L.J., "Tables of radar cross-sections of water spheres", Technical report n° 9, University of Arizona.

MAGUET M. and SERPOLAY R., 1973, "Action de l'acide alginique et de quelques-uns de ses dérivés sur les brouillards de laboratoire", Journal de Recherches Atmosphériques, Vol. VII, n° 2, pp. 83-90.

MIE G., 1908, "Beiträge zur optik trüber Medien, speziell kolloidaler Metallösungen", Ann. der Phys. XXV, pp. 377.

PAUGAM J.-Y. and SERPOLAY R., 1970, "Modification de la densité optique des brouillards par ensemencement d'alginate pulvérulent. Comparaison avec les ensemencements de NaCl", Communication presented to 89th Congrès de l'Association Française pour l'Avancement des Sciences, Brest 6-11 July 1970, published in Journal de Recherches Atmosphériques, Vol. IV, 2ème année, n° 3, pp. 101-106.

SERPOLAY R., 1971, "Projet d'expérimentation sur la modification des brouillards à toutes températures par voie physico-chimique", Communication presented to the Joint Conference on Aeronautical Meteorology of S.M.F. and A.M.S., Paris 24-25 May 1971.
Published in 1971, Journal de Recherches Atmosphériques, Vol. V, n° 4, pp. 185-191.

SERPOLAY R. and ANDRO M., 1972, "Précipitation locale d'une nappe de brouillard par ensemencement à base de chlorure de sodium", Journal de Recherches Atmosphériques, Vol. VI, n° 1-2-3, pp. 529-535.

SERPOLAY R. and ANDRO M., 1973, "Salt drizzles extracted from unsaturated air layers by seeding with hygroscopic nuclei", Proceedings of the International Conference on Weather Modification, pp. 55-61.Tashkent.

WALDTEUFEL P., Mai-Juin 1973, "Atténuation des ondes hyperfréquences par la pluie : une mise au point", Ann. des Telec., T. 28, n° 5-6, pp. 255-272.

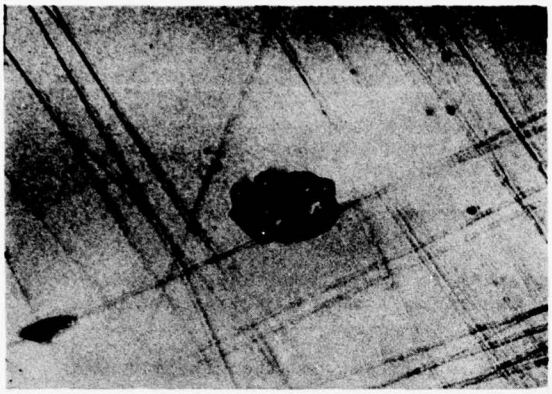

(a)

(b)

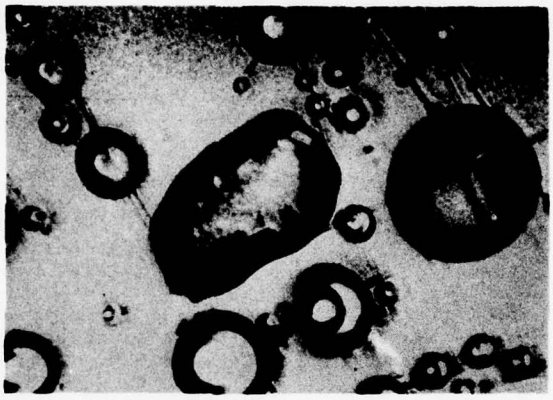

(c)

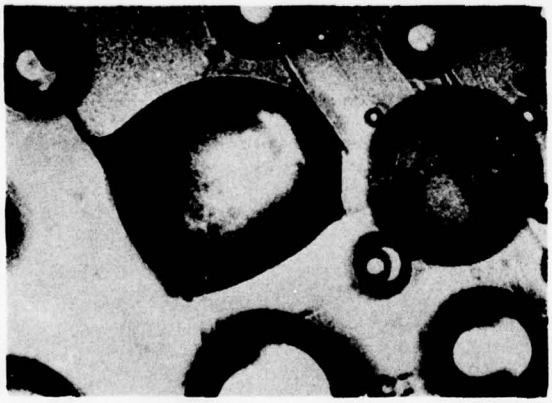

(d)

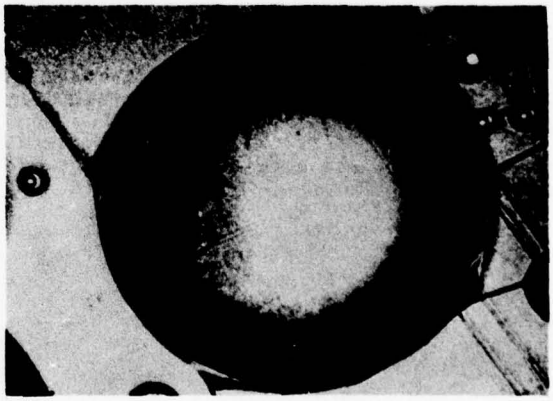

(e)

Fig. 1 - Different growth stages of a single sodium alginate particle of about 40 µm in size suspended on a web's thread (a) in a stream of cloudy air. The growth proceeds by direct capture of cloud droplets or by coalescence with other cloud drops captured by web's threads in its vicinity (b to e). Let us note the opacity of the particle during the growth process and the final size reached (about 160 µm).

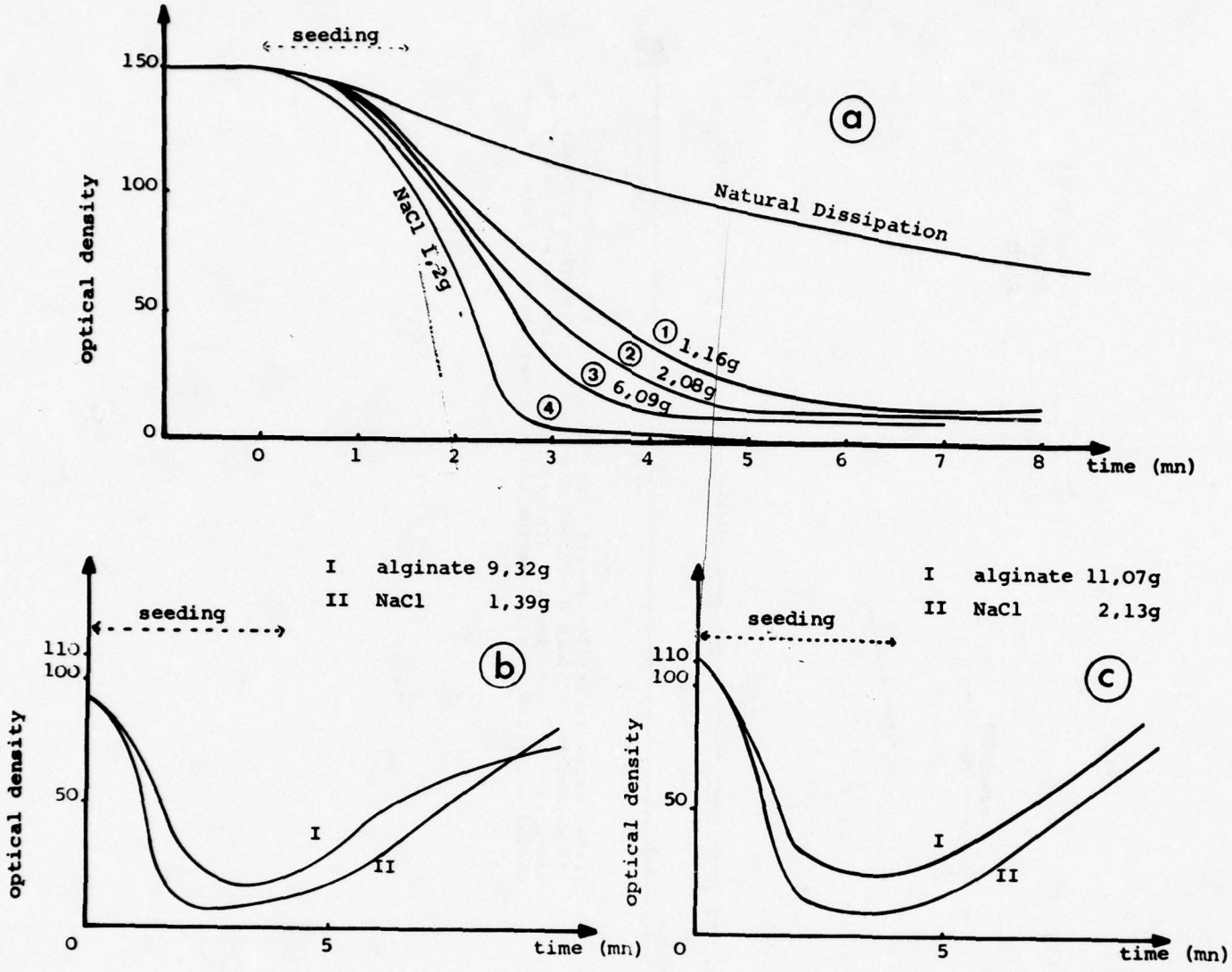

Fig. 2 - Optical density variations versus time in an artificial fog seeded with sodium alginate or sodium chloride. (a) type 1 experiments ; (b) and (c) type 2 experiments (refer to the text).

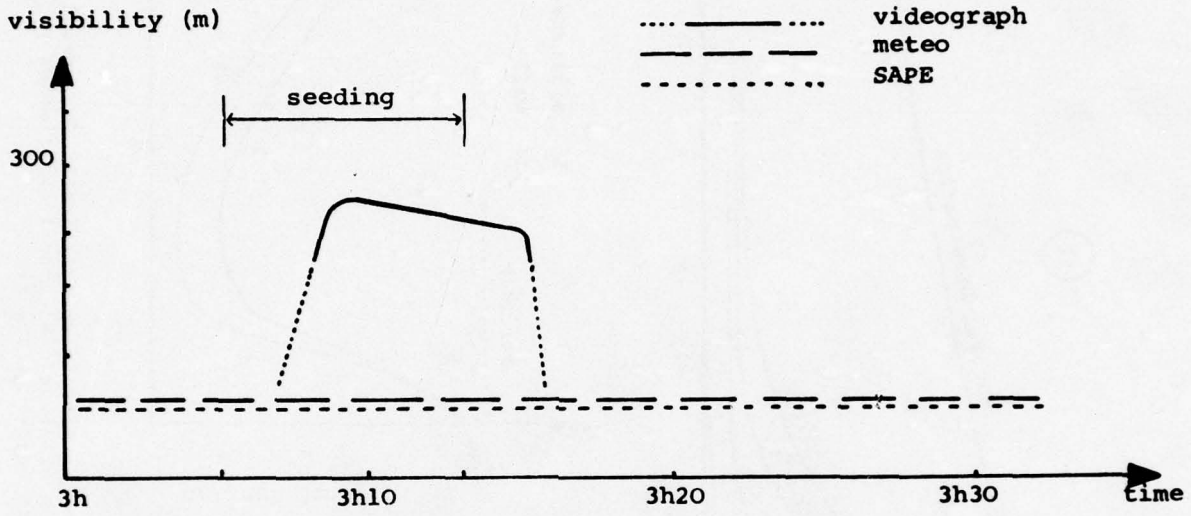

Fig. 3 - Visual range variations versus time during a field experiment (15 September 1971) in a natural fog seeded with sodium alginate. Meteo and SAPE measurements are recorded in sites located out of the seeded area. Let us note the low and constant level of these values.

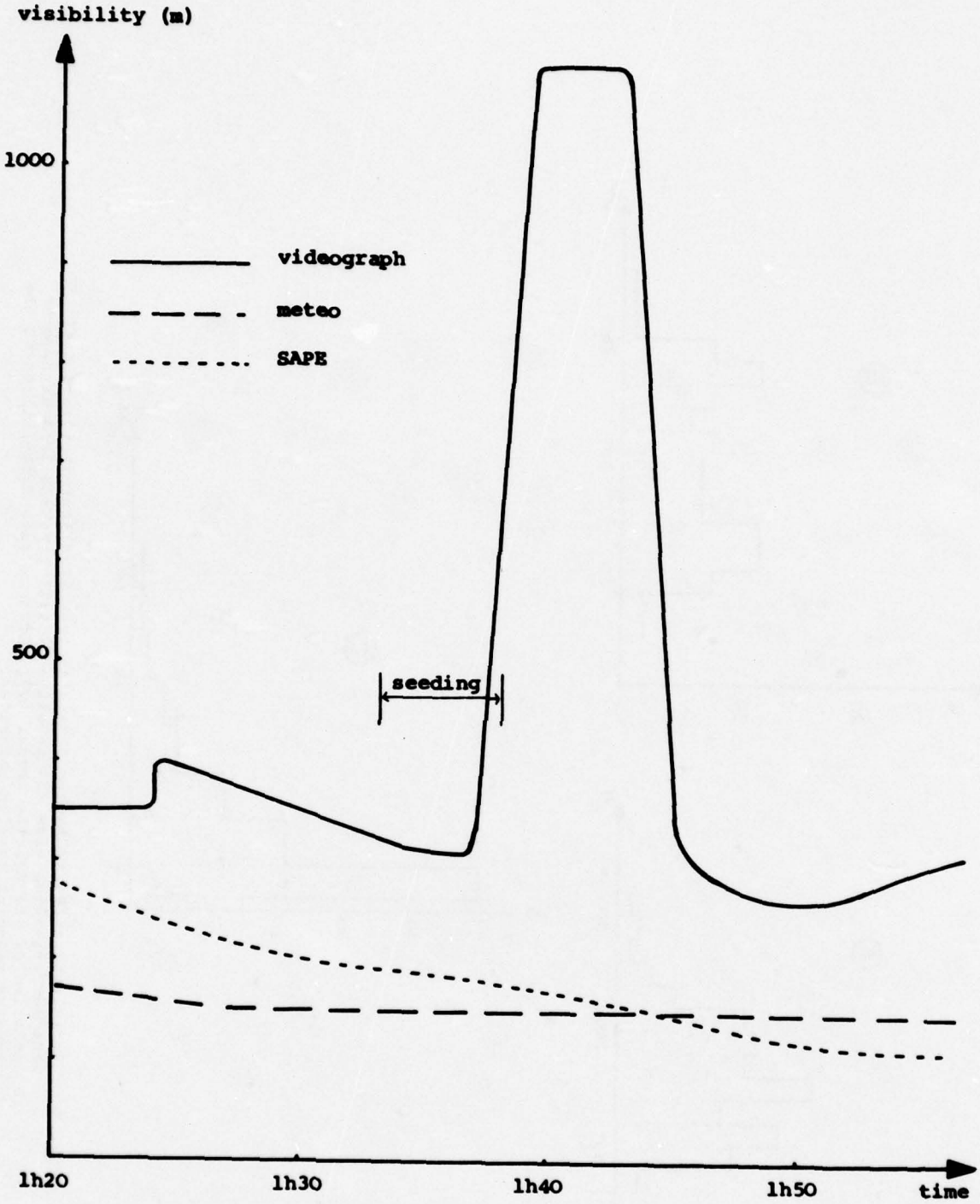

Fig. 4 - Visual range variations versus time during a field experiment (29 September 1971) in a natural fog seeded with sodium chloride. The improvement resulting from the seeding has been recorded by the "Videograph" in an area corresponding to a briny drizzle.

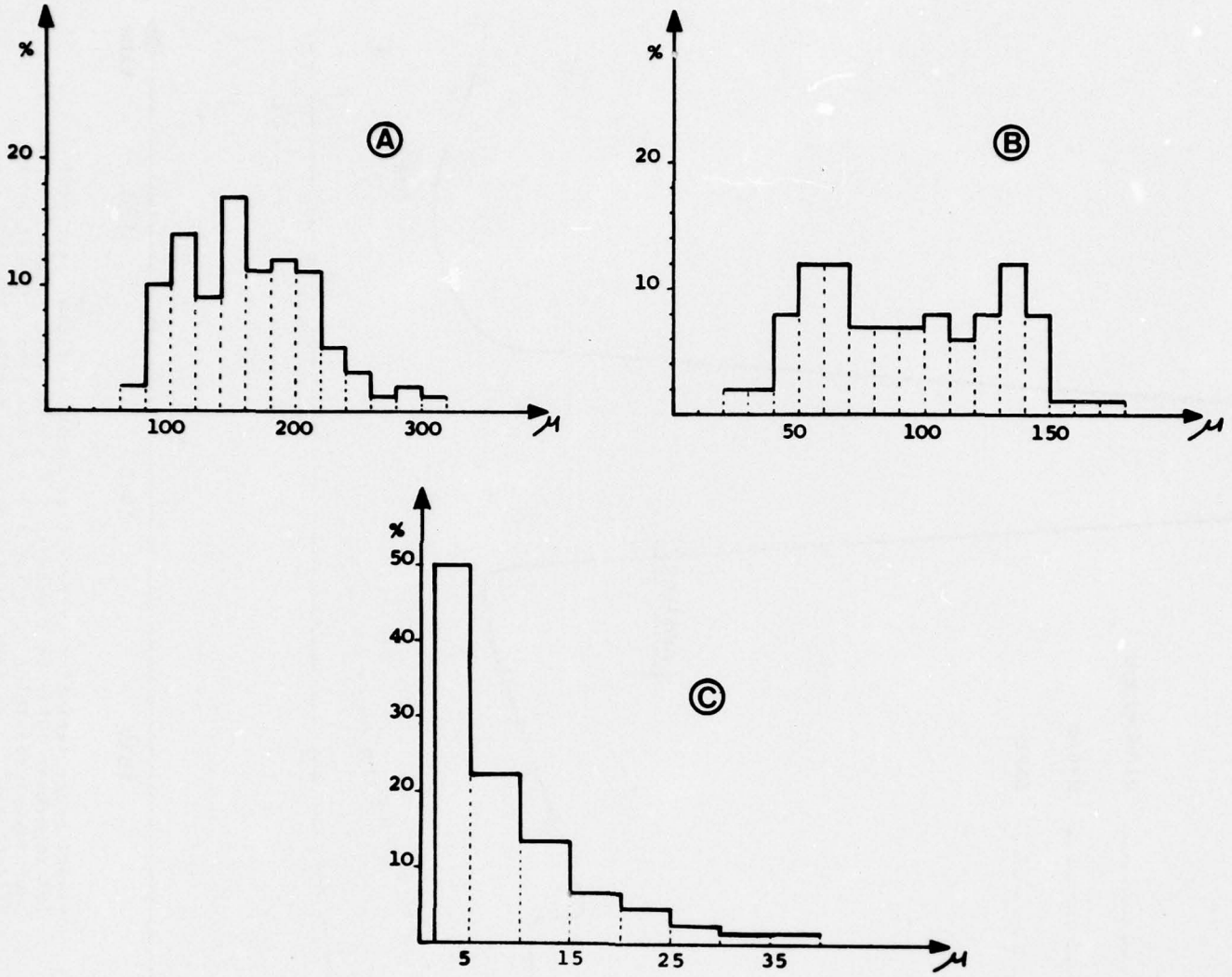

Fig. 5 - Experiment of 29 September 1971 -(A) Drop size distribution and (B) the corresponding size distribution of salt crystals left after evaporation of the drizzle drops. (C), particle size distribution of the seeding material (sodium chloride).

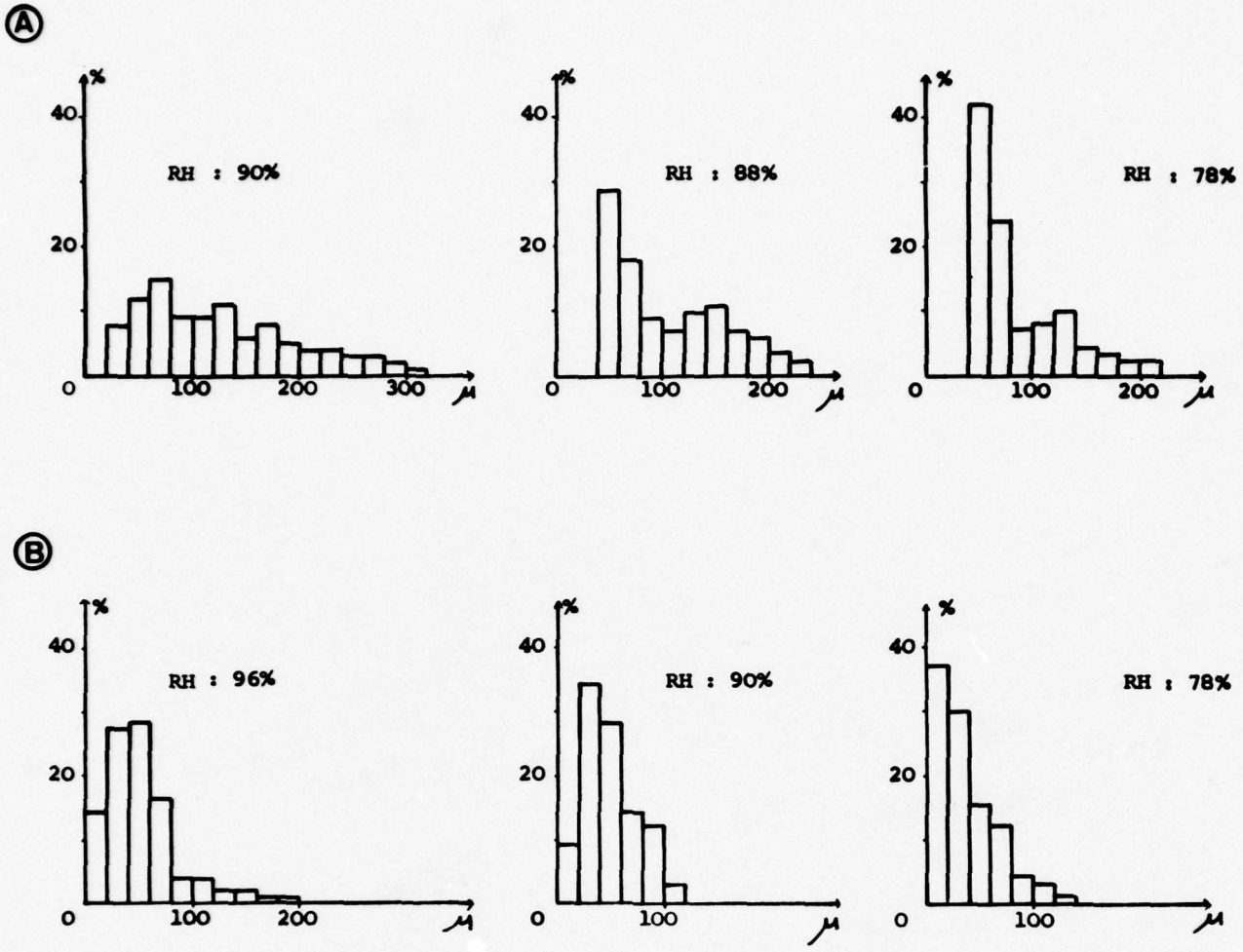

Fig. 6 - (A) Drop size distributions and (B) size distributions of salt crystals left after evaporation of drizzle drops induced by seeding moist air layer with sodium chloride at decreasing relative humidity.

SESSION I, ROUND-TABLE DISCUSSION

MODIFICATION OF NON-IONIZED MEDIA

Participants at Round Table: H.J.Albrecht (Chairman)
G.Hänel,
H.Jeske,
E.Kleinjung,
E.Lampert,
R.Serpolay.

By way of introduction, H.J.Albrecht referred to the present initial state of research in modifying non-ionized media for purposes of affecting wave propagation and to the degree of difficulty thus encountered, also in reviewing achievements up to the present. He pointed out that, in some areas of the topic being dealt with, it is yet unknown in which way the technological development may improve the capability of intentionally modifying the propagation environment and thereby extend usefulness and reliability of communication links. It was also mentioned that, at this early stage, the entire field is definitely a challenging one, and that its progress should certainly be watched.As a general procedure, it was agreed to adhere to a sequence of discussion topics in accordance with the order of paper presentations; the audience was invited to fully participate.

As an initial comment, reference was made to one of the conclusions of the first paper, namely the possibility of redistribution and dissolution of precipitation in such a way that communication links would not be affected. E. Kleinjung pointed out that this may perhaps be achieved by what is called "overseeding" clouds; in certain cases, this process might lead to the dissolution of precipitation inasmuch as a complete ice-crystalization would occur. He emphasized, however, that this is only possible in very few cases as the dynamics of the cloud are not involved. Another consequence of "overseeding" supercooled clouds may be the redistribution of precipitation. Examples were reported by Weickmann for the "Great Lakes winter snowstorms" where an increase in the number of ice crystals by seeding resulted in a decrease in intensity and a spreading over larger areas of the snowstorms. Redistribution may sometimes be connected with orographic seeding and seeding of frontal clouds. Also, redistribution may refer to seeding with a delayed action upon precipitation. R.Serpolay supported these comments and added that appropriate experiments had been done; he also referred to the subject of fog dispersal. He mentioned that supercooled fog seeding by liquid propane never led to overseeding, but, on the contrary, produced sometimes snowflakes which had diameters of the order of one or a few centimetres.

Referring to the production of snow from precipitation, and possibly dry snow with minimum effects upon the larger part of the electromagnetic wave spectrum, H.J.Albrecht again drew attention to the difference between the aims of present-day weather modification and the modification objectives for propagation purposes. He mentioned that, in this case, the criterion is a minimum effect of precipitation on propagation and not necessarily the complete disappearance of rain clouds. In other words, the importance of considering this criterion was emphasized as the actual aim. He was supported by L. Boithias (France) whose comments enlarged upon this difference in criteria and also included remarks on the more meteorological character of some of the contributions of this session. In a reply, R.Serpolay unterlined the significance of knowing the interface area between meteorology and propagation research and that meteorological conditions have to be considered when initiating a modification process. It was pointed out that appropriate investigations are essential. P.Halley (France) supported the views just presented and also referred to some work of intentionally changing thunderstorm effects in connection with electrical power lines.

Some additional comments again referred to the subject of dissolving or redistributing rain clouds for the benefit of communication purposes and also to fog dispersal. G. Hänel supported the importance of taking meteorological conditions into account; as an example, the presence of strong winds would prevent the use of modifying materials. In addition, he emphasized that our present knowledge does not allow us to fully understand the simultaneous action of the processes which modify particles, such as coagulation, coalescence and sedimentation. Especially the consequences of coagulation or coalescence of particles of different chemical compositions are not known exactly enough He added that, for a controlled modification, calm conditions are essential and that only effects restricted in time and location can be expected. W.Attmannspacher(Germany) also emphasized that, today, it is only possible to modify precipitation in special cases and with local effect; a thunderstorm cannot be destroyed or moved away. Thus only in special cases there may be an improvement of propagation conditions. G.Tacconi (Italy) then discussed statistical aspects of modifying propagation media; information available at this very early stage of research is not adequate.-Calculation of propagation behaviour may be possible with rainfall of known intensity and drop-size distribution; as an opposite example, effects of hail cannot be estimated easily, depending, for instance, on a water film around an ice nucleus.

As a new item, H.J.Albrecht referred to P.Halley's comments on lightning modification or on the artificial initiation of lightning by a wire connection with ground. Apart from supporting P.Halley in the view that it was unfortunate not to have a contribution

describing recent and detailed results obtained in this field in France, he pointed out that basic experiments were first performed several years ago in the United States. He then suggested what he described as a possible speculation at this juncture, namely that under certain conditions the capability of initiating lightning artificially could have an extremely important bearing on communications and that one of the conditions would be of more meteorological nature inasmuch as the question whether or how reproducible such modification could be. If the artificial initiation of lightning out of a thunder-cloud would mean that the same thunder-cloud would not be able to produce lightning for a certain period to follow this initiation, this capability might well mean that a relatively lightning-free period would follow and that this period would be under relative control. This, however, would then lead to relatively low noise levels in that period which could yield a higher signal-to-noise ratio on communication links. He emphasized that such a development would certainly be of interest in communication work and could be considered a great advance. Meteorologists present were invited to particularly comment on this possibility. E. Kleinjung remarked that the seeding of volumes below thunder-clouds by means of chaff material had led to corona discharges at the ends of chaff fibres - followed by marked decrease in lightning activity - and that this was in fact similar to the experiments of rockets with a wire connection to ground. It was mentioned that present knowledge cannot be considered adequate and that investigations have not been made with this possibility in mind. W.Attmannspacher drew attention to experiments planned to take place at Hohenpeissenberg in Germany with an artificial initiation of lightning by the Hochspannungslaboratorium of the Technical University of Munich. J. Belrose (Canada) mentioned that the only objective of lightning initiation which, in his opinion, was first achieved some fifteen years ago in the United States (by Williamson ?) , was, in the past, a measurement of the resulting waveform at the bottom end of the wire, in connection with propagation studies on these VLF waves.

J. Belrose then went on to mention two aspects which had not been covered in this session so far. In particular, he referred to a possible contamination of the environment and to experiments of influencing a tropospheric volume by sound waves and thus causing pressure-perturbation modification. No contamination is connected to the latter changes; the modification is effective when the modifying equipment is switched on and disappears when the modifying transmitter is switched off. G. Hänel replied that contamination by cloud seeding does not present any problem whatsoever, because of the minute amount of material used. With reference to J. Belrose's second comment, meteorologists were asked to comment on this rather important topic and on such experiments. H. Jeske described briefly methods of measuring tropospheric parameters by means of acoustic radar and also by a combination of this with electromagnetic radar equipment (radio-acoustic-sounding-system); he said that this work is continuing. H.J.Albrecht expressed hope that details of modification experiments by acoustic means would come forward at an appropriate time.

The discussion was then led to chaff-produced scatter propagation and appropriate models. G.Tacconi referred to the usefulness of a detailed mathematical description of the communication behaviour of such links. E. Lampert commented on appropriate possibilities existing in principle.

In conclusion, the discussion may be summarized as a very successful exchange of results presently available in the various disciplines connected with the subject of artificially modifying non-ionized media, here mainly represented by the earth's troposphere. Scientific research in this field being in the beginning stage and this meeting being the first one actually addressing anthropogeneous changes to the troposphere as a propagation medium, the round-table discussion contributed considerably to the recognition of the state of the art as well as of the predominant direction of progress. This, and the relevant suggestions for the most promising areas of research, as well as the establishment of interdisciplinary contact are the general results, actual stimulation of projects, such as propagation-oriented modification of precipitation characteristics, fog dispersal, etc., the more detailed ones.

SESSION II

MODIFICATION OF IONIZED MEDIA BY EM WAVES

IONOSPHERIC MODIFICATION INDUCED BY HIGH-POWER H F TRANSMITTERS - POTENTIAL FOR COMMUNICATION AND PLASMA PHYSICS RESEARCH

W. F. Utlaut
Office of Telecommunications
Institute for Telecommunication Sciences
Boulder, Colorado 80302
U.S.A.

SUMMARY

High-power, HF, ground-based radio transmitters have been used to intentionally modify the electron temperature and density in the ionosphere since 1970. Transmitting facilities having power-aperture products of the order of 10^4 MWm^2 have been used, and they provide a power density in the F region of a few tens of microwatts per square meter. One transmitter facility, known as Platteville, is located near Boulder, Colorado. The observations reported here were obtained using this facility which used an 18 dBi gain ring array antenna fed with as much as 2 MW, average power, to produce the ionospheric modification. Many unanticipated physical phenomena have been observed and new understanding has been gained in plasma physics because of this ability to carry out experiments on the ionosphere. Perhaps more importantly, however, it has been shown that the modified region acts as a significant radio scatterer to radio frequencies at least as high as UHF. Thus, it has been possible to demonstrate a potential usefulness of ionospheric modification for telecommunication purposes. Voice, teletype, and facsimile transmissions have been sent, via the scattering region above the modifier, between ground terminals separated by several thousands of kilometers and using frequencies which would not otherwise have been useful for those paths. Surprisingly, it has also been shown that ionospheric modification and a significantly large scatterer in the ionosphere can be produced with relatively low power and simple antennas -- a few hundred kilowatts and dipole antennas, for example.

The basis for heating and modifying the F region of the ionosphere is that very strong absorption of a radio wave occurs in a region in which the radio frequency is near the local electron plasma frequency. The plasma frequency f_N is given by

$$f_N^2 = \frac{Ne^2}{4\pi^2 \varepsilon_o m} \tag{1}$$

where N, e, and m are, respectively, the number density, charge, and mass of the electrons, and ε_o is the permittivity of free space. The absorption occurs when the electron collides with a heavy particle; energy is extracted from the radio wave and added to the random thermal energy of the electron. The rate at which energy is absorbed by electrons, in the F region where the plasma and operating frequencies are much greater than the collision frequency, is, approximately,

$$Q = \frac{1}{2} \frac{Ne^2 \nu}{m \omega^2} E_o^2 \tag{2}$$

In equation (2), ω is the angular frequency of the radio wave, ν is the collision frequency of the electrons and E_o is the maximum value of the radio wave electric field.

As the electrons become hotter, they lose only a small part of their excess energy to ions upon collision because the electron mass is so much smaller than the ion mass. The rate at which electrons lose energy to heavy particles by collisions is given by

$$L_\nu = \frac{3}{2} N \delta \nu K (T_e - T_o) \tag{3}$$

where T_e and T_o are the temperatures of electrons and heavy particles and K is Boltzmann's constant. The quantity δ is the mean fractional loss of excess energy per collision, and for elastic collisions it is equal to $2m_e/m_i$, assuming that most of the collisions are with ions. If the collision frequency in the F region is taken to be of the order of 10^3, and the ions are assumed to be 0^+, the relaxation time $(\delta\nu)^{-1}$ is of the order of 10 seconds. Thus, because the heating radio wave spends a relatively long time in the region when ω is near f_N, as a result of its lowered group velocity, and because of the relatively long time-constant of 10 s for electron cooling, appreciable heating of electrons is possible. Such heating is described as being caused by ohmic dissipation, or as deviative absorption. As electron temperature increases, the plasma pressure increases, and the plasma expands along the

earth's magnetic field lines. Electrons are constrained to spiral along magnetic field lines and thus can diffuse, and heat can be conducted more readily along these lines than across them.

Two other factors have important bearing upon the amount of heat the radio wave emanating from the earth's surface will deposit in the F region. One is the effect the lower ionosphere has on a wave as it passes through; the other is the effect the earth's magnetic field has upon wave propagation. The major loss of heating wave energy in the underlying ionosphere occurs in the daytime in the D region, between 60 and 90 km. Although in this region electron densities are relatively low, collision frequencies are high, and a significant amount of nondeviative absorption occurs. In the normal daytime ionosphere, radio frequencies used for ionospheric modification might be expected to suffer of the order of 3 dB attenuation in passing through the lower ionosphere. Additional attenuation in the D region of a few decibels is also caused by the high power heating wave itself, because of the heating and subsequent increase in collision frequency it causes. One consequence of this modification of the D region is that strong cross-modulation may be imposed upon other radio waves passing through that region. The second factor is the influence of the earth's magnetic field. Because of the existence of the geomagnetic field, the ionosphere is a doubly refractive magnetoionic medium. When a radio wave enters the ionosphere there are two modes by which it propagates, one in which the electric vector rotates clockwise (ordinary, or o-mode) and the other counter-clockwise (extraordinary, or x-mode). The two modes have different velocities of propagation, traverse different paths in the ionosphere, and cause quite different modification effects in the ionosphere. Our experience has shown that the o-mode produced the more significant effects for telecommunication purposes, and the major results of scattering discussed below were obtained with the heating transmitter producing o-mode excitation.

Radio waves intense enough to appreciably modify the energy balance through ohmic heating can, in addition, set off parametric decay instabilities. A parametric instability is a periodic modulation of some parameter of an oscillating system at such a frequency and with sufficient amplitude that the oscillations become unstable. In the ionosphere, the additional absorption of energy due to excitation of parametric instabilities, termed "anomolous" because of the nonlinear dependence of dissipation on RF power density, creates an intense turbulent plasma wave spectrum. One important consequence of this is the production of short-scale ($\sim$ 3 meter) field-aligned plasma density fluctuations, which is a source of some of the higher frequency scattering that is observed.

Much of the impetus for improving theoretical understanding of the basis of ionospheric modification came from several completely unanticipated experimental results. The first salient unexpected result, when experimentation began near Boulder, Colorado, was the production of spread F. This suggested the possibility that field-aligned structure in the ionosphere would exist. Thus, HF through UHF monostatic and bistatic radio observations, at different ground locations and from aircraft, and spaced receiver measurements of satellite signals which passed through the modified region were made. The results from these observations showed that the modified region provided a large radar cross section, ranging from as high as 10^{9} m^{2} at HF to 10^{4}m^{2} at UHF.

Three different kinds of scattering are observed from the F region. One, in which the received signal is virtually unchanged from that transmitted, is believed to result from specular scatter from electron density structure aligned with the earth's magnetic field. This scatter has been termed field-aligned scatter (FAS). The second kind results in two received signals, one being shifted upward and the other downward from that transmitted by an amount nearly equal to the frequency used for modifying the ionosphere (a frequency ranging from about 0.5 to 1.0 of the maximum plasma frequency in the ionosphere). These shifted signals are believed to result from plasma oscillations propagating very nearly along the earth's magnetic field lines. The scattering phenomenon resulting in the shifted frequency signals has been termed plasma-line scatter (PLS). The two scattering modes are observed to have dissimilar characteristics. Field-aligned scattering is highly aspect sensitive with respect to the direction of the geomagnetic field; PLS is found to be much less aspect sensitive. The region of strongest scatter for the FAS mode is found to occur in the modified region where the radar line-of-sight is perpendicular to the geomagnetic field, and is independent of the height at which the modifier frequency matches the plasma frequency in the ionosphere. However, the scattered signal intensity is maximized when the perpendicularity locus and the frequency matching height nearly correspond and becomes smaller as the distance between them increases. For the PLS the maximum back-scattering signal occurs at the altitude of maximum heating, which occurs at the height where the ionospheric plasma frequency equals the heater frequency. Variation in scattering cross-section with probing frequency also differs for the two scattering modes; the FAS cross-section is greater at VHF than at UHF, whereas the PLS cross-section is greater at UHF than at VHF. The third kind of scattering is believed to be Bragg scattering from ion-acoustic waves, which propagate nearly along the earth's magnetic field lines, and has been termed ion-acoustic scatter (IAS). The received signal in this case is very nearly equal to that transmitted, differing only by a few kilohertz in accordance with ion-acoustic frequencies. Fewer observations have been made of the IAS and less is known about its characteristics than for FAS and PLS.

Strong FAS has also been observed to come from the E region of the ionosphere, at about 110 km altitude, when frequencies appropriate to the lower plasma frequencies existing there are used for modification. From a limited amount of data, the E-region FAS seems to have a large radar cross section over a greater range of frequencies than that found for F-region FAS. The degree of aspect sensitivity of the E-region FAS has not been measured. It is possible that it is less aspect sensitive than the F-region FAS since it is likely that irregularities are produced in a limited-height region. Thus the irregularities should not be as elongated as in the F region, where the great length along the field contributes to the high degree of aspect sensitivity.

A theoretical model to describe the modified ionosphere above Platteville, and the FAS which it makes possible, has been developed based on the radar and transmission measurements discussed above. The physical model of the disturbance generated above Platteville is a volume containing small electron density fluctuations in a diffuse region centered above the heater at a height where the heater frequency equals the local ionospheric plasma frequency. The strength of irregularities falls off above and below this altitude with a Gaussian scale length of 7.5 km (15 km between 1/e points). The horizontal dimensions of the volume are set by the width of the heater beam which is of the order of 1/3 radian, or 100 km in diameter near the altitude of 300 km. In essence, the volume is a pancake-shaped region with diffuse boundaries, located at the reflection height defined by the heater frequency and filled with field-aligned electron density irregularities. The rms intensity of the electron density fluctuations at the center of the disturbed volume is 1 to 1.5 percent, when full heater power is used.

Using the information gained from the various diagnostic experiments and the scattering model, communication experiments were planned and executed. Signal transmission statistics were collected and various communication messages were relayed by the scattering region created over Colorado, at all hours throughout a day. The observations demonstrated that it is possible to operate VHF communication circuits, using conventional modulation techniques, antennas and transmitters, over paths several thousand kilometers in length by way of scattering from the field-aligned, heater-induced irregularities at any time of day. The circuit must have the proper geometry, because of the scattering aspect sensitivity, and the frequency of the heating transmitter must be adjusted to produce intense electron density irregularities at the altitude appropriate for the geometry of the path. The communication zones at the earth's surface that might be established by this phenomenon extend several thousand kilometers in a magnetic east-west direction, but only a few hundred kilometers in north-south directions. Their exact shape depends upon geomagnetic latitude and altitude at which the heating is done, but, typically communications appear to be possible over several million square kilometers of the earth's surface by this phenomena. One problem is that while additional paths for communication circuits may be established using this technique, it is also possible that increased interference, resulting from scattering of VHF or UHF signals into areas where they would not normally be expected to propagate may result from intentional or unintentional ionospheric modification. During the experimental program such interference effects did not cause complaints.

Many effects are produced when the ionosphere is illuminated with sufficient energy and with frequencies matching the plasma frequencies there. Most of the phenomena associated with these effects are not well understood and both theoretical and experimental efforts are required to place these in better perspective. This is particularly true for the changes which are caused in the D and E regions. There are some very pronounced changes observed to occur in the D region when illuminated by the Platteville transmitter, but only preliminary measurements have been made. They do suggest that changes in both electron collision frequency and density occur over an extended height range and, in addition, the chemistry and reaction rates in the D and E region may be modified from what normally exists.

Scattering cross sections at various frequencies have only been measured at the one geomagnetic latitude above Colorado. It is desirable to determine the variation of ionospheric modification with geographic location, altitude, radiated power, and elevation angle; and what are the adverse or constructive consequences to other telecommunication signals encountering the modified regions.

For those desiring greater details about the various phenomena mentioned above two publications, and the references contained therein, may be useful. These are: (a) Radio Science, Vol. 9, No. 11, Nov. 1974 (special issue on ionospheric modification) and (b) Proceedings of the IEEE, Vol. 63, No. 7, 1022-1043, July 1975.

DISCUSSION

H. Soicher: It was mentioned that the ionospheric effects after transmitter turn-on are instantaneous. How long after transmitter turn-off do the various ionospheric effects disappear ?

W. F. Utlaut: The phenomena leading to the large radar cross-sections, parametric instabilities and plasma waves which are produced, disappear promptly with heater turn-off at VHF and UHF and within tens of seconds at HF. However, spread-F exists for varying amounts of time after turn-off.During the day, spread-F in the F2-region disappears within several minutes while that in the F1-region disappears within a minute. During the evening hours, spread-F persists for tens of minutes after turn-off and has been observed to last for hours when created during the middle of the night, sometimes remaining until sunrise in the ionosphere.

E. Thrane: Which frequencies were you using for your measurements of cross-modulation as a function of heating power ?

W. F. Utlaut: In the slide shown the heater frequency was 7.4 MHz and the cross-modulation was observed on a 60 kHz signal. Cross-modulation measurements have been made of frequencies of 20 and 60 kHz and 2.5 MHz using various heater frequencies.

L.W. Barclay: 1) What heating frequencies were used in the observations of E-region scatter ? ------ 2) How does the rcs, or some other similar parameter, vary with the ratio of heating frequency to f_oF2 ?

W. F. Utlaut: 1) Heater frequencies used for E-region scatter ranged from about 2.7 to 3.5 MHz, frequencies below the E-region maximum plasma frequency.
2) The radar cross-section of the scattering volume in the F-region does not appear to be dependent upon heater frequency as long as that frequency is properly chosen so as to maximize heating at the proper altitude corresponding to that giving specular reflection for the monostatic or bistatic radar path.

THE HEATING EXPERIMENT AT ARECIBO

W. E. Gordon
Rice University
Houston, Texas

H. C. Carlson
Institute for Physical Sciences
University of Texas at Dallas
Richardson, Texas

SUMMARY

The ionized atmosphere over the Arecibo Observatory can be illuminated by HF waves in the frequency range 5-12 MHz with an incident power density of 10^{-3} watts per square meter at the bottom of the ionosphere, resulting in

(a) normal absorption producing fractional changes in electron temperature of a few 10's percent near and just below reflection height for O and X modes, and

(b) anomalous absorption with plasma waves enhanced by a few orders of magnitude when the frequency of the incident wave matches the local plasma frequency. This condition can be achieved for ordinary mode polarization, but the extraordinary wave is reflected in the ionosphere before the matching is achieved. Thus, plasma wave instabilities are excited by O-mode waves only.

This paper describes the Arecibo Observatory experiments and summarizes the results. Muldrew and Showen detail some special features of the results, Minkoff applies the results to communications, and Stubbe and Kopka outline plans for experiments in a new facility.

1. INTRODUCTION

The experimental arrangement includes the "heater" and the diagnostics illustrated in Figure 1. The heater is an United States Department of Commerce 100 kilowatt transmitter connected to the TCI (Technology for Communications International) log periodic feed in the 1000-foot dish. The diagnostics consist of the incoherent scatter radar ionosondes and photometers. The incoherent scatter radar yields electron temperature, ion temperature, electron density and plasma wave intensity in a sample volume as small as 1 km on a side. The ionosondes are located at the Observatory and at Los Caños 10 km north of the Observatory. The photometers are located at the Observatory and observe the airglow at 6300Å.

The current interest in the modification experiments goes back to Platteville where, under the direction of W. F. Utlaut with the support of the Department of Defense, the spectacular observations were begun in 1969. The heating experiments began at Arecibo in 1970 under the direction of the authors with the participation of a large number of scientists from many institutions and with the support of the Department of Defense and more recently the National Science Foundation.

The heating experiments at Arecibo have yielded a number of interesting results derived from the normal absorption of radio waves in the ionosphere (Showen, 1972; Kantor, 1971; Gordon, Showen and Carlson, 1971; Gordon and Carlson, 1974) and from the anomalous absorption of the high frequency (5-10 MHz) waves and the excitation of plasma instabilities (Carlson, Gordon and Showen, 1972; Fejer, 1972; Kantor, 1972; Sipler and Biondi, 1972; Dias and Gordon, 1973; Haslett and Megill, 1974; Kantor, 1974; Gordon and Carlson, 1976). The experiments at Arecibo and at Boulder have stimulated the development of plasma theory (Perkins and Kaw, 1971; Kruer and Valeo, 1973; Kuo and Fejer, 1972: DuBois and Goldman, 1972; Valeo, Oberman and Perkins, 1972; Weinstock and Bezzerides, 1972; Arnush, Fried and Kennel, 1974; Fejer and Graham, 1974; Perkins, Oberman and Valeo, 1974; Weinstock, 1974). Eight theses have been produced on this subject at Rice (Showen, 1969; Kantor, 1971; Dias, 1971; Kantor, 1972; Dias, 1973; Misener, 1974; Showen, 1975; Duncan, 1976) and four theses are planned (Duncan, Ph.D.; Fleisch, M.S., Ph.D.; Djuth, Ph.D.).

2. CONCLUSIONS

Although the anomalous absorption results are more interesting to communicators, note in passing that O-mode heating of the ambient electron temperature is easily measured (Figure 2). Deviative absorption, ray tracing and heat balance calculations are consistent with (1) the magnitude of the increase of electron temperature, typically peaking at 400°K with higher values at night, (2) the location of the heating, typically 4° to 9° north of the Observatory in accord with the refraction of the HF wave, (3) the volume, matched to the HF beam when mapped in two or three dimensions, and (4) the thermal relaxation times of a few tens of seconds. The ion temperature is unchanged within error bars of tens of degrees K.

The anomalous absorption of the HF wave excites plasma lines exhibiting spectral features (decay mode line, growing mode line, image of decay mode line) (Figure 3), which in general can be explained by linear parametric theory. Observation of an additional broad spectral feature has led to an extension of the theory, although the predictions of Perkins that energy would cascade through the spectrum as one excited line acts as a

source for its neighbor has been disproved by Showen who finds that the broad feature forms first and then breaks into a series of spikes (the reverse in time of the prediction). The decay times are consistent with the wave damping theory and offer a new tool for collision frequency and photoelectron studies. The cascading of energy from the enhanced plasma line into neighboring lines was predicted by Perkins. Showen observed with a 2 ms time resolution the development of the enhanced spectral features following the sudden turn-on of the HF transmitter (Figure 4). Earlier observations by Showen with a 20 ms resolution did not resolve the structural development. The present observations provide the detail with which to test Perkins' predictions and Showen (1975) finds that the broad feature forms in the first 2 ms after HF excitation and that it subsequently breaks up into lines contrary to the time sequence predicted. Fluctuations of the plasma line intensities over two orders of magnitude show distribution functions suggesting upper threshold saturation in the ionospheric plasma for higher HF transmitted power levels (Figure 5). Ion component spectra have been measured with frequency resolution that needs to be improved substantially before they contribute significantly to the results (Figure 6 shows the thin slab in which the enhanced ion line is observed.)

Enhanced plasma lines excited by a powerful HF radio wave originate in the sporadic-E layer (Figure 7) when the blanketing frequency exceeds the exciting frequency confirming that the plasma is overdense for the exciting frequency. Around the time when the blanketing frequency falls through the exciting frequency large fluctuations in the plasma line intensities are observed suggesting the possibility of overdense patches drifting through the sampled volume (Figure 8) (Gordon and Carlson, 1976).

An HF enhanced plasma line was observed for the first time on the topside of the ionosphere by Kantor. The enhanced plasma line on the bottomside (200 km altitude) was simultaneously observed. The topside line at about 270 km may have been excited, according to Muldrew, by coupling of the transmitted O-mode into a Z-mode near 180 km, and propagation of the Z-mode from 180 to 270 km where it would be strongly absorbed.

Muldrew (1976) finds enhanced plasma lines simultaneously with and at heights just below the regularly observed enhanced plasma lines. The characteristics of the new lines are quite different from those regularly observed and Muldrew is developing an explanation for them.

Meriwether, Sipler and Wickwar were surprised by the observation of transient suppression of λ6300 airglow when the ionosphere was illuminated by an O-mode HF wave. The usual observation with this illumination is an enhancement in the airglow attributed to the impact excitation by additional electrons above 2 ev generated by the HF wave. The transient suppressions are typical of X-mode illumination of the ionosphere and are attributed to a temperature dependent change in the dissociative recombination coefficient. These processes compete and apparently the conditions of the experiment were sufficiently unusual that the suppression process dominated. This deserves careful examination! Sipler believes that the same thing may have been observed once at Platteville, but it does not seem to have been reported anywhere.

Given the photometer and radar data (and present understanding), there is a separate problem to be examined. It is to gain an understanding of what affects the O-mode enhancements. We have obtained enhancements in May and October 1972, and for the first time this April good cases of little or no enhancement. Radar data is available for electron temperature, ion temperature, electron density and plasma line intensities (both on and off the HF frequency). Additionally, there are two competing theories available to describe the energization of electrons by the HF.

Duncan has observations of the asymmetry in the powers of the upshifted and downshifted plasma lines that he believes will refute Fejer's explanation of this difference being due to the lines originating in different parts of the Airy distribution. The frequency asymmetry in the upshifted and downshifted lines, first observed by Kantor, has been reobserved by Duncan (1976) (Figure 9) who associates it with a high, local diffusion velocity. It appears that the ionosphere is always descending when plasma lines are observed -- rising energetic electrons are being replaced by thermal electrons from above.

3. FUTURE PLANS

The scientific questions to be examined in the future arise from ongoing work and are in two areas, aeronomy and plasma physics. In the area of aeronomy, the observations provide for studies of (1) collisional and other damping mechanisms at various heights and times, (2) thermal processes associated with the loss of the energy given to the electrons by the HF waves, and (3) the temperature dependent reaction rates associated with the airglow in the manner of Biondi, Sipler and Carlson.

In the area of plasma physics the spectral details of the HF excited lines continue to provide challenges. Basic questions of excitation and quenching mechanisms pose difficulties for the experimenters and clues for the theoreticians. The large fluctuations of the line intensities on a wide range of time scales tackled by Showen awaits a full explanation. The critical observations of the enhanced ion line and the enhanced plasma line are yet to be made. The weak, elusive lines tentatively found at a number of frequencies in the spectrum, or at the same frequency but at different heights in the F region, await confirmation and explanation. The enhanced plasma lines observed in blanketing sporadic E open a path for studying the structure of the medium

(electron density gradients) and its response to HF waves by comparing the results in the E region with those in the F region.

We propose to mount one heating experiment this summer using the current arrangements at Arecibo and adding a second frequency of observation in the HF band. It should yield information on scatterers that will be of interest to communicators.

REFERENCES

ARNUSH, D., B. D. FRIED and C. F. KENNEL, 1974, "Parametric Amplification of Propagating Electron Plasma Waves in the Ionosphere," J. Geophys. Res. 79, 1885-1893.

CARLSON, H. C., W. E. GORDON and R. L. SHOWEN, 1972, "High Frequency Enhancements of the Incoherent Scatter Spectrum at Arecibo," J. Geophys. Res. 77, 1242-1250.

DIAS, LUIZ A.V., 1971, "High Frequency Radio Heating of the Ionosphere," M.S. Dissertation, Rice University.

DIAS, LUIZ A.V., 1973, "Observations of Artificially Induced Enhancements in the Ionospheric Backscatter Spectrum, Ph.D. Dissertation, Rice University.

DIAS, L.A.V. and W. E. GORDON, 1973, "The Observation of Electron Cyclotron Lines Enhanced by HF Radio Waves," J. Geophys. Res. 78, 1730-1732.

DuBOIS, D. F. and M. V. GOLDMAN, 1972, "Spectrum and Anomalous Resistivity for the Saturated Parametric Instability," Phys. Rev. Letters 28, 218.

DUNCAN, L. M., 1976, "Enhanced Plasma Wave Spectral Asymmetries," M.S. Dissertation, Rice University.

GORDON, W. E., H. C. CARLSON and R. L. SHOWEN, 1971, "Ionospheric Heating at Arecibo: First Tests," J. Geophys. Res. 76, 7808-7813.

GORDON, W. E. and H. C. CARLSON, 1974, "Arecibo Heating Experiments," Radio Science 9, 1041-1047.

GORDON, W. E. and H. C. CARLSON, 1976, "The Excitation of Plasma Lines in Blanketing Sporadic-E," accepted for publication in J. Geophys. Res.

FEJER, J. A., 1972, "Variability of Plasma-Line Enhancement in Ionosphere Modification Experiments," J. Geophys. Res. 77, 273-275.

FEJER, J. A. and K. N. GRAHAM, 1974, "Electron Acceleration by Parametrically Excited Langmuir Waves," Radio Science 9, 1081-1084.

HASLETT, J. C. and L. R. MEGILL, 1974, "A Model of the Enhanced Airglow Excited by RF Radiation," Radio Science 9, 1005-1019.

KANTOR, I. J., 1971, "Artificial Heating Paradox of the Lower Ionosphere," M.S. Dissertation, Rice University.

KANTOR, I. J., 1972, "Enhanced Plasma Lines Excited by HF Waves," Ph.D. Dissertation, Rice University.

KANTOR, I. J., 1974, "High Frequency Induced Enhancements of the Incoherent Scatter Spectrum at Arecibo, 2," J. Geophys. Res. 79, 199-208.

KRUER, W. L. and E. J. VALEO, 1973, "Nonlinear Evolution of the Decay Instability in a Plasma with Comparable Electron and Ion Temperatures," Phys. Fluids 16, 675-682.

KUO, Y. and J. A. FEJER, 1972, "Spectral Line Structures of Saturated Parametric Instabilities," Phys. Rev. Letters 29, 1667-1670.

MISENER, S. L., 1974, "Induced Heating Effects in an Irregular Ionosphere," M.S. Dissertation, Rice University.

MULDREW, D. B., 1976, "Plasma-Line Observations at Multiple Heights," presented at AGARD Meeting on Artificial Modification of Propagation Media, Brussels, April 1976.

PERKINS, F. W. and P. K. KAW, 1971, "The Role of Plasma Instabilities in Ionospheric Heating by Radio Waves," J. Geophys. Res. 76, 282.

PERKINS, F. W., C. OBERMAN and E. J. VALEO, 1974, "Parametric Instabilities and Ionospheric Modification," J. Geophys. Res. 79, 1478-1496.

SHOWEN, R. L., 1969, "Artificial Heating of the Lower Ionosphere," M.S. Dissertation, Rice University.

SHOWEN, R. L., 1972, "Artificial Heating of the Lower Ionosphere," J. Geophys. Res. 77, 1923-1933.

SHOWEN, R. L., 1975, "Time Variations of HF Induced Plasma Waves," Ph.D. Dissertation, Rice University.

SIPLER, D. P. and M. A. BIONDI, 1972, "Measurements of $O(^1D)$ Quenching Rates in the F Region," J. Geophys. Res. 77, 6202-6212.

VALEO, E., C. OBERMAN and F. W. PERKINS, 1972, "Saturation of the Decay Instability for Comparable Electronic and Ion Temperatures," Phys. Rev. Letters 28, 340-343.

WEINSTOCK, J. and B. BEZZERIDES, 1972, "Nonlinear Saturation of Parametric Instabilities," Phys. Rev. Letters 28, 481.

WEINSTOCK, J., 1974, "Enhanced Airglow, Electron Acceleration, and Parametric Instabilities," Radio Science 9, 1085-1087.

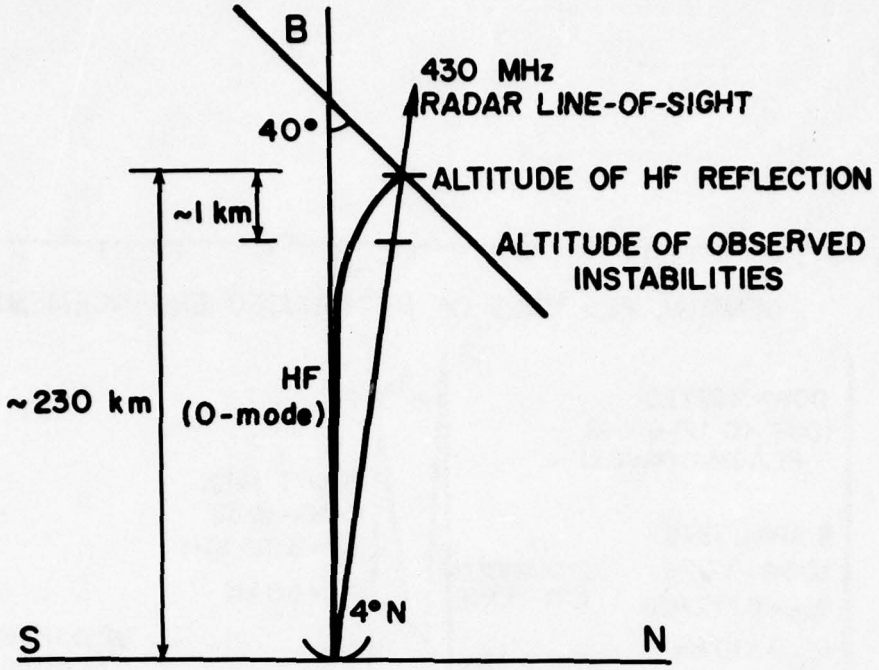

Fig.1. A schematic of the experimental configuration. The incoherent backscatter radar is directed 4° north of vertical, intersecting the center of the modified volume corresponding to an O-mode HF pump. The height below reflection for the observed instabilities is determined by the radar wavelength and the parametric instability frequency matching condition.

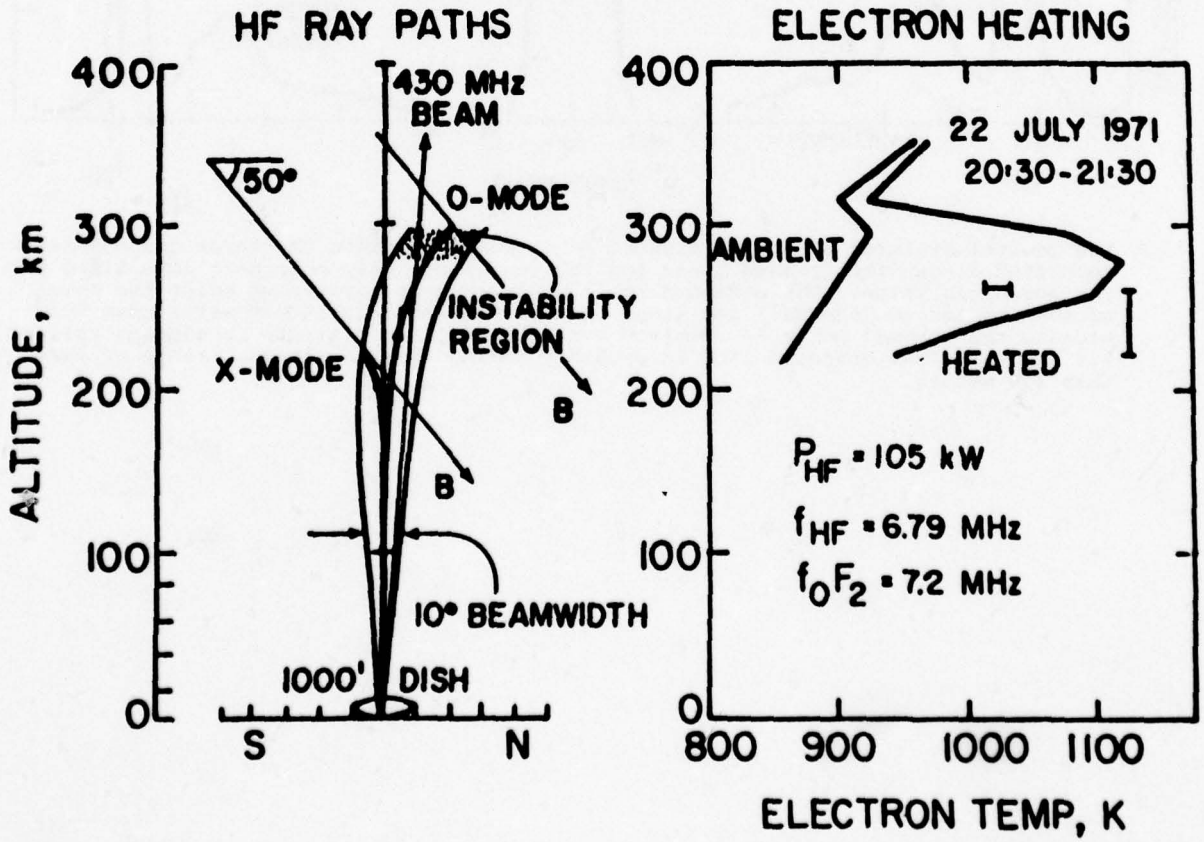

Fig.2. The ray paths for the HF waves and the resulting electron heating.

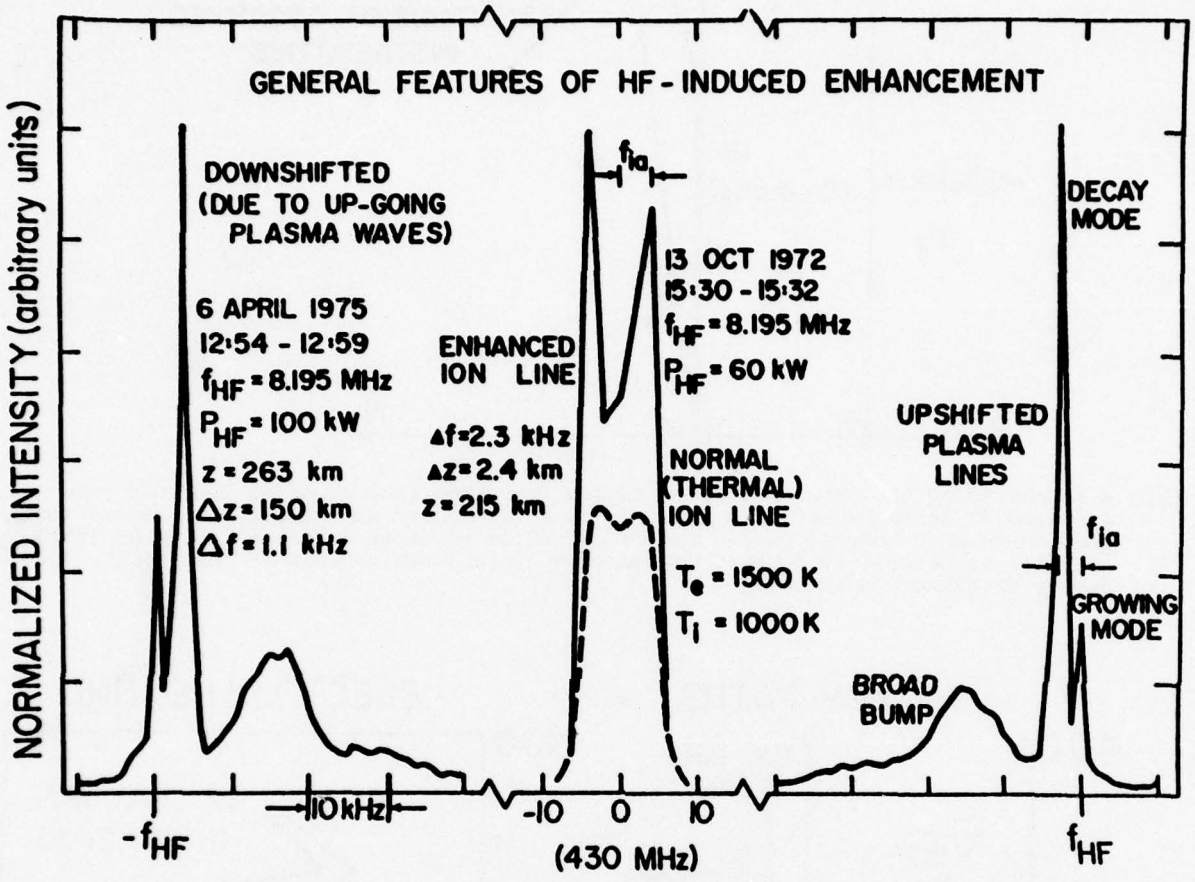

Fig.3. The general features of the HF induced enhancements include the three components -- upshifted/downshifted plasma lines and the ion line. They have been normalized to the same peak value. The enhanced ion line is seen to have about twice the power of the unenhanced (thermal) ion line. The actual ratio is much greater than two because the thermal power is received over the complete altitude resolution cell of 2.4 km, while the enhanced line is probably coming from an altitude range of less than 300 meters.

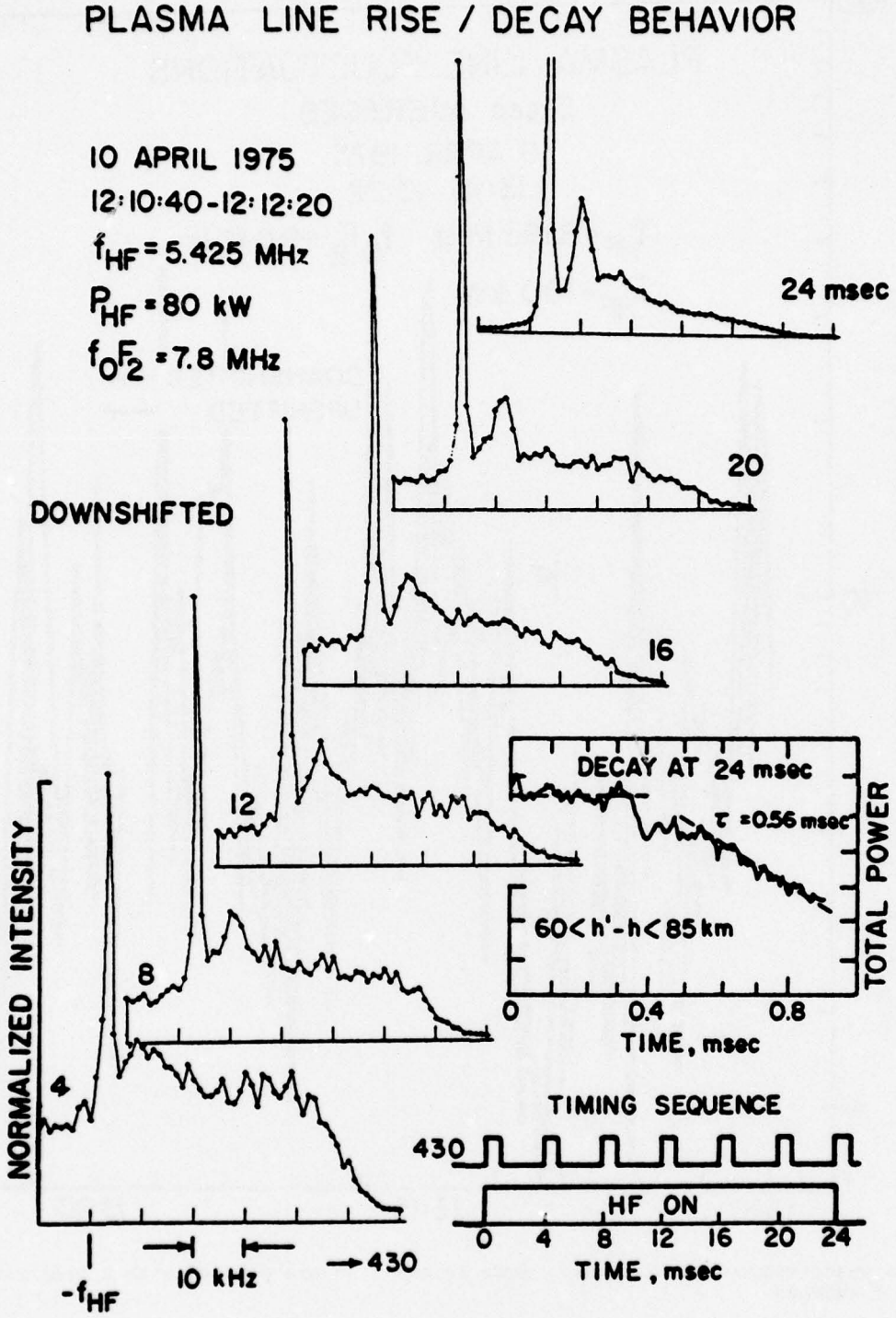

Fig.4. The rise and decay of the plasma line are presented. The time resolution for the rise is 4 milliseconds; for the fall measurement it is 7 μsec. Four milliseconds after HF turn-on the decay peak is seen to be well developed and very narrow. At its side is a broad noise bump. As time progresses through to the last measurement at 24 milliseconds, this broad bump sharpens into a peak. This peak is displaced by about three times the ion acoustic frequency.

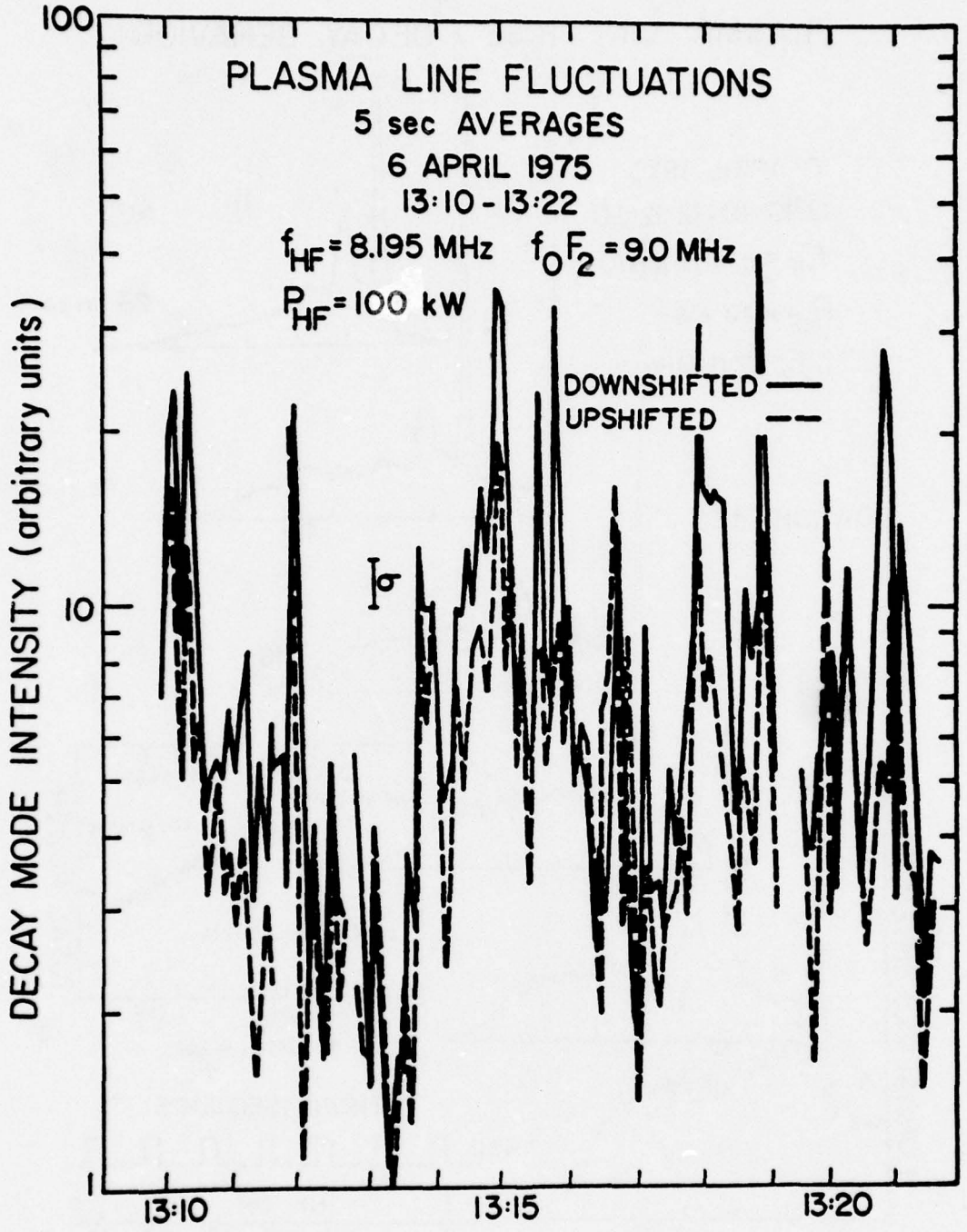

Fig.5. The upshifted/downshifted decay mode intensities are plotted with a time resolution of 5 seconds.

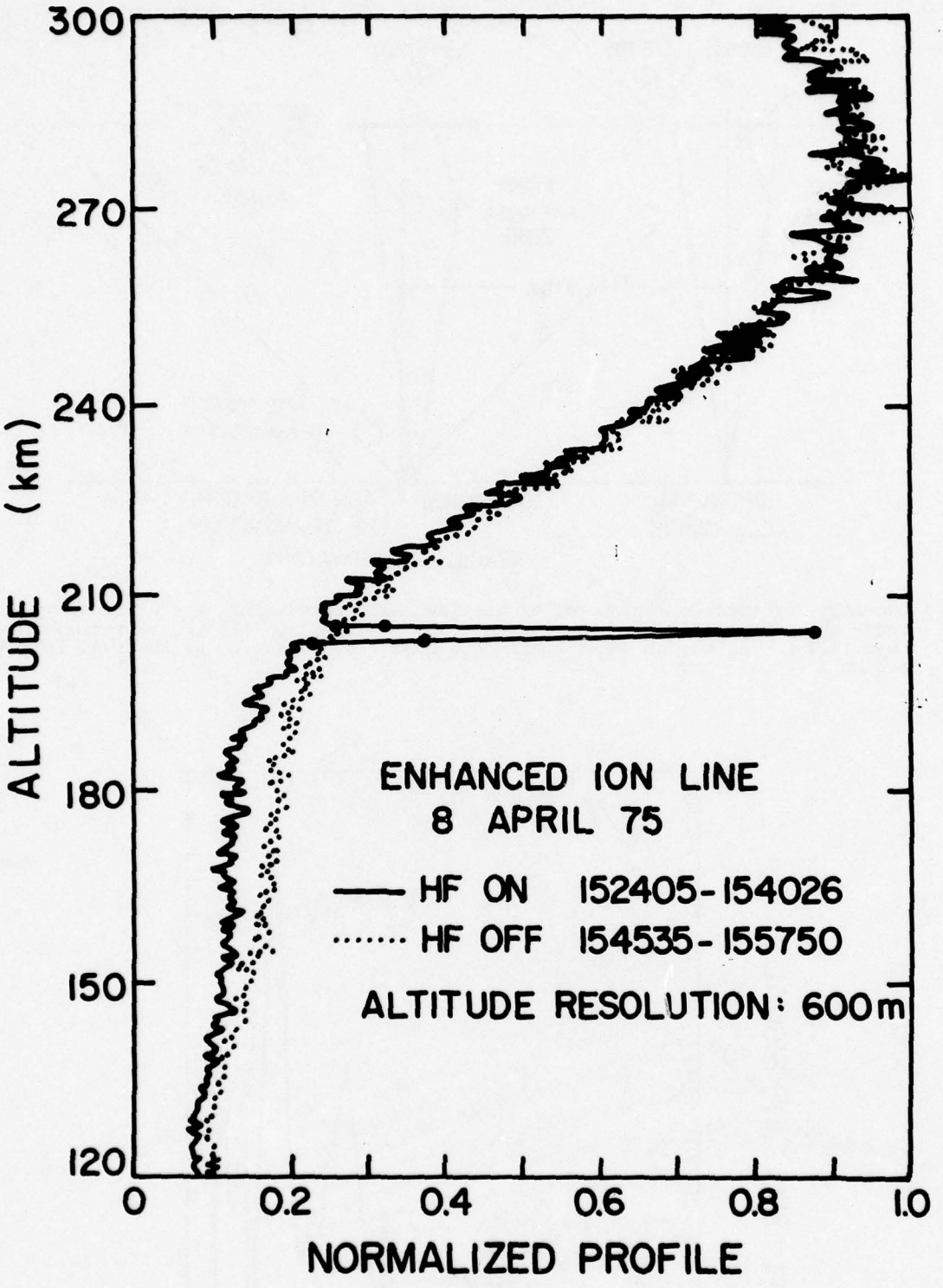

Fig.6. Normalized profile of the ionosphere, including the enhanced ion line for the HF ON cycle. The observable instability is shown to come from a narrow altitude range.

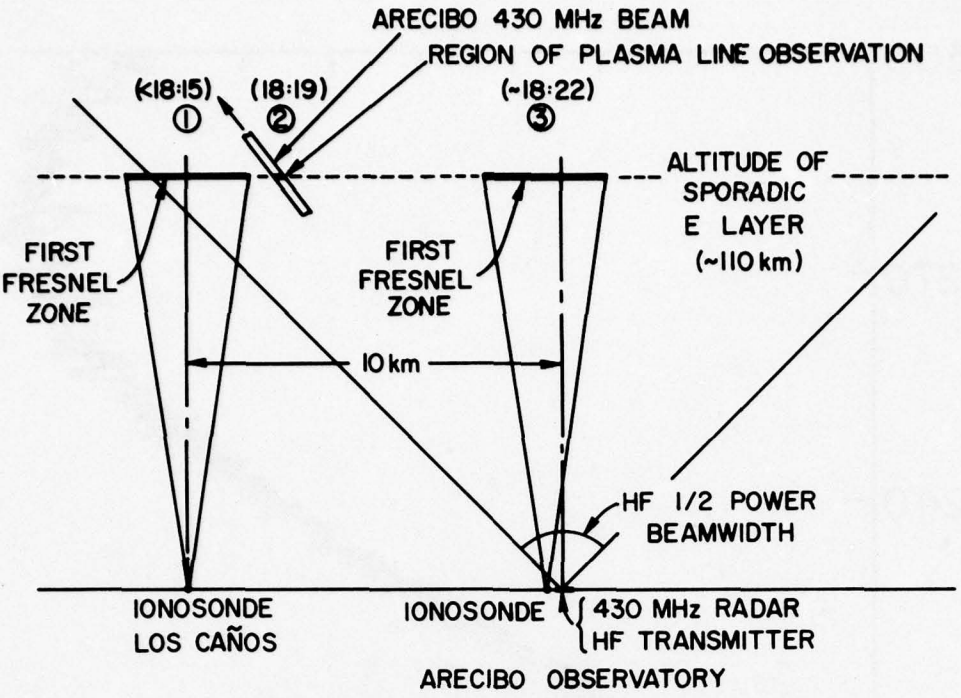

Fig.7. Geometry for Arecibo regions of HF heating and observations by 430 MHz diagnostic radar and two ionosondes. E_{sb} ceases to be observed by 1815 AST at region 1, and near 1822 AST at region 3; HF enhanced plasma lines cease to be observed from region 2 at 1819 AST.

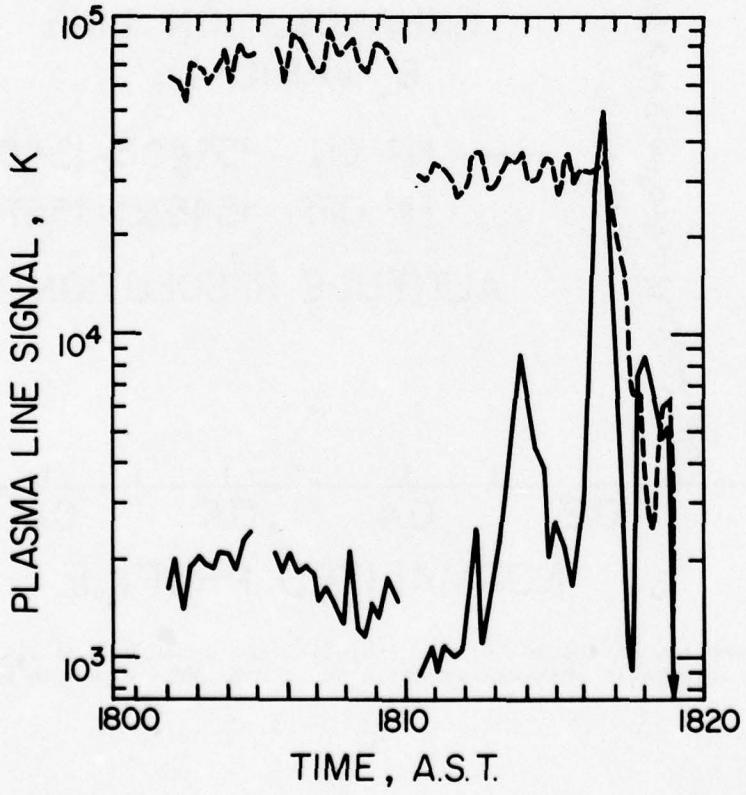

Fig.8. Peak plasma line signal into a 2.2 kHz band. The normal photoelectron enhanced E-region plasma line intensity is of order 10°K. Dashed curve is the upshifted line, full curve the downshifted line.

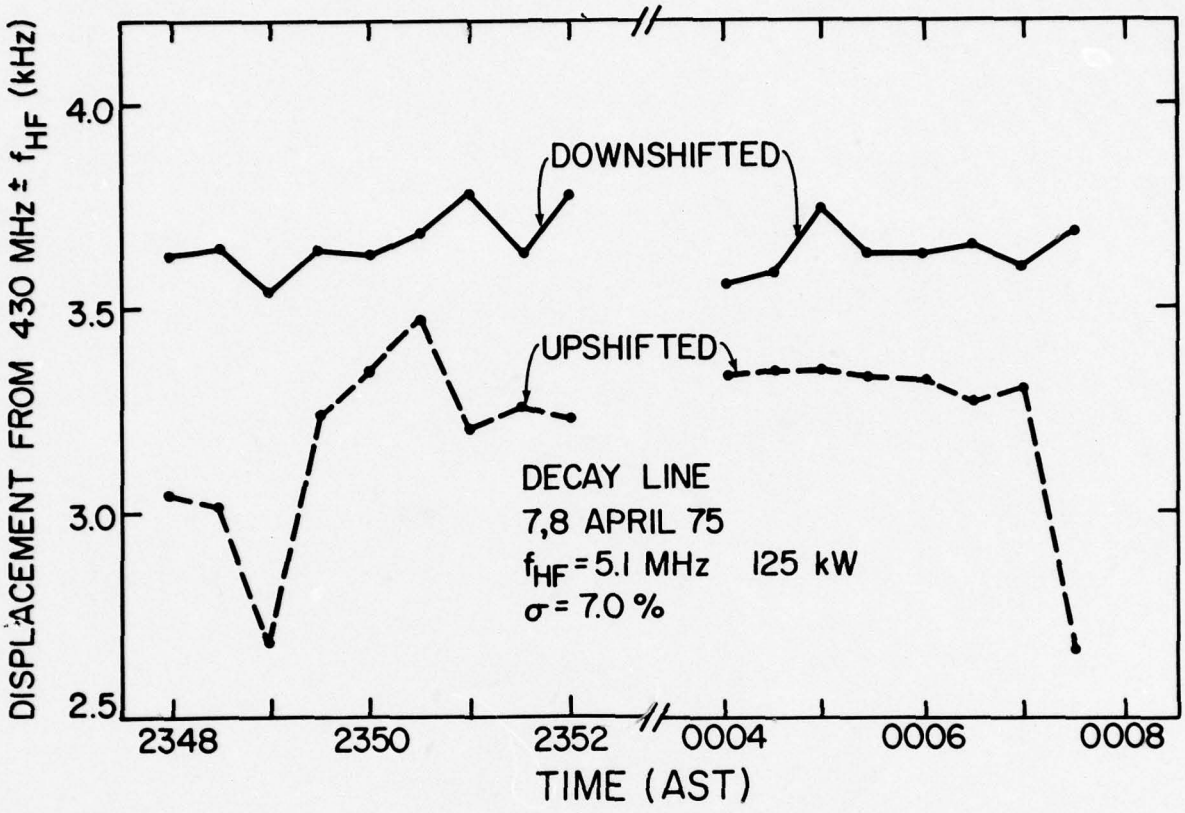

Fig.9. Experimental data illustrating the frequency asymmetry between upshifted and downshifted plasma lines corresponding to the decay instability. The frequency is measured from 430 MHz ± the HF frequency, displaced toward the radar frequency.

A REVIEW OF VHF/UHF SCATTERING FROM A HEATED IONOSPHERIC VOLUME

J. Minkoff and I. Weissman

80 West End Avenue, New York, New York 10023, USA

ABSTRACT

It is observed that an ionospheric volume in the F-layer subjected to high-power HF illumination becomes an effective scattering medium for radio signals in the VHF/UHF-frequency range. The experimental results are representative of a field-aligned scattering geometry for which the first such observations of VHF/UHF scattering from a heated ionospheric volume are presented. Two distinct and markedly dissimilar scattering modes are observed: center-line and plasma-line scattering. Center-line scattering is observed at the transmitted radar frequency f; plasma-line scattering is observed as a pair of sidebands at $f \pm f_h$ where f_h is the heater frequency. Center-line scattering is highly aspect sensitive with respect to the direction of the geomagnetic field, $\vec{B}$; plasma-line scattering is found to be much less aspect sensitive, if at all. By means of bistatic measurements it is determined that center-line scattering takes place from field-aligned irregularities. The longitudinal scale size of the irregularities, L, is found to be greater than the maximum antenna diameter, 85'. Because of fundamental limitations imposed by the spatical-resolution capability of the measurement system no more exact estimate for L is possible. A striking reversal in frequency-dependence is found between the center-line and plasma-line modes. The per-unit-volume center-line backscatter cross-section is found to be ~7 dB greater at VHF than at UHF; the per-unit-volume plasma-line backscatter cross section is found to be at least 11 dB less at VHF than at UHF. For both modes the scattering cross section is found to be effectively turned on and off very rapidly in response to the heater excitation. The spectra of the scattered signals, for both modes, are found to be quite complex, consisting of both narrow-band and wide-band components. Narrow spectral peaks having 3-dB widths of the order of tens of Hertz are often observed superimposed on a wide-band component essentially flat over the 100-Hz unambigous frequency interval corresponding to the 0.01-sec interpulse spacing. The spatial configuration of the heated volume is investigated; significant differences are observed depending on whether f_h/f_0F_2 is greater or less than unity.

INTRODUCTION

This paper presents a review of results of VHF/UHF scattering from a heated ionospheric volume in the F-layer over Platteville, Colorado. The ionospheric heating, by means of a high-power HF illumination was carried out by the Institute of Telecommunications Sciences under the direction of Dr. W. F. Utlaut. These results, as well as a large number of other results at optical as well as radio frequencies, are contained in a special issue of Radio Science, Vol. 11, November 1974. The reader is referred to this issue for details not covered below.

SCATTERING MODES

All experimental results presented here were obtained using radars located at the White Sands Missile Range (WSMR) for which the relevant radar parameters are presented in Fig. 1. The experimental geometry was ideal for field-aligned scattering measurements. For these results, with a 15-deg elevation angle, the radar line-of-sight intersected the magnetic field at perpendicular incidence at an altitude of ~290 km directly above the heater. As shown in Table I, the experiments were carried out over a period of two years covering all seasons. A-scope presentations of radar echoes under optimum backscatter conditions are presented in Fig. 2. Two very different scattering modes were observed which were denoted as Center-Line Scattering (CLS) and Plasma-Line Scattering (PLS). For CLS the transmitted and received frequencies were the same, aside from small Doppler shifts due to ionospheric drift. For PLS the scattering was observed as a pair of sidebands at $f \pm f_h$ where f_h was the heating frequency. In Fig. 2, it is seen that the received PLS power at VHF was approximately 28 dB greater than the CLS power. At UHF it is seen that the backscattered CLS and PLS power are nominally equal. When the relative sizes of the scattering volumes are taken into account, it is found that for CLS the per-unit-volume VHF scattering cross section exceeds the per-unit-volume UHF scattering cross section by approximately 7 dB. For PLS, however, the per-unit-volume UHF cross section exceeds the per-unit-volume VHF scattering cross section by at least 11 dB. Thus, it was determined that, in this frequency range, the scattering properties of heated volume exhibit a reversal in frequency dependence between CLS and PLS. That is, in this frequency range the CLS cross section decreases with increasing frequency, whereas the PLS cross section increases with increasing frequency (Minkoff et al., 1974a).

ASPECT SENSITIVITY

VHF/UHF CLS was first observed in June 1971 with the RAM radar. One of the first things we wanted to determine was the location of the scattering region. Originally it was expected that, because of Landau damping considerations, the scattering region would be a very narrow horizontal layer located at the altitude where f_h was equal to the local plasma frequency f_p. To determine the location of the scattering region an elevation scan experiment was carried out. In this experiment, for a fixed azimuth, the scattering location was determined as a function of range and elevation angle. The result of such an experiment at UHF is shown in Fig. 3 in a Range Time Intensity (RTI) presentation. It is seen that the locus of maximum scattering does not fall along the line which defines the horizontal scattering layer. Instead it is coincident with the locus of points where the radar line-of-sight intersects the magnetic field at perpendicular incidence, which is referred to here as the perpendicularity contour, $C_\perp$. This was determined by plotting the locus of maximum scattering as shown in Fig. 4 and, under the crude assumption that the magnetic dip angle was constant across the heated volume, calculating the angles between the line-of-sight and the magnetic field over the locus of maximum scattering. It is seen that the difference from perpendicularity between the line-of-sight and the magnetic field, $\hat{B}$, is very small across the entire scattering region, with the small differences easily within the error made by the assumption of a constant dip angle. This experiment was carried out numerous times always with the same results. It was further determined that this is a special case of a more general situation in which the CLS signals are effectively specularly reflected off the magnetic field lines. Thus, for CLS, it was determined that maximum scattering was always determined by the geometry relative to $\hat{B}$ independent of the heating altitude h_f. Although maximum backscatter was observed when the heating took place at the point where perpendicularity to the magnetic field was achieved (where $h_f \sim 290$ km), for heating below the perpendicular point (say $h_f = 260$ km) the backscatter was nevertheless maximized when the radar line-of-sight satisfied the perpendicularity criterion, and not when the line-of-sight was directed at the altitude h_f. Backscatter was observed for h_f values as small as 255 km. Thus, the heating effects were found to be spread out over at least 50 or 60 km, and not confined to a narrow layer as originally believed.

PLS was first observed at RAM in January 1972, and similar experiments were carried out. Results of sequential elevation scans between upper and lower PLS and CLS are shown in Fig. 5 in an RTI presentation. Although the regions are similar in appearance they have different slopes. The locations of maximum scattering corresponding to the RTIs are shown in Fig. 6. The CLS region is coincident with the perpendicularity contour, as before, but PLS is not. The PLS, in fact, is maximum where the maximum heating takes place, in this case at 290 km. The droop of the scattering region to the north for PLS was observed consistently. A more extreme case is shown in Fig. 7. For $h_f \sim 200$ km, PLS is observed at approximately 200 km; for h_f 240 km the scattering is observed at ~240 km. In both cases the northward droop is observed. It is seen that for these large angles-of-incidence to $\hat{B}$ (~ 5-6 deg) no CLS is observed. For PLS, it was found that maximum backscatter was always determined by the altitude of maximum heating effects independent of the geometry relative to $\hat{B}$. Thus, PLS was determined to be much less aspect-sensitive than CLS. Whether or not PLS is in fact aspect-sensitive at all, and if so to what extent, was not determined by these experiments. We note that since PLS was always nominally at the altitude where the heating frequency was equal to the local plasma frequency, PLS can be equivalently described as a pair of sidebands at $f \pm f_p$.

TIME-DEPENDENT BEHAVIOR

The only significant similarity observed between PLS and CLS was in their time-dependent behavior. In both cases the scattering was found to be turned on and off very rapidly in response to turn-on and turn-off of the heater. A qualitative result is presented in Fig. 8. This figure shows a CLS RTI in response to various square-wave modulations of the heater power. A more quantitative result of a measurement of decay and rise time of the scattering in response to sudden heater turn-off and turn-on is shown in Fig. 9. Prior to turn-off the heater was operating CW for a time period of the order of minutes during which strong backscatter (i.e., ~ 40 dB SNR) was being received. The data consisted of digital samples, and the reduction procedure employed a form of spatial averaging in which, for each received echo, the largest value of signal amplitude over five range cells located in the center of the echo was selected. The results were plotted vs time, and a least-square fit was made which is presented in the figure.

The overall response is seen to be complicated, especially in the regions immediately after turn-off and at turn-on. For a rather long period of 27.5 sec, however, the least-square estimate of the rate of change of received power is seen to be a perfect fit to an exponential in time. Because of this it is of interest to interpret this decay in terms of a diffusion model, since a function of the form $n(x,t) = A_e^{-t/\tau} \sin k_s x$ satisfies the diffusion equation:

$$\frac{\partial n}{\partial t} = D \frac{\partial^2 n}{\partial x^2} \qquad (1)$$

where $\tau = 1/k_s^2 D$. The interpretation in this case is that, for backscatter, the radar signal selects that spatial Fourier component of the electron-density fluctuations whose wavelength is one-half the transmitted radar wavelength. The amplitude, A, in the well-known analogy to Bragg scattering, is proportional to the spatial frequency spectrum of

electron-density fluctuations in a plane perpendicular to $\vec{B}$ evaluated at $k_s = 2k = 4\pi/\lambda$, where λ = radar wavelength. Under this interpretation of the data, the signal decays as if this Fourier component of the electron-density fluctuations smoothed out by process of diffusion in planes normal to $\vec{B}$ with a diffusion constant, D, equal to 3 cm^2/sec, where D is determined from the straight-line portion of the curve as shown. We also note that this model predicts a decay time constant which goes as λ^2. This interpretation is in qualitative agreement with the trend which has been observed throughout these experiments. That is, it has been found consistently that the observed rate of decay is greater for scattering at greater radar wavelengths.

The CLS and PLS spectra were also observed to be quite similar. As discussed in detail in Minkoff and Kreppel (1976), for both modes there were essentially three categories: (1) narrow band ($\sim$10 Hz spectral width); (2) wideband (at least as wide as the 100-Hz unambiguous interval corresponding to the 10^{-2} sec interpulse spacing in the transmitted waveform); (3) composite structure, consisting of a narrow-band peak superimposed on a flat wideband component. As discussed in the above quoted reference, these spectral characteristics and the scattering geometry indicate that the mechanism responsible for these PLS results are different from that responsible for the plasma-line scattering observed at the Aerocibo Ionospheric Observatory (Gordon and Carlson, 1974).

Examples of spectra at VHF only are presented in Figs. 10 and 11. These figures show average periodograms representing a total observation time of 2.5 sec each. The spectra are representative of the scattering from separate independent range cells separated by $\sim$4.5 km (corresponding to the 30-μsec transmitted VHF pulse). A spectral broadening with range is seen in Fig. 10a. In general, it was found that the scattering was most narrow band at the southern periphery of the heated volume, although not to the same marked degree as that shown in 10a.

PROPERTIES OF THE HEATED VOLUME

Because of the narrow beamwidths, the WSMR radars were useful for studying the characteristics of the heated volume. Significant differences were observed depending on whether f_h/f_oF_2 was greater than or less than unity. For f_h/f_0F_2 less than one, the heated volume was confined essentially to the heater beamwidth. However, for f_h/f_0F_2 greater than one many differences were observed. In particular, when the heater frequency exceeded f_0F_2 penetration effects were observed. An example is shown in Fig. 12. This figure presents an RTI during an azimuth scan with fixed elevation angle. The time intermittencies shown are the result of an on-off heater modulation and do not bear on this discussion. The heated volume is observed to resemble a doughnut with penetration, and therefore reduced heating effects, taking place in the center directly over the heater. At this time the heater frequency just exceeded f_0F_2, the penetration took place directly above the heater, and the scattering was very weak. At the periphery of the heated volume, however, because of the secant factor, penetration did not take place and backscatter was observed. In addition, for $f_h > f_0F_2$ the heated volume was observed to become significantly spread out in an east-west direction. An example is shown in Fig. 13. It is interesting to note that, in addition to the maximum which takes place at the location of the heater, an additional maximum during the spreading was observed at an angle of 13 deg, which is exactly in the plane of the magnetic meridian. This effect can probably be explained by detailed ray-tracing calculations.

SCATTERING MORPHOLOGY

In order to develop a scattering model of the heated volume, it was necessary to determine whether or not the scattering was taking place from field-aligned irregularities. For this purpose and experiment employing a mobile aircraft-based bistatic receiver was carried out. The basic concept of this experiment is as diagrammed in Fig. 14. For a field-aligned irregularity of length L the scattering in a plane containing $\vec{B}$ is confined to an angle on the order of $\frac{\lambda}{L}$. However, in the perpendicular (east-west) direction the scattering would be greatly spread out in comparison. In this experiment, the aircraft flew on a north-south flight path and measured the extent of the scattering region over the ground. Having located the region, the aircraft then flew to the west to determine the westward extent of the scattering. One such experiment employed 15 and 30 MHz radars operated by the Raytheon Company in addition to the RAM VHF/UHF radar. Figure 15 presents a result at 15 MHz. It is seen that the north-south extent of the scattering region is of the order of 150 km. In the orthogonal direction, however, it is seen that scattering was observed as much as 600 km to the west of the north-south path, at which point the aircraft was forced to turn back because of fuel considerations. A similar result to the east would presumably also have been observed. Thus it was determined that the scattering was taking place from field-aligned irregularities. Good agreement has been obtained between the observed north-south location of the scattering zone and that obtained via ray-tracing calculation (Minkoff et al., 1974b).

SCATTERING CROSS SECTION (CLS)

The per-unit-volume scattering cross section is an interesting quantity both for communications applications as well as for describing the physics of the phenomena. For an underdense plasma, under the Born approximation, Booker (1956) has derived the per-unit-volume differential cross section:

$$\sigma = r_e^2 \overline{|\Delta n|^2}\, S(k_x,k_y,k_z) \tag{2}$$

where r_e is the classical electron radius, $\overline{|\Delta n|^2}$ is the variance of the electron-density fluctuations and $S(k_x,k_y,k_z)$ is the wave-number spectrum of the electron-density fluctuations. For aspect-sensitive scattering we visualize long, thin columns of ionization aligned with $\hat{B}$. In this case, the spectrum can be written separably (Minkoff, 1973) as: $S = S_L S_T$ where the longitudinal and transverse spectra S_L and S_T describe the spatial-frequency content of the electron-density fluctuations parallel and perpendicular to $\hat{B}$, respectively. S_L and S_T are characterized by the longitudinal and transverse coherence lengths, L and T, which are measures of the dimensions parallel and perpendicular to $\hat{B}$ over which collective scattering effects take place. For reasonably small angles-of-incidence, α, to the magnetic field the longitudinal spectrum, which has an angular width λ/L and describes the aspect sensitivity of the scattering, takes the form: $S_L(2k\alpha)$.

The remaining quantities we denote collectively as the backscatter coefficient which, for statistical fluctuations in the electron density axially symmetric with respect to $\hat{B}$, takes the form:

$$b(k) = r_e^2\, \overline{|\Delta n|^2}\, S_T(2k) \tag{3}$$

$b(k)$ is thus a per-unit-volume measure of the magnitude of the Fourier component at $\lambda/2$ of the electron-density fluctuations.

Measurement of S_L is, in general, difficult since it requires excessively high angle resolution (Minkoff, 1973). For these experiments it was only possible to determine that L was greater than the diameter of the RAM antenna, 26 m. Thus, complete specification of the scattering cross section is not possible. It is, however, possible to calculate the received power in terms of $b(k)$ alone, independently of precise knowledge concerning the aspect sensitivity. It can be shown (Minkoff, 1974) that:

$$P_R = \frac{\pi P_T D^3 b(k) \Delta}{8R^2} \tag{4}$$

where P_T and P_R are the transmitted and received power, D the effective antenna diameter, Δ the range resolution cell, and R the range; in this expression beam filling in azimuth is assumed.

A calculation of $b(f)$ ($f = \frac{ck}{c\pi}$, c = speed-of-light) representative of maximum CLS backscatter for these experiments is presented in Fig. 16. (Insufficient data were obtained for similar PLS calculations.) No scattering was ever observed at 1300 MHz. The symbol ⬡ denotes the AMRAD minimum detectable signal which falls just above the extrapolated tail of the curve. In addition to backscatter measurements, $b(k)$ is also useful for calculating received power in bistatic geometries since, for an axial bistatic angle ϕ, ($=\pi$ in backscatter) $b(k)$ takes the form (Minkoff, 1973):

$$b\left(k \sin \frac{|\phi|}{2}\right) = r_e^2 \overline{|\Delta n|^2}\, S_T\left(2k \sin \frac{|\phi|}{2}\right) \tag{5}$$

Thus, the bistatic power for an angle ϕ can be predicted from backscatter measurements by considering an equivalent frequency $f_{eq} = f \sin \frac{|\phi|}{2}$. From the shape of the curve in Fig. 16, it is seen that, for fixed f, the bistatic cross section is larger than the backscatter cross section. This was verified experimentally (Minkoff, 1974).

In addition to calculating scattered power levels, $b(k)$ is also useful for calculating the rms fractional electron-density deviation. This is obtained by making use of the normalization:

$$\int_{-\infty}^{\infty}\int_{-\infty}^{\infty} S_T(k_y,k_z)\,dk_y\,dk_z = (2\pi)^2 \tag{6}$$

which for axial symmetry of S_T becomes:

$$\int_0^{\infty} kS_T(k)\,dk = 2\pi$$

Hence if,

$$m = \int_0^{\infty} kb(k)\,dk \tag{7}$$

then

$$\overline{|\Delta n|^2} = 2m/\pi r_e^2 \tag{8}$$

The calculation of m from Fig. 16 is discussed in Minkoff (1974). A value $m = 2.52 \times 10^{-2}$ is obtained from which $\overline{|\Delta n|^2} = 2 \times 10^{19}\ (el/m^{-3})^2$. The fractional

deviation $\overline{(|\Delta n|^2/n^2)}^{1/2}$ is also of interest. This is dependent on the value chosen for n which, however, can be related to the heater frequency f_h since maximum heating takes place where f_h is equal to the local plasma frequency f_p. Taking 6 MHz as a representative value, for which $n = 4.5 \times 10^{11}$ el m^{-3}, we obtain $\overline{|\Delta n|^2} = 10^{-4}$ for an rms fractional deviation of 1%. Since for all the experimental results presented here the minimum value of f_h was about 5 MHz we obtain the maximum fractional deviation by choosing the corresponding value of n, 3.1×10^{11} el m^{-3}, for which the rms fractional deviation is 1.5%.

Now we note that variations in $|\Delta n|^2$ result in an upward or downward shift in the curve of $b(f)$, the shape presumably remaining the same. This enables upper and lower bounds on $\overline{|\Delta n|^2}$ for these experiments to be easily estimated since a shift by x dB results simply in a change in $\overline{|\Delta n|^2}$ by a factor of $10^{0.x}$. Choosing for x the values ± 5 and + 10 we obtain the dashed curves shown in Fig. 16. The results of this analysis are summarized in Table II. It is seen that, unless S_T takes a sudden unexpected increase below 40 MHz, for these experiments a reasonable upper bound on the rms fractional electron density deviation under the maximum heating conditions is 2.6%, and that values as large as 4% or 5% were probably never achieved.

TABLE I. EFFECTS OF VERTICAL DISPLACEMENT OF $b(f)$ ON VALUES OF $(\overline{|\Delta n|^2})^{1/2}$ and $(\overline{|\Delta n|^2/n^2})^{1/2}$

x (dB)	$(\overline{\lvert\Delta n\rvert^2})^{1/2}$ (el m^{-3})	f_h	$(\overline{\lvert\Delta n\rvert^2/n^2})^{1/2}$ (per cent) f_h = 5 MHz 6 MHz	(max. values)	
10	1.4×10^{10}		3.2	4.6	Too large
5	8.0×10^{9}		1.8	2.6	Upper bound
0	4.5×10^{9}		1.0	1.5	Average value
-5	2.5×10^{9}		0.6	0.8	Lower bound

TABLE II. LIST OF EXPERIMENTS

EXPERIMENT DATES	TRANSMITTING SITES	RECEIVING SITES AND FREQUENCIES
June 1971	RAM DUCK (HF)*	RAM - VHF/UHF AC - VHF/HF
July 1971	RAM	RAM - VHF/UHF
October 1971	RAM	RAM - VHF/UHF
January 1972	RAM	RAM - VHF ($f \pm f_h$)/UHF (includes X-mode observations at VHF)
February 1972	RAM	RAM - VHF ($f \pm f_h$)/UHF ($f \pm f_h$) AC - VHF
April - May 1972	RAM	RAM - VHF ($f \pm f_h$)/UHF ($f \pm f_h$) Santa Fe Site - VHF El Centro Site - VHF AC - VHF
August 1972	RTMS	RTMS - VHF/UHF
December 1972	RTMS	RTMS - VHF
February 1972	RTMS	RTMS - VHF/UHF
September 1973	RTMS	RTMS - VHF/UHF

* DUCK Site 10 miles east of RAM

$f \pm f_h$ denotes plasma-line observation, AC denotes aircraft-based bistatic receivers.

REFERENCES

Booker, H. G. (1956). A theory of scattering by nonisotropic irregularities with application to radar reflections from the aurora, J. Atmos. Terr. Phys., 8, 204-221.

Gordon, W. E. and Carlson, Jr., H. C. (1974), Arecibo heating experiments, Radio Sci., Vol. 9, No. 11, pp. 1041-1047, November 1974.

Minkoff, J., Analysis and interpretation of aspect-dependent ionospheric radar scatter, Journal of Geophysical Research, Vol. 78, 3865, July 1973.

Minkoff, J., Kugelman, P. and Weissman, I., Radio frequency scattering from a heated ionospheric volume, 1, VHF/UHF field-aligned and plasma-line backscatter measurement, Radio Sci., Vol. 9, No. 11, pp. 941-955, November 1974a.

Minkoff, J., Laviola, M., Abrams, S. and Porter D., Radio frequency scattering from a heated ionospheric volume, 2, bistatic measurements, Radio Sci., Vol. 9, No. 11, pp. 757-963, November 1974b.

Minkoff, J., Radio frequency scattering from a heated ionospheric volume, 3, cross-section calculations, Radio Sci., Vol. 9, No. 11, pp. 997-1004, November 1974.

Minkoff, J. and Kreppel R., spectral analysis and step response of RF scatttering from a heated ionospheric volume, Journal of Geophysical Research, June 1, 1976.

Thome, G. D. and Blood, D. W., First observations of RF backscatter from field-aligned irregularities produced by ionospheric heating, Radio Sci., Vol. 9, No. 11, pp. 917-921, 1974.

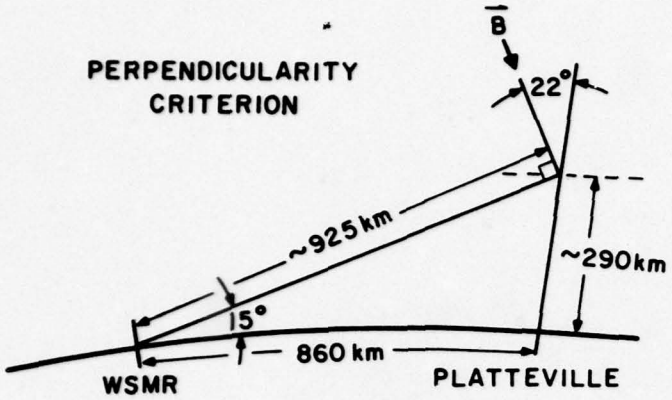

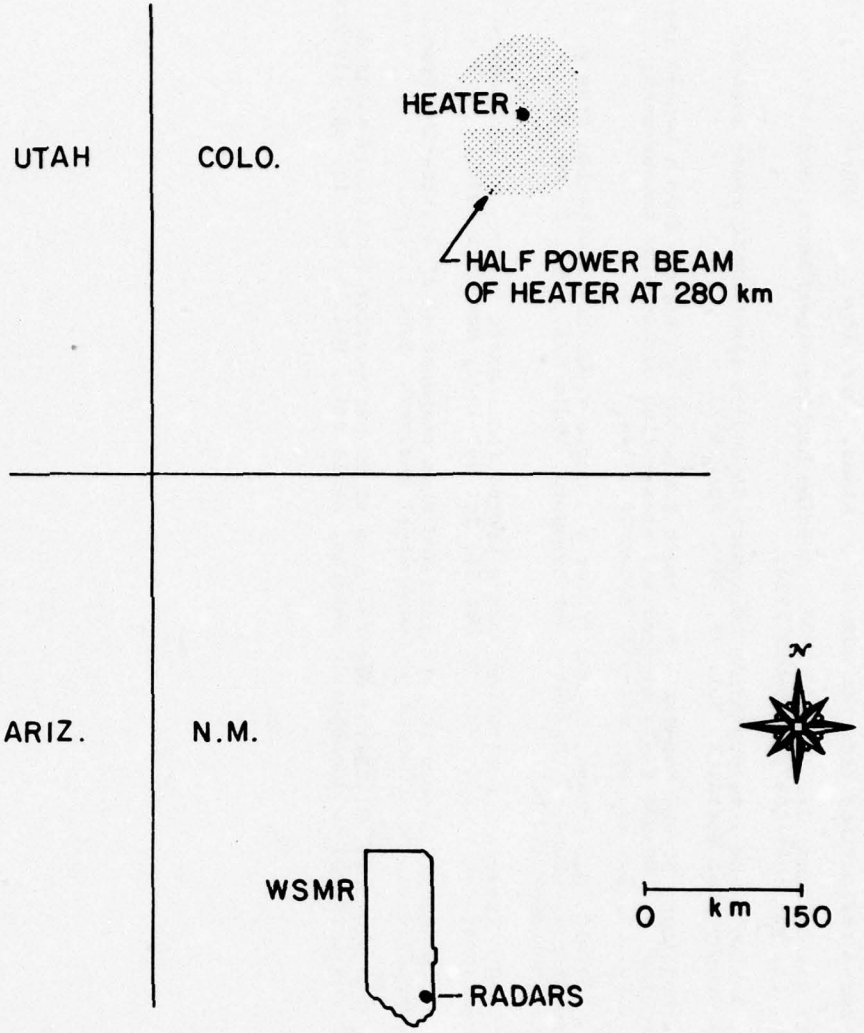

RADAR PARAMETERS

	RAM (VHF)	RAM (UHF)	AMRAD
Frequency (MHz)	157.5	435	1300
Peak Power (MW)	10	12	10
Max. Pulse-width (μsec)	30	10	8
Nominal PRF (sec^{-1})	100	100	50
Antenna 3-dB Beamwidth (deg)	5.2	2.0	0.9

Fig. 1. White Sands - Platteville experiment geometry. The azimuthal heading between the radars at White Sands and the heater is 8^0. The magnetic dip angle at Platteville is 68^0 and the declination is 13^0. For a 15^0 radar elevation angle, the line-of-sight is perpendicular to B above the heater at an altitude of about 290 km.

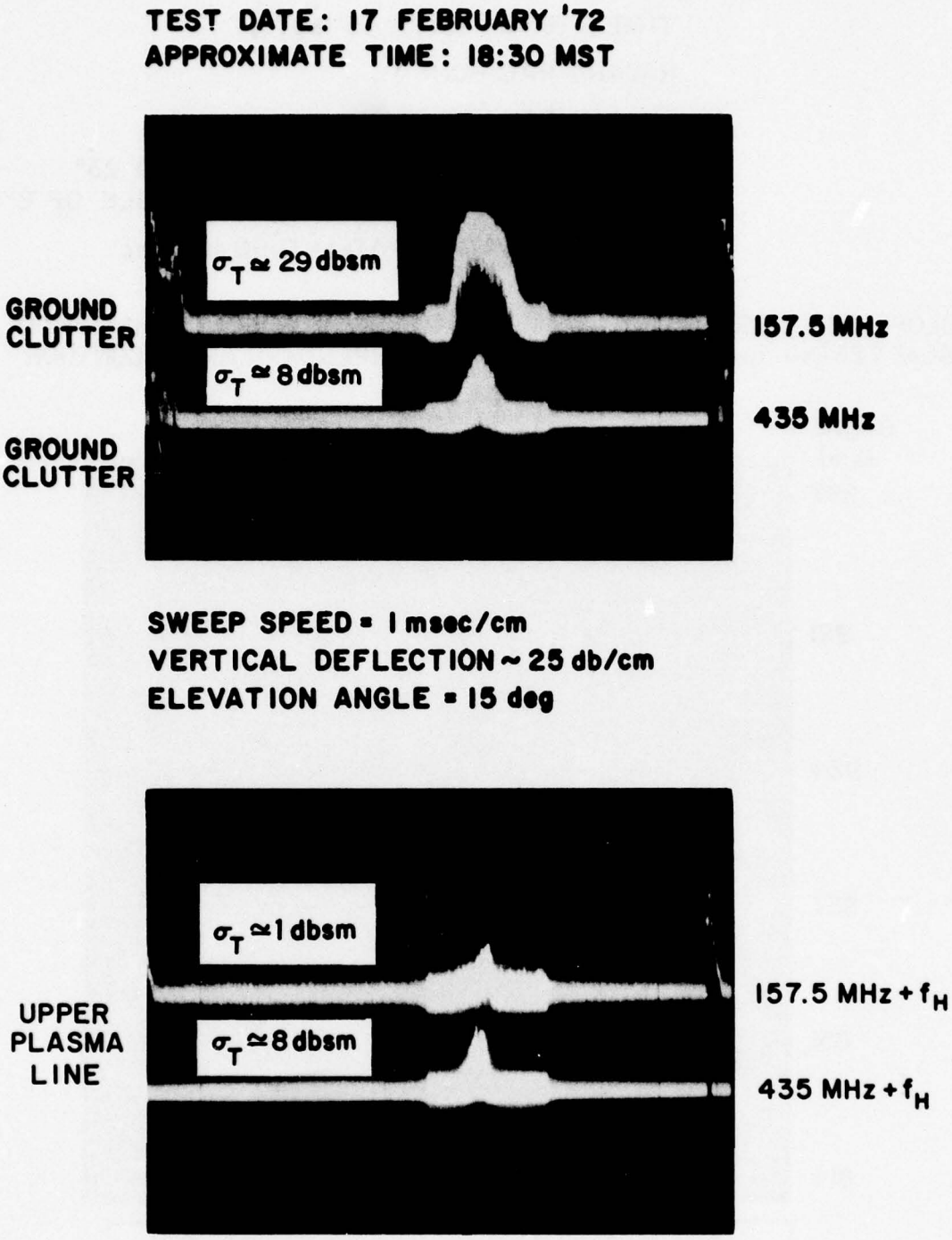

Fig. 2. A-scope presentations of typical large center-line and plasma-line radar echoes from the heated volume under optimum scattering conditions (15^0 RAM elevation angle, $h_f \simeq 290$ km, heater power $\simeq 2$ MW). The thicker base-line trace in the vicinity of the echo is due to an image intensifier in the oscilloscope. Note the absence of ground clutter in the plasma-line A-scope trace; the spikes shown on the ends of the trace represent leakage of the transmitted pulse into the receiver. σ_T is the ordinary radar cross section calculated from peak values of received power (not properly normalized with respect to per-pulse scattering volume).

DATE : 13 OCTOBER 71

TIME : 19:12–19:15:45 MDT

RADAR : RAM–UHF

PULSEWIDTH : 10 μsec

EVENT : ELEVATION SCAN FROM 8° TO 23°
AT A CONSTANT AZIMUTH ANGLE OF 8°

ELEVATION RATE = 0.50 deg/sec

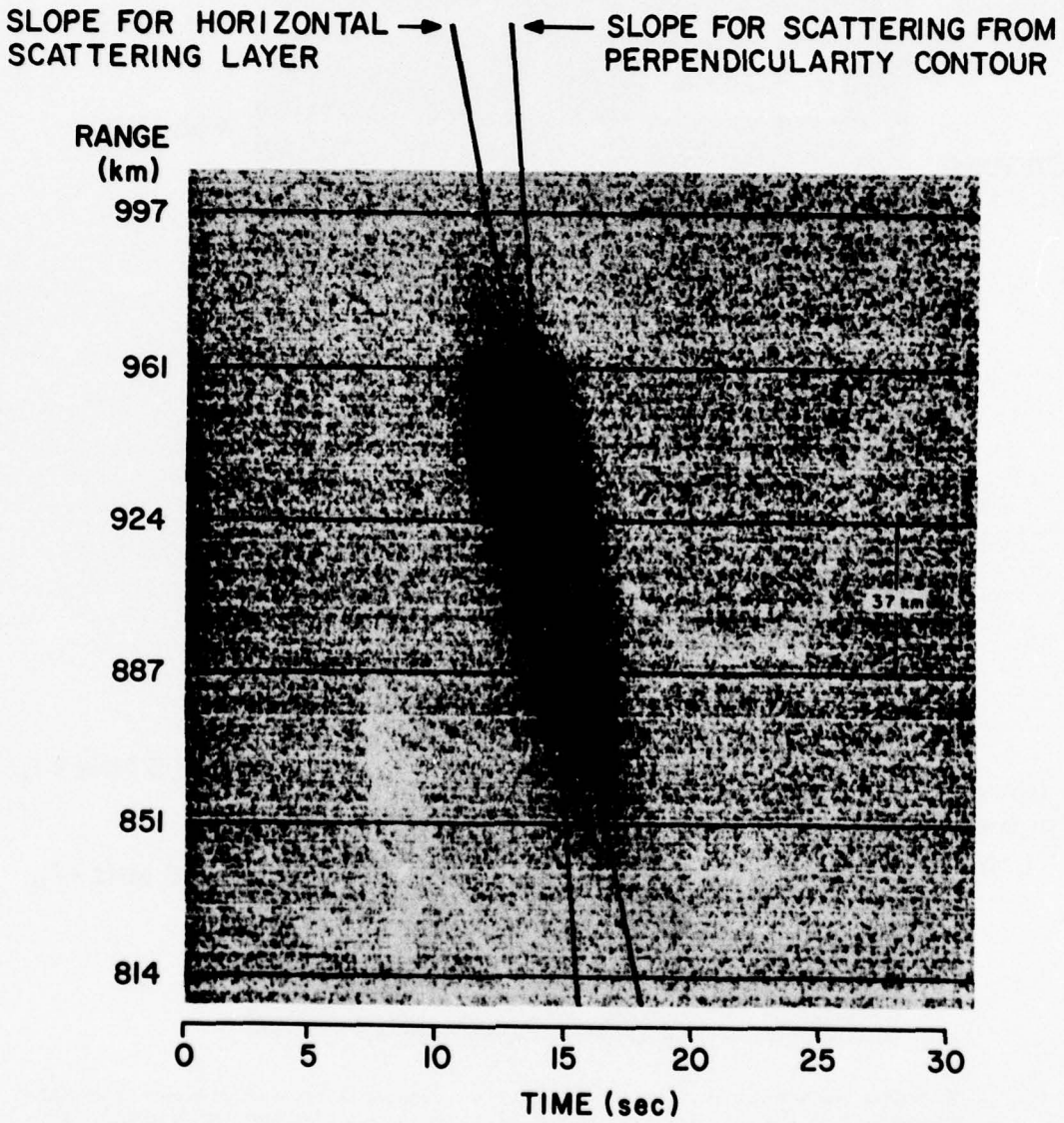

Fig. 3. Results of UHF elevation-scan experiment indicating a planar sacttering region aligned with $C_{\perp}$.

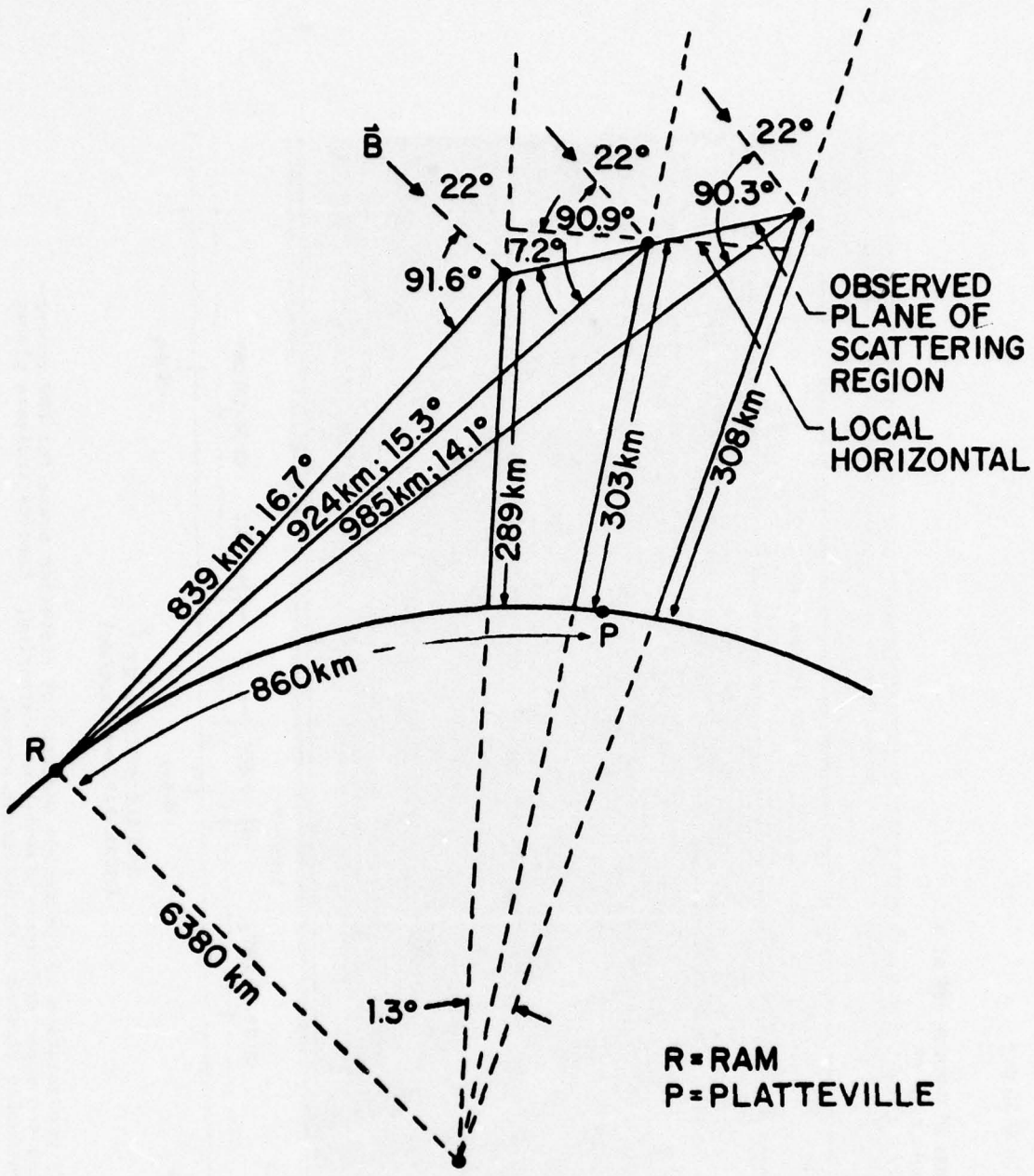

Fig. 4. Resulsts of analysis of experimental measurement shown in Fig. 4, determining the orientation of the locus of points of maximum scattering in relation to the direction of the geomagnetic field, B. From these results it was first determined that the locus of points of maximum backscatter for the center-line mode coincides with $C_{\perp}$.

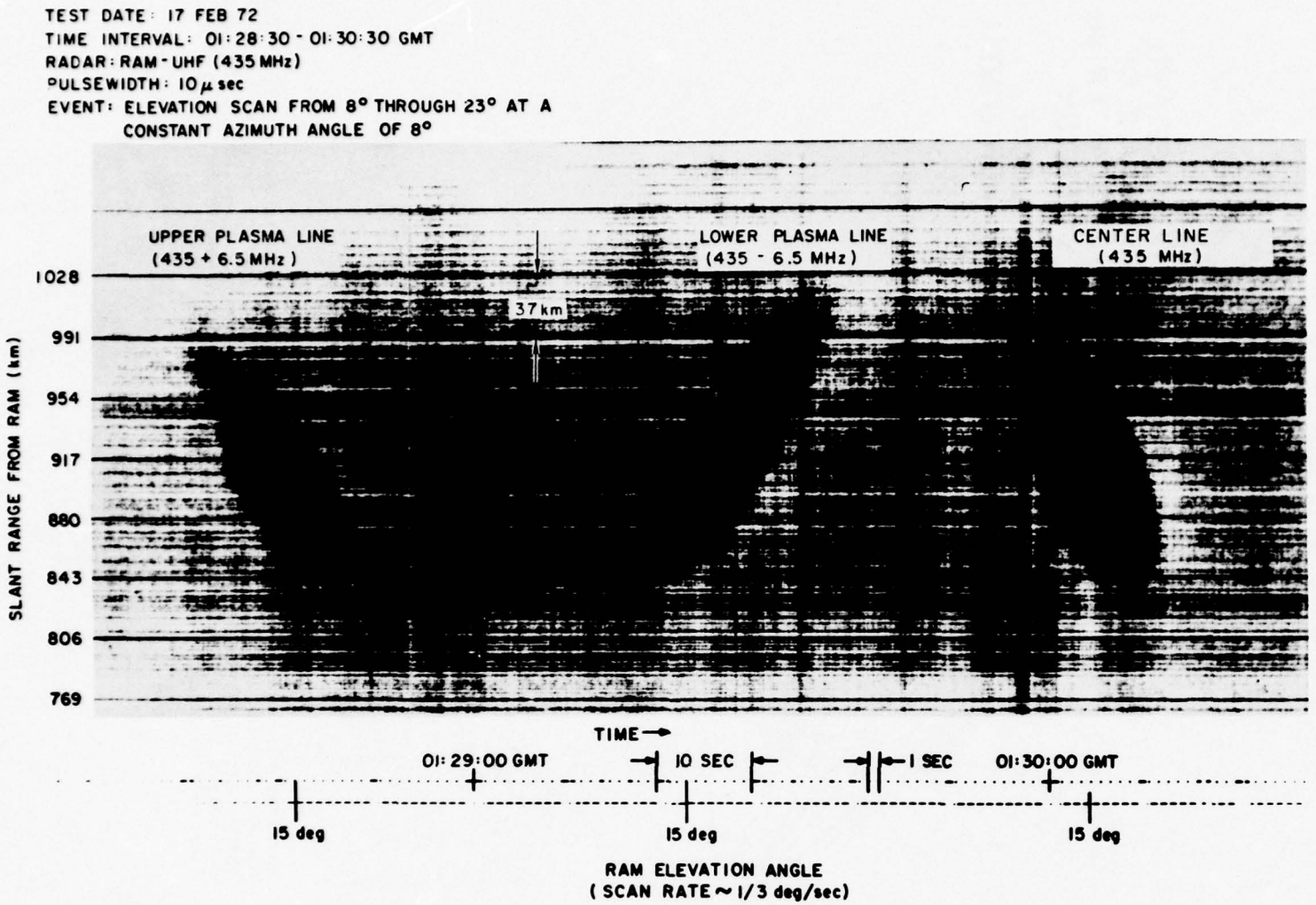

Fig. 5. RTI presentation of continuous sequence of elevation scans for UHF center-line and upper and lower plasma-line scattering. Results indicate planar scattering regions with different slopes.

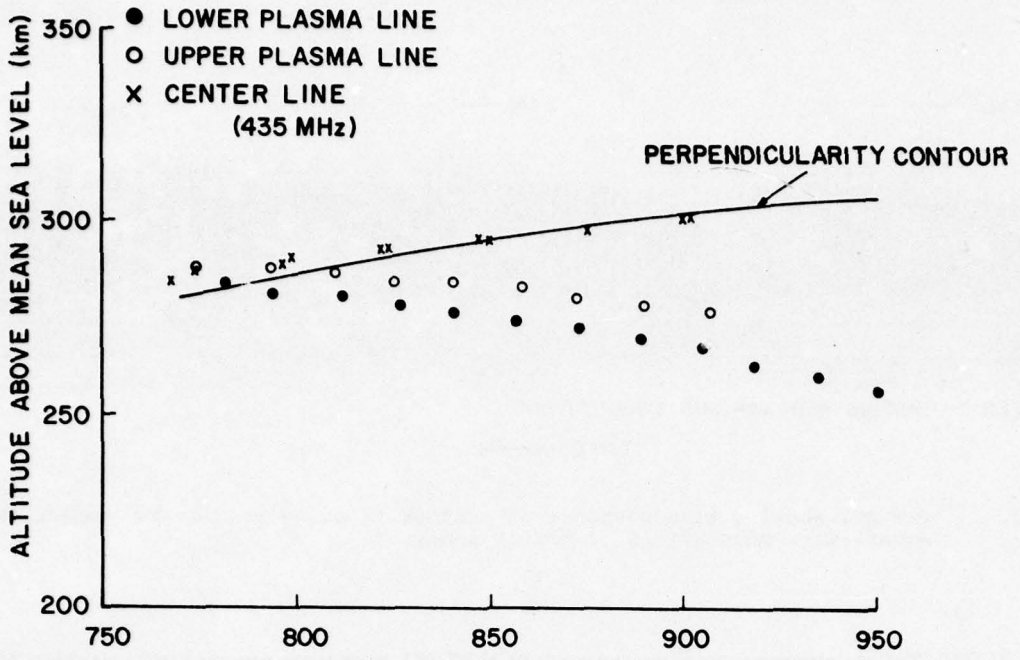

Fig. 6. Locations of loci of maximum scattering for experimental results of Fig. 5. The perpendicularity contour, $C_\perp$, shown in this figure was calculated from a 99-term spherical-harmonic expansion of the geomagnetic field (Thome and Blood, 1974). The locus of points of maximum scattering for the plasma-line measurements intersects $C_\perp$ at an altitude of 290 km but is otherwise completely distinct from $C_\perp$. This indicates that (a) plasma-line scattering is much less aspect sensitive than center-line scattering, and (b) the location of the scattering region from the center line is determined by h_f, independently of the geometry relative to B. At this time $h_f \simeq 290$ km.

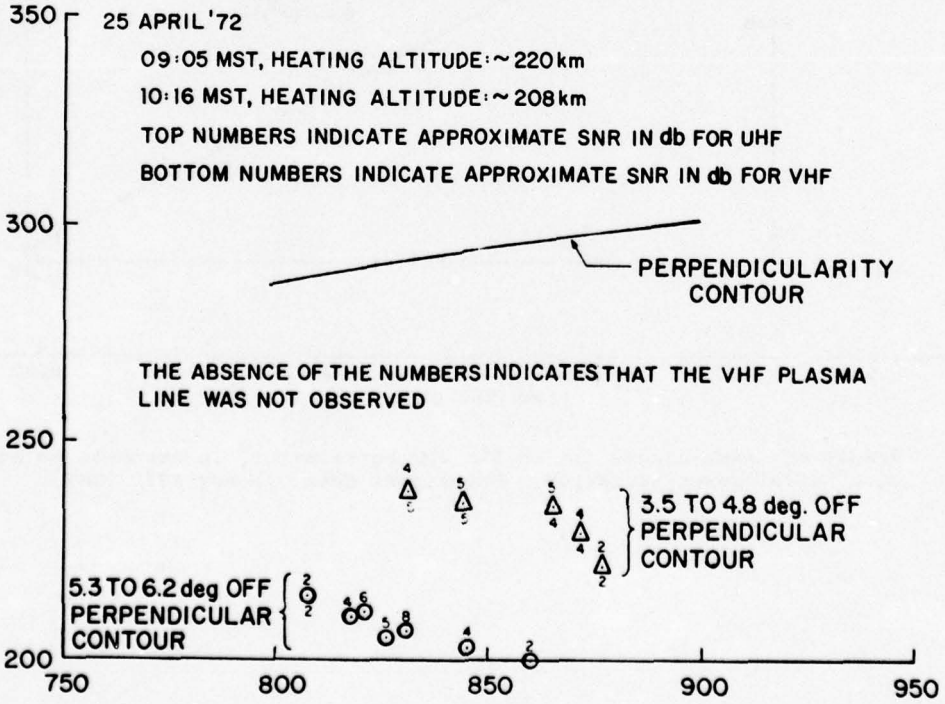

Fig. 7. Location of VHF and UHF plasma-line scattering regions as functions of h_f. No center-line scattering was observed at this time. Note that the scattering at UHF is stronger than at VHF. Triangles are data points for $h_f \simeq 220$ km. Circles are data points for $h_f \simeq 208$ km.

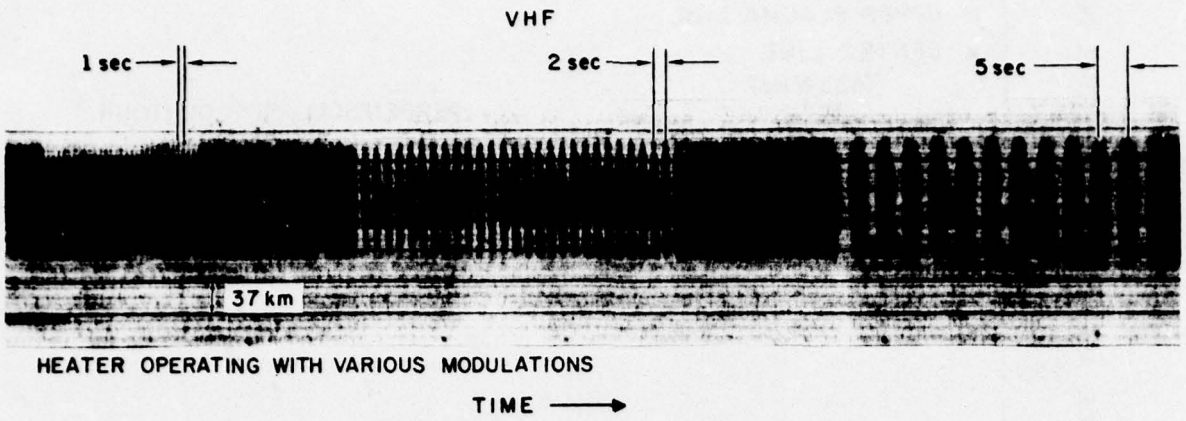

Fig. 8. VHF RTI showing time-response of scattering cross section to various on-off square-wave modulations of heater power.

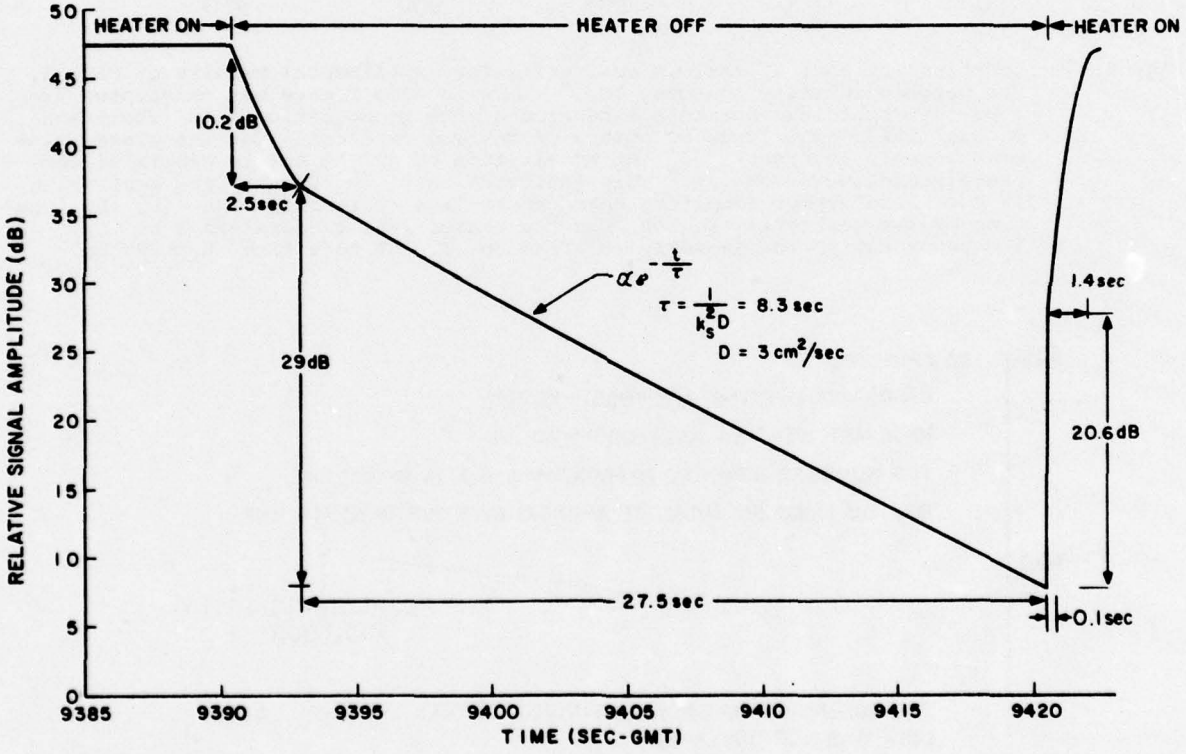

Fig. 9. Result of least-square fit to RAM VHF backscatter, in response to step-function heater-power variation. Experiment date: 5 May 1972 (GMT).

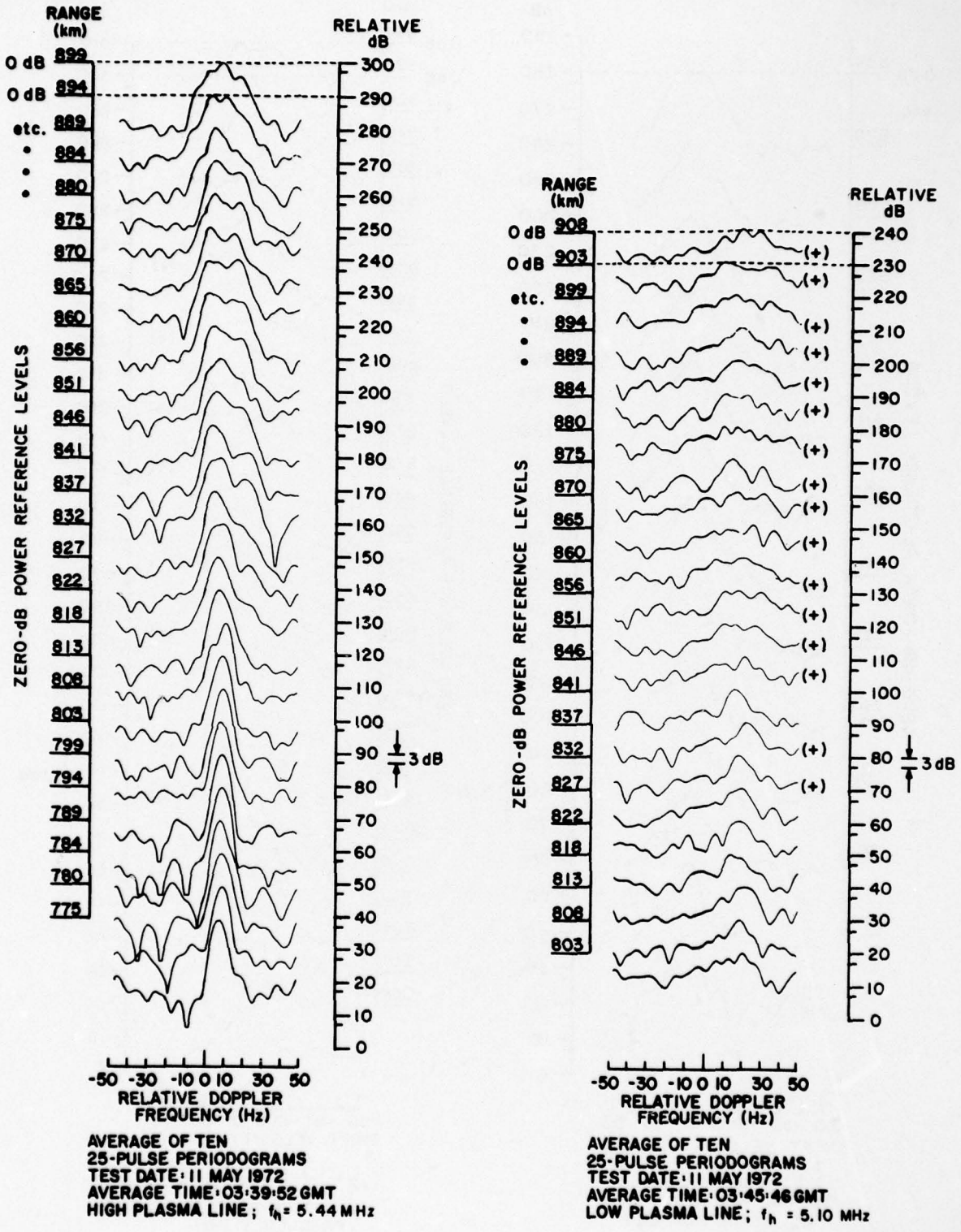

Fig. 10. Range sequence of average periodograms.

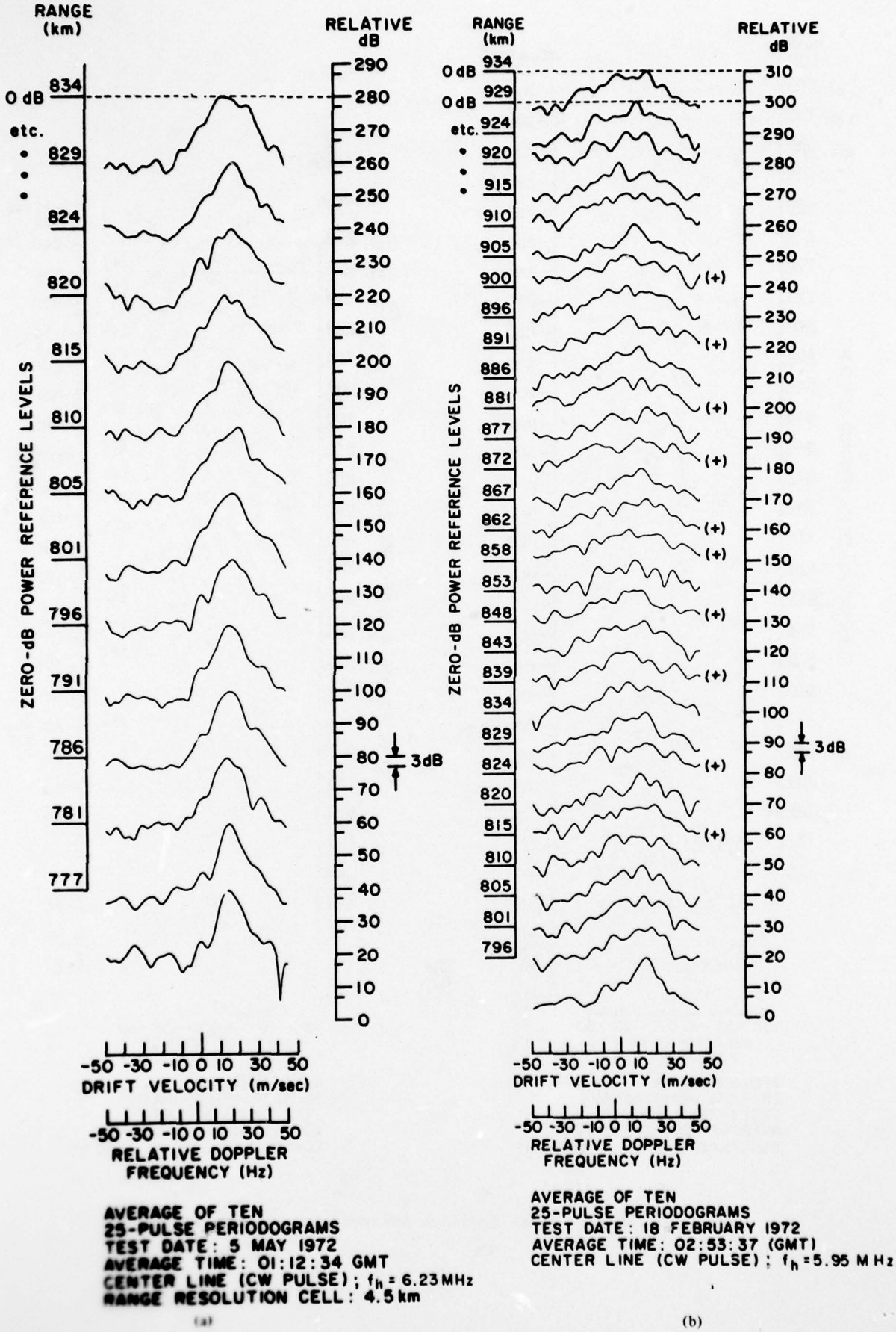

Fig. 11. Range sequence of average periodograms.

DATE : 13 OCTOBER 71

TIME : 19:33:10 - 19:33:46 MDT

RADAR : RAM - UHF

PULSEWIDTH : 10 μ sec

EVENT : AZIMUTH SCAN FROM 0.2° TO 18.7°
AT A CONSTANT ELEVATION ANGLE OF 15°

AZIMUTH RATE = 0.53 deg/sec

f_h = 5.10 MHz $f_0F_2 \approx$ 5.06 MHz

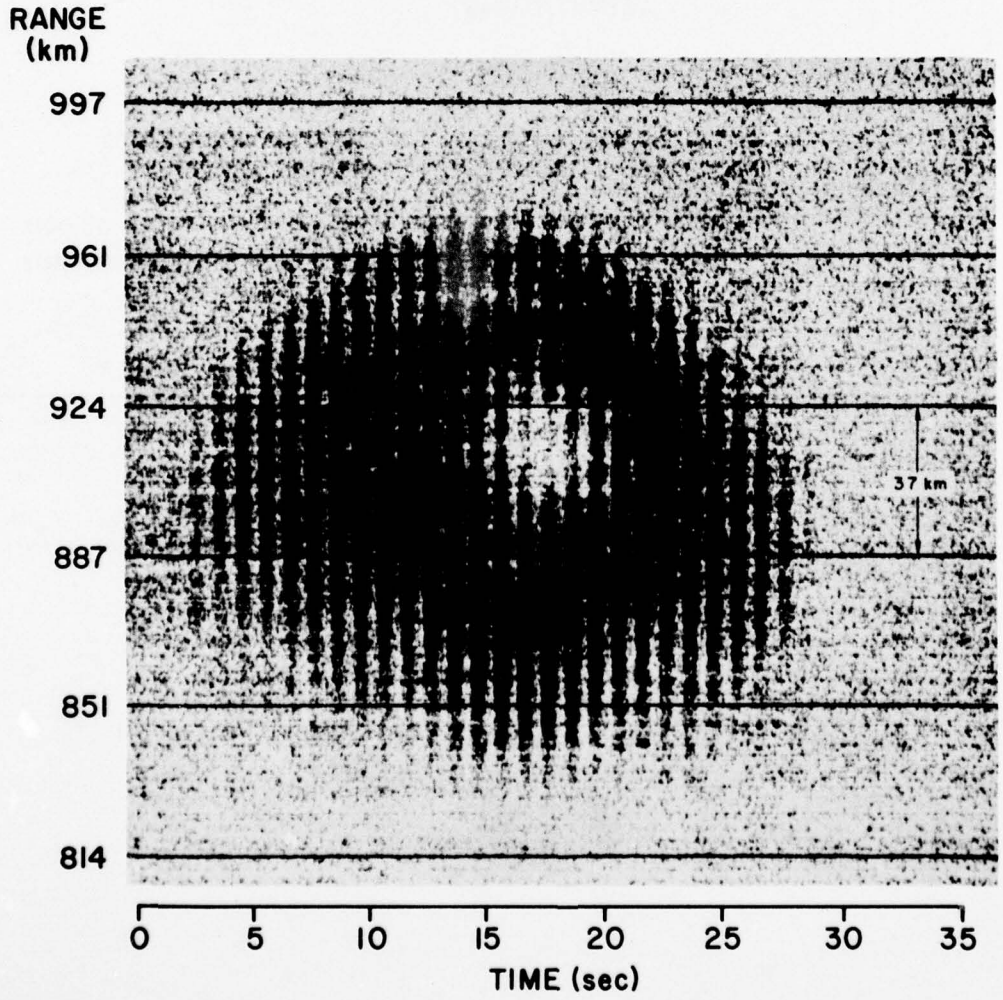

Fig. 12. RTI of azimuth scan of heated volume at fixed elevation angle (the periodic intermittencies in the figure result from a 5-Hz on-off square-wave modulation of the heater power and do not bear on this discussion). Since f_h/f_0F_2 is only slightly greater than unity, penetration occurs in the central region of the heater beam only.

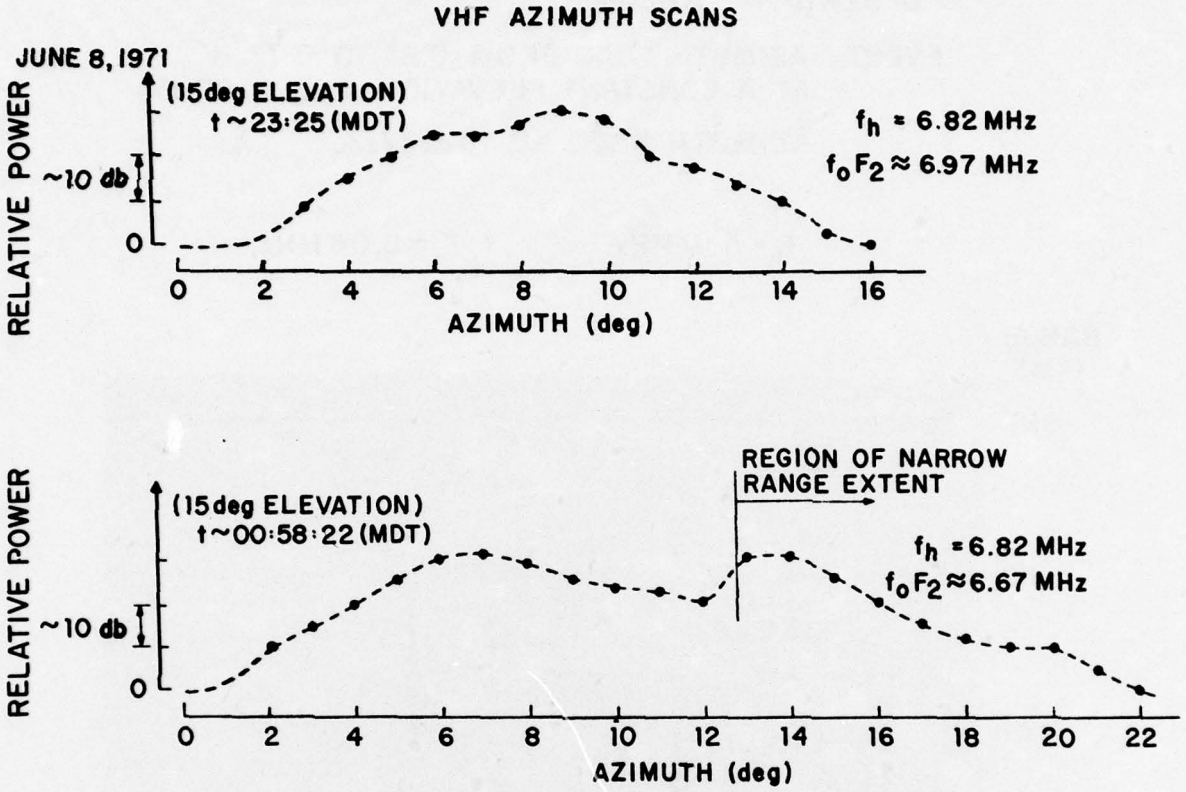

Fig. 13. Illustration of observed east-west spreading of heated volume for $f_h/f_0F_2 > 1$. Note the second peak at 13° in the lower figure, for which radar line-of-sight was exactly in the plane of the magnetic meridian.

SCATTERING BY FIELD ALIGNED STRUCTURES

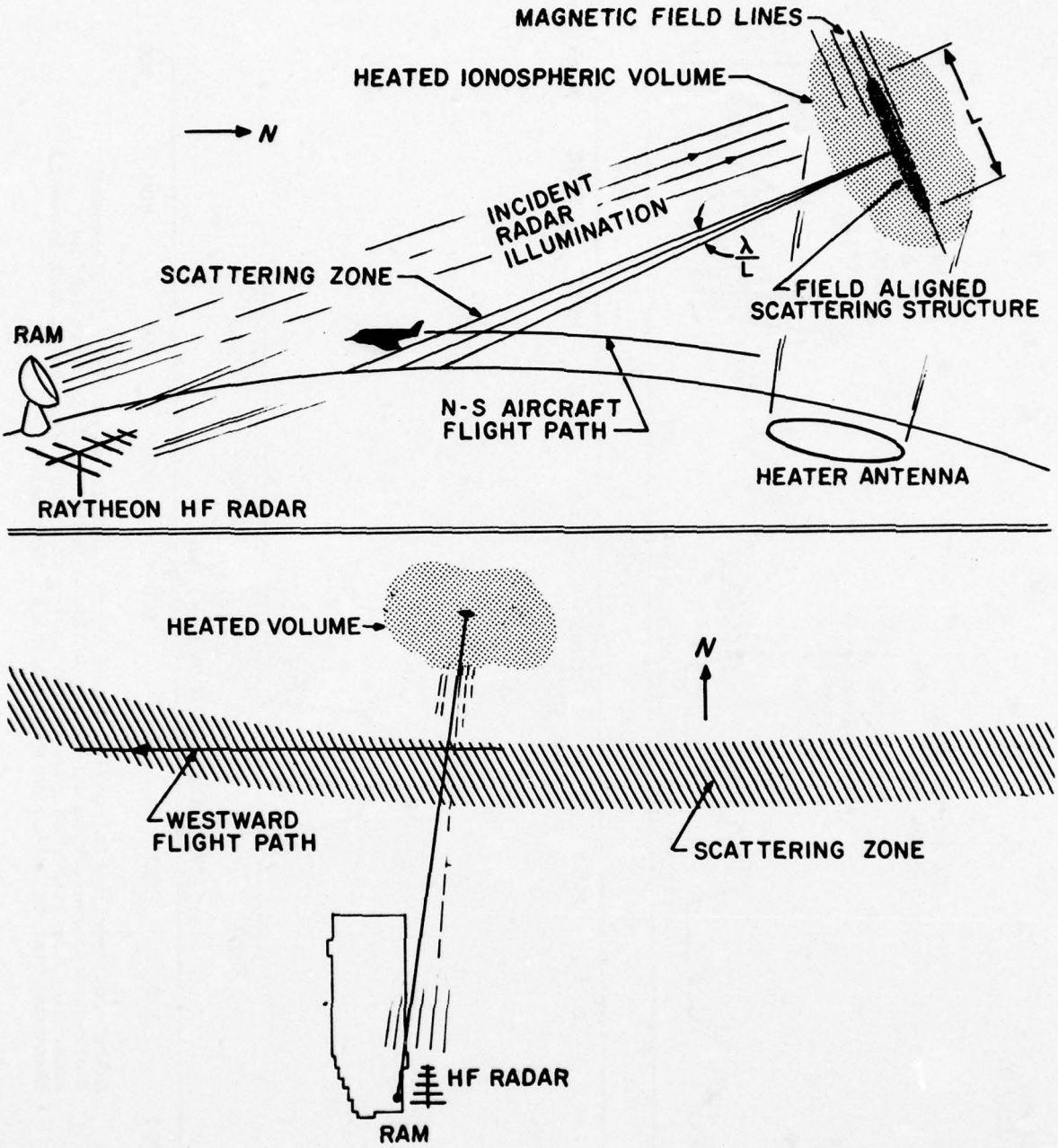

Fig. 14. Diagram of experiment using aircraft-borne, bistatic receivers.

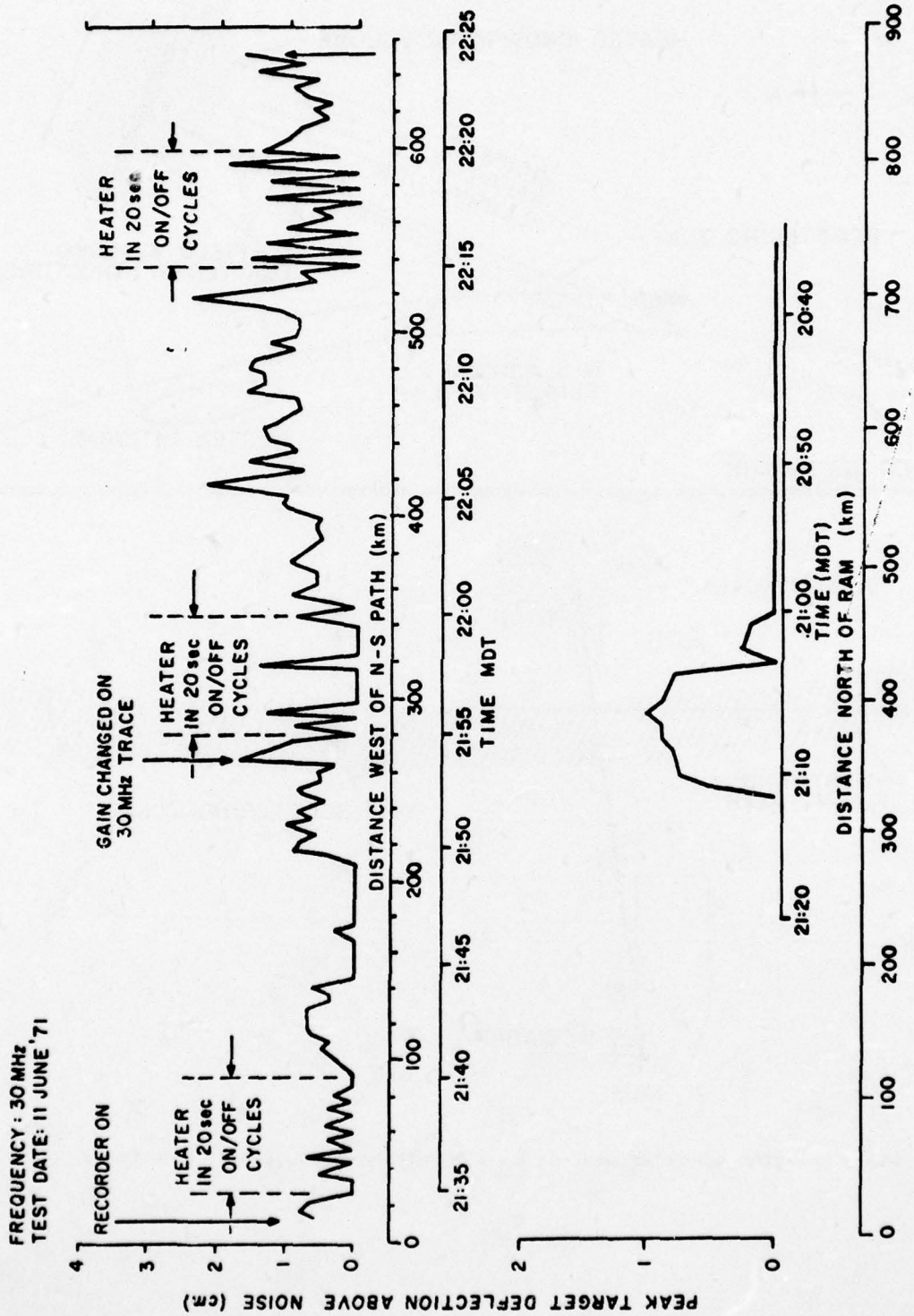

Fig. 15. Example of experimental results which first established presence of elongated field-aligned scattering structures within a heated volume. This follows from observed scattering zone during east-west flight (top) being much broader than zone observed during north-south flight (bottom).

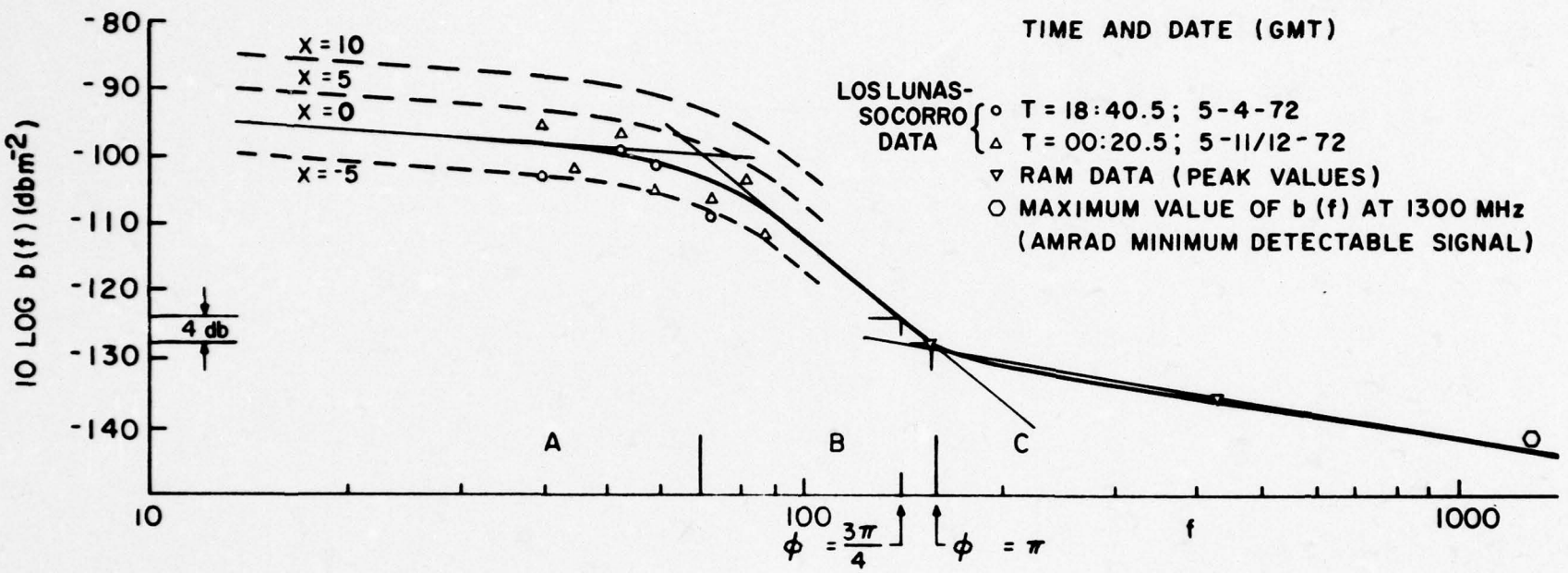

Fig. 16. The backscatter coefficient (b(f) as determined from experimental data using Eq.(4). The width of the curve is nominally 100 MHz from which T 3 m. Varying $\overline{|\Delta n|^2}$ results in vertical displacement of b(f), the shape presumably remaining the same. By using this procedure uppern and lower bounds on $\overline{|\Delta n|^2}$ for these data are calculated from the dashed curve corresponding to x = ± 5 dB, respectively; the results of this analysis are summarized in Table II. The values of $\phi = \pi$ and $\phi = 3\pi/4$ refer to a comparison of the measured backscatter and axially-bistatic cross section as discussed in Minkoff (1974). As indicated in the figure, the theoretically predicted increase in cross section for the axially-bistatic case is 4 dB.

ON THE IONOSPHERIC MODIFICATION EXPERIMENT PROJECTED AT MPI LINDAU: SCIENTIFIC OBJECTIVES

P. Stubbe and H. Kopka
Max-Planck-Institut für Aeronomie, 3411 Katlenburg-Lindau 3,
F.R. Germany

SUMMARY

An ionospheric modification experiment is planned by the Max-Planck-Institut für Aeronomie to be carried out near Tromsø, Norway. The scientific objectives include (a) the study of parametric instabilities, for which the EISCAT incoherent scatter system will be a highly flexible diagnostic instrument, (b) of non-linear electromagnetic wave propagation effects, especially in relation to the polar electrojet, (c) determination of certain parameters of aeronomic interest, (d) modification of natural polar electrojet instabilities, and (e) extension of the diagnostic capabilities of the EISCAT incoherent scatter facility.

1. INTRODUCTION

An ionospheric modification experiment is planned by the Max-Planck-Institut für Aeronomie to be carried out near Tromsø, Norway. This experiment, which would be the third of its kind, derives its motivation from (a) the special ionospheric conditions in the auroral zone and (b) the extraordinary accumulation of highly valuable diagnostic equipment in the Tromsø area, the most important being the tristatic two-frequency steerable EISCAT incoherent scatter facility.

Some basic data on the site and on the experiment are listed in the following table:

LOCATION	Tromsø, Norway	
	$\varphi_G = 69.6^oN$, $\lambda_G = 19.0^oE$	
	$\varphi_M = 67.1^oN$, $I = 78^o$, $L = 6.2$	
EXPERIMENT	Frequency	2.75 - 8.00 MHz
	Power	1 MW
	Antenna gain	> 22 dBi
	ERP	> 150 MW
	Construction period	1976 - 1978

2. AVAILABLE DIAGNOSTIC EQUIPMENT

Before outlining the scientific goals, it may be appropriate to briefly describe the available main diagnostic equipment. It should be mentioned that most of this equipment has been or will be built independent of our experiment, but that in all cases a close cooperation has been agreed upon.

a) EISCAT European Scatter Facility

The EISCAT incoherent scatter facility will consist of two independent systems, a tristatic UHF system (933 MHz) with the transmitter at Tromsø and receivers at Tromsø, Kiruna (Sweden) and Sodankylä (Finland), and a monostatic VHF system (224 MHz) at Tromsø. The UHF transmitting antenna will (most likely) be fully steerable, the VHF antenna will (probably) be steerable in the magnetic N-S-meridian. The basic data are summarized in the following table:

	UHF	VHF
Frequency	933 MHz	224 MHz
Wave length	0.32 m	1.34 m
Average power	250 kW	300 kW
Peak power	2 MW	5 MW
Pulse length	20μs - 10ms	20μs - 1ms
Antenna gain	48 dB	44 dB

b) Partial Reflection System (A. Haug, University of Tromsø)

The partial reflection system presently in operation has a frequency of 2.75 MHz. An extension to one or two higher frequencies is planned in order to expand the height coverage and to achieve an overlap with the EISCAT measurements.

c) VHF-Pulse-Radar (R. Greenwald, MPI Lindau)

This radar consists of two independent monostatic systems, operating at 140 MHz, located at Trondheim (Norway) and Sauvamaki (Finland). The azimuthal range covered is 28^{o} with an angular resolution of 3.5^{o}. The radial resolution is 7.5 - 15 km, corresponding to a pulse length of 50 - 100 μsec. The radar aims at polar electrojet instabilities.

d) VHF-CW-Radar (P. Czechowsky, MPI Lindau)

This system operates at 145 MHz. The transmitter is located at Borlänge (Sweden), the receiver at Lycksele (Sweden). The receiving antenna covers an azimuthal range of 90^{o} with a resolution of 10^{o}. The two radar systems are complementary with the pulsed system giving distance information and the CW system affording a better frequency resolution.

e) Airglow Photometer (G. Lange-Hesse and H. Lauche, MPI Lindau)

The photometer will be designed to scan a circular area with a radius of 300 km in the F region and a resolution of 8 x 8 km^2. The main purpose will be to measure the 6300 Å and 5577 Å intensities, but searches for other lines are also intended.

f) Narrow-Beam-Riometer (E. Nielson, MPI Lindau)

This riometer works at a frequency of 51.4 MHz. Its antenna has a beam width of 16^{o} which agrees closely with the beam width of the heating antenna. Thus, the riometer sees the same area in the D region which is modified by the heater.

g) Dynasonde

The dynasonde will be part of the heating facility. It will be used for real time monitoring of the ionospheric state during a modification experiment and for determining electron density profiles, ionospheric absorption, echolocations, ionospheric response times, echo spreading and scintillations.

The locations of the diagnostic instruments specified above are shown in Fig. 1.

3. SCIENTIFIC OBJECTIVES

Two of the scientific objectives will be described in some detail, while the others will only be briefly sketched.

a) Study of parametric instabilities

The electromagnetic heating wave (ω_0, $\underline{k}_0$), if above a certain threshold and in the ordinary mode, feeds part of its energy into an electron plasma wave (ω_1, $\underline{k}_1$) and an ion acoustic wave (ω_2, $\underline{k}_2$). This process,

the so called decay instability, is subject to the frequency and wave number matching conditions

$$\omega_0 = \omega_1 + \omega_2 \tag{1a}$$

$$\underline{k}_0 = \underline{k}_1 + \underline{k}_2 \tag{1b}$$

A radar is able to detect these enhanced electron and ion fluctuations, if the Bragg condition

$$\pm \underline{k} = \underline{k}_t - \underline{k}_r \tag{2}$$

is satisfied with $\underline{k}$ belonging to the plasma wave under consideration and $\underline{k}_t$, $\underline{k}_r$ denoting the wave vectors of the transmitted and received radar signals, respectively. For monostatic operation we have $\underline{k}_r = -\underline{k}_t$, so that $k = 2k_t$. Thus, the radar sees, out of the full angular and frequency spectrum of the enhanced plasma waves, just one spectral component. Its direction of propagation is determined by the radar geometry, its wavelength is determined by the radar frequency.

It is desirable, therefore, to have a radar system which allows observations at different frequencies and under different angles. The EISCAT system offers this flexibility. Let us first discuss the possibilities provided by the monostatic VHF system and by the UHF system in monostatic operation:

Since both the radar and the heating beams will be steerable, it appears that one can study parametric instabilities in the full available angular range. This is not necessarily so, however. If we insert into (1) the dispersion relations $\omega(k)$ for electromagnetic, electron plasma, and ion acoustic waves and furthermore assume a linear $N_e(z)$ profile, we find that the altitude at which the radar sees the plasma fluctuations is given by

$$z_R = z_0 - H \cdot 2\ 10^{-6}\ \frac{T_e}{1000}\ \frac{f_R^2}{f_H^2} \tag{3}$$

with H the linear electron density scale height ($N_e = N_{eo}(1 + \frac{z-z_0}{H})$), z_0 the height at which the heating wave is reflected for vertical incidence, f_R the radar frequency, and f_H the heating frequency. Some typical values for $z_0 - z_R$ are given in the following table (T_e = 2000 K):

		f_H[MHz]	2.75	4.00	6.00	8.00
f_R = 224 MHz (VHF)	H = 25 km	z_0-z_R[km]	0.66	0.31	0.14	0.08
	H = 50 km	z_0-z_R[km]	1.33	0.63	0.28	0.16
	H =100 km	z_0-z_R[km]	2.65	1.25	0.56	0.31
f_R = 933 MHz (UHF)	H = 25 km	z_0-z_R[km]	11.5	5.4	2.4	1.4
	H = 50 km	z_0-z_R[km]	23.0	10.9	4.8	2.7
	H =100 km	z_0-z_R[km]	46.0	21.8	9.7	5.4

One has to make sure that the heating wave is reflected at an altitude $z > z_R$ which prohibits propagation at large angles φ with respect to the vertical. This is illustrated in Fig. 2.

In the VHF case z_0-z_R is very small. Consequently, the maximum allowed φ is roughly given by the Spitze-angle φ_S

$$\varphi \leq \varphi_S = \arcsin\left\{\sqrt{\frac{f_L/f_H}{1+f_L/f_H}}\cos I\right\} \tag{4}$$

with f_L = 1.4 MHz the gyro-frequency and I = 78° the dip angle. For f_H in the range 2.75 to 8.00 MHz, φ_S ranges from 6.9° to 4.6°, a typical value being 6°. Thus, the angular range φ^* with respect to the magnetic field is approximately

$$\text{VHF:} \qquad 6^\circ < \varphi^* < 18^\circ \tag{5}$$

This is, however, a very careful estimate. In reality the angular range may be a few degrees wider, particularly for lower heating frequencies.

In the UHF case, the maximum allowed φ exceeds φ_S considerably. For a rough estimate we employ the sec-law of oblique propagation, again in conjunction with a linear $N_e(z)$ profile. Thereby, we obtain the following relation between the propagation angle φ and the reflection height z

$$\sin^2\varphi = \frac{z_o - z}{H} \tag{6}$$

Inserting (3), the maximum allowed φ, φ_o, follows to be

$$\text{UHF:} \qquad \sin^2\varphi_o = 2\cdot10^{-6}\,\frac{T_e}{1000}\,\frac{f_R^2}{f_H^2} \tag{7}$$

With T_e = 2000 K, f_R = 933 MHz and f_H ranging from 2.75 to 8.00 MHz, φ_o ranges from 43° to 14°. Thus, with respect to the magnetic field, we have

$$\text{UHF:} \qquad \begin{aligned} -31^\circ < \varphi^* < 55^\circ \quad & \text{for } f_H = 2.75 \text{ MHz} \\ -\ 2^\circ < \varphi^* < 26^\circ \quad & \text{for } f_H = 8.00 \text{ MHz} \end{aligned} \tag{8}$$

The accessible φ^*-range in the monostatic VHF and UHF cases is illustrated in Fig. 3.

Next let us look into the case of UHF operation using the remote receivers. The height z_R at which the radar sees the enhanced plasma waves is now given by

$$z_R = z_o - H\,2\cdot10^{-6}\cos^2\Theta\,\frac{T_e}{1000}\,\frac{f_R^2}{f_H^2} \tag{3a}$$

where Θ is half the angle between $\underline{k}_t$ and $\underline{k}_r$. Thus, the maximum allowed propagation angle of the heating wave is

$$\sin^2\varphi_o = 2\cdot10^{-6}\cos^2\Theta\,\frac{T_e}{1000}\,\frac{f_R^2}{f_H^2} \tag{7a}$$

Evaluating (7a) together with the geometric conditions of the transmitter-receiver-setup (see Fig. 4), we arrive at the following maximum allowed values of φ^*, φ^*_{max}, which, by accident, are approximately equal for Kiruna and Sodankylä:

$$\text{UHF:} \qquad \begin{aligned} \varphi^*_{max} &\approx 62^\circ \quad \text{for } f_H = 2.75 \text{ MHz} \\ \varphi^*_{max} &\approx 41^\circ \quad \text{for } f_H = 8.00 \text{ MHz} \end{aligned} \tag{9}$$

These values relate to a backscatter altitude of 250 km.

Summarizing, we may say that the EISCAT facility is a very well suited instrument for studying parametric instabilities. The angular spectrum with respect to the magnetic field may be scanned up to angles of at

least 41^0, at best 62^0. Especially important, small angles down to $\varphi^* = 0$ are included, so that extremely strong lines in the backscatter spectrum are to be expected. According to Perkins, Oberman and Valeo (1974), this small angle scattering should exceed the level observed at Arecibo by a factor 10^4.

b) Study of nonlinear wave propagation effects

In addition to those nonlinearities which generally occur in a sufficiently strong D region (Ginzburg and Gurevich, 1960), there is a special electrojet nonlinearity that deserves particular attention. Suppose we heat the ionospheric region which carries the polar electrojet (PEJ). A change in the electron temperature T_e causes a change in the Pedersen and Hall conductivities and, thus, in the PEJ current density $\underline{j}$. If we now switch the heating wave in an on-off-cycle, we periodically change T_e and j (see Fig. 5). Thereby, the dc current obtains an ac component, so that the heated ionospheric area is turned into a huge antenna radiating at a frequency corresponding to the pulse repetition rate and its harmonics. We want to roughly estimate the power radiated by this "D region antenna".

First, we calculate the full electron temperature increase ΔT_e which relates to heating times long compared with the characteristic time τ. Heat production is determined by the absorption rate of the heating wave, heat loss is mainly governed by rotational and vibrational excitation of N_2 and O_2. With the corresponding loss rates taken from Stubbe and Varnum (1972), the resulting non-linear energy equation is numerically solved.

Second, we calculate the Pedersen and Hall conductivities, σ_P and σ_H, for the electron temperatures $T_e = T_n$ (before heating) and $T_e = T_n + \Delta T_e$ (saturated heating). This gives us the full overhead current density change (again relating to heating times long compared with τ)

$$(\Delta j_o)_{P,H} = [\sigma_{P,H}(T_n+\Delta T_e) - \sigma_{P,H}(T_n)]\, E \tag{10}$$

with E the horizontal electric field. For the radial dependence of Δj we assume

$$\Delta j = \Delta j_o \exp\left(-\frac{r^2}{r_o^2}\right) \tag{11}$$

(see Fig. 5) with $r_o = z\, tg\alpha$ (z = altitude, α = half width of heating beam). The subscripts P, H have now been dropped for convenience.

Third, we calculate the amplitude of the periodic current density variation, Δj_1. The maximum possible Δj_1 is $\frac{1}{2}\ \Delta j$, but for a pulse repetition rate f not small compared with $1/\tau$ Δj_1 is smaller:

$$\Delta j_1 = \frac{1}{2}\,\Delta j\, [1 - \exp(-\frac{1}{4f\tau})] \tag{12}$$

Fourth, we calculate the current amplitude ΔI. With x and y the coordinates perpendicular and parallel to Δj_1, respectively, we easily find

$$\Delta I(y) = \frac{1}{2}\int_0^{\infty}\int_{-\infty}^{+\infty} dx\, dz\, \Delta j_o(z) \exp(-\frac{x^2+y^2}{r_o^2})\, [1 - \exp(-\frac{1}{4f\tau(z)})] \tag{13}$$

or, after replacing r_o by $z\, tg\alpha$ and carrying out the integration over x:

$$\Delta I(y) = \frac{\sqrt{\pi}}{2}\, tg\alpha \int_0^{\infty} dz\, z\, \Delta j_o(z) \exp(-\frac{y^2}{z\, tg\alpha})\, [1 - \exp(-\frac{1}{4f\tau(z)})] \tag{13a}$$

Fifth, we calculate the average of $\Delta I(y)$ over the length $2r_o$, $\overline{\Delta I}$. For r_o we take the value at $z = z_{max}$ with z_{max} the altitude where $\Delta j_o(z)$ has its maximum. We thereby obtain

$$\overline{\Delta I} = \frac{1}{2r_o} \int_{-\infty}^{+\infty} \Delta I(y)\, dy \approx \frac{\pi}{4} tg\alpha \int_{0}^{\infty} dz\, z\, \Delta j_o(z)\, [1-\exp(-\frac{1}{4f\tau(z)})] \tag{14}$$

Sixth, we assume that $\overline{\Delta I}$ constitutes a line current flowing at altitude z_{max} in an "antenna" of length $2r_o = 2\, z_{max}\, tg\alpha$. We treat this "antenna" as a Hertzian dipole in free space (thereby neglecting ground reflection, ducting and guiding of the radiated VLF wave), which has the radiation resistance

$$R_S = 80\, \pi^2\, \frac{4z_{max}^2\, tg^2\alpha}{\lambda^2} = 320\, \pi^2\, \frac{z_{max}^2\, f^2\, tg^2\alpha}{c^2} \quad [\frac{V}{A}] \tag{15}$$

Thus, we arrive at the following expressions for the radiated power

$$P \approx \frac{1}{2}\, R_S\, \overline{\Delta I}^2 \tag{16}$$

or

$$P \approx 10\ \pi^4\, \frac{z_{max}^2\, f^2\, tg^4\alpha}{c^2} \left[\int_{o}^{\infty} dz\, z\, \Delta j_o(z)\, [1 - \exp(-\frac{1}{4f\tau(z)})]\right]^2 \tag{16a}$$

The assumption of a Hertzian dipole breaks down for $f > 10^4$ Hz. We have based the results to be shown in the following on equ. (16a). For $f \gg 1/\tau(z_{max})$, however, one may carry the approximation one step further. Taking a parabolic profile for $\Delta j_o(z)$,

$$\Delta j_o(z) = \Delta j_{max} \left[1 - (\frac{z-z_{max}}{Y})^2\right] \tag{17}$$

one obtains

$$P \approx \frac{10}{9}\, \pi^4\, \frac{z_{max}^4\, Y^2\, \Delta^2 j_{max}\, tg^4\alpha}{c^2\tau^2(z_{max})} \tag{18}$$

Note that the right hand sides of (16a) and (18) have to be multiplied by 1V/A. P is now frequency independent since the frequency dependencies of R_S and $\overline{\Delta I}^2$ cancel each other out. For values of f not obeying $f \gg 1/\tau(z_{max})$, the frequency dependence of R_S predominates. Therefore, for lower frequencies, P decreases with decreasing f.

We have not yet performed a complete case study to the efficiency of the "PEJ - D region-antenna". The results of one particular example, however, are shown in Figs. 6 and 7. We see from Fig. 7 that for frequencies above about $5 \cdot 10^3$ Hz a radiated VLF power of the order 100 VA can be expected. It remains to be investigated whether this is enough to cause secondary effects like particle precipitation due to stimulated pitch angle diffusion of trapped particles.

c) Determination of aeronomic parameters

Ohmic and anomalous heating of the ionosphere lead to a number of phenomena which can be used for a determination of certain parameters of aeronomic interest (Meltz and Perkins, 1974, and papers referenced there in). Among those are chemical rate coefficients, energy transfer rates, neutral wind velocities, and airglow quenching rates. The availability of a partial reflection system will make it possible to determine, as a function of altitude and electron temperature, the recombination rate in the D region. This appears to be an especially attractive application.

d) Modification of natural plasma instabilities

Both the type I (two stream) and type II (gradient drift) electrojet instabilities depend, through their thresholds and growth rates, on the electron temperature (e.g. Sudan, Akinrimisi and Farley, 1973). To be

more specific, the minimum required electron drift velocity across B is larger for larger electron temperatures in both cases. Thus, by altering the electron temperature, one may affect the instabilities, the ultimate being a disruption. This possibility of having an active influence may add new prospects to the study of PEJ instabilities.

e) Extension of the diagnostic capabilities of the incoherent scatter system

The excitation of parametric instabilities leads to a number of additional lines in the incoherent backscatter spectrum (e.g. Carlson, Gordon and Showen, 1972) which bear some additional information on the macroscopic ionospheric plasma parameters: The frequency difference between growing mode and decay line contains additional temperature information, the frequency asymmetry between upshifted and downshifted plasma lines yields the electron drift velocity, and the plasma line decay time after switch-off allows to determine the electron collision frequency. Particularly important appears the determination of the electron velocity. Since the ion line gives the same kind of information on the ion velocity, one can now measure the field aligned current strength, a highly valuable quantity for studying ionosphere-magnetosphere interactions.

REFERENCES

Carlson H.C., W.E. Gordon and R.L. Showen	1972	High frequency induced enhancements of the incoherent scatter spectrum at Arecibo, J. Geophys. Res. 77, 1242
Ginzburg V.L. and A.V. Gurevich	1960	Nichtlineare Erscheinungen in einem Plasma, das sich in einem veränderlichen elektromagnetischen Feld befindet, Fortschr. d. Phys. 8, 97
Meltz G. and F.W. Perkins	1974	Ionospheric modification theory: Past, present, and future, Radio Sci. 9, 885
Perkins F.W., C. Oberman and E.J. Valeo	1974	Parametric instabilities and ionospheric modification, J. Geophys. Res. 79, 1478
Stubbe P. and W.S. Varnum	1972	Electron energy transfer rates in the ionosphere, Planet. Space Sci. 20, 1121
Sudan R.N., J. Akinrimisi and D.T. Farley	1973	Generation of small-scale irregularities in the equatorial electrojet, J. Geophys. Res. 78, 240

DISCUSSION

E. Thrane: When estimating the electron temperature resulting from the heating, what assumptions did you make about the electron cooling process ?

P. Stubbe: We assumed the electron gas to be cooled by means of rotational and vibrational excitation of O_2 and N_2 .

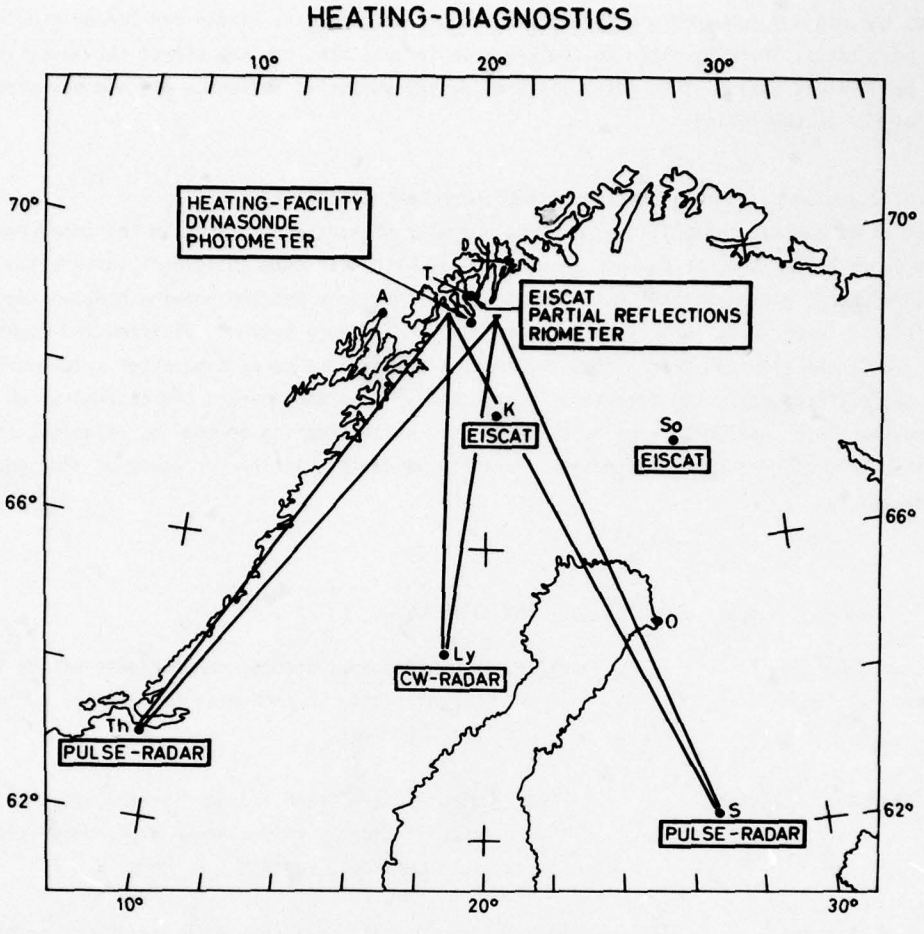

Figure 1

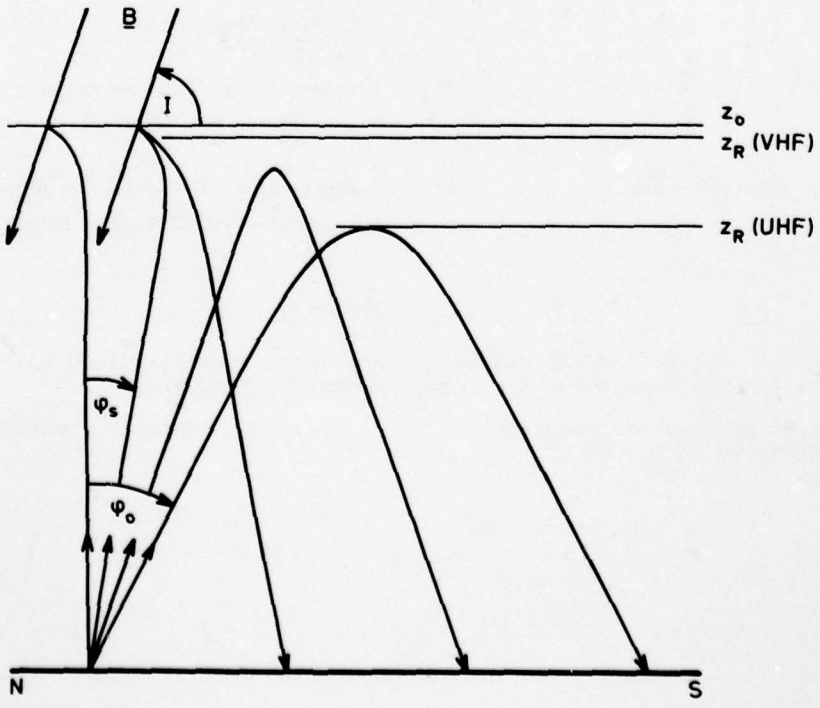

Figure 2

AD-A036 355 ADVISORY GROUP FOR AEROSPACE RESEARCH AND DEVELOPMENT--ETC F/G 20/14
ARTIFICIAL MODIFICATION OF PROPAGATION MEDIA.(U)
JAN 77 H J ALBRECHT

UNCLASSIFIED AGARD-CP-192 NL

2 OF 3
ADA036355

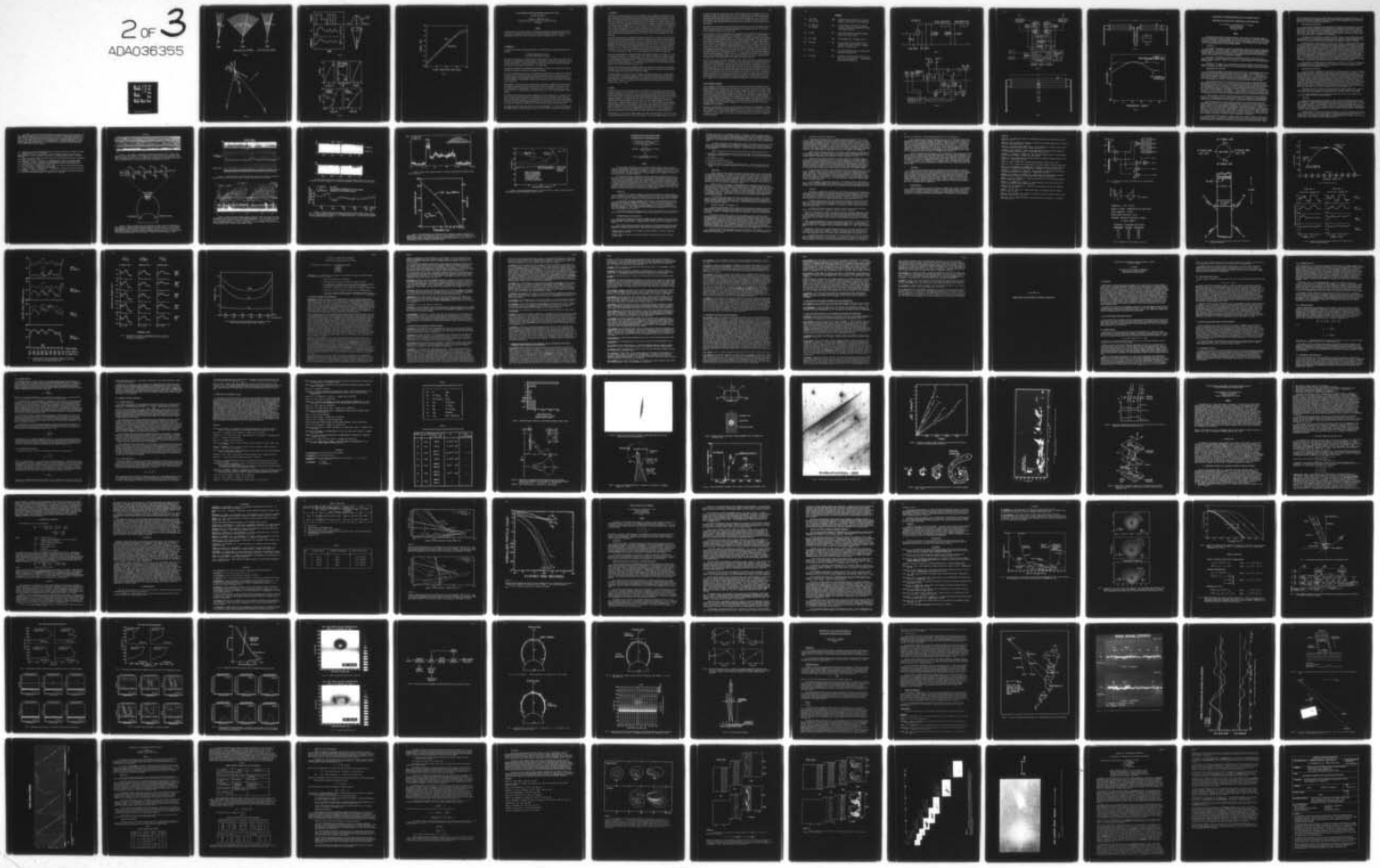

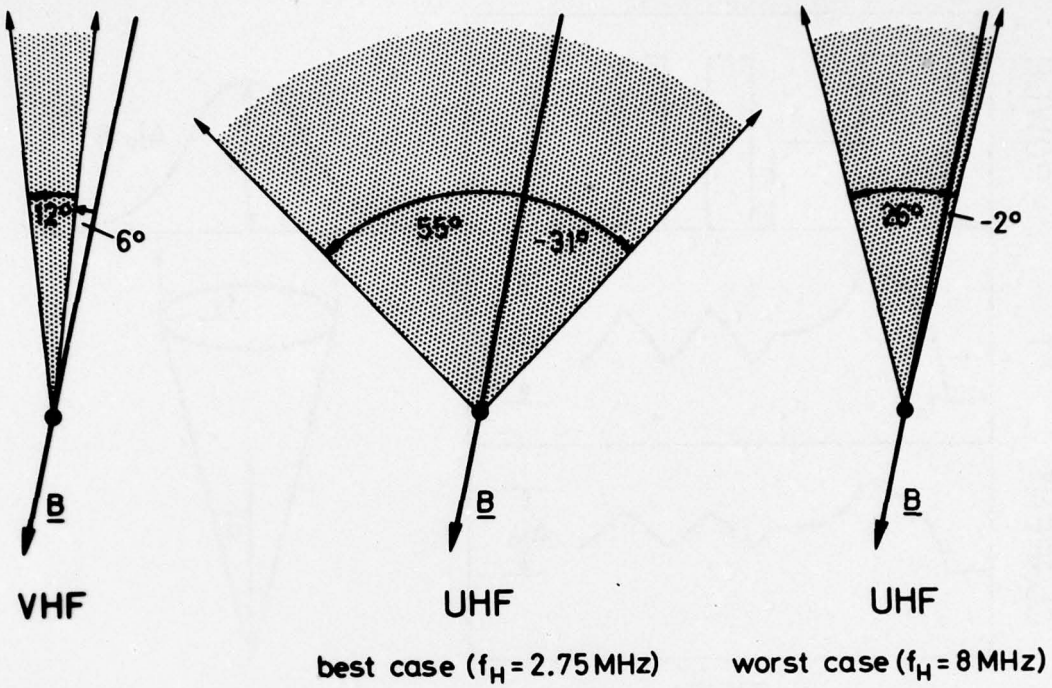

Figure 3

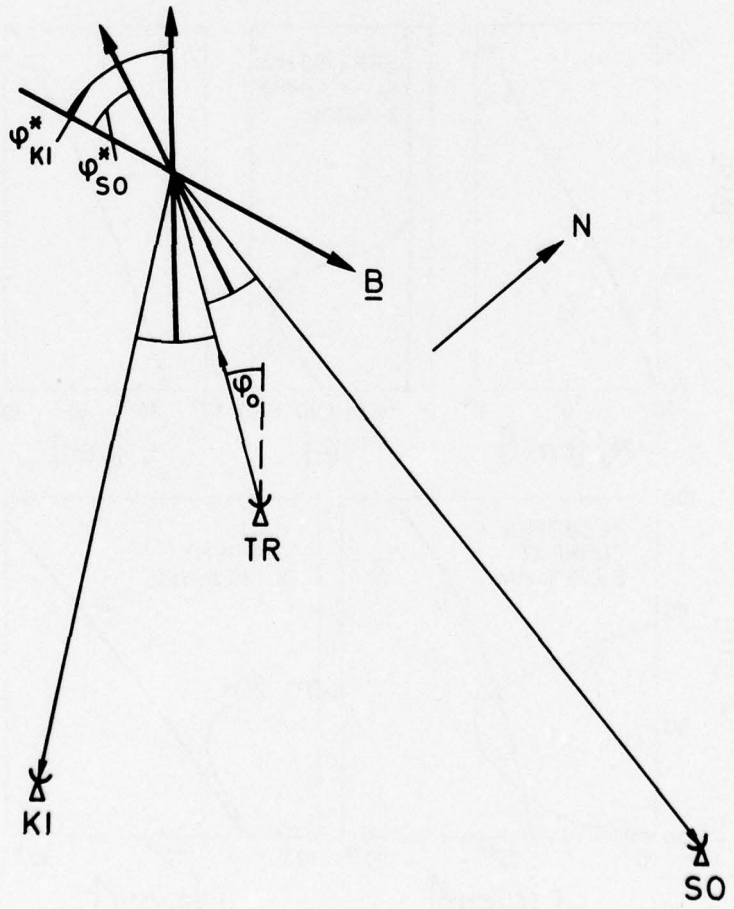

Figure 4

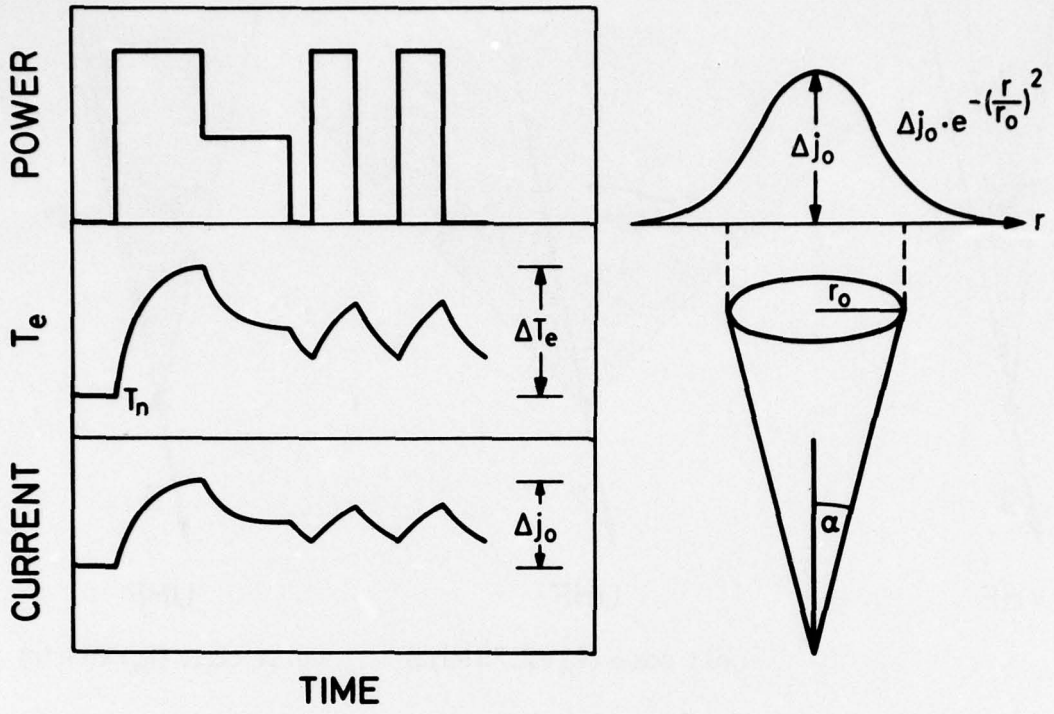

Figure 5

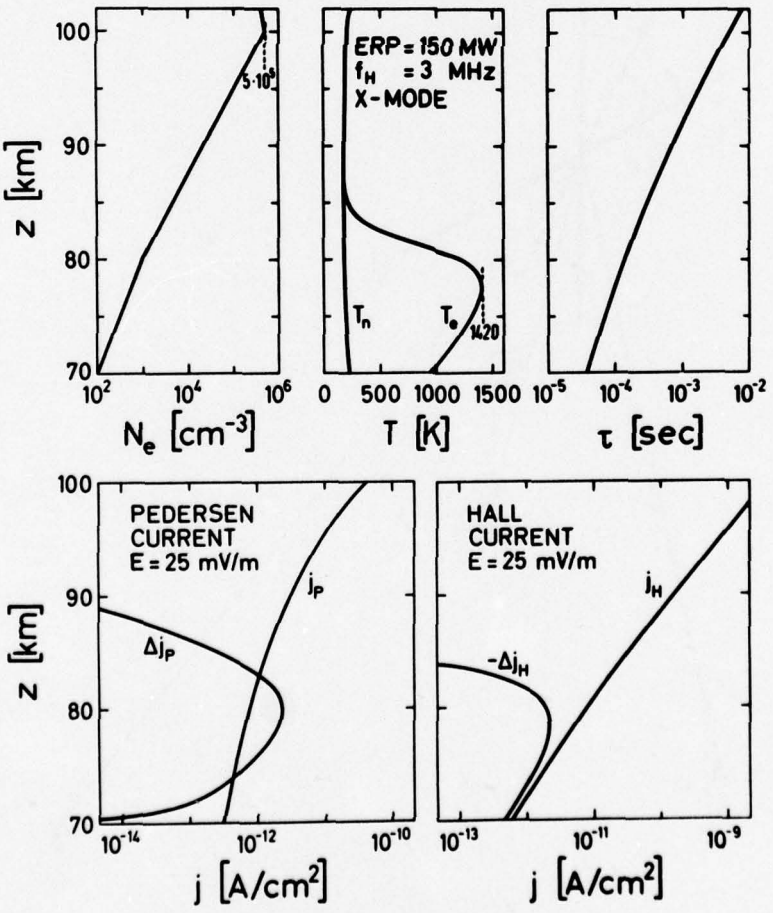

Figure 6

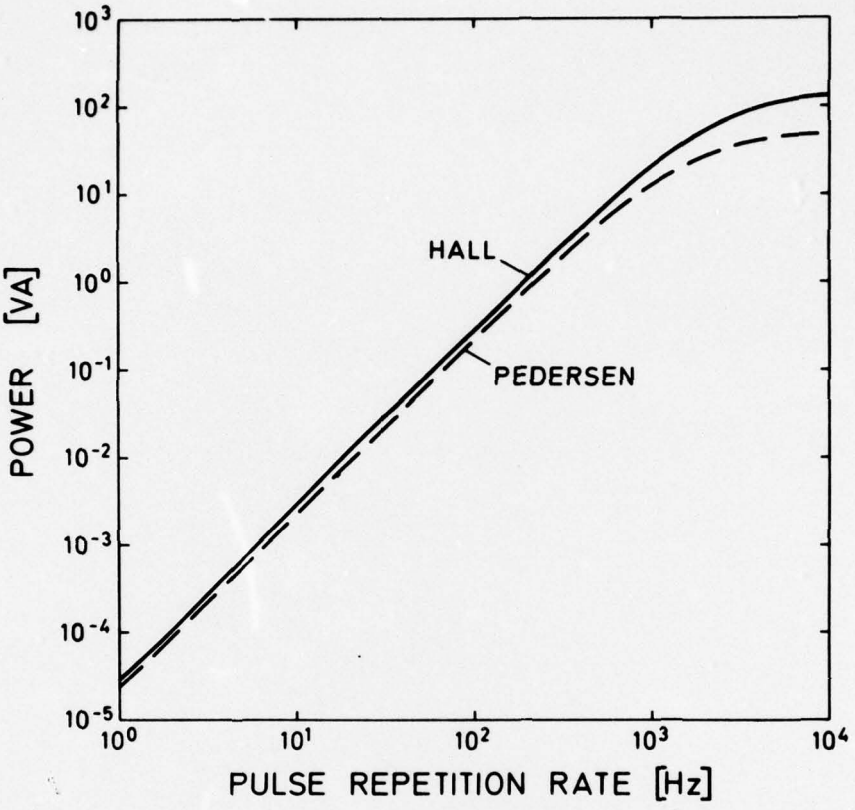
POWER [VA]
PULSE REPETITION RATE [Hz]
HALL
PEDERSEN
10^3
10^2
10^1
10^0
10^-1
10^-2
10^-3
10^-4
10^-5
10^0
10^1
10^2
10^3
10^4

Figure 7

ON THE IONOSPHERIC MODIFICATION EXPERIMENT PROJECTED AT MPI LINDAU: PRACTICAL REALIZATION

H. Kopka, P. Stubbe and R. Zwick
Max-Planck-Institut für Aeronomie, 3411 Katlenburg-Lindau 3,
F.R. Germany

SUMMARY

This paper outlines the technical design of the ionospheric modification experiment described in the preceding paper. The heating facility will consist of 10 100 kW transmitters, feeding into arrays of 5 x 6 corssed dipoles. There will be three such arrays to cover the frequency range 2.75 - 8.00 MHz.

1. INTRODUCTION

To produce the ionospheric modifications described in the preceding paper, one needs power densities of the order

$$2 \text{ m W/m}^2 \text{ at 80 km height (D-region)}$$
$$0{,}1 \text{ m W/m}^2 \text{ at 300 km height (F-region)}$$

These densities correspond to an effective isotropic radiated power of about 150 MW. In practice, of course, the power is radiated upwards to the region where it is most effective, rather than isotropically. Thus the required power densities in the region where they are needed are achieved with an upward directed beam using high gain antenna arrays and transmitter of much lower power.

The appropriate antenna gain is determined by the propagation conditions, by the region which can be observed and by the spatial resolution of the diagnostic equipment.

For the most interesting F-layer effects, the excited plasma instabilities, only those rays are effective which reach a level of reflection at which the "heating" frequency is equal or very near equal to the local plasma frequency. Within the magnetic meridian plane this is given by those rays which produce the "spitze" phenomena. For the geomagnetic conditions near Tromsø this leads to a beam width for the antenna array of about $\pm 6^{\circ}$.

The beam width of the modifying array for effects within the D-region is determined by the beam width of the diagnostic equipment, which involves mainly partial reflection measurements. This implies a circle of 25 km diameter at D-region heights or a beam width of $\pm 10^{\circ}$. As a compromise we decided on a beam width of 8.5°; that is, an antenna gain of 22-23 dB. With this gain, a total transmitter power of 1 MW is required.

For the modification experiments one needs - depending on the type of modification - to be able to select either of the two characteristic waves. Thus the antenna must be able to produce circularly polarized waves with either sense of rotation. This can be done most easily by using crossed linear single antennas, with a phase difference of 90° between each corssed pair. An antenna gain of 22-23 dB can be realized with an array of 5x5 crossed pairs of single half wave linear antennas, including the ground reflection.

The frequency range is fixed at the lower end at twice the gyrofrequency; i.e. 2,75 MHz. At the upper end the frequency must reach the maximum value of f_0F_2, which for 1978-1982 is estimated to be about 8 MHz.

2. Transmitter

The power of 1 MW could be obtained from a single transmitter. But the problems of distribution with the correct phase over the total frequency range, including maintaining the 90^0 phase difference, are formidable. The 90^0 phase difference could be obtained by using two transmitters but the distribution of high power with correct phase over a wide frequency band to 25 single antennas still presents a major technical problem. Further, the construction of 500 kW transmitters is beyond our experience and because of the high cost the purchase of commercial units is out of question. We therefore decided to use 10 transmitters each of 100 KW. Two transmitters feed each row of 6 crossed pairs of linear antennas (a 5 x 5 array fulfills the power requirements but a 6 x 5 array makes the interconnections simpler) with one linear antenna of each pair fed from one transmitter and the orthogonal linear antenna fed from the other transmitter. The 90^0 phase shift between the two halves of each row is made at the transmitter input side of the system.

The use of 10 transmitters has two important advantages in addition. First it makes it very easy to shift the antenna beam in the plane perpendicular to the row direction merely by varying the phase difference at the inputs of the transmitters connected to the 5 rows. Secondly it makes it possible to transmit two frequencies simultaneously by dividing the transmitters and rows into two groups and using two frequency generators. Thus the planned double frequency experiments become very easy. Fig. 1 shows the diagram of a transmitter. It is a linear class AB amplifier, using a solid state wide band exciter and driver (driving power 1,5 KW), so that only the transmitter output section has to be tuned and matched. The output π - L circuit is designed for a VSWR $<$ 2:1, output impedance 50Ω and 40 dB harmonic suppression.

Due to the coupling between the antennas the antenna input impedances change for all antennas, if at one row the matching conditions, i.e. the input current of its antennas is changed. By a computer simulation for the antenna array (based on the Hallèen integral equation [1], [2]) we have found, that the process of tuning and matching converges within 4 or 5 steps by tuning and matching the transmitters one after another (during tuning and matching of one transmitter the nine others are fixed) and repeating the whole procedure, after tuning and matching the series of ten.

The tuning and matching are done by an automatic control. The control units are based on a conventional technique, using a phase discriminator between grid and anode voltage and a voltage discriminator between the output terminal and a certain part of the anode of voltage.

The tuning elements are controlled by special equipment, after they have been preset to approximately correct positions for the selected frequency by a small minicomputer associated with the Dynasonde (see basic diagnostics). The same minicomputer controls the sequence of successive transmitter tuning and matching and its iteration. A flow diagram of the control system for each transmitter and for the total system is shown in Fig. 2 and 3.

3. Antenna

As useful antennas for the full frequency range of 2.75-8 MHz we first considered log. periodic antennas arranged as crossed pairs with 25 pairs in a 5 x 5 array. Each log. periodic antenna should radiate downwards and be reflected at the ground. This requires that the radiating region of the log. periodic antenna should always be about 0.25λ above ground. The spacing between the antennas should be 0.4λ at the lowest frequency. Although it is possible to construct a single log. periodic antenna with these properties ($\approx 0{,}25\lambda$ height, radiation downwards) with a max. VSWr < 2:1 over a frequency range of 3:1 this is no longer true for a large log. periodic antenna array [3], [4]. In an array the mutual coupling between the different antennas produces strong resonances in the frequency range, especially at frequencies at which normally the transition from one main radiating element to the next (using a coarse structure) would occur. In the case of an array either the VSWR would be much higher than 2:1 or the log. periodic structure must be made much finer by using a smaller apex angle, which means using higher antenna towers.

Cost estimates have shown, that it becomes cheaper to use three narrow band antennas in the form of arrays of simple folded dipoles or parallel wire full wave dipoles. To cover the frequency range of 2.75 - 8 MHz

the range is divided into three parts each with a relative bandwidth of 37%. A bandwidth of 37% can be covered easily either with folded dipoles (Fig. 4) [4] or fullwave dipoles with frequency compensation. Calculations show that the VSWR for these "narrow band" antennas is better than 1.6:1. Further the required height for the lowest frequency band is 22 m, which is considerable less than the 30 m for the log. periodic antennas envisaged previously (and this was for an isolated log. periodic antenna and not for an array).

Additionally, the inter-element spacing within each array varies by only 37% over the frequency band, so that the spacing can be such as to give almost maximum gain over the whole band (Fig. 6). In this way we get an avarage additional gain of about 1,5 dB.

On the other hand, of course, we need three times the number of baluns, power dividers, approximately 2.5 times the length of cable and additionally 30 coax-switches. But fortunately, due to the narrow band requirements of the baluns and power divider it is possible to use simple line elements and $\lambda/4$ transformers, instead of the very expensive wide band ferrit core baluns and transformers. The input impedance of a single antenna (folded dipole or full wave) is approximately 500-600Ω. It is rather complicated to make line baluns for these impedances using conventional coaxial cable for the feeder system. Instead, we connect a pair of parallel dipoles by balanced open 600Ω lines and connect the midpoint of the line by a 4:1 balun to 75Ω coaxial cable. To do this we need an even number of antennas in each row. However, the new arrangement using 6 antennas per row and 5 rows requires only 3/5 the number of baluns and about 3/5 the length of cable that of the previously planned 5 x 5 array. In prices the changes nearly compensate, so that we have now decided on an antenna field of 6 x 5 crossed dipoles which gives a gain of approximately 24 dB or 250 MW effective power. This is more than necessary for the most F-layer modification experiments but for the D-region modification we want as much power as possible.

The three 75 coax lines of each row are connected to power dividers consisting of simple 50Ω to 25Ω transformers (Input 50Ω/100 KW, output 3 x 75 in parallel). These power dividers are constructed from two $\lambda/4$ transformer lines with Chebycheff behaviour for the reflection coefficient. The mismatch over the frequency range is less than 1.05:1. The transformers with a total length of $\lambda/2$ (corresponding to each band midpoint frequency)are part of the feeding system and shorten the line length considerably. They are constructed from aluminium tubing of 100 mm outer diameter. The same tubing is also used as the outer conductor for the 100 KW coax lines. This coax line construction is similar to that used in the Boulder experiment and originally in the Jicamarca equipment [5], [6]. However, the weather conditions at Tromsø require additionally, that the connections of the tubes be waterproof. The total feeding system consists of 9000 m line for 100 KW (100 mm outer diameter) and 9000 m for the 35 KW (60 mm outer diameter).

4. Basic diagnostic equipment

The main diagnostic instrument will be the EISCAT facility, the partial reflection equipment and photometers. Additionally as an integral part of the heating facility a digital ionosonde will be used. (Dynasonde[7]) which will be constructed at Boulder. With this instrument we can measure the time delay, phase and amplitude of a wave reflected by the modified ionosphere. Their interpretation is partly done in real time by using the available software developed by J.W. Wright et al and additional software developed for the heating experiment. We shall thus be able to determine and set very quickly the optimum frequency, power and special program of measurements by using the Dynasonde computer, which communicates directly with the minicomputer that controls the transmitters. A further (and in practice very important) use of the Dynasonde computer lies in the automatic documentation in print and tape storage form of the various programmes and their parameters.

Additionally the Dynasonde will be used as probe transmitter and receiver for a complementary cross-modulation experiment, in which the heating transmitters are used as the disturbing transmitter in a complementary manner. That is, instead of using short disturbing pulses, we will use a CW heating signal which is pulsed off with short pulses. In this way we can use the cross modulation technique for investigating the modified D-region.

REFERENCES

[1]	V.W.H. Chang and R.W.P. King	1968	Theoretical Study of Dipole Array of N Parallel Elements; Radio Science, Vol. 3, No.5, May 1978
[2]	R.L. Tanner and M.G. Andreasen	1967	Exact calculation of arbitrary wire antennas; TCI Report, Technology for Communications International, Mountain View Cal.
[3]	R.H. Kyle	1970	Mutual Coupling Between Log.-Periodic Antennas; IEEE T-AP Vol. AP 18, Jan 1970
[4]	E.M.T. Jones	1975	Private communication, TCI Mountain View Cal.
[5]	P.W. Arnold	1973	An HF High-Power Vertically Directed Array For Ionospheric Modification; NBS Dept. of commerce Boulder, Col. OT Report 73-21
[6]	G.R. Ochs	1965	The Large 50 MC/S Dipole Array at Jicamarca Radar Observatory; NBS Report 8772
[7]	J.W. Wright	1975	Development of Systems for Remote Sensing of Ionospheric Structure and Dynamics - Dynasonde; NOAA SEL-Preprint 206, Boulder, Col.

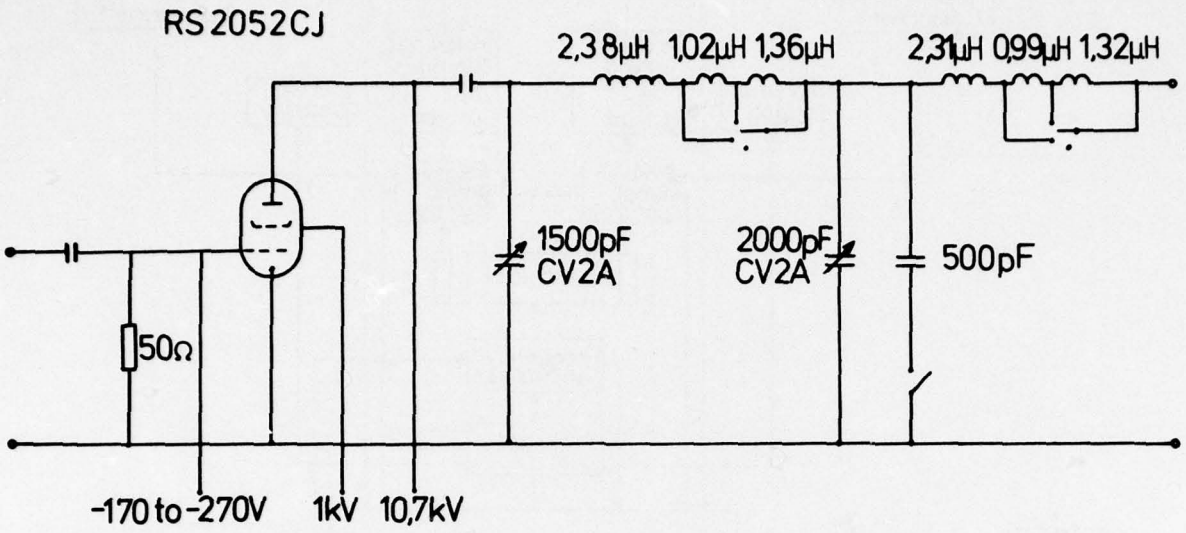

Figure 1

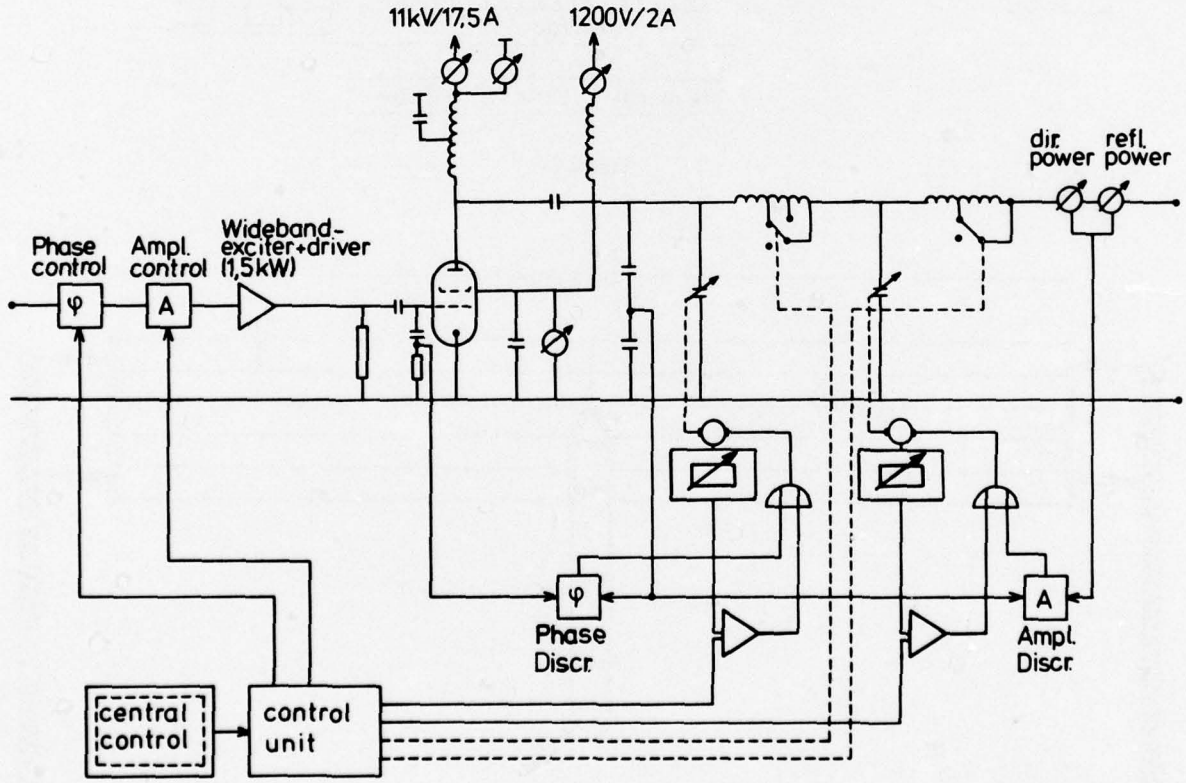

Figure 2

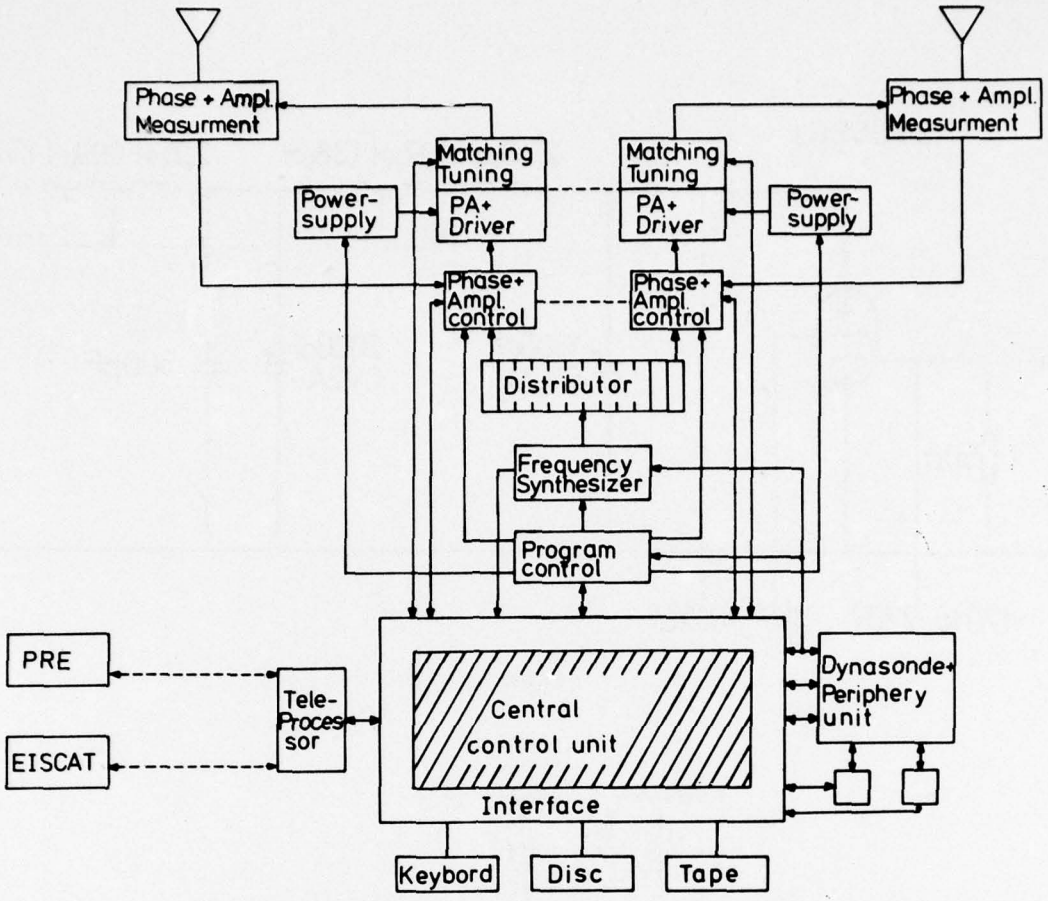

Figure 3

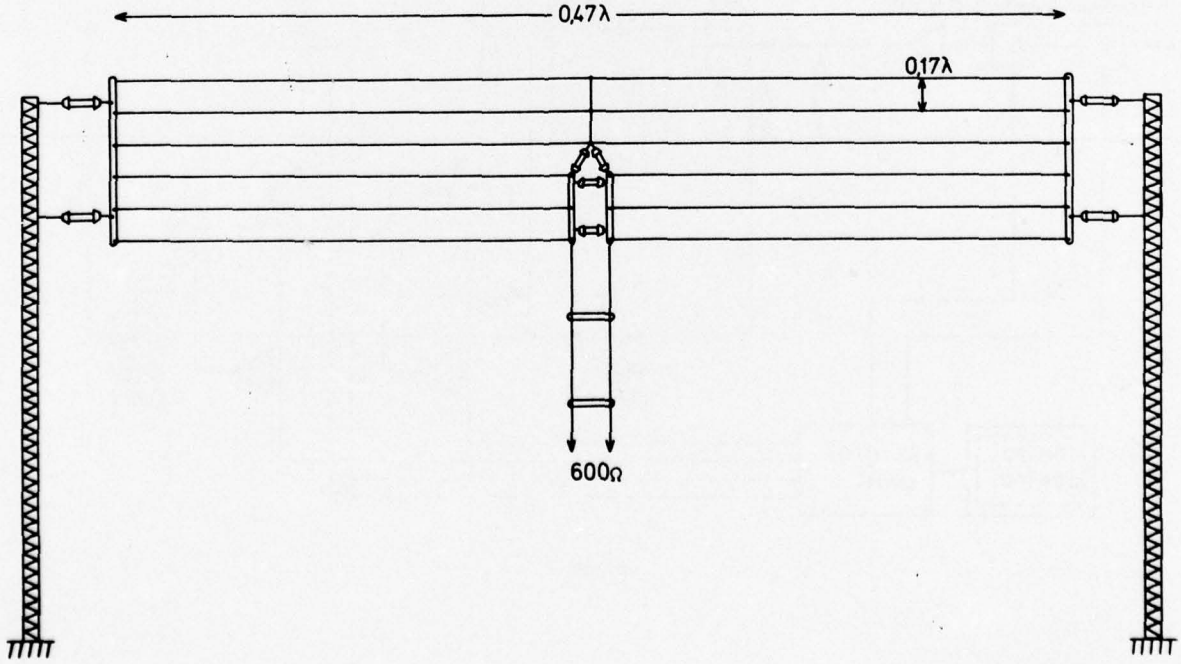

Figure 4

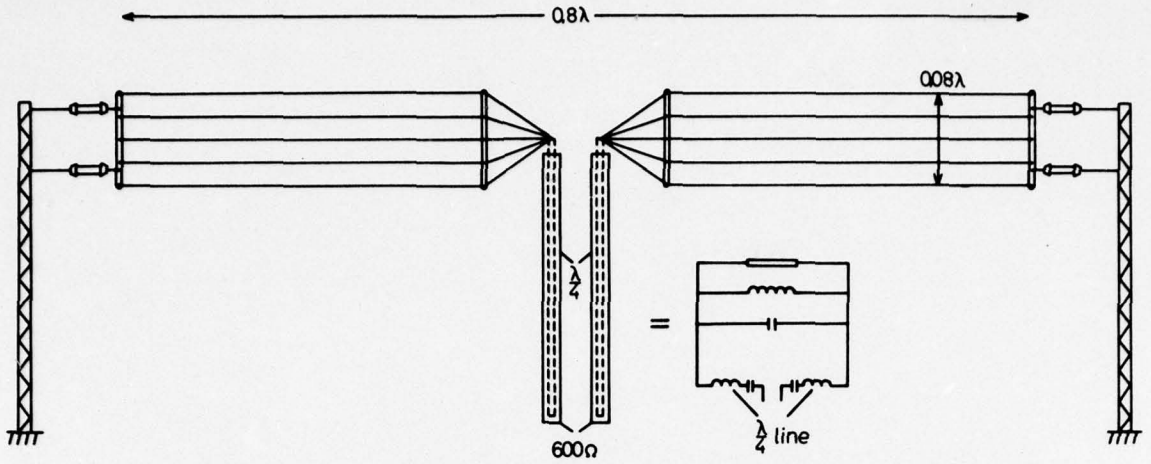

Figure 5

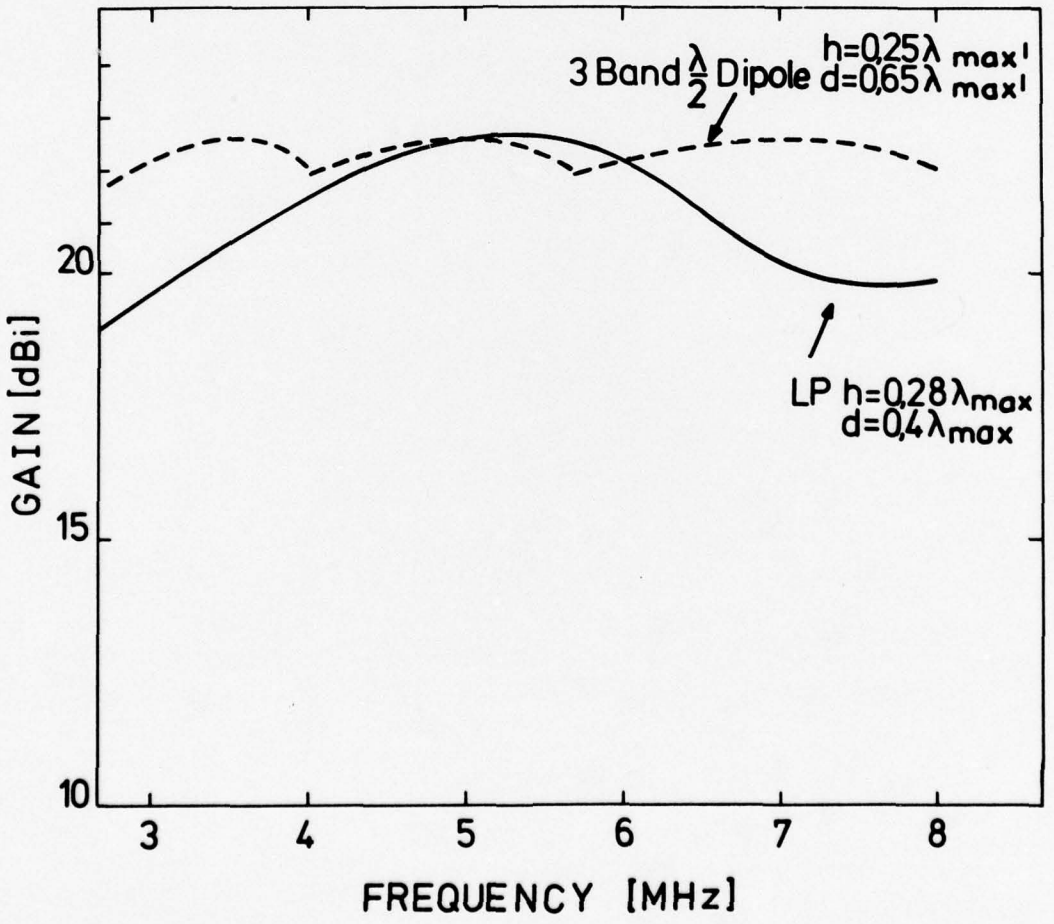

Figure 6

MODIFICATION OF THE PROPAGATION CHARACTERISTICS OF THE IONOSPHERE (AND THE MAGNETOSPHERE) BY INJECTION INTO THE MAGNETOSPHERE OF WHISTLER-MODE WAVES

R. A. Helliwell, J. P. Katsufrakis and P. A. Bernhardt
Radioscience Laboratory
Stanford University
Stanford, Ca. 94305
USA

SUMMARY

Wave-induced precipitation of energetic electrons is known to modify the ionosphere. Natural whistler emissions scatter energetic electrons into the loss cone resulting in >30 keV Bremmstrahlung Xray bursts and in temporary (~30 sec) enhancements of the electron density between 70 and 90 km. In an attempt to bring these ionospheric perturbations under man's control, coherent whistler-mode VLF signals are being injected into the magnetosphere from Siple Station, Antarctica. Future experiments may involve transmission of VLF signals from satellites such as the Space Shuttle.

1. INTRODUCTION

The purpose of this paper is to describe a new technique for modifying the electrical properties of the lower ionosphere. Electromagnetic waves in the whistler-mode frequency range are used to precipitate energetic electrons into the D and E regions. Advantage is taken of the amplifying properties of the magnetosphere which can increase the power density of a whistler-mode wave by three orders of magnitude. During and after the amplification process, energetic electrons are scattered in pitch angle producing an increase in the particle flux that is absorbed by the ionosphere.

The energy of the precipitating electrons is converted into ionization, heat, airglow, and Bremsstrahlung Xrays. The absorbed energy which goes into ionization alters the electrical properties of the earth-ionosphere waveguide. Changes in the strength of a VLF wave propagating in this waveguide may be as much as 6 db.

The balance of this paper will 1) review the direct and indirect evidence for wave-induced ionospheric perturbations, 2) suggest evidence of pitch-angle scattering of energetic electrons in the magnetosphere by coherent wave-particle interaction, and 3) discuss further experiments that might be performed.

2. BREMSSTRAHLUNG XRAY EXPERIMENT

The first direct evidence of the control of electron precipitation by electromagnetic waves was obtained in an experiment performed at Siple Station, Antarctica on January 2, 1971 [Rosenberg et al., 1971]. A balloon at 30 km altitude recorded Bremsstrahlung Xrays above an energy of 30 keV. Simultaneously, ground recordings were made of natural VLF noise in the very low frequency range. A substorm event occurring at the time produced an interesting one-to-one correlation between bursts of Xrays and bursts of VLF noise as shown in Figure 1. Analysis of conjugate point recordings showed that the bursts of VLF noise were in fact triggered by whistlers which were excited by northern hemisphere lightning discharges.

A cross-correlation analysis was performed on the Xray count rate and the integrated amplitude of the VLF emissions between 2 and 6 kHz. It was found that the VLF wave packets arrived earlier than the Bremsstrahlung Xrays by 0.3 to 0.4 seconds. Using the known properties of the whistler-mode and assuming that the precipitation resulted from a cyclotron resonance interaction between the waves and the particles, the interpretation of Figure 2 was developed. In this picture energy exchange between electrons and whistlers occurs when the electrons see a Doppler shifted wave frequency equal to their own gyrofrequency. This is called cyclotron resonance, the condition for which is given by $\Omega = \omega - kv$ where ω = electron gyrofrequency, ω = wave frequency, k = wave number, v = parallel velocity of electron. The waves can grow during this process and at the same time reduce the average pitch angle of the interacting particles. Some of the particles close to the loss cone will thereby be forced into the loss cone and will be precipitated.

A significant point is that the strong Xray bursts were associated only with whistler triggered emissions. This indicates that signals injected from the ground play a dominant role in the wave-particle interactions in the magnetosphere. We conclude therefore that the use of manmade waves approximating the characteristics of a whistler should be very effective in controlling precipitation into the ionosphere.

Wave-induced perturbations of the ionospheric electron density can be observed in another way. Long distance VLF propagation in the earth-ionosphere waveguide is very sensitive to properties of the D and the E regions as is well known [Potemra and Rosenberg, 1973]. Observations at Eights, Antarctica have revealed a surprising association between VLF subionospheric propagation and whistlers. An example is shown in Figure 3. Earth-ionosphere waveguide propagation of Station NSS from Annapolis to Eights Station, Antarctica is shown in the lower panel. A strong whistler is seen in the upper panel at about the middle of the record. At the same time the signal strength of NSS increases by about 6 db. The signal strength then slowly recovers to its previous value (the full recovery is not shown in the figure). Recovery times typically run about 10-70 seconds, the average being close to 30 seconds. Apparently each strong whistler produces sufficient precipitation to change the electrical properties of the waveguide.

Indirect evidence of precipitation is found in observations of the wave-particle interactions that accompany precipitation. The mechanism for the amplification of VLF signals is thought to be the same one which accounts for wave-induced electron precipitation. Consider the amplitude of variable pulse length signals transmitted at Siple Station and received at Roberval, Quebec as illustrated in Figure 4. Amplifi-

cation of pulses increases as the pulse length increases until saturation is reached (at 250 msec in this case). Amplification (and precipitation) grows with pulse length until the number of energetic particles remaining to be bunched (or scattered) is exhausted. Analysis of the maximum amplification available may indicate a limit on the maximum precipitation possible.

3. WAVE-INDUCED NOISE SUPPRESSION

In the course of observations of VLF signal amplification using the Siple transmitter a surprising new effect was discovered. Sometimes the amplified signal is accompanied by a suppression of background natural noise in a narrowband just below the transmitter carrier frequency. Within this band, which is about 50-200 Hz wide, the natural noise is attenuated by as much as 6 db (Figure 5). Thus a conventional subionospheric signal channel at VLF could under these conditions exhibit an increase in signal-to-noise ratio of 6 db. This assumes of course that the VLF receiver is located in a region where the major component of the background noise is generated in the magnetosphere.

The mechanism of wave-induced noise suppression is not fully known. We are considering mechanisms involving the effect of a strong wave on the particle population. Figure 6 illustrates the scattering of resonant particles out of a band where the suppressed noise lies (Umran Inan, private communication, 1976). The particles thus scattered may participate in ionospheric modification by corpuscular ionization.

Another mechanism of signal suppression, which may be of interest in connection with communication problems, is the attenuation of amplified waves by other signals at nearly the same frequency. For example it is observed that Siple pulses can be amplified 30 db and then attenuated by 3 db or more when the echo of the previous signal is received. Here the mechanism is better understood. It is known that amplification requires relatively monochromatic wave trains. Broadband noise is not amplified very much. If during amplification a second signal is added to the first at a slightly different frequency then the spectrum is broadened and the amplification is reduced. The suggested explanation is that the phase bunching of resonant particles is not as effective when the spectrum is broad. It is necessary for the resonant electrons to see a phase stable wave train throughout the bunching process, which may occupy a distance of about 1000 km in the magnetosphere. Wave components extending over a frequency range such that the electron sees one or more phase reversals during its traversal of the interaction region cause reduced bunching efficiency. It is believed that this mechanism accounts for the suppression of growth by echoes of the transmitted pulse. Thus any signal being amplified in the magnetosphere and being used for communication could in principle be attenuated by simply adding another wave at a slightly different frequency.

In some cases, an amplified wave may be attenuated by its own echo. In Figure 7, a 30 second pulse is attenuated by the echo 4.1 seconds after the signal was keyed. The value of 4.1 seconds is the round-trip propagation time in the magnetospheric duct. A similar effect is noted when the echo of a short pulse coincides with the reception of a later pulse.

4. MAN-MADE PRECIPITATION EVENTS

It is clear from the experiments just described that it should be possible to control the precipitation of energetic electrons. Experiments to test this idea have been performed at Siple Station. Coherent whistler-mode signals were injected into the magnetosphere and were observed at the conjugate point at Roberval, Quebec [Helliwell and Katsufrakis, 1974]. Amplification of 30 db was frequently observed, making the amplified signals as strong as any natural signals observed in the magnetosphere. However precipitation effects directly connected with these signals have not yet been seen. The reason we believe is that the optimum frequency for amplification and triggering is close to half the gyrofrequency on the path. At such frequencies the energy of the interacting particles is relatively low, of the order of a few kev (Figure 8). These particles when precipitated are absorbed well above the D region. Thus the Xray and VLF perturbation experiments mentioned earlier do not have sufficient sensitivity to detect the effects of low energy particles. Work is in progress to look for various effects, such as auroral type emissions and magnetic field perturbations, that may be connected with the Siple transmissions. Some interesting results have already been obtained but no conclusive relationships have yet been demonstrated.

Enhancement of the E and D regions with the precipitation of energetic electrons with a characteristic energy of 45 keV and an energy flux of 2 ergs/cm^2/sec is illustrated in Figure 9 [Bell, 1976]. Fluxes of this energy may be produced by propagating high power VLF signals around a 2 kHz frequency.

Bell [1976] has suggested that high energy precipitation may be used for the generation of ULF radiation by modification of the E-region conductivity.

5. CONCLUSION

Natural wave-induced precipitation has been observed in the form of enhanced Bremsstrahlung Xrays and perturbation of VLF sub-ionospheric propagation. In order to duplicate these observations using the Siple transmitter, it appears to be necessary to radiate more power at the lower frequencies (i.e., 2-4 kHz) that is presently available. The radiated power levels at the low end of the frequency range are not as high as found in many whistler and VLF emissions. However it is expected that integration techniques will make possible a significant increase in the sensitivity of the various detection methods. The advantage of a controlled source is the ability to accurately time the excitation of precipitation and thereby provide a basis for long term integration.

Another approach to the control of precipitation by waves is to place a transmitter in a satellite, such as the Space Shuttle. Then the losses involved in coupling the energy into the magnetosphere would be greatly reduced. In addition a much larger range of wave normal angles could be excited. It is conceivable that a large increase in the precipitated flux could be obtained by this means, giving rise to much larger effects in the ionosphere than have already been observed.

The probability of detecting wave-induced particle precipitation would be greatly increased if VLF waves could be injected into a duct at a known location. The release of gases (such as H_2) which chemically deplete the ionosphere may be used to create artificial ducts in the magnetosphere [Bernhardt et al., 1976]. At night, the ionospheric hole resulting from the release of chemically reactive gases will be filled by field aligned flow of plasma out of the magnetosphere. The depleted magnetospheric flux tube may be used as a duct to guide VLF waves. The injection of strong VLF signals from satellite into artificially created ducts may provide for the first time the ability to produce wave-induced controlled electron precipitation at a given location.

Bailey, D. K., 1968, "Some Quantitative Aspects of Electron Precipitation in and Near the Auroral Zone", Reviews of Geophys., Vol. 6, 3, 289-346.

Bernhardt, P. A., A. V. da Rosa and C. G. Park, 1976,"Chemical Depletion of the Ionosphere", AGARD/EPP Specialists' Meeting on Artificial Modification of Propagation Media, Paper No. 19, Brussels, 26-30 April.

Bell, T. F., 1976, "ULF Wave Generation Through Particle Precipitation Induced by VLF Transmitters", submitted to J. Geophys. Res., 1975.

Helliwell, R. A. and T. L. Crystal, 1973, "A Feedback Model of Cyclotron Interaction between Whistler-Mode Waves and Energetic Electrons in the Magnetosphere," J. Geophys. Res., 78, 7357, 7371.

Helliwell, R. A. and J. P. Katsufrakis, 1974, "VLF Wave Injection into The Magnetosphere from Siple Station, Antarctica," J. Geophys. Res., 79, 2511-2518.

Helliwell, R. A., J. P. Katsufrakis and M. L. Trimpi, 1973, "Whistler-Induced Amplitude Perturbation in v.l.f. Propagation," J. Geophys. Res., 78, 4669-4688.

Potemra, T. A. and T. J. Rosenberg, 1973, "VLF Propagation Disturbances and Electron Precipitation at Midlatitudes," J. Geophys. Res., 78, 1572.

Rosenberg, T. J., R. A. Helliwell and J. P. Katsufrakis, 1971, "Electron Precipitation Associated With Discrete Very-Low-Frequency Emissions," J. Geophys. Res., 76, 8445-8452.

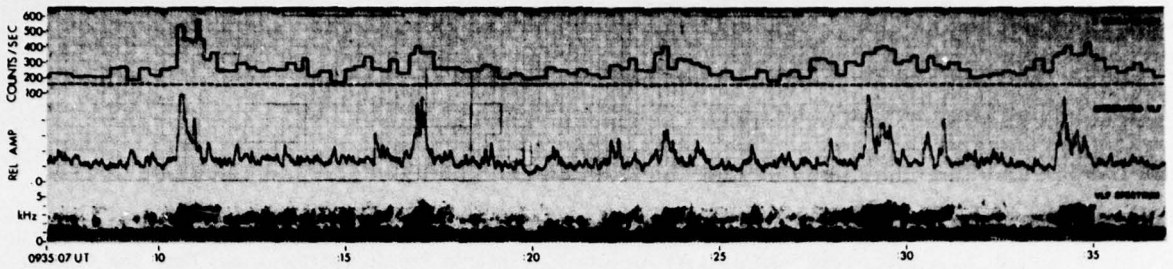

Figure 1. A 30 s segment of simultaneous recordings of Xray count rate for E > 30 kev (top), integrated vlf amplitude from 0.6 to 5 kHz (middle), and vlf spectrum from 0 to 5 kHz (bottom) at Siple Station, Antarctica, on 2 January 1971. The dashed line in the top portion of the figure refers to the cosmic-ray background level of ca. 175/c/s. (Because of a plotting error the Xray record must be shifted 0.15 s to the right relative to the vlf records.) (figure 1, Rosenberg et al. [1971]).

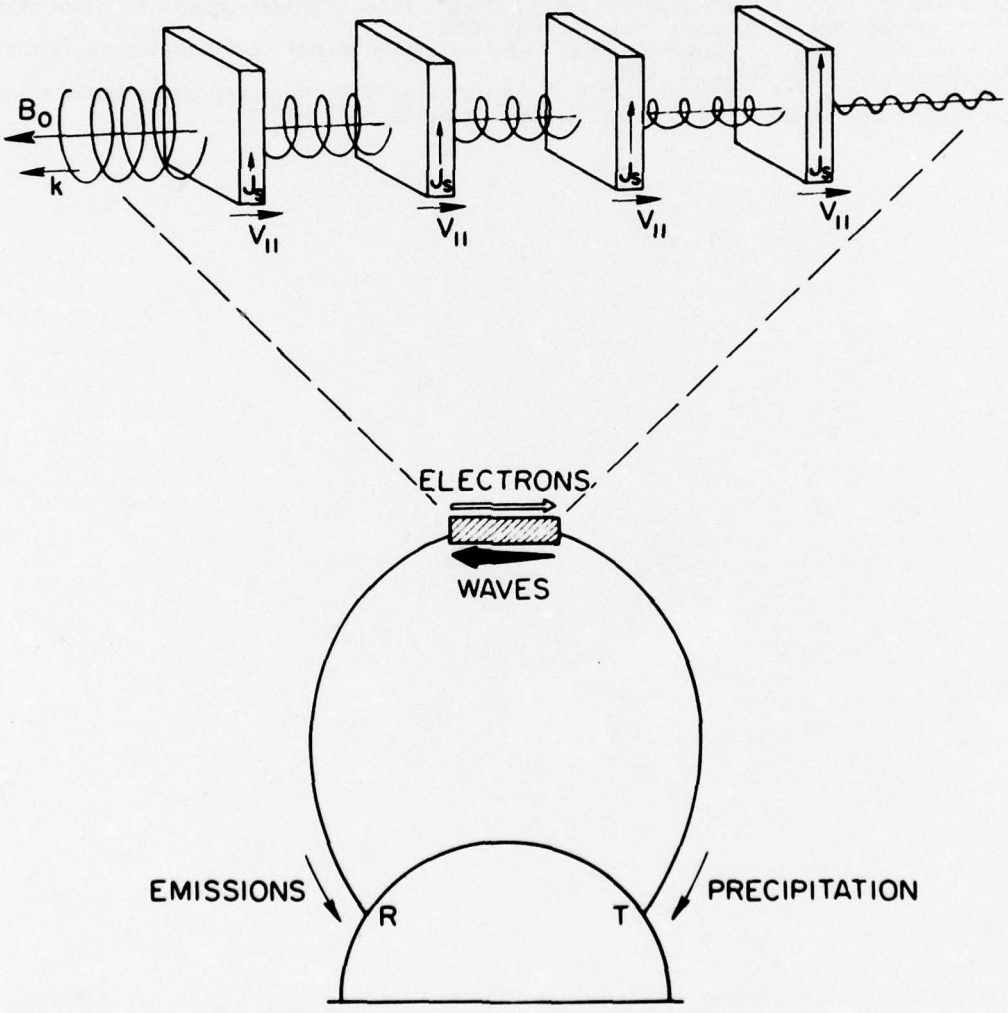

Figure 2. Sketch of interaction region, or emission cell, model. Circularly polarized waves transmitted from T resonate with oppositely traveling electrons near the equator. The train of electron sheets represents a continuous stream of resonant electrons. The resonant electrons in each sheet are phase-bunched by the wave, producing a transverse stimulated current J_s. The change in wave amplitude shown across each sheet results from the addition of the wave component generated by J_s. Emissions travel to R, and the scattered electrons are precipitated at T (figure 1, Helliwell and Crystal [1973]).

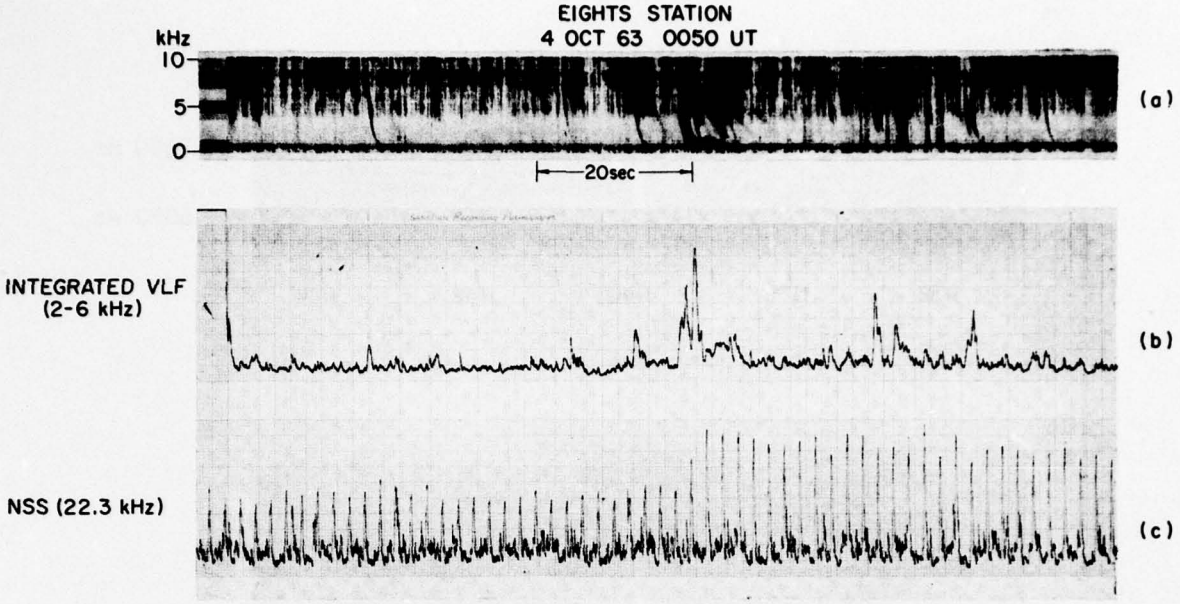

Figure 3. (a) Whistler spectra; (b) whistler amplitude, 2-6 kHz; and (c) NAA pulse transmissions observed at Eights Station, Antarctica (figure 2, Helliwell, Katsufrakis and Trimpi [1973]).

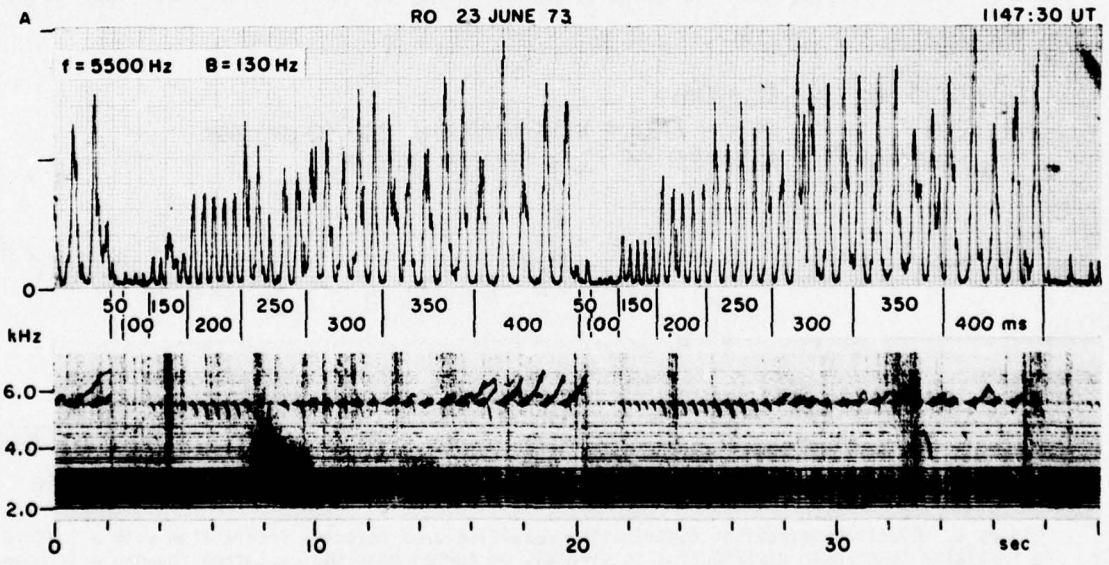

Figure 4. Variable pulse length sequence received at Roberval. Lower panel shows the spectrum, and upper panel shows the amplitude in a 130 Hz bandwidth centered on 5.5 kHz. Pulse lengths vary from 50 to 400 ms in 50 ms steps as indicated by the numbers between panels. A two-hop whistler, with echoes at ca. 3 kHz, appears at 8-10 s; its source is the sferic at 4.2 s. A strong well defined two-hop whistler component extending up to 5.5 kHz is seen at about 8.2 s and corresponds to the one-hop delay of the Siple pulses (figure 2, Helliwell and Katsufrakis [1974]).

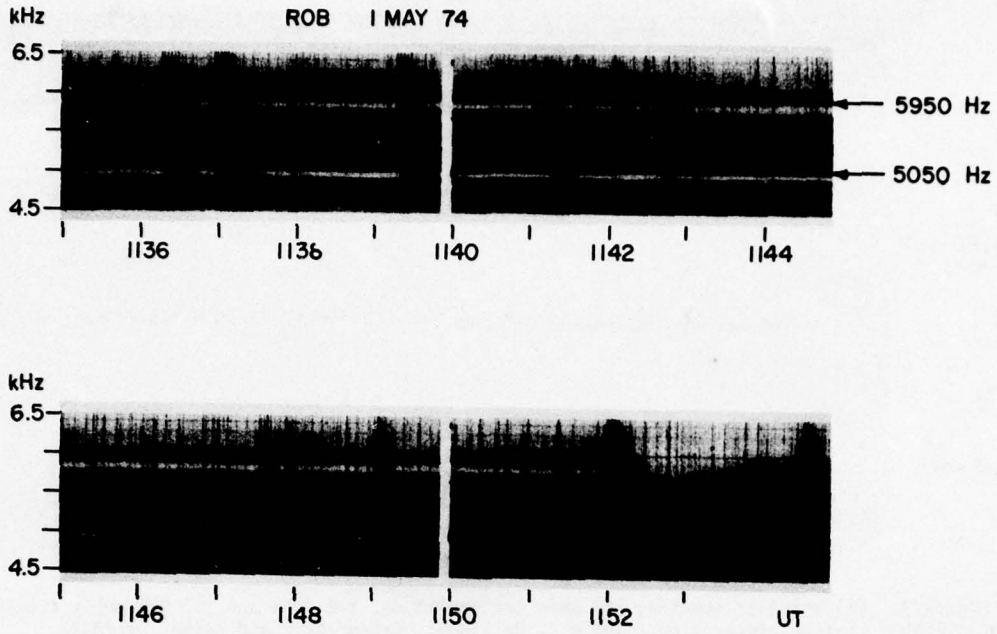

Figure 5. Roberval spectrograms illustrating "quiet bands" immediately below the 5,950- and 5,050-Hertz transmitter frequencies. The transmissions terminated at 1152 Universal Time (lower right).

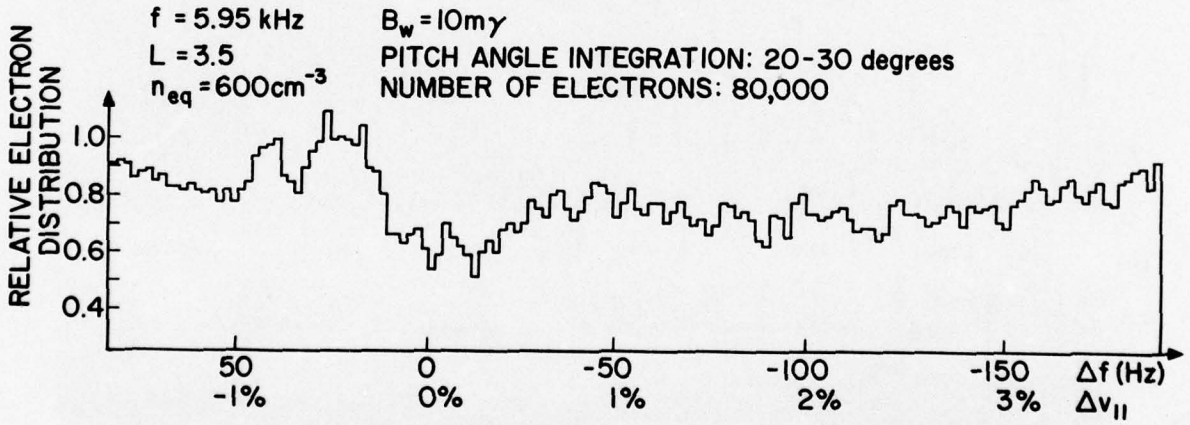

Figure 6. Electron velocities distribution resulting from resonant interaction with a 5.95 kHz wave. An initially istotropic distribution is strongly perturbed near the cyclotron resonance frequency ($\Delta f = 0$). The scattering of electrons out of the frequency band below $\Delta f = 0$ account for the production of noise suppression bands in Figure 5.

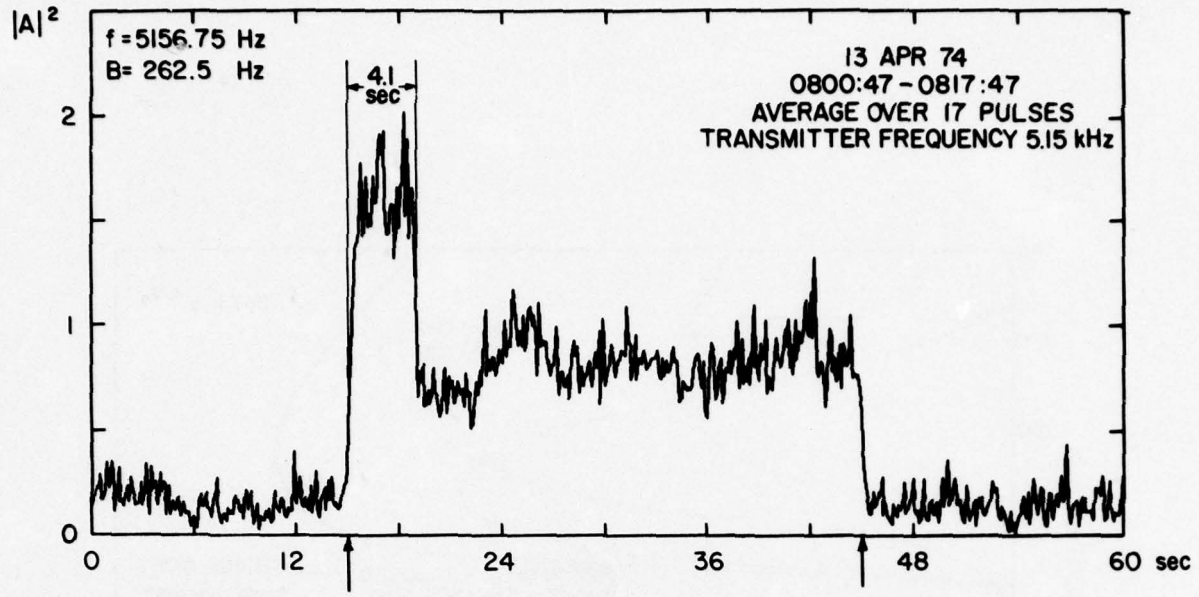

Figure 7. Average of the squared amplitude of 17 successive 30-second Siple transmitter pulses received at Roberval.

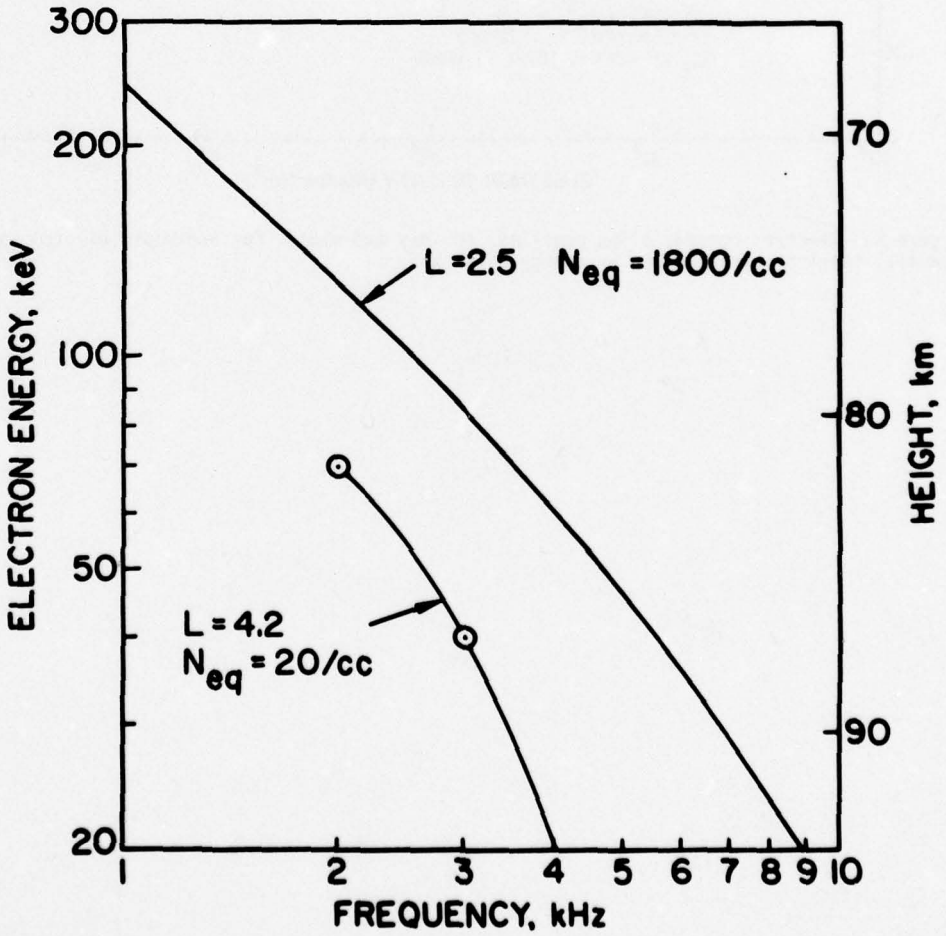

Figure 8. Relation between electron energy and whistler frequency for equatorial regions of the magnetosphere. The two curves represent an L shell of 2.5 with an equatorial electron concentration of 1800 cm^{-3} and an L shell of 4.2 with an equatorial electron concentration of 20 cm^{-3}. The right scale shows the approximate height of penetration of the energetic electrons whose energies are given on the left scale (Figure 9, Helliwell, Katsufrakis and Trimpi [1973]).

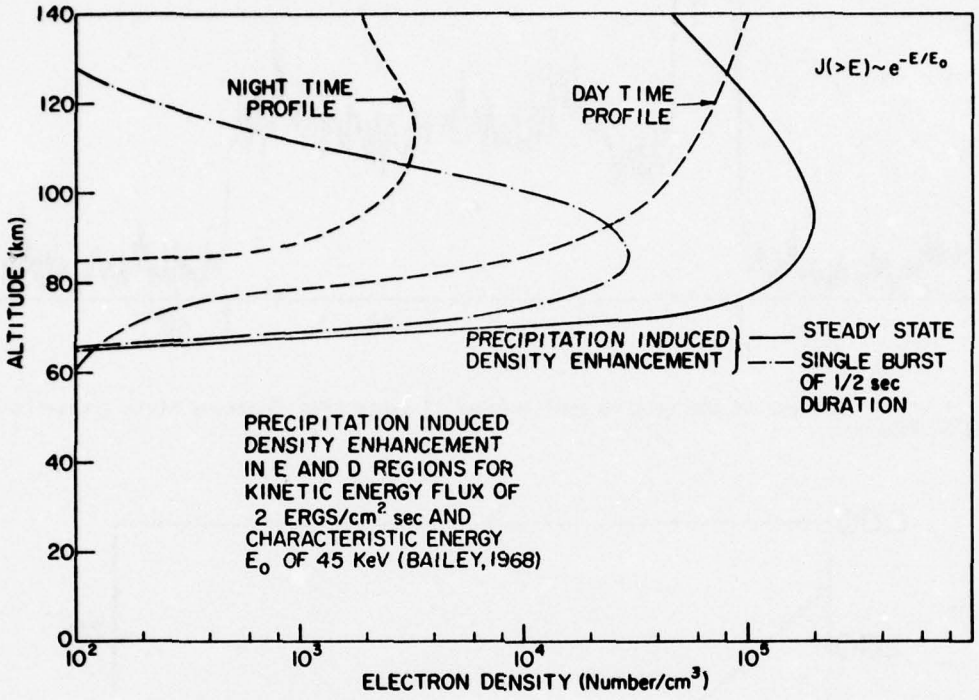

Figure 9. Electron concentration profiles, for day and night, for isotropic electron precipitation with exponential spectra characterized by energy of 45 keV.

LOW FREQUENCY ELECTRIC FIELD VARIATIONS DURING HF TRANSMISSIONS ON A MOTHER-DAUGHTER ROCKET

T.J. Rosenberg[†], N.C. Maynard[*], J.A. Holtet,
N.O. Karlsen, and A. Egeland
The Norwegian Institute of Cosmic Physics
Oslo, Norway

T. Moe
Department of Physics, University of Bergen
Bergen, Norway

and

J. Trøim
Norwegian Defence Research Establishment
Kjeller, Norway

SUMMARY

HF wave propagation experiments have been conducted on Mother-Daughter rockets in the polar ionosphere. Swept-frequency transmissions from the Mother, nominally covering the range from 0.5 to 5 MHz in both CW and pulse modes, are received by the Daughter. In the most recent rocket of the series, the Mother also contained an AC electric field spectrometer covering the frequency range from 10 Hz to 100 kHz in four decade bands. This paper examines the low frequency response of the ionosphere with respect to waves emitted from the onboard HF transmitter.

During off periods, the low frequency data indicated the presence of background noise levels which were in substantial agreement with previous rocket and satellite measurements of AC electric field variations in the E- and F-regions. Marked intensity enhancements, particularly below 10 kHz, occurred in the F-region during on periods in the CW mode. Specific features were noted at HF frequencies near 1.1 and 1.7 MHz and between approximately 2.4 and 2.9 MHz. None of these features occurred consistently at frequencies which could clearly be identified with critical frequencies of the ionospheric plasma. It is suggested that the observed ELF/VLF electric field variations are electrostatic oscillations associated with field-aligned density irregularities contained in a turbulent region created by the transmitted HF radiowaves. Calculations indicate that the size of the turbulent region extended no further than ~ 100 m from the transmitter, a result which is consistent with the observations.

1. INTRODUCTION

In recent years the capacity to modify the earth's plasma environment by artificial means has increased substantially our knowledge of fundamental interactions occurring in the ionosphere and magnetosphere. The methods which have been used include electron guns, ion releases, and radiowave propagation. Here, we will be concerned with modification techniques which inject HF wave energy into the ionosphere.

It is well known that heating experiments conducted from the ground produce plasma turbulence in the F-region (UTLAUT, 1975; GORDON and CARLSON, 1974). Likewise, it has been shown that HF transmissions from rockets (FOLKESTAD and TRØIM, 1974; FOLKESTAD et al., 1976) and satellites (PALMER and BARRINGTON, 1973) can stimulate resonances at or near certain critical frequencies associated with the local plasma environment. Topside sounder (PALMER and BARRINGTON, 1973) and rocket (MATSUMOTO et al., 1975; 1974; MIYATAKE et al., 1974) observations also have shown that the ionosphere has a low frequency response when stimulated by HF radiowaves.

In this paper we examine the response of an AC electric field spectrometer covering the frequency range from 10 Hz to 100 kHz during HF transmissions from a rocket launched into the polar ionosphere.

2. INSTRUMENTATION AND FLIGHT CONDITIONS

The electric field data were obtained by instruments on a Mother-Daughter rocket launched from Andøya Rocket Range in northern Norway. The electric field experiment, carried by the Mother, consisted of two independent systems connected to orthogonal antennas. Figure 1 gives a block diagram of one system.

One of the main purposes of the launch was to conduct an HF wave propagation experiment between the separated sections of the rocket payload. The transmitter, also carried by the Mother, was swept exponentially in frequency between 0.55 and 3.3 MHz in both CW and pulse modes. The duration of one

[†]Permanent address: Institute for Fluid Dynamics and Applied Mathematics, University of Maryland, College Park, Md. 20742, USA.

[*]Permanent address: Laboratory for Planetary Atmospheres, Goddard Space Flight Center, Greenbelt, Md. 20771, USA.

transmission period was 8.4 s and consisted of four 2.1 s intervals in which the transmitter was first on in the CW mode, then off, then on in the pulse mode, and off again. Twenty-eight fixed-frequency receivers covering the full range of transmitted frequencies were located in the Daughter section. Figure 2 summarizes the operating characteristics of the HF transmitter. Figure 3 illustrates the orientation and position of the two orthogonal electric field antenna systems with respect to the HF transmitter and antenna.

The rocket, called Polar 4, was launched shortly after 1927 UT (2027 local time) on 13 December 1974 into a disturbed ionosphere during a breakup auroral display. The rocket traversed a distinct auroral form during the downward leg of the trajectory. The magnetometer at the launch site registered 300-500 gammas negative disturbance in the X-component; several db of absorption were recorded by the 27.6 MHz riometer.

Figure 4 illustrates the rocket trajectory and indicates the following important events:

a) Separation of the Mother-Daughter sections at 50 s into the flight. The relative separation speed was constant at approximately 1 m s^{-1}. Near the end of the flight the two sections were separated by ~ 350 m.

b) HF transmitter on at 56 s.

c) Electric field experiment on at 90 s.

d) HF transmitter off for 25 s near apogee.

e) Passage of the rocket over an auroral arc between 285 and 350 s. Within this interval of flight time, HF receivers on the Daughter recorded noise of natural origin in the frequency range 0.6 - 1.1 MHz.

3. OBSERVATIONS

Figure 5 shows the typical response of the four spectrometer channels of the A antenna system for two transmission periods. The B antenna system gave qualitatively similar results. The signal level is enhanced above "background" in channels 1, 2, and 3 in the CW mode and in 1 and 2 in the pulse mode. The largest relative enhancement occurs in spectrometer channel 1. Slight decreases in the signal level are observed in channel 4. Several minima and maxima appear in channels 1, 2, and 3 in the CW mode, but the response in the pulse mode is rather featureless. The return to "background" in each channel is reached ~ 0.5 s after the transmitter is turned off. This decay time is the same in both the CW and the pulse modes and is the fall time of the spectrometer response.

Several features of the response of the spectrometer in the CW mode and most aspects of the response in the pulse mode are attributable to instrumental effects. Post-flight testing of the electric field experiment (on a similar unit) revealed that the spectrometer had a transient response when the transmitter was turned on at the beginning of a sweep and off at the end of a sweep. The effects were most noticeable in channel 1 in the CW mode. For example, the relative maximum at 0.6 MHz, and the one following transmitter turn-off, both of which occur almost exclusively in spectrometer channel 1, are related to the switching transients. In particular, the decay of the 0.6 MHz peak has a slope commensurate with the instrumental decay time. Plasma responses in the pulse mode were influenced by the effects of continuous switching transients.

In the remainder of this paper we consider only the responses in the CW mode. The frequency-dependent structure in spectrometer channels 1, 2, and 3 above approximately 1 MHz is considered to be evidence of plasma stimulation by the HF transmitter. To place this aspect of the data in perspective, we first examine the data obtained during the transmitter off periods to determine the signal levels that constitute the background response.

3.1. Spectrometer response - HF transmitter off

A measure of the background intensity in each of the four channels was obtained for each transmission period by averaging the intensity levels during the last second of the off periods immediately preceding and following the operation of the transmitter in the CW mode. The results are shown as the solid curves in Figure 6. No attempt was made to remove the rocket spin (0.31 Hz) or coning (0.0036 Hz) modulations.

These solid curves show that from 90 to 385 s the background intensity levels were larger at the higher frequencies. This can be understood as arising from the presence of natural emissions, primarily broadband auroral hiss, which would contribute mainly to spectrometer channels 3 and 4 (MAYNARD and JOHNSTONE, 1974). Near the end of the flight, when the rocket fell below 130 km altitude, the background levels increased markedly in channels 1 and 2 and decreased in 3 and 4. The decrease for frequencies above 1 kHz is probably related to a relatively sharp cutoff of broadband auroral hiss below 130 km that has been observed in other rocket measurements at auroral latitudes with similar electric field instrumentation (HOLTET, 1973). The increase for frequencies below 1 kHz has also been observed previously and is interpreted as being mainly due to electrostatic waves with frequencies below approximately 1.5 kHz created from two-stream interactions within the auroral electrojet (HOLTET, 1973).

Note that the first three spectrometer channels show some evidence of an enhancement in the background intensity near 290 s. This enhancement occurred near the region of the auroral arc and HF noise through which the rocket passed.

3.2. Spectrometer response - HF transmitter on

The dashed curves in Figure 6 show the response of each channel averaged over the 2.1 s CW intervals. These curves clearly illustrate an intensity enhancement in channels 1, 2, and 3 relative to their respective background levels both as depicted in the solid curves and during the 25 s interval near apogee when the transmitter was off. The response of channel 4, however, was not influenced appreciably by the operation of the transmitter. Note, as mentioned previously for the solid curves in Figure 6, that the intensity levels increased in channels 1 and 2 and decreased in channels 3 and 4 when the rocket fell below 130 km. Furthermore, the levels become nearly equal to the background levels determined previously. This suggests again that below 130 km (that is, in the E-region), the intensity levels were mainly of natural origin and were not appreciably influenced by the operation of the transmitter.

Having illustrated the average response in the CW mode, and those aspects of the data that can be attributed to natural or instrumental causes, we now consider specific transmitter-induced effects in the ionospheric plasma. Based on the foregoing discussion, such effects are limited primarily to HF frequency-dependent enhancements in the signal levels recorded in channels 1, 2, and 3.

Figure 7 shows the response of channels 1, 2, and 3 averaged over 7 transmission periods during five intervals covering that portion of the flight which was above 130 km. Several maxima and minima appear consistently throughout the response in a given channel and/or in different channels. In considering the frequency structure exhibited in these records, one might expect the transmitter to be particularly effective in stimulating the ionospheric medium as the frequency sweeps through certain resonance frequencies associated with the local plasma environment. Such frequencies would include the electron gyrofrequency and harmonics, the plasma frequency, and the upper hybrid resonance frequency. The variation of these resonance frequencies along the rocket trajectory is illustrated in Figure 8.

In general, specific features of the low-frequency response in the CW mode did not occur consistently at frequencies that can clearly be identified with any of the critical frequencies mentioned. For example, the onset of plasma-stimulated response occurs near 1.1 MHz which is significantly below the electron gyrofrequency. Relative maxima occur below the plasma frequency but not necessarily at the gyrofrequency. Some of the other features at higher frequency are close to the upper hybrid resonance and/or second harmonic of the gyrofrequency. An altitude dependence of some of these features is suggested in the averaged data of Figure 7, but is not easily discernible in studying the responses during individual transmission periods.

It is of interest to note that HF receiver data on this flight and from two similar Mother-Daughter flights (FOLKESTAD and TRØIM, 1974; FOLKESTAD et al., 1976) show that cone resonances occurred below the local electron gyrofrequency and between the plasma and upper hybrid frequencies. These data, although we do not discuss them here, also point to the occurrence of other resonance phenomena as well.

4. DISCUSSION

The absence of broadband data from the electric field experiment precludes the identification of the frequency characteristics of the stimulated emissions that have contributed to the response of the spectrometer. However, broadband data obtained in a Japanese rocket program (MATSUMOTO et al., 1975; 1974; MIYATAKE et al., 1974) have revealed a variety of frequency spectra of VLF plasma waves when the ionospheric medium was stimulated by an onboard HF transmitter. Significant differences in the instrumental parameters of the Polar 4 and Japanese experiments make a detailed comparison difficult.

The general features of the Polar 4 data can perhaps be understood in terms of the following model. HF radiowave energy absorbed by the plasma creates a turbulent region in the vicinity of the transmitter. This turbulent region is considered to be the site of ionospheric density irregularities. Nonlinear mechanisms associated with the presence of the irregularities excite electrostatic oscillations in the ELF/VLF range.

No attempt will be made to justify this model on the basis of specific physical processes. However, the following plausibility arguments are offered in support of the model.

a) The HF receiver measurements on this flight, and previous results (FOLKESTAD and TRØIM, 1974; FOLKESTAD et al., 1976) suggest the need for a nonlinear coupling region to explain observed frequency conversion phenomena at HF. Such a region will probably be most efficiently created in the relatively strong field near the transmitting antenna. Most of the emitted wave energy will probably be electrostatic because the short antenna is very inefficient for electromagnetic transmission at the frequencies employed.

b) Results of heating experiments show that artificial spread-F is produced by HF transmissions (UTLAUT, 1975; GORDON and CARLSON, 1974). Generation mechanisms proposed to explain artificial spread-F involve the production of field-aligned density irregularities (GEORGES, 1970; PERKINS and VALEO, 1974; CRAGIN and FEJER, 1974), in agreement with previous observations (ALLEN et al., 1974; THOME and PERKINS, 1974).

c) Low-frequency electrostatic noise has been observed in association with natural equatorial spread-F (HOLTET et al., 1976). The f^{-1} frequency dependence of this noise and of the power spectra of associated F-region irregularities (DYSON et al., 1974) is consistent with the Polar 4 results showing a much larger enhancement of noise in the lowest frequency spectrometer when the transmitter is on.

In applying this model to the Polar 4 data it is useful to estimate the size of the turbulent region that might be associated with the transmitter. Such an estimate is difficult to make with a high degree of confidence because it is not well known just what fraction of the energy fed to the antenna is actually emitted as electrostatic waves and what power densities are required to excite various in-

stabilities. Nevertheless, a crude estimate has been arrived at in the following way.

Heating experiments show that power densities as low as 0.1 $\mu W\ m^{-2}$ deposited in the F-region can stimulate a turbulent condition leading to field-aligned irregularities and spread-F (UTLAUT, 1975). Adopting this value as a threshold we estimate the radius of a sphere, with the Polar 4 transmitter at the center, on the surface of which the power density falls to the threshold value. The calculation is based on a 50 Ω antenna impedance, the voltages listed for the CW mode in Figure 2, a 1% antenna efficiency, and radiated power decreasing isotropically as r^{-4} for the electrostatic case. These assumptions lead to a radius of approximately 10 m. The radius can be increased to approximately 50 m by assuming that the radiated power decreases isotropically as r^{-2} for the electromagnetic case. A more realistic situation would consider the fact that propagation may be strongly dependent on the orientation of the transmitting antenna with respect to the magnetic field direction.

Despite the roughness of these estimates, it would be difficult to argue strongly that the main heating volume (or turbulent region) extends much beyond a few hundred meters from the transmitter. This result is, in fact, consistent with the AC electric field data. It is clear from the individual transmission periods that the low frequency response returns to the natural background in less than 1 s after the transmitter is turned off. Heating experiments have shown (UTLAUT, 1975) that spread-F conditions can endure for a long time after transmitter turn-off (minutes to hours, depending on the time of day). In 1 s the rocket moves ~ 1 km. Consequently, if a turbulent region $\gtrsim$ 1 km had been created around the Polar 4 transmitter, it would have been evident even during the off period. Such does not seem to have been the case.

5. CONCLUSIONS

Rocket observations of AC electric field variations show that the ionospheric plasma above ~ 130 km altitude has a low frequency response when stimulated by HF radiowaves from an onboard transmitter. Specific features of this low frequency response did not occur consistently at any HF frequency that could clearly be identified with such ionospheric critical frequencies as the electron gyrofrequency and harmonics, the electron plasma frequency, or the upper hybrid resonance frequency. The general features of the electric field data are described in terms of a model in which HF radiowave energy is absorbed by the ionospheric plasma and creates a turbulent region in the vicinity of the transmitter. Using as a threshold value the power density required to stimulate artificial spread-F, the size of the turbulent region is estimated to extend no further than ~ 100 m from the transmitter. This result is consistent with the observations.

6. ACKNOWLEDGEMENTS

Helpful discussions were held with K. Folkestad, B. Maehlum, and L. Lyngdal. This cooperative research program was supported by the National Aeronautics and Space Administration and the Royal Norwegian Council for Scientific and Industrial Research. Also we acknowledge the support of personnel in the Laboratory for Planetary Atmospheres of the Goddard Space Flight Center and in the Division for Electronics of the Norwegian Defence Research Establishment in the implementation of this experiment.

REFERENCES

ALLEN, E.M., G.D. THOME and P.B. RAO, 1974, HF Phased Array Observations of Heater-Induced Spread-F, Radio Sci., 9, 905.

CRAGIN, B.L. and J.A. FEJER, 1974, Generation of Large-Scale Field-Aligned Irregularities in Ionospheric Modification Experiments, Radio Sci., 9, 1071.

DYSON, P.L., J.P. McCLURE and W.B. HANSON, 1974, In Situ Measurements of the Spectral Characteristics of F Region Ionospheric Irregularities, J. Geophys. Res., 79, 1497.

FOLKESTAD, K. and J. TRØIM, 1974, A Resonance Phenomenon Observed in a Swept Frequency Experiment on a Mother-Daughter Ionospheric Rocket, J. Atmos. Terr. Phys., 36, 667.

FOLKESTAD, K., J. TRØIM and J. BORDING, 1976, Interpretation of Signals Detected on a Mother-Daughter Rocket in the Polar F-Region, J. Atmos. Terr. Phys., 38, 335.

GEORGES, T.M., 1970, Amplification of Ionospheric Heating and Triggering of Spread-F by Natural Irregularities, J. Geophys. Res., 75, 6436.

GORDON, W.E. and H.C. CARLSON, 1974, Arecibo Heating Experiments, Radio Science, 9, 1041.

HOLTET, J.A., 1973, Electric Field Microstructures in the Auroral E-Region, Geophys. Norvegica, 30.

HOLTET, J.A., N.C. MAYNARD and J.P. HEPPNER, 1976, Variational Electric Fields at Low Latitudes and their Relation to Spread F and Plasma Irregularities, submitted to J. Atmos. Terr. Phys., 38.

MATSUMOTO, H., S. MIYATAKE and I. KIMURA, 1975, Rocket Experiment on Spontaneously and Artificially Stimulated VLF Plasma Waves in the Ionosphere, J. Geophys. Res., 80, 2829.

MATSUMOTO, H., S. MIYATAKE and I. KIMURA, 1974, Frequency Spectra of VLF Plasma Waves Observed by Japanese Ionospheric Sounding Rocket K-9M-41, Rept. Ionos. Space Res. Japan, 28, 89.

MAYNARD, N.C. and A.D. JOHNSTONE, 1974, High-Latitude Day Side Electric Field and Particle Measurements, J. Geophys. Res., 79, 3111.

MIYATAKE, S., H. MATSUMOTO and I. KIMURA, 1974, Rocket Experiments on Non-Linear Wave-Wave Interaction in the Ionospheric Plasma, Space Res., 14, 369.

PALMER, F.H. and R.E. BARRINGTON, 1973, Excitation of Ion Resonances by the Isis 2 HF Transmitter, J. Geophys. Res., 78, 8167.

PERKINS, F.W. and E.J. VALEO, 1974, Thermal Self-Focusing of Electromagnetic Waves in Plasmas, Phys. Rev. Lett., 32, 1234.

THOME, G.D. and F.W. PERKINS, 1974, Production of Ionospheric Striations by Self-Focusing of Intense Radio Waves, Phys. Rev. Lett., 32, 1238.

UTLAUT, W.F., 1975, Ionospheric Modification Induced by High-Power HF Transmitters, Proceedings of the IEEE, 63, 1022.

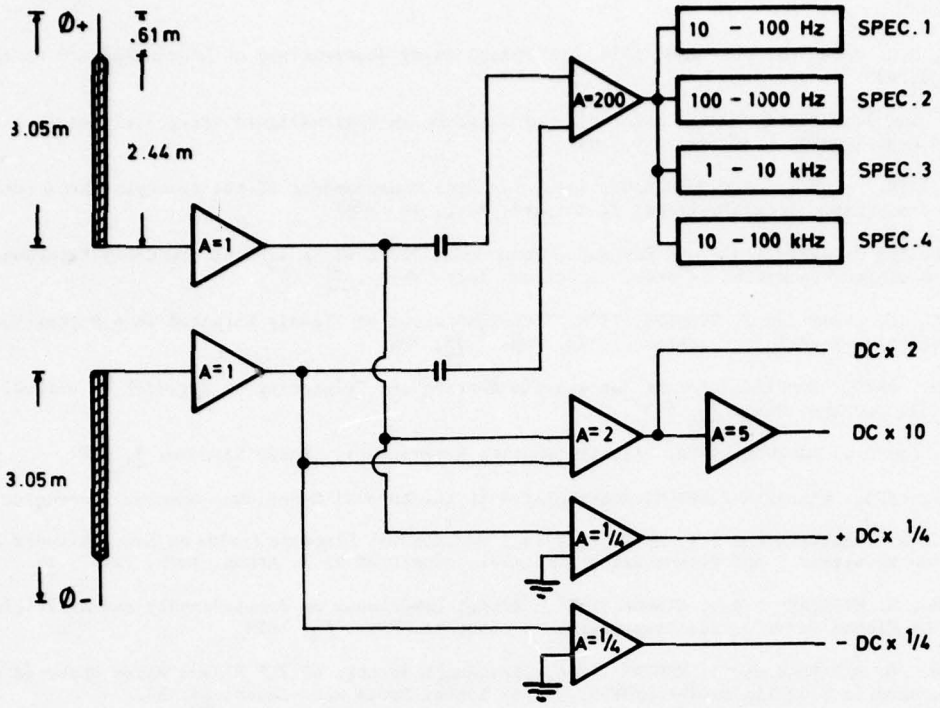

Fig. 1. Block diagram of one axis of the AC/DC electric field experiment on Polar 4.

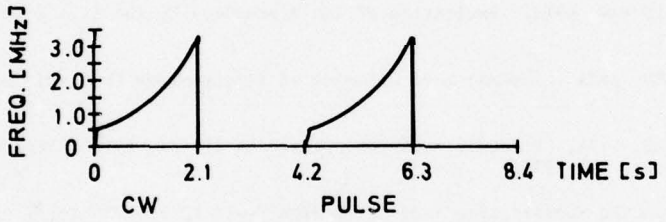

FREQUENCY : 0.55 - 3.3 MHz

FORM OF SIGNAL : UNMODULATED CW AND PULSE

PULSE DURATION : 6.55 ms

PULSE REPETITION RATE : 50 Hz

ANTENNA : BALANCED ELECTRICAL DIPOLE ,
1 m HALF LENGTH

POTENTIAL AT ANTENNA FEED POINT

FREQ.[MHz]	CW [Vpp]	PULSE [Vpp]
0.6	150	400
1.0	130	300
2.0	110	250
3.0	100	150

Fig. 2. Parameters of the HF transmitter on Polar 4.

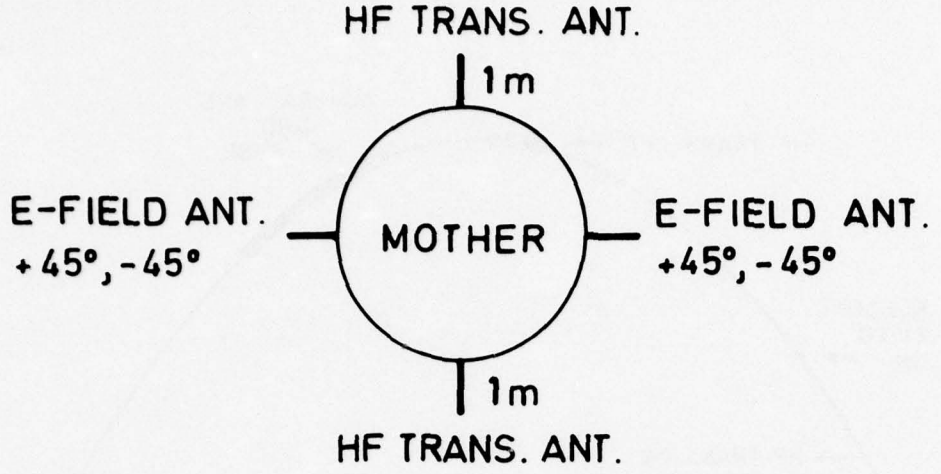

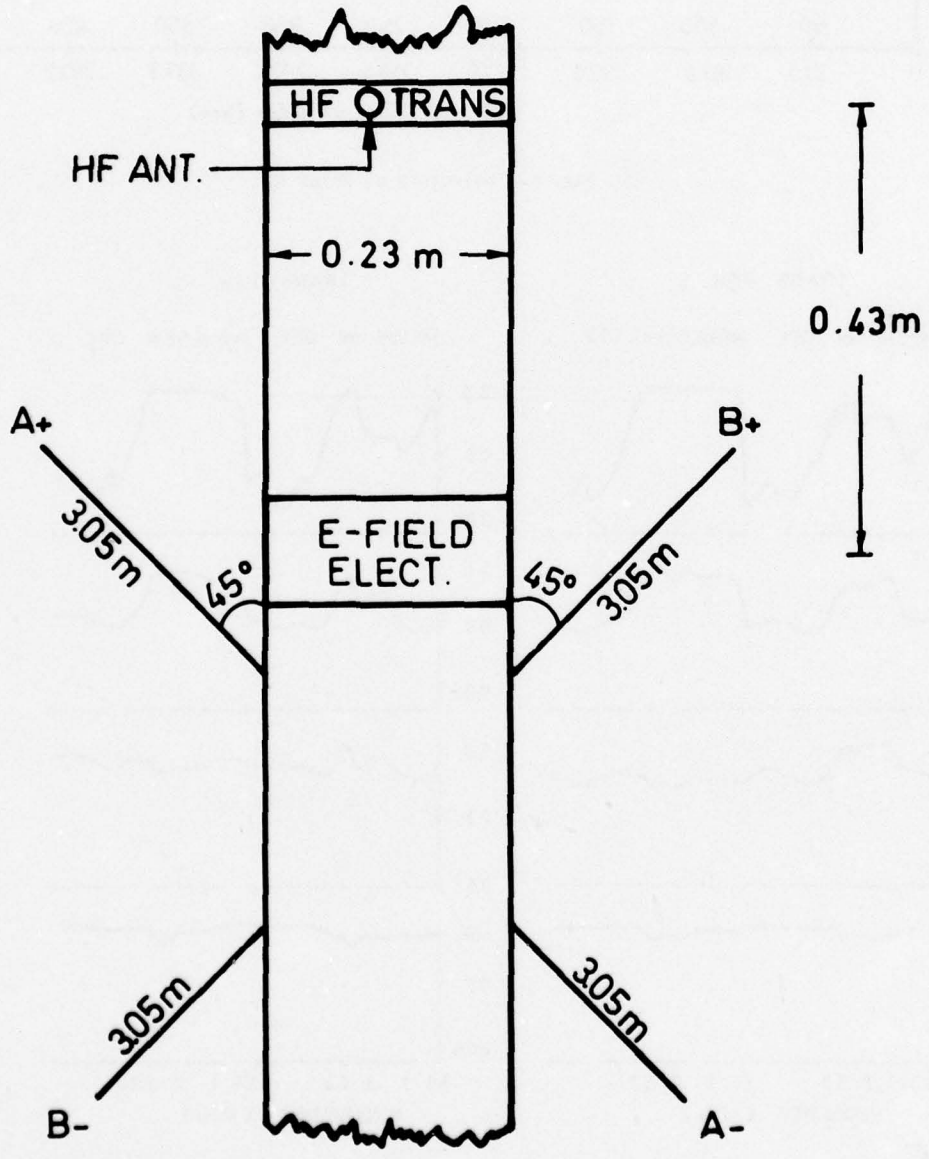

Fig. 3. Antenna orientation and position for the electric field and HF transmitter experiments.

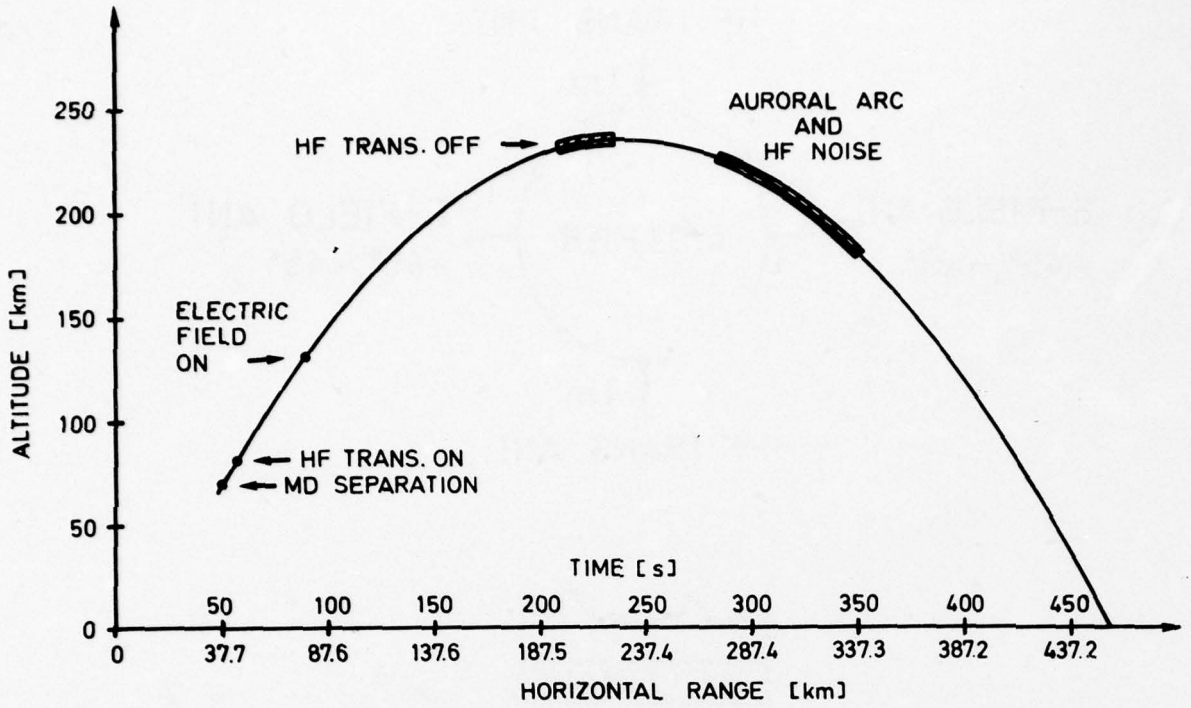

Fig. 4. Trajectory of Polar 4.

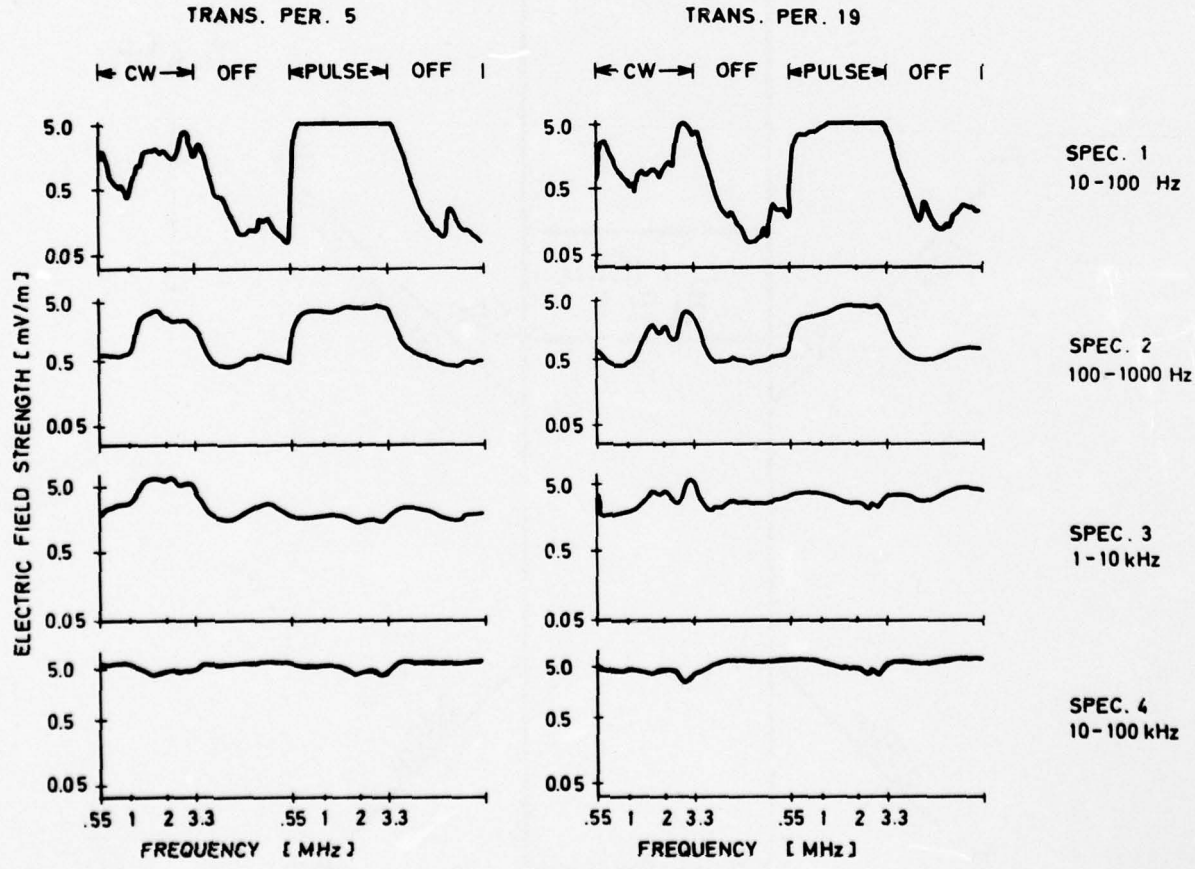

Fig. 5. Response of the four spectrometer channels of the A antenna system for two transmission periods.

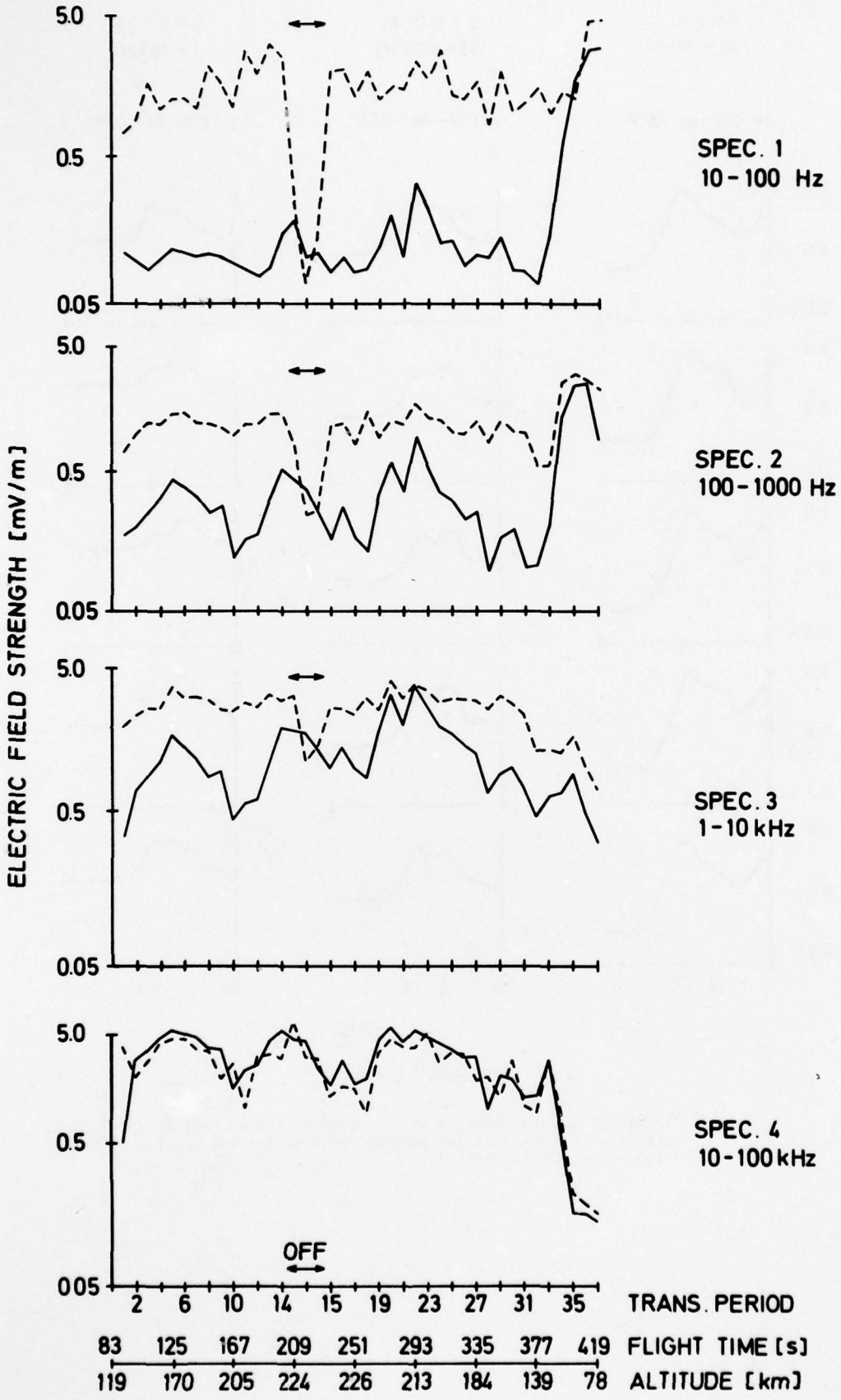

Fig. 6. Average response of the four spectrometer channels in each transmission period during intervals when the transmitter is off (solid curves) and on in the CW mode (dashed curves).

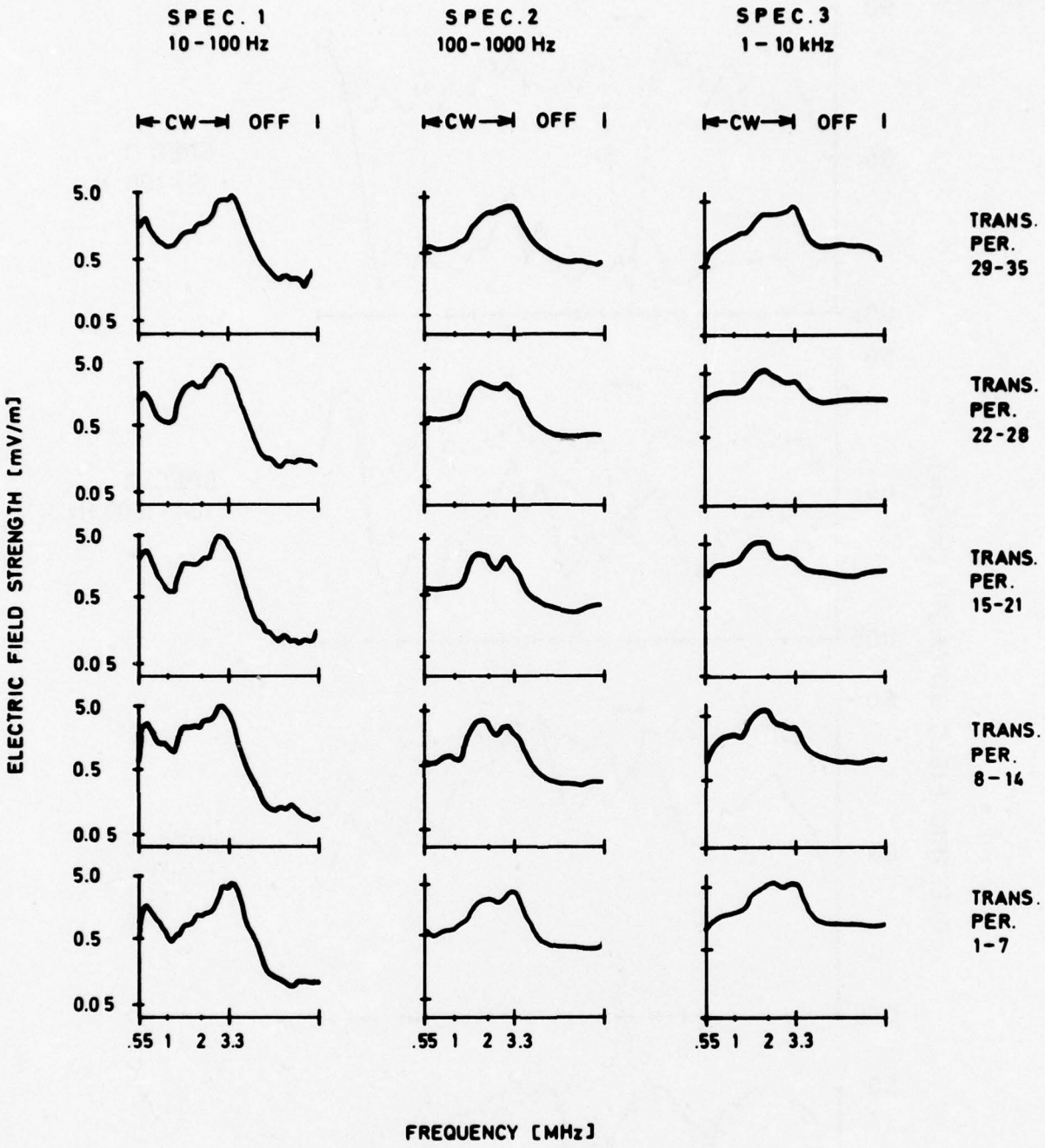

Fig. 7. Average CW and off response of spectrometer channels 1, 2, and 3 in intervals of 7 transmission periods (58.8 s) for the portion of the flight above 130 km altitude.

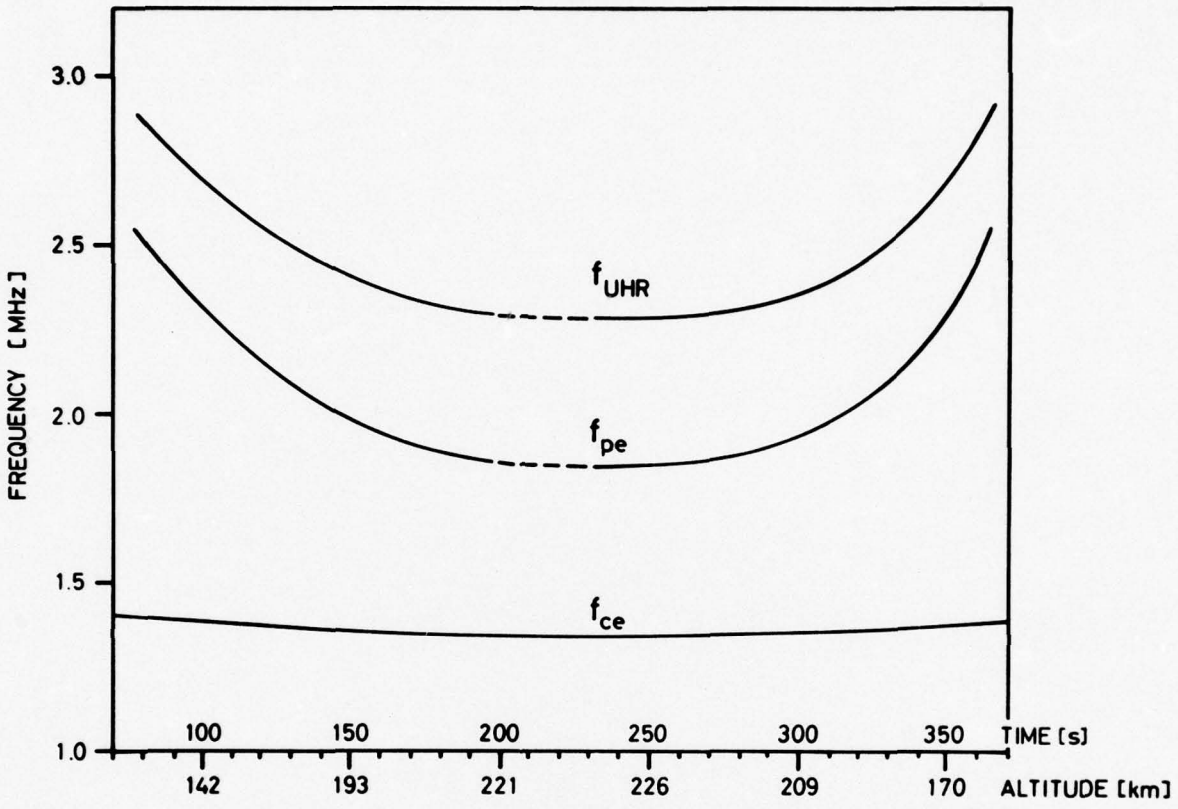

Fig. 8. Variation of electron gyrofrequency, plasma frequency, and upper hybrid resonance frequency along the Polar 4 trajectory.

SESSION II, ROUND-TABLE DISCUSSION

MODIFICATION OF IONIZED MEDIA BY EM WAVES

Participants at Round Table: W.E.Gordon (Chairman)
F.H.Hibberd,
H.Kopka,
J.Minkoff,
P.Stubbe,
W.F.Utlaut

W.E.Gordon: May I suggest that we organize the discussion around the following topics and proceed with them in order:

1. Plans for modification experiments.
2. Observations that were not reported in today's sessions.
3. The communication parameters and their observed values, scattering cross-section, bandwidth, aspect sensitivity and geometry.
4. Inadvertent modification of the ionosphere by powerful transmitters.
5. Interaction of the modified ionosphere with the magnetosphere.
6. The study of natural processes in the ionosphere by modification experiments. (This topic was added at the suggestion of H. Soicher)

1. Plans for Modification Experiments

J.Belrose: In Canada, we have been thinking about doing the ionospheric modification experiment for quite some time. In the early 1970's I started thinking about it and it seemed like a very good experiment to do, especially in conjunction with the Upper Atmosphere Observatory, which was to be located in upstate New York and was proposed to be a joint United States/Canadian program to study the upper ionosphere at a magnetic latitude near L=4. The ionospheric modification facility that we were proposing was going to cost several million dollars and was to be located due north of that facility. That facility, the Upper Atmosphere Observatory, was to be an incoherent scatter radar and was going to be able to tilt the radar beam in a north-south plain. To date neither of these major projects has been funded. A year ago we decided to try to do something with facilities that we could muster on hand without any great resources.

We have been doing the partial reflection experiment at Ottawa for many years. The partial reflection experiment involves generation of high power pulses so that you can observe backscatter from the D-region from the lower ionosphere. The high power amplifier is capable of 800 kW pulses at a frequency of 2.66 MHz, with a maximum pulse width of 250 μs. We have been using 50 μs or shorter pulses for the partial reflection experiment. We built large antenna arrays for the partial reflection experiment at Ottawa, mainly to direct the beam more vertically upwards and be sure that the backscatter was in fact coming from overhead, and not particularly to increase the signal-to-noise ratio. The antenna array consists of twenty-five 100-foot towers. Between each 100-ft-tower there is a half-wave dipole antenna. It is a 40 dipole antenna array covering a little over thirteen acres of land, and the estimated gain is about 24 decibels over isotropic. Its fixed frequency is 2.66 MHz. The transmitter has a 100 kW driver, the main amplifier and a pair of the largest air-cooled tubes in the world which are capable of 200 kW of transmitted power each but we do not have the required amount of drive for that kind of cw power. The power supply delivers 20 kV at a quarter of an amp and this will be replaced by a power supply that will deliver 20 kV at 3 amps and the pulse length will be stretched from 250 μs to 10 ms. The maximum pulse rate will be about 5 pulses per second.

Relative to the diagnostics, the type of scatter that you have been hearing about, mainly as investigated in the United States work at the Platteville facility, was the field-aligned irregularity type of scatter. It was my opinion that we would not be able to generate this kind of scatter, although I heard W.F.Utlaut this morning say that it started rather quickly, but I do not know if it starts within 10 ms which is the maximum duration of our transmitter pulse. Anyway, that kind of geometry is not favorable for Canada because the earth's magnetic field is almost vertical, and to do the kind of communications experiments that W.F.Utlaut was talking about this morning you would have to have the transmitter and receiver locations outside the country of Canada. The kind of backscatter that we will be looking at is the plasma wave scatter, and the initial experiment that we will be doing will be with a transmitter and receiver facility located at the foot of the field line which is being heated by the facility at Ottawa.

The diagnostic probes we will be using, VHF and UHF transmitters, are rather modest diagnostic probes if you compare them to the Arecibo situation.We will be using 1 kW transmitters.The antenna systems will be basic building blocks of sixteen 13.7 dB-gain antennas -- 16 of them in a broadside array. At the UHF frequency there will be 4 of these building blocks, so if you put them all together you get 64 antennas. Since they are in building blocks, depending on what signal-to-noise ratio you can manage to

achieve as backscatter from the region, you can transmit on one 16 antenna array and receive simultaneously on two 16-element antenna arrays, or you can combine all four sets of 16 antennas together to make a 64 antenna array and transmit and receive on the same array.

If we could in fact generate field-aligned irregularities or something that would last for a longer period of time than the 10 ms pulse, we have a very large antenna array at Ottawa, a Mill's cross, with a row of dipoles 1.2 km long in one direction and 800 m long in the other direction. There are about 79 receivers in this antenna array and each one comes out separately as a receiver tied to an antenna, so in fact you could direction-find very beautifully on any kind of field-aligned irregularities.

That is the plan, which is very, very modest compared to what we were talking about at the beginning when we started to contemplate doing the ionospheric modification experiment at Canadian latitudes. For the time scale, we are engaged in doing it now. The transmitter will probably be on the air sometime this summer. We hope to have the UHF diagnostic probe in the field by the fall.

W.F.Utlaut: In Russia, an active program appears to be carried out in the vicinity of Gorky using three different transmitters. The lowest frequency, I believe, is very close to the gyro frequency, and there are other transmitters that are operating up in the 5-10 MHz region. Apparently, the higher frequency transmitters at least have been modulated with a VLF signal and, as I understand it, an amplified VLF signal which is detected some distance away, is generated in the ionosphere. That is about all I know about it.

W.E.Gordon: There are certainly Russian publications in the field. Ginzburg, Guravitch and others have published papers on subjects that we have been discussing; therefore, it is clear that they are not only interested in the theories, which their papers have covered very nicely, but that they are also performing some experiments.

F.Hibberd: The only Russian papers that I have seen published have been theoretical papers. In just the last year or two there have been some experimental results coming out. On the point of the proposed experiment W.F.Utlaut suggested that, in Russia, a low frequency modulation of a high frequency wave is used; have you any idea of the process involved ?

W.F.Utlaut: I do not know what the process is.

P.Stubbe: It could be something like the modulation of a current flowing in the E-region, or it could be this energetic effect where you produce electron temperature fluctuations at twice the frequency so you would get more of the combination frequencies like 2 f_o plus or minus the probing frequency.

T.J.Rosenberg: I know that, in Russia, some work has been done with VLF transmitters. I would not call it a facility, but I believe there are transmitters on a ship where in essence something like the transmitter experiment at VLF has been done. The ship was situated itself in the Indian Ocean near the magnetic conjugate point of a station in the Soviet Union where ionospheric effects produced by VLF could be observed. I think some information is available in the literature, although I cannot off-hand suggest the papers.

2. Observations not reported in Today's Session

W.E.Gordon: There have been other experiments, of course, that had to do with modification of the ionosphere, and in particular there was one in the D-region. Would you like to say a word, Dr. Showen, about what you did a few years ago and that may remind people of other things that have been done.

R.L.Showen: At Arecibo we had a 40 MHz transmitter and it was possible to double and triple the electron temperature in a range from, say, 80 to 120 km. We were able to measure the electron collision frequency and the G factor, which is also obtained in cross-modulation experiments, so this is the first time that mention of a collision frequency was made from the ground at those altitude ranges.

W.E. Gordon: And this experiment was performed, in particular, to modify the D-region and to use the diagnostic of incoherent scatter to check on the results. Would participants at the Round Table have any comments they would like to make on D-region modification, a subject we have not covered here very well.

W.F.Utlaut: I do not know that I can say a lot more; I have already indicated that there seem to be a variety of complex phenomena going on in the D-region. I did show you some examples of the incremental continuation of a 2.6 MHz signal which, if you recall, had as much as a 6 dB (this was two way) attenuation imposed upon it very promptly with a turn-on and disappearing very promptly with a turn-off of the transmitter. There is other information that would suggest that one would normally expect that the extra-ordinary mode would receive greater attenuation in passing through the D-region than does the ordinary mode. We found with the high power transmitter, however, that the reverse was the case, which seems to have no explanation on a theoretical basis. I do not know what that may be unless there is evidence, of course, that the electron temperature is changing drastically but it is also possible that the whole electron dis-

tribution in the D-region changes very quickly. The integrated attenuation is dependent upon both of those factors. The D-region seems to undergo a very pronounced change, and I only wish that we were able to transmit now and observe it more because I think that there is undoubtedly a lot that could be learned about the D-region.

J. Belrose: I am not really very well prepared to make the comments on the amount that you can increase the temperature in the D-region. I wish that I had brought with me the paper by R.A. Smith that was presented at the last AGARD conference concerned with modification of the ionosphere by electromagnetic waves (CP No. 138, Non-linear effects in electromagnetic wave propagation, edited by J. A. Fejer, 1974). He showed, from his point of view, that large temperature changes in the D-region were absolutely impossible. Unfortunately, I have forgotten the details of his work and I just bring it to the attention of the panel members up here and, in particular, to P. Stubbe who showed a graph this morning suggesting very, very large temperature changes in the D-region. R.A.Smith in Armidale, Australia, has been doing high-power interaction experiments in the D-region for many years. He had a 500 kW transmitter and a 40 dipole antenna array adjusted so that he could transmit either polarization on a frequency fairly near the gyro-frequency. Unfortunately, very little of his work has been published.

P. Stubbe: Well, unfortunately, I have not read the paper by R.A. Smith that you have just been citing, but we have made systematic calculations of the effect of the heating wave on the electron temperature increase in the D-region, and we found that it is possible to get an increase by a factor of 10 and in some cases even more. The task to perform the calculations is in itself relatively simple and, since the order of magnitude is fully in agreement with what G. Meltz has done, I have no reason to doubt that one can reach such temperature increases in the D-region.

J. Belrose: R.A. Smith did not agree with those calculations,so therein the controversy lies. I am not in a position to argue for him since I do not remember the details of his paper, but I think it is very important that you look at the paper because there is a conflicting opinion.

W. E. Gordon: It is important that we look at the paper. It is also important that some experimenter comes to the rescue of the theoreticians and decides which one is right.

F.H. Hibberd: I am a close colleague of R.A. Smith. Many years ago we did work together in this field, but I have been away from the field now for quite a long time. I have tried hard to persuade R. A. Smith to publish what he has because it is extremely valuable material; some of it was presented at the Edinburgh meeting.

W. E. Gordon: In the meantime, it is clear that we should be reading the former AGARD publications.

E. Thrane: I would like to make a comment as a representative of the old school of cross-modulation work when the custom was to use very low powers.We used the cross-modulation theory of course, but at one time while I was in Boulder I tried to extend this in a very simple fashion to a very high power. It is easy to see that you can get fairly high electron temperatures, but my problem was that even though you could raise the electron temperature by a significant factor it does not produce a very great cross modulation. I understand from what W. F. Utlaut said this morning that he had measured up to 40 % cross-modulation. This indicates there are some processes that we have neglected and do not understand at all.

A. Egeland: I would like to mention some experiments which at least would have some great influence on the physical understanding of what is going on in producing these irregularities which greatly influence communication, and that is in connection with active experimental satellites. As you all know, there have already been a few accelerators carried on board rockets (mainly electron guns) and there are quite a few more planned. As a matter of fact, we have carried out the first one with an electron gun in Norway where you really can very well control the energy of the particle sent out. At the same time (and I think that is very important for the physics) that we measure the electric field about DC and AC, we as well measure the electron density and perhaps also the optical emissions. In connection with Spacelab, of course, some very large active experiments are planned.

3. Communication Parameters and Their Observed Values, Scattering Cross-Section, Bandwidth, Aspect Sensitivity, and Geometry.

W. E. Gordon: What I suppose is the main reason for this meeting has to do with the communication parameters and the problems in communication that arise because of the modification of the ionosphere. Perhaps the intention was to improve communications by doing something on purpose to the ionosphere. This morning we had two papers which gave a fine review of the current situation. W. F. Utlaut's paper contains a good bit of the information and it was supplemented nicely by J. Minkoff in the summary of the experiments he did and with some reference to the experiments that Stanford did. Are there any questions that you who are in the communications business, in particular, would like to address to either of those experts or anyone else on the subject of what one might expect,given an ionosphere that is modified by high-power EM waves -- could you make an estimate for a particular link of what signals you would expect on that path ? I think they have given you the basic elements and I think the calculation is all quite doable, but I would like to make sure that each of you feels the same about it. You might press

further if there are some phases of the problem that you feel were only touched on and they may, in fact, have some additional data to offer. The question of the scattering cross-section -- are you satisfied with the data as it was presented and do you feel that you understand fully what they mean by scattered cross-sections and how you might use them to calculate the signal on a particular path ?

H. Flüss: I have a question concerning the cross-section. What is the dependence of polarization of the cross-section ?

J. Minkoff: We did not find any dependence of the polarization. It did not make any difference. We did experiments with circular polarization as well as with linear polarization, and in a backscatter experiment we found no variation with polarization.

H. Flüss: My second question is, what is the cross-section for higher frequencies (GHz-region) ?

J. Minkoff: The highest frequency observed is at 435 MHz. We had a radar at 1300 MHz and during times of very strong scattering conditions we were able to point that radar exactly where it should have been and no scattering was observed. Therefore, the curve I drew really only goes up to 435 MHz. I arbitrarily extended it and then I calculated the minimum detectable signal that that 1300 MHz radar could have seen, and it is right on the curve; however, that is a dubious point and I really do not think we can make any claims above 435 MHz.

W. F. Utlaut: G. Meltz has proposed that it would be possible using X-mode for illumination to create so-called Bernstein waves which he estimates would have a large cross-section, even at S-band, but this has not been verified. That is only a theoretical calculation, so some experimenters might want to consider this in some of their plans.

W. E. Gordon: I have a question, or a clarification, about the earlier question on the dependence on polarization. You said you used circular polarization, and that should have no problems. Presumably if you use linear polarization, and I think you did some experiments with linear polarization, should there not be a Faraday-rotation problem or is the Faraday rotation so small that it does not matter ?

J. Minkoff: I think the answer is that it is very small and does not matter. The data that I presented this morning was all with circular polarization. Later on in the program we had another radar which had vertical polarization; however, none of the data on these curves here were obtained using that and so there was no correction necessary.

W. E. Gordon: In the data that was presented to you, there were some interesting points about the bandwidth of the path that might be created by a modification of the ionosphere and, in particular, that there is a very large difference between the bandwidth that might be created by a modification in the F-region and a modification in the E-region. Is that a point that anyone has any questions about ?

W. F. Utlaut: The typical time-delay spread for the F2-region was of the order of a millisecond; it did vary somewhat with time of day and so on. The time-delay spread for the E-region was of the order of 150 microseconds -- appreciably shorter. Now I think that, in part, the F-region-time-delay spread is due to the size of the volume that is illuminated by the heater transmitter and so it is conceivable that one could use a higher gain antenna, essentially modifying a smaller region of the ionosphere, and perhaps reduce that time-delay spread in the F-region.

W. E. Gordon: That is certainly true. That is a trick that was used in tropospheric propagation paths to help the bandwidth. It may not be feasible in practice to build the antenna the size that is required in order to gain that advantage. These bandwidths, in effect, then turn out to be something like a kHz in the F-region and 5 or 6 kHz for the E-region, although you say you did not have any experimental data on the E-region. Is that right ?

W. F. Utlaut: No communication experiments other than just the radar backscatter observations on this.

W. E. Gordon: And the experiments on the F-region scatter did show bandwidths like a kilohertz ?

W. F. Utlaut: Voice communications of 3 kHz were perfectly adequate. However, using a 30 kHz FM , it was of a very inferior quality and sometimes not even understandable.

G. Tacconi: From the communication point of view, the more significant parameter should be, in my opinion, bandwidth time.

W. F. Utlaut: In other words, you are asking what the fading rate of the signal is. It is a few cycles, almost like ordinary HF transmissions. I thought you were asking a question on availability and maybe I did not make that clear today, but this is an available channel round-the-clock -- we were able to operate 24 hours per day by choosing proper frequencies for modifying the ionosphere.

W. E. Gordon: If you had a voice channel, or a channel with some information that required a kHz bandwidth, would it be available continuously ?

W. F. Utlaut: I think the answer is yes; it would be available continuously. Actually, the 1 kHz bandwidth is probably the minimum; at times, however, it would open up to 2 or 3 kHz.

J. Beirose: I wonder if W. F. Utlaut or somebody on the panel could comment on the bandwidth for the parametric instability, the plasma-line scatter. This bandwidth seems to be fairly uncertain from what one can read in the literature. For example, the temperature of the line seems to depend upon the resolution of the resolving instruments to measure it. You get a sort of higher temperatures and narrower lines, depending on how you reduced your data.

W. E. Gordon: I will make a comment, but I do not want to preempt either of you. I do not know the experimental answer to the question you have asked, but if you think of the scattering as being produced by the region in which the instabilities exist, that is a very thin region. The region is not as thin as a kilometer or a fraction of a kilometer that we sometimes see at Arecibo, but that is simply because we are looking at a particular frequency. The instability region itself is probably of a thickness of about 10 km and it is spread over the area that is illuminated by the beam, and that would give you something like a pancake 10 km thick and 50 km in diameter, so you can look at that I think and get some multipath kind of calculation which would give you a bandwidth.

Are there any other questions or comments relative to the communication parameters? I hope that is a reflection on how well W. F. Utlaut and J. Minkoff did this morning. I think they did a fine job, and I suspect that the information got across. You do know that these papers will be available in the Proceedings, although that may be a few months before you see them. The final question in the communication parameters is the problem of aspect or geometry of the path, and in terms of what is known about the field alignment problems, the information is available. There is adequate theory to describe the kind of scattering one gets from any elongated scatterer.

J. Minkoff: We never really had a chance to measure it. I should say one thing, plasma-line scattering is observed to be strongest when the heating was taking place near the perpendicular point. We also made measurements at lower altitudes where the scattering was much less and the angle of incidence to the magnetic field was about 5 or 6 degrees, which indicates that maybe there is some aspect sensitivity. However, that experiment was compromised by the fact that it took place in the daytime (the low altitude experiment) in the presence of the D-layer and it is possible that absorption of the heating wave could have reduced the amount of heating and therefore the plasma-line signal was less. The higher altitude plasma-line signal at the perpendicular point took place at night with no D-layer, so certainly it is a lot less aspect-sensitive, but you cannot say at this time that it is not at all aspect-sensitive.

4. Inadvertent Modification of the Ionosphere

W. F. Utlaut: There are a couple of things that one might say. One is that there are a number of high power LF through HF transmitters that are already in existence and others that are being planned that go to even higher powers, powers of the order of 10 MW or so. Now while these are designed primarily for oblique transmission, it is still possible (if you consider the side lobes of any normal transmitter) that there can be appreciable power that is essentially radiated vertically, or near vertically, and so there may well be a number of places around the world where there is unknown and unintentional modification of the ionosphere taking place. To go one step further, we did try on a few occasions, using another array which was designed for low take-off angles, to try to illuminate the ionosphere at a substantial distance from the Platteville facility. When we turned on the transmitter, a short time after trying to illuminate at this distant point spread F began to show on the ionosonde under that heated region. But, perhaps more importantly, there was also a phenomenon of an upward travelling wave in the ionosphere. Travelling waves are seen on ionograms normally as little hooks that start at the very highest point and move downward in height and in frequency as a travelling wave moves over the sight. I have talked with many knowledgeable people who have looked at many ionogram records and they have never seen a travelling disturbance moving upward because of the nature of normal disturbances in the ionosphere. They are moving forward with a tilt so that they always look as though they are moving down. So I think that we have a few occasions where it is clear that we were able to modify the ionosphere at some distance from the heating transmitter itself, operating on a frequency which was low enough so that it was still below the maximum critical frequency at the remote point that we were trying to modify. Therefore I think there is a concern and, maybe some of you know, there are even questions which have been raised within the CCIR now as to what the possible unintentional modification effects from existing high power ground transmitters might be.

W. E. Gordon: That is a rather remarkable observation from at least two points of view.

L. W. Barclay: I certainly appreciate the points that W. F. Utlaut has made, but I would also like to point out that there are some communication transmitters which have vertically pointing antennas too. There are at least one or two medium frequency transmitters that use horizontal dipoles for transmission. Calculations of the cross-modulation from these, although much more severe because of the higher power densities, show that the geographical extent is quite small. There are also some HF transmitters which use almost vertical incidence antennas and these are used for tropical broadcasting.

W. E. Gordon: May I come back to the point you were making a moment ago. You obviously produce some modification because the ionosonde responded with spread-F. It is difficult to see how you could satisfy under those conditions the necessary condition for a plasma instability to develop. For the plasma instability you require that the incident wave frequency match the plasma wave frequency, and this problem is not unlike the problem of the X-mode case. If you propagate vertically, what happens with X-mode is that it is reflected before it reaches a frequency in the plasma, matching the transmitted frequency, and it seems to be that the refraction will do the same thing to your situation. There is a question of how fast the spread-F occurs, of course. Can you comment on that?

W. F. Utlaut: I cannot give you precise times, but it was clear that it was there not promptly; it took 30 seconds, or maybe even a minute or more, before there was the development of the spread-F. It developed slowly, but it became quite an appreciable amount of spread.

Another thing that we have done is to phase the array at low power levels with the transmitter and steer the beam of the vertically directed array off from vertical, tipping it almost to 45° from vertical. We observed the heating transmitter signal itself on the ground, and it is clear that out 300 km, or 400 km away, that the heating wave itself (when we have full power on) has very deleterious effects. It causes it to fade very rapidly and very deeply, whereas if we came on with low power first and made the measurement we did not have the ionospheric modification and it was just an ordinary ionospheric reflection. It may be that trying to go to too high a power transmitter, at least for short distances, may defeat itself in the fact that it is destroying the characteristic of the signal just due to the irregularities in the turbulence of the ionosphere.

W.E. Gordon: That should have some interesting consequences for the communications people. Are there any further comments on the inadvertent modification problem ? Apparently mankind is polluting his environment in all kinds of ways, including the ionosphere.

5. Interaction of the Modified Ionosphere with the Magnetosphere

W. E. Gordon: Let us proceed to the ionosphere/magnetosphere coupling. We have touched on it more than once in the discussion so far, and I wonder if anyone has more to say.

P. A. Bernhardt: I forgot to mention that it is planned (or proposed, at least) to put a VLF transmitter on the Spacelab and in that way get away from coupling through the ionosphere into the magnetosphere by just sticking the transmitter above the instrument.

6. Study of Natural Processes in the Ionosphere by Modification Experiments

A. Egeland: I was mainly interested in the production of this field-aligned irregularity, and I just want to ask what is the main source for production of this field-aligned irregularity in connection with heating experiments. Is it the electric field ?

W. F. Utlaut: I am not sure that I really know the answer. I think that there are two kinds of field-aligned irregularities, at least. Apparently just the heating (even relatively low power heating) itself somehow sets up the instabilities that will create field-aligned irregularities that can be observed at low HF frequencies. In order to produce the kinds of irregularities that are seen at VHF and UHF one requires the beating of plasma waves and electrostatic waves to produce this transverse irregularity (Perkins has developed the theory). I think these are the source of the backscatter that is seen at 157 and 435 MHz and it seems clear that, if you look at the radar cross section as a function of frequency, that there are two different slopes so it looks as though there are probably two distinct kinds of phenomena going on.

H. Soicher: Can we cause the effects of a magnetic storm, for example, by any of the artificial modifications ? Can we explain L-band scintillations with artificial modification ?

W. F. Utlaut: I do not know about creating a magnetic storm; I would not want to take credit for it. Certainly, I think we learn something about a possible understanding of spread-F creation. With the satellite transmissions -- I do not know whether I mentioned that these transmissions were made on frequencies ranging from 135 to 400 MHz through the artificial modification -- the scintillations look exactly like they do with natural scintillation. We had no opportunity to observe at L-band. We know that there is at least a three-meter structure in the ionosphere that is created and probably much shorter than that even if J. Minkoff's extrapolation of curves up to 1300 MHz is correct. There would have been cross sections seen had we looked at higher frequencies. There must be a whole spectrum of irregularity sizes created. That does not say we know about it, but it does offer a facility, I think, for observing the kind of things you are asking about.

P. Stubbe: I would like to say a few words to your first question, which was more general. First, one should think that one can learn from these experiments because one produces instabilities of the same kind that nature also does, but at second look it is a different process. Nature does it mainly by drawing the energy from kinetic energy and feeds it into some wave mode and here the conversion is from an electromagnetic wave into a more or less electrostatic mode. But the results of all these processes are the

same, namely an enhanced level of electrostatic fluctuation. If on this basis some secondary processes are caused, they may be the same. For instance, if you produce by electromagnetic wave an electron plasma wave which has a very high intensity, then this may serve as a mother wave to produce a daughter wave and this, for instance, could be involved in the process of forming field-aligned irregularities. This is the process of Perkins that you were mentioning. So, I think that when you are at the stage where you have excited plasma waves then the whole thing is identical -- only the step from the energy source to the enhanced plasma wave level is completely different.

W. E. Gordon: If I might add to that, I think the objectives of many of the people who work at Arecibo in ionospheric modification experiments are simply to try to understand what is going on in the atmosphere, both from the point of view of aeronomy and by making use of the ionosphere as a plasma laboratory. I am sure that P. Stubbe and his colleagues, in becoming very involved in EISCAT, have similar motivations.

E. Thrane: I would like to ask one question that has been bothering me the last fifteen minutes. Dr. Utlaut, how is it (this is about cross modulation again) that the extraordinary wave causes most cross modulation but has least absorption in the D-region ?

W. F. Utlaut: I assumed someone was going to ask that question because it has bothered me too, but that seems to be the phenomenon that is existing.

W. E. Gordon: That is a good paradox, perhaps one on which to end the session. You have time at the beer hall or wherever it may be after the session to think about serious problems, and this is a good one to leave with you. If anyone has the answer, I am sure that J. Belrose, who is Chairman of the session tomorrow morning, would be glad to hear from you and perhaps even offer you a minute to speak. Let me thank the participants at the round table and the audience for a very stimulating hour. The session is adjourned.

SESSION III

MODIFICATION OF IONIZED MEDIA BY CHEMICAL SUBSTANCES

Modification of Ionized Media by Chemical Substances - A Review of Physical Processes

G. Haerendel

Max-Planck-Institut für Physik und Astrophysik
Institut für extraterrestrische Physik
8046 Garching b. München, Germany

1. Introduction

"Modification of ionized media by chemical substances" lets us think in the first place of man-made releases of gases in the upper atmosphere. The cheapest way of accomplishing this is by chemical reactions, such as the Ba - CuO reaction, which yield a neutral metal vapor. The ionization is provided by exposure of the gas to the UV radiation of the sun. But there are other ways of modifying the ionized medium. Plasma can be created by means of a plasma generator or accelerator, but, of course, at a higher expense of energy. Or, one can inject a neutral gas with which the natural ionosphereic plasma undergoes reactions, such as electron attachment, charge exchange, or ion-molecule reactions which lead finally to enhanced losses by dissociative recombination. Modification can also arise in a natural way by selective transport processes. In the lower ionosphere, this selection is mainly provided by the differing recombination rates of the different ion species. Metal ions above the turbopause have a much longer life-time than the characteristic time-scales of transportation, in contrast to the dominant ions, NO^+ and O_2^+. In the higher ionosphere or magnetosphere, the transport process itself can be selective. Diffusive separation, as it occurs in the polar wind, is the simplest example. Less well understood are processes related to anomalous resistivity of field-aligned currents which may accelerate different ion species even in opposite directions, since one species may be preferentially coupled to the parallel electric field and the other to the electron current (Haerendel, 1976).

Modification means creation of an inhomogeneous composition of the ionzed component which may or may not be accompanied by a change of total mass-density and pressure. The aim of this paper is to survey briefly the host of processes initiated by such modifications. Before doing so, I will summarize the common plasma injection techniques and some of the natural modification processes.

2. Artificial and Natural Modification Processes

I do not intend to give a complete survey of all possible modification techniques, but will confine this discussion mainly to chemical releases and to some natural modification processes. Recently, interest has grown in more indirect modification techniques by releasing freon or other molecules with which the natural plasma reacts rapidly (s. contributions of Mendillo (1976) and Bernhardt et al. (1976) to this symposium). These techniques will not be covered here.

2.1. Chemical Releases

Historically the first deliberate plasma injection was made by Marmo et al. (1959) with Cs vapor. Thermite reactions, in which a compound of the element to be injected is reduced by Al or Mg, were mainly used. Initially, the same type of reaction was applied in barium release experiments (Föppl et al., 1965), but later on replaced by the more efficient Ba - CuO reaction with an excess of Ba (Föppl et al., 1967):

$$n\ Ba + CuO \longrightarrow BaO + Cu + (n - 1)Ba$$

n is typically 2.5. The same reaction works well with Eu and Li. The efficiency for barium is in the proximity of 10 - 15% relative to the total weight.

Recently, titanium - boron reactions have been introduced as heat sources for evaporating metals of higher vapor pressure such as Ba and Li (Alford and Reed, 1969). Since the reaction product, TiB_2, is a solid and both atoms relatively light, a clean and perhaps more efficient evaporation of the added metal can be achieved. Whenever weight is critical, this may be an attractive new technique. Table 1 is a list of molecules which have been released in the upper atmosphere. Figure 1 taken from an excellent summary of chemical release techniques by Thiokol (1975) shows the amounts of materials that have been released up to now in rocket experiments. The dominance of barium demonstrates the great interest in ionospheric modification.

Shaped or hollow charges have proven to be very useful tools for injections of ion beams along the magnetic lines of force up to high altitudes, i.e. deep into the magnetosphere (Michel, 1969, 1974; Wescott et al., 1972, 1974). Forward velocities of up to 20 km/sec, but dominantly between 8 and 15 km/sec, are characteristic of the fast part of the velocity distribution. Figure 2a shows the distribution achieved with the charge shown in Figure 2b. By proper choice of cone angle, liner thickness, and shape of the explosive can one optimize the resulting velocity distribution of the ion jet. In our recent experiments we have been aiming at a relatively narrow velocity range. Figure 3 shows such a jet at an altitude of

3700 km. Its length is 1000 km and the width of the bright structure 20 km. In addition to particle tracing this technique can be used to create artificial ducts for VLF waves in the magnetosphere.

The elements used so far for chemical releases of plasmas were Li, Cs, Ba, Eu. U_{238} is another good candidate because of its low ionization potential. The alcali metal ions Li^+, Na^+, Cs^+ do not have resonance lines in the optical window of the earth's atmosphere and can, therefore, only be used if other than optical detection techniques are employed, such as radar reflections or in situ measurements. Table 2 summarizes some of the properties of these elements.

2.2. Natural Modification Processes

The most important recombination process of metal ions (M^+) in the low ionosphere are three-body reactions, e.g.:

$$M^+ + O_2 + A = MO_2^+ + A$$

and subsequent dissociative recombinations of MO_2^+. A is any third neutral collision partner. Since the probability of such collisions decreases rapidly above 100 km, the life-time of metal ions becomes very long. The dominant molecular ions, O_2^+ and NO^+, however, are subject to dissociative recombination with rate coefficients of the order $\alpha_{rec} = 10^{-7}$ cm^3 sec^{-1}. Hence, any pile up or depletion of the total plasma density in the lower ionosphere will have a more severe effect on metal ions than on the dominant ions, which tend to re-establish quickly their chemical equilibrium. This way the relative composition of the various ionic constituents can change severely. Regions where this tends to occur most expressedly are (1) the regions of sporadic E, i.e. regions of wind shear; (2) the underside of the ledge of the night-time F2 layer at sub-equatorial latitudes, where the ions lifted by the equatorial fountain effect "rain" down; and (3) regions of strong shear flows in the polar ionosphere, where the Pedersen current, which is carried by the ions, has appreciable divergences. Mg^+ and Fe^+ are the most abundant naturally occurring metal ions. They originate by the evaporation of micro-meteorites at 80 - 90 km altitude and become ionized after upward transport by charge exchange with O_2^+ and NO^+.

Of particular interest are today natural modifications of the magnetospheric plasma by upward acceleration of ionospheric ions. Either heating in regions of strong anomalous electric resistivity or the action of a strong parallel electric field, both in the presence of dense field-aligned currents, may be responsible for this effect. The relation to field-aligned currents, which tend to flow in thin sheets, implies a very inhomogeneous modification of the magnetosphere through this mechanism. Reports of high densities of NO^+, O_2^+, N_2^+ at altitudes up to 1100 km (Taylor, 1974), of energetic O^+ in the magnetosphere (Shelley et al., 1972, 1974), and of outward directed field-aligned ion flows in plasma sheet (Paschmann et al., 1976) and plasma mantle (Frank et al., 1976) confirm the presence of these ions. Their possible effects on magnetospheric dynamics and the propagation or generation of plasma waves is likely to become a fascinating subject of future research. Barium shaped charge experiments have recently demonstrated beyond doubt that electrostatic acceleration of ions into the magnetosphere does occur (Haerendel et al., 1976).

3. Processes Initiated by Modification of the Ionized Medium

There are essentially three classes of effects that are related to inhomogeneous plasma distributions. The first class comprises those effects which result from the balance of forces: inertial, pressure, magnetic, and resistive forces. The second class contains the changes of transport processes arising from electrostatic polarization fields set up by inhomogeneities of the electrical conductivity, both collisional and inertial, the latter occurring when the wave frequency exceeds the collision frequency. The third class are the effects of inhomogeneities on the propagation of electromagnetic and plasma waves; they are of particular interest to this symposium. Many of these effects may lead to instabilities, to further secondary effects and feed-backs. Of particular interest are those processes which are characteristic of a cold and hot plasma interface, as we have between ionosphere and magnetosphere. It is to a large extent this aspect that will maintain or even enhance the demand for active plasma experimentation in the near earth space over the next decade or so.

At the same time, many of these experiments are providing tracers for natural processes, in particular of the electric and magnetic fields. This property has been in the foreground of most of the chemical release experiments till now and will certainly be further exploited.

3.1. Enhancements of Pressure

In this class of effects we must distinguish between the balance of pressures perpendicular and parallel to the magnetic field. The initial phase of many plasma injections is characterized by diamagnetic effects. The decay of magnetic cavities is an interesting subject of investigation. In the lower ionosphere the pressure balance is maintained by interactions of the ionized component with the much denser neutral atmosphere. Parallel to the magnetic field ambipolar diffusion and sedimentation dominate. Above the F2 maximum, the ionized and neutral components become decoupled, and the balance of total plasma pressure parallel to $\underline{B}$ is a subject of interest. A few experimental and theoretical results from this field will now be summarized.

3.1.1. Diamagnetic Cavities

When the pressure, p , of an injected plasma exceeds the energy density of the ambient magnetic field, $B^2/8\pi$, a magnetic cavity is formed. In the ionosphere this is not an important effect for chemical releases, because the photo-ionization time-scales are so long that plasma densities above 10^7 cm^{-3} can hardly be generated. Even with an initial energy of 100 eV, as they are achieved in shaped-charge injections of barium, the energy density would stay at least one order of magnitude below the magnetic pressure. Plasma injections with plasma generators, however, although they have normally a much lower total output of ions, lead to the formation of magnetic cavities within the first few meters from the source (Zhulin et al., 1972). The study of the development of such a cavity, in particular of its collapse is a very fascinating plasmaphysical experiment. In the sounding rocket project PORCUPINE we had scheduled the ejection of a Cs-source from the main diagnostic payload (Sagdeev et al., 1976), which would have provided such an experiment (Figure 4) (Unfortunately, the rocket motor exploded shortly before burnout, and no data were obtained.).

With chemical releases in the higher magnetosphere the situation is different (Pilipp, 1971). $\beta = 8\pi p/B^2$ exceeds unity within a substantial volume. Figure 5 is a sketch of the situation for a release of about 2 kg of Ba vapor at an altitude of 5 R_E using a Scout rocket (Haerendel, 1973). Figure 6 shows magnetic field data from inside the cavity. The field is decreased by 2 orders of magnitude, but recovers quickly within about 1.5 min. This recovery was faster than expected. Furthermore, there are indications of micro-instabilities causing a fast diffusion of $\underline{B}$ back into the cavity and heating the plasma at the same time. This heating manifested itself in an unusually fast longitudinal expansion of the barium plasma.

The diamagnetic effects created by artificial injections are short-lasting or, with an continuously operating source, confined to the very neighborhood of the source. They are, however, strong modifications of the environment and useful tools for experimental studies of processes which play important roles in the laboratory, possibly at the magnetopause, in cometary atmospheres and many other situations. Subsequent to the diamagnetic phase, plasma boundary layers with gradient lengths below the ion gyro-radius may be maintained for a little while whereas the electrons are already completely magnetized. This again is a fascinating subject of plasma physics.

3.1.2. Ambipolar Diffusion

When the plasma density of the ionosphere is locally enhanced, it is subject to several transport mechanisms. Parallel to the magnetic field ambipolar diffusion, sedimentation and drag by the neutral wind are the prevailing processes. Transverse to $\underline{B}$, convection, possibly connected with strong shears, dominates, very often breaking up into small scale convection because of instabilities that will be mentioned later on. Transverse diffusion has not yet been established as a significant effect, except for anomalous diffusion in diamagnetic cavities (see above). But ambipolar diffusion of a finite cloud is an interesting theoretical subject (Haerendel and Scholer, 1967; Simon and Sleeper, 1972; Rozhanskii and Tsendin, 1975). It turns out that parallel as well as transverse to $\underline{B}$ the ions dominate the rate of diffusion and an approximate diffusion equation for a cylindrical inhomogeneity is:

$$\frac{\partial n}{\partial t} = \frac{\partial}{\partial z}\left(D_{a_\parallel} \frac{\partial n}{\partial z}\right) + \frac{1}{r}\frac{\partial}{\partial r}\left(r\, D_\perp \frac{\partial n}{\partial r}\right)$$

with

$$D_{a_\parallel} = \left(1 + \frac{T_e}{T_i}\right) D_{i_\parallel}$$

$$D_\perp \cong \left(1 + \frac{T_e}{T_i}\right) D_{i_\perp} \quad .$$

Since $D_{i_\perp} / D_{i_\parallel} \ll 1$ where diffusion plays an essential role (F layer) it can for all practical purposes be considered as one-dimensional parallel to $\underline{B}$ and proceeding with $D_{a_\parallel}$.

When releases are made in the upper F-region, where the coupling with the neutral atmosphere is weak, one has to be aware that the heat content of the injected plasma may not be quickly exchanged with the background. In experiments at the magnetic equator at about 500 km altitude (2 kg charges only) we could observe for more than 10 min a locally enhanced parallel diffusion coefficient. This is only understandable if the temperature of the barium cloud remained higher than the (measured) background temperature by about 60% for this period.

3.2. Enhancements of Total Mass Density

If the total mass density of the ionized component if significantly affected by a plasma injection, inertial or gravitational forces in the disturbed region may become important. Under almost all circumstances will the initial bulk velocity of the injected plasma be different from that of the background. Eventually, however, both will become equal, unless there is a constant external force acting transverse to $\underline{B}$, like gravity at the equator. The momentum exchange with the ambient plasma is an important problem, in particular because of the inhomogeneity of the magnetosphere-ionosphere system, which introduces complex long range coupling effects by emission and dissipation of Alfvén waves. The gravitational force may lead to the Rayleigh-Taylor instability.

3.2.1. Momentum Transfer

The momentum density of a certain volume in space be suddenly enhanced owing to plasma injection, and the total velocity vector be different from that of the undisturbed environment. After the diamagnetic phase, the magnetic field pervading the injection region can be considered as frozen-in, i.e. injected and pre-existing plasma tend to move relative to the surrounding plasma. The corresponding change of the magnetic field leads to the excitation of Alfvên waves which propagate approximately along the magnetic field and communicate the change of motion to other regions in space outside the injection region. Thereby, momentum is exchanged along a flux-tube with a time-scale:

$$\tau_o = \frac{M_{ion}}{2F \rho_a v_A} ,$$

where M_{ion} is the total injected mass, F the cross-section transverse to $\underline{B}$, ρ_a the ambient density and v_A the Alfvên velocity. This process has been dealt with by Scholer (1970).

If the injection occurs in the magnetosphere, the propagation of the Alfvên waves and the coupling with the dissipative ionosphere poses many interesting problems which pertain equally to some natural magnetic pulsations (pc 5) or, for instance, to the interaction of Io and Jupiter. In the aforementioned barium release from a Scout rocket we observed a very slow momentum exchange lasting up to several hours, depending on the mass density within a certain flux-tube. Such a dependence is to be expected from the above equation. Figure 7 shows a picture of the resulting density structure, and Figure 8 the square-root of the angular separation from the field line through the release point as a function of time. The different slopes show the density dependent accelerations, the brightest features being the slowest. One of the unexpected results was the absence of any strong oscillatory effects which were predicted as a consequence of Alfvên wave reflection at the ionosphere (Scholer, 1970).

This experimental situation is closely related to the physics of cometary plasma tails. In that case, however, $\underline{B}$ is relatively weak as compared with the momentum density of the plasma flow. Therefore, the field becomes strongly distorted while it is still anchored in the coma of the comet. The well-known rays, which point away from the sun, are formed. In order to study the effects more closely, one could in fact think of creating an artificial comet by releasing several 100 kg of barium outside the magnetopause. This may be an experiment for the 80's.

In the ionosphere we can treat the momentum exchange in an electrostatic way, since the travel time of an Alfvên wave is much shorter than the time of momentum exchange. This time-scale is dictated by the balance of the inertial and frictional forces on a flux-tube. The friction is caused by ion-neutral collisions; therefore, the integrated Pedersen conductivity, Σ_p, enters:

$$\tau_1 = \frac{M_{ion} c^2}{F \Sigma_p \cdot B^2} .$$

It turns out that τ_1 lies typically between 10^{-2} and 10^{-1} sec. For optical tracing from the ground it is not detectable. However, diagnostic instrumentation close to a plasma emitter should discover the finite momentum transfer time. We were hoping to measure the distortion of a plasma spiral originating from the rotating Cs-plasma generator (Figure 9) to be ejected from the PORCUPINE payload. The maximum expansion of the spiral upstream in the sense of the ambient convection would give an answer on τ_1.

3.2.2. Rayleigh-Taylor Instability

A gravitational force, $\underline{g}$, transverse to the magnetic field leads to a transverse drift:

$$\underline{u}_g = \frac{\underline{g} \times \underline{B}}{\Omega B}$$

where Ω is the gyrofrequency. u_g is proportional to the molecular weight, μ. At the magnetic equator, u_g is approximately: $u_g = 0.3 \cdot \mu$ [cm/sec]. In spite of the small magnitude of this drift it may have far reaching effects, since the corresponding ion current can set up strong polarization fields at any existing inhomogeneity. The magnitude of this field depends on the effective transverse conductivity which allows for a certain amount of short-circuiting. If the conductivity of the lower F and E regions is reduced, as it happens in the equatorial ionosphere at sunset, the damping of vertical convective motions is reduced; the Rayleigh-Taylor instability can work. We have essentially the situation of a heavier fluid on top of a lighter one at the steep ledge of the F2 layer. Its growth rate is (Balsley et al., 1972)

$$\gamma = \frac{g}{\nu_{eff} H} ,$$

where ν_{eff} is a weighted average of the ion-neutral collision frequency and H the scale height of the plasma component. With $H \approx 20 - 50$ km growth rates of several times 10^{-3} sec^{-1} can exist. It is now widely

believed that equatorial spread F, a wide range of irregularities in the night-time equatorial F-region, is initiated by this process.

One feature of this instability is very remarkable: the irregularity creates apparently elongated "bubbles" which rise up by several 100 km, even above the F maximum (Woodman and La Hoz, 1976; Kelley et al., 1976), rather than leading to enhanced downward transport of higher density regions. Inside these "bubbles" or "holes" short-wave irregularities form which are effective radar scatterers. Figure 10 shows an example of rising patches of 3 m irregularities as measured by the Jicamarca radar. On the other hand, we were very surprised when we placed barium clouds into the theoretically unstable F-layer during spread F that no visible fine-structure was created. One of the few examples of barium clouds without striations. This anomaly is still unexplained.

3.3. Changes of Electrical Conductivity

3.3.1. Pedersen Conductivity

In a weakly ionized plasma such as the ionosphere, the electrical conductivity is proportional to the number density of charged particles. Inhomogeneities of the density lead necessarily to polarization fields, which in turn affect the electric drift, $\underline{u}_E = c \frac{\underline{E} \times \underline{B}}{B^2}$. The high electrical conductivity parallel to $\underline{B}$ has the consequence that a whole magnetic flux-tube gets involved. Therefore, we must not only take into account the primary inhomogeneity, but all the plasma along the magnetic lines of force, in particular the section through the E-layer where the Pedersen- and Hall-currents flow. For small transverse wave-lengths electric polarization fields can be short-circuited above this layer, thus the effective integrated conductivity becomes reduced (Farley, 1959) and the polarization fields enhanced. Subsequent distortions and small-scale irregularities can develop more rapidly and cause the familiar striated appearance of barium clouds.

A vast literature exists on the subject of distortions (Lloyd and Haerendel, 1973; Perkins, Zabusky, and Doles, 1973; Zabusky, Doles, Perkins, 1973) and on formation of striations by the cross-field instability (Simon, 1963; Linson and Workman, 1970; Völk and Haerendel, 1971). One of the decisive processes in this context is the set up of secondary irregularities in the region of return current owing to the fact that the communication along magnetic field lines is achieved by electron currents, whereas the dissipative part of the transverse current, the Pedersen current, is carried by the ions. Hence, any divergence of $\underline{E}_\perp$ leads to a divergence of the ion flow and thus pile up and depletion of the previously unaffected background plasma. This way image clouds and image striations develop below and above the primary irregularity (Figure 11). The physics becomes very complex and escapes analytical treatment. Numerical modeling has been successfully applied to these problems.

In brief, whenever we modify the ionosphere, somewhere electrostatic coupling leads to a subsequent modification of other layers along the same flux-tube. Most efficient is the modification if applied to the region of maximum transverse electrical conductivity. Chemical releases in this range of altitudes are, however, less effective because oxidation of the neutrals is competing with the photo-ionization process. Cs seems to be more appropriate than barium for such applications. An effective artificial modification of the E-layer can be achieved by electron attachment as for instance with releases of SF_6 or by an immediate injection of metal ions by means of plasma generators.

In this connection we should remind ourselves of the existence of appreciable amounts of natural metal ions, mainly Mg^+ and Fe^+ in the E-layer. They can pile up in regions of wind-shears or strongly divergent Pedersen currents (Figure 12). Once their distribution has become inhomogeneous they tend to create secondary irregularities via the cross-field instability, be it only because the critical ratio of gyro- and collision frequencies, on which the transverse conductivities depend, varies approximately as $\mu^{-1/2}$. Not much is known about the role of these meteoric ions in the creation of ionospheric fine-structure, but the subject is worth exploring. Our group is at present developing a TV-camera to be flown on a balloon with the aim to take pictures of the ionosphere in the light of the Mg^+-resonance lines at 2800 Å. This technique may help elucidating such processes.

3.3.2. Inertial Conductivity

Large-scale ionospheric irregularities are quite often accompanied by short wave-length structure. This is of particular importance for the backscatter of radio-waves above the critical frequency. Spread F and type II irregularities in the E-region are good examples. The underlying mechanisms are not yet completely understood, in particular in the upper F-layer. When collisions are rarer, other effects may take over; the ion inertia becomes important. In the presence of a varying electric field the ions get a mobility in the direction of $\underline{E}$ and the corresponding velocity is for $\omega \ll \Omega_i$:

$$\underline{u}_p = \frac{1}{\Omega_i} c \frac{\dot{\underline{E}}_\perp}{B} .$$

This ion current can take over the role of the Pedersen current in the lower ionosphere and lead to somewhat changed growth-rates of instabilities such as the Rayleigh-Taylor or cross-field instabilities. $\omega - \underline{k}\underline{v}_0$ must exceed the collision frequency for inertial effects to become effective. With typical drift velocities of tens of hundreds of m/sec this applies to wave-lengths below about 1 km in the F-layer.

Of particular significance are ion inertial effects in connection with the often observed shear flows. Above the E-layer shear flows correspond to $\frac{\partial E_x}{\partial x} \neq 0$. Any drift in the direction of the divergent electric field will lead to a $\frac{dE_x}{dt}$ experienced by the ion and thus to an additional mobility in the direction of E_x , which the electron does not possess. The resulting electric current can be destabilizing in certain situations. In general, we should not be surprised to see shear flows accompanied with small scale irregularities down to the range of meters. In this field much theoretical works has still to be done.

4. Modification of the Propagation of Waves

In this paper I have focused the attention on processes which influence the dynamics of density changes of an ionized medium. Once such variations in density are established they will influence the propagation of waves, be it the diagnostic waves of ground-based radar, the radio waves of a commercial broadcasting station, the TM signals of a satellite, the signals of a point-like radio source, the whistler waves in a magnetospheric duct, or plasma waves trapped in regions of enhanced cold plasma in the magnetosphere. If the waves are excited by energetic particles, their propagation properties have strong consequences on their growth and, therefore, on the energy transferred to them from the particles. This means, in addition, that the accompanying scattering of the particles is also affected by the propagation properties of the waves. Modification of the propagation medium can thus cause a wide field of secondary effects (Brice, 1970). The interest in these processes as well as the desire to understand the mere propagation of the waves, stimulates us to design various artificial modification experiments. Chemical releases are a relatively inexpensive means to achieve them. However, plasma generators and accelerators appear more frequently in space, in particular in the planning for Spacelab. Phenomena as magnetic cavities and sharp plasma boundaries with scale-lengths below the ion gyro-radius can be set up with their help and can be studied far into the non-linear regime of any occurring instability. Large-scale plasma seeding in the magnetosphere and tracing of transport processes between solar wind and the inner magnetosphere are more ambitious tasks for future applications of the chemical release technique. It is quite apparent that the earth's environment as a plasma laboratory has not at all been fully exploited.

References

Alford, G., and R. Reed, Jr., An Analytical and Laboratory Investigation to Develop More Effective Methods for Producing Dense Barium Ion Clouds, RADC-TR-69-366 Thiokol Report, Oct. 1969.

Balsley, B.B., G. Haerendel, and R.A. Greenwald, J. Geophys. Res. 77 (1972) 5625.

Bernhardt, P.A., A.V. da Rosa and C.G. Park, Chemical Depletion of the Ionosphere, This Symposium (1976).

Brice, N., J. Geophys. Res. 76 (1971) 4698.

Farley, D.T., J. Geophys. Res. 64 (1959) 1225.

Föppl, H., G. Haerendel, J. Loidl, R. Lüst, F. Melzner, B. Meyer, H. Neuss and E. Rieger, Planet. Space Sci. 13 (1965) 95.

Föppl, H., G. Haerendel, L. Haser, J. Loidl, P. Lütjens, R. Lüst, F. Melzner, B. Meyer, H. Neuss and E. Rieger, Planet. Space Sci. 15 (1967) 357.

Frank, L.A., K.L. Ackerson and D.M. Yeager, Observations of Atomic Oxygen (O^+) in the Earth's Magnetotail, University of Iowa Report 76-5 (1976).

Haerendel, G., and M. Scholer, Space Research VII, North-Holland Publ. Comp., Amsterdam (1967) 509.

Haerendel, G., in Space Research XIII, Akademie Verlag, Berlin (1973) 601.

Haerendel, G., Coordinated Measurements with Eiscat, Sounding Rockets, and Balloons Aimed at Plasma-physical Studies,
Haerendel, G., E. Rieger, A. Valenzuela, H. Föppl, First Observation of Electrostatic Acceleration of Barium Ions into the Magnetosphere,
Proc. Symposium on Present and Future European Programmes on Sounding Rockets and Balloon Research in the Auroral Zone, Schloß Elmau, Germany (1976) in press.

Kelley, M.C., G. Haerendel, H. Kappler, A. Valenzuela, B.B. Balsley, D.A. Carter, W.A. Ecklund, C.W. Carlson, B. Häusler, and R. Torbert, Evidence for a Rayleigh-Taylor Type Instability and Upwelling of Depleted Density Regions During Equatorial Spread F, submitted to Geophysical Research Letters (1976).

Linson, L.M., and J.B. Workman, J. Geophys. Res. 75 (1970) 3211.

Lloyd, K.H., and G. Haerendel, J. Geophys. Res. 78 (1973) 7389.

Marmo, F.F., J. Pressman, and L.M. Aschenbrand, Planet. Space Sci. 1 (1959) 291, 306.

Mendillo, M. and J. Forbes, Spatial-Temporal Development of Molecular Releases Capable of Creating Large-Scale F-Region Holes, *This Symposium* (1976).

Michel, K.W., Verhalten der Ba-Ionenstrahlen aus Hohlladungen beim Nike-Tomahawk Experiment, MPI-PAE/Extraterr. 19 (1969).

Michel, K.W., Acta Astron. 1 (1974) 37.

Paschmann, G., O. Bauer, G. Haerendel, H. Rosenbauer and N. Sckopke, HEOS 2 Plasma Observations in the Near-Earth Plasma Sheet, presented at the AGU Intern. Conf. on Solar-Terrestrial Physics, Boulder (1976).

Perkins, F.W., N.J. Zabusky and J.H. Doles III, J. Geophys. Res. 78 (1973) 697.

Pilipp, W., Planet. Space Sci. 19 (1971) 1095.

Sagdeev, R.Z., I.A. Zhulin, V.A. Dokukine, J.J. Ruzhin, and G. Haerendel, PORCUPINE EXP. 12: Cesium Plasma Source, in "Project PORCUPINE" ed. by G. Haerendel, Max-Planck-Inst. Rep. (1976) 88.

Scholer, M., Planet. Space Sci. 18 (1970) 977.

Shelley, E.G., R.G. Johnson, and R.D. Sharp, J. Geophys. Res. 77 (1972) 6104.

Shelley, E.G., R.G. Johnson, and R.D. Sharp, in Magnetospheric Physics ed. by B.M. McCormac, Reidel, Dordrecht-Holland (1974) 135.

Simon, A., Phys. Fluids 6 (1963) 382.

Simon, A., and A.M. Sleeper, J. Geophys. Res. 77 (1972) 2353.

Taylor, Jr., H.A., J. Atmosph. Terr. Phys. 36 (1974) 1815.

Thiokol Research Report "Chemical Releases from Space Shuttle Payloads", Publ. No. 75243 (1975).

Völk, H.J., and G. Haerendel, J. Geophys. Res. 76 (1971) 4541.

Wescott, E.M., H.M. Peek, H.C.S. Nielsen, W.B. Murcray, R.J. Jensen, and T.N. Davis, J. Geophys. Res. 77 (1972) 2982.

Wescott, E.M., E.P. Rieger, H.C. Stenbaek-Nielsen, T.N. Davis, H.M. Peek, and P.J. Bottoms, J. Geophys. Res. 79 (1974) 159.

Woodman, R.F., and C. La Hoz, Radar Observations of F-Region Equatorial Irregularities, submitted to J. Geophys. Res. (1976).

Zabusky, N.J., J.H. Doles III, and F.W. Perkins, J. Geophys. Res. 78 (1973) 711.

Zhulin, I.A., V.I. Karpman, and R.Z. Sagdeev, in Critical Problems of the Magnetosphere, ed. by E.R. Dyer, National Academy of Sciences (1972) 245.

DISCUSSION

P.A. Bernhardt: What were effects of NH_3 release ?

G. Haerendel: Just shock wave effects.

J. Lemaire: What is the order of magnitude of the time scale $\tau_1 = M_{ion} c^2 / 4\pi \Sigma_P B^2$ compared to $\tau_0 = M_{ion} c^2 / 2\pi \rho_a v_A$?

G. Haerendel: $\tau_0 \simeq$ hours

$\tau_1 \simeq 10^{-2}$ sec (?)

TABLE 1

Typical Chemicals Used in High Altitude Experiments (Thiokol, 1975)

Ba	Sr	C_2H_2
Na	Al $(CH_3)_3$	NH_3
Li	Al $(C_2H_5)_3$	B_2H_6
Cs	SF_6	B $(C_2H_5)_3$
Eu	NO	Fe $(CO)_5$
K	NO_2	Pb $(C_2H_5)_4$
Ca	CS_2	Kerosene
Al	CO_2	Misc. explosives

TABLE 2

Properties of Elements Suitable for Artificial Ionospheric Plasma Clouds

Element	U_{ion} [eV]	Resonance Lines of Ions [Å]	α_{ion}	t = theory t = experiment
Li	5.39	199.28	$2.9 \cdot 10^{-4}$ sec^{-1}	t
Na	5.12	372.07	$1.1 \cdot 10^{-5}$ sec^{-1}	t
Sr	5.69	4077.77 4215.52	$< 2.2 \cdot 10^{-4}$ sec^{-1}	t , e
Cs	3.87	926.75	$6.5 \cdot 10^{-4}$ sec^{-1}	t
Ba	5.21	4554.04 4934.09	$5 \cdot 10^{-2}$ sec^{-1}	e
Eu	5.67	4129.74 4205.05	$5 \cdot 10^{-3}$ sec^{-1}	e
U	6.05	4090.20 4241.67	?	

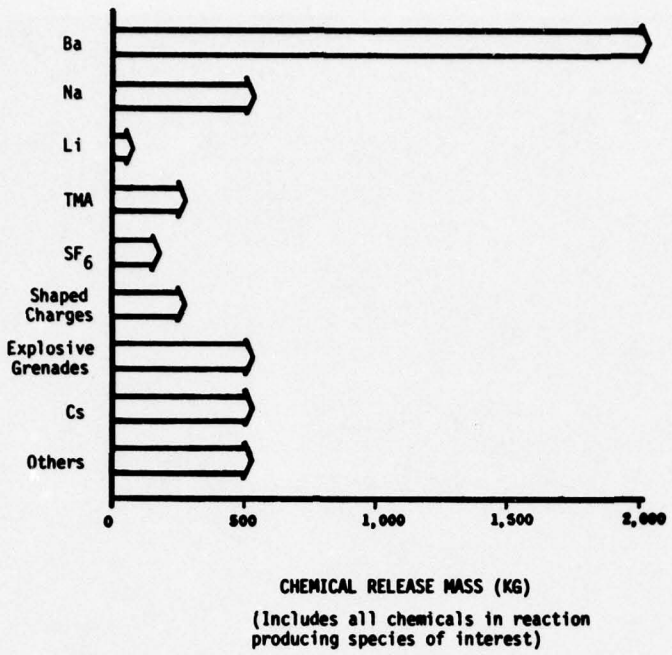

Figure 1: Approximate Usage of Chemicals in High Altitude Experiments (Thiokol, 1975).

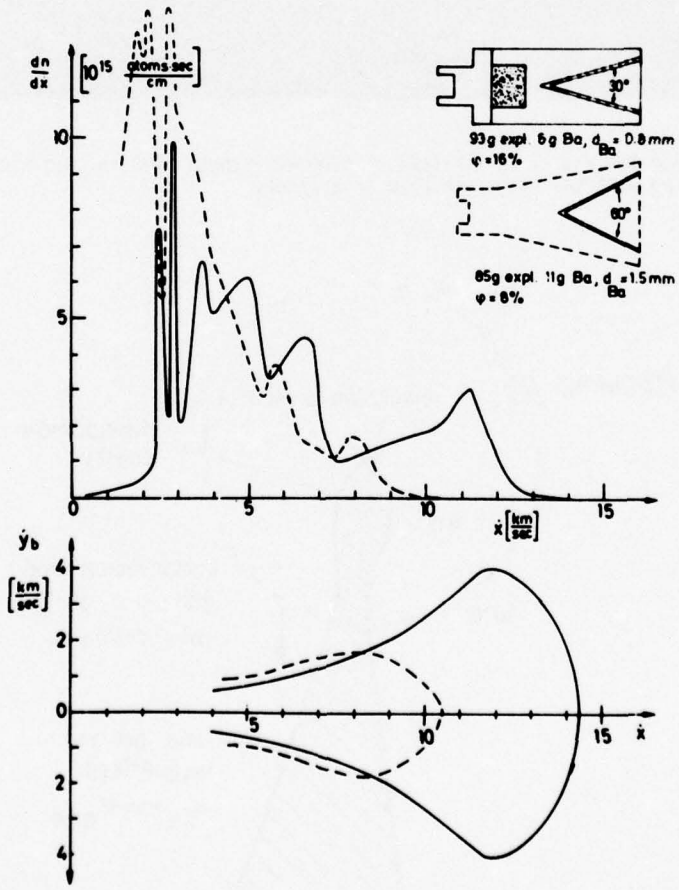

Figure 2a: Distribution of Ba Vapour Atoms Over Forward Velocity $\dot{x}$ and Transverse Velocity $\dot{y}_b$ of the Boundary of the Distribution as Measured in the Laboratory by Michel (1969, 1974). —— cone angle 30^0 , ---- cone angle 60^0 .

Figure 2b: (upper right-hand corner) Configurations of Shaped Charges.

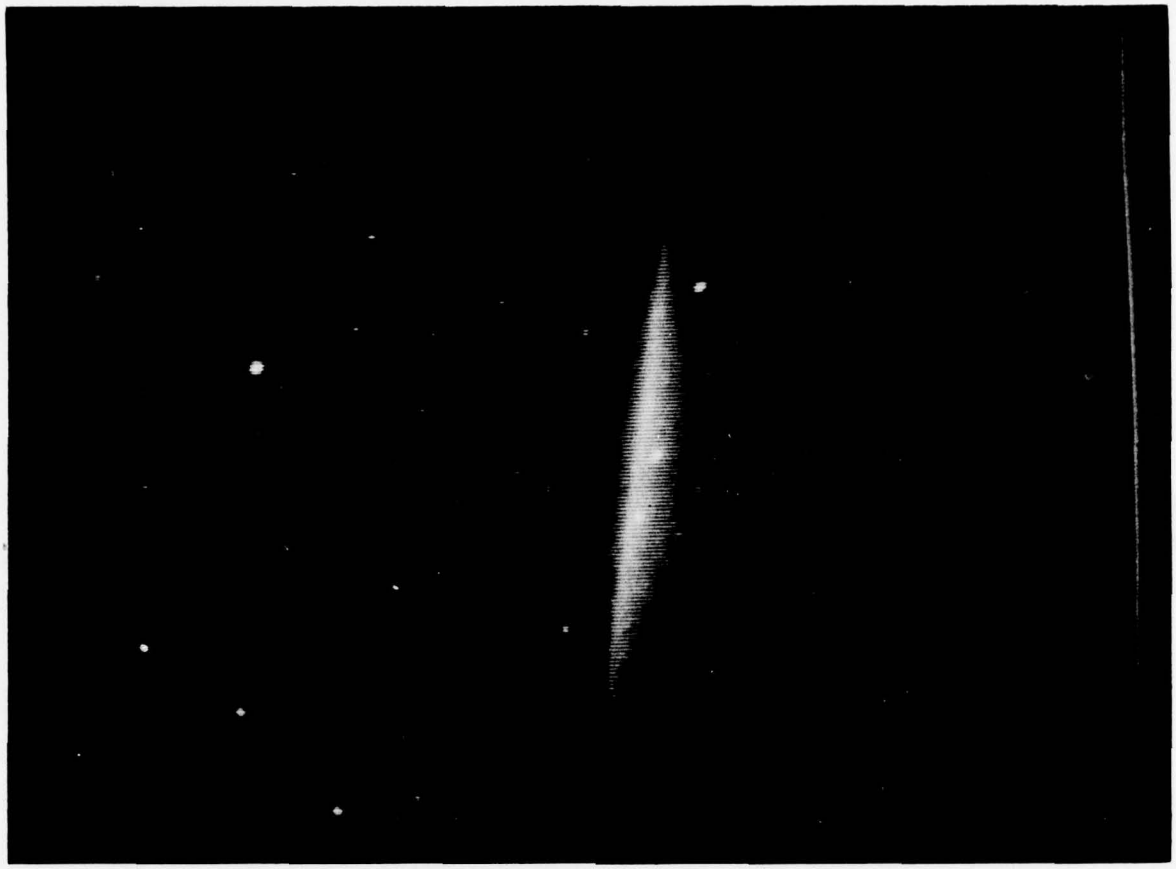

Figure 3: Barium Ion Jet at an Altitude of 3700 km. Length 3700 km, Width of Core 20 km, 5 Minutes After Injection From Antarctica.

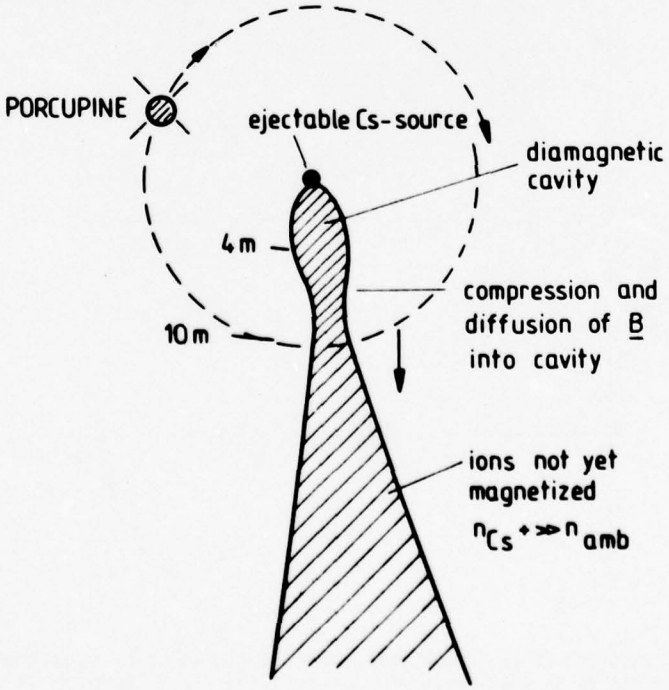

Figure 4: Sketch of Cs-Plasma Beam Near Source. Configuration of Experiment 12 on PORCUPINE (Sagdeev et al., 1976).

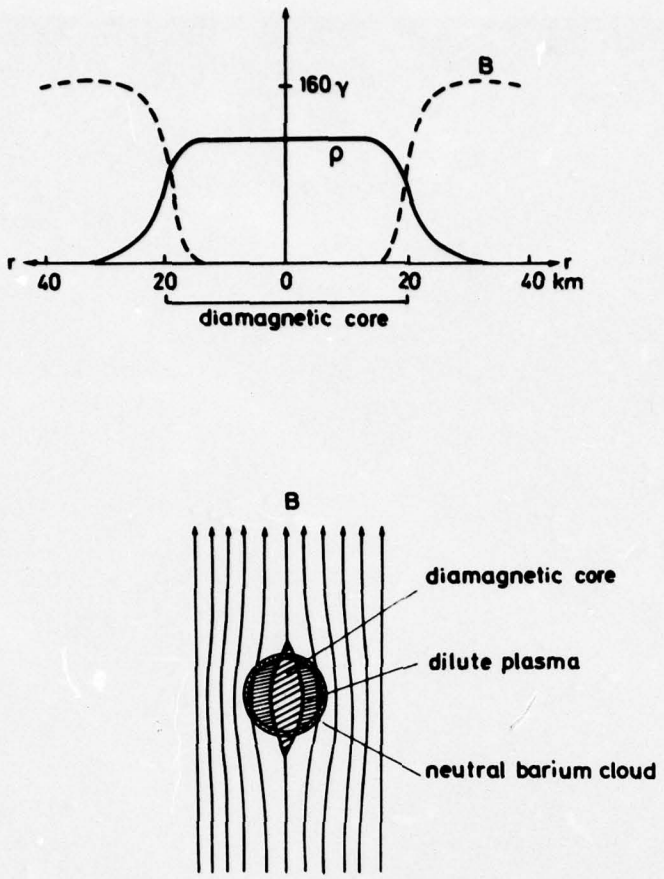

Figure 5: Sketch of Initial Configuration of Plasma and Magnetic Field in a Release at an Altitude of 5 R_E.

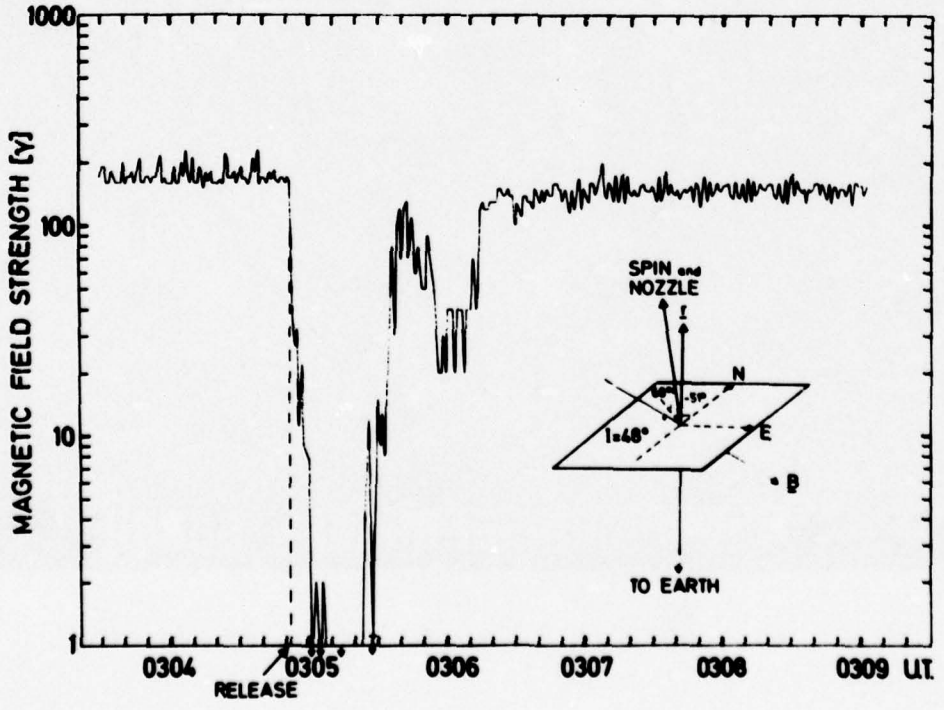

Figure 6: Observed Perturbation of Magnetic Field in Release at 5 R_E Altitude (Haerendel, 1973).

Figure 7: Barium Cloud at 5 R_E Altitude After 15 Minutes (Haerendel, 1973).

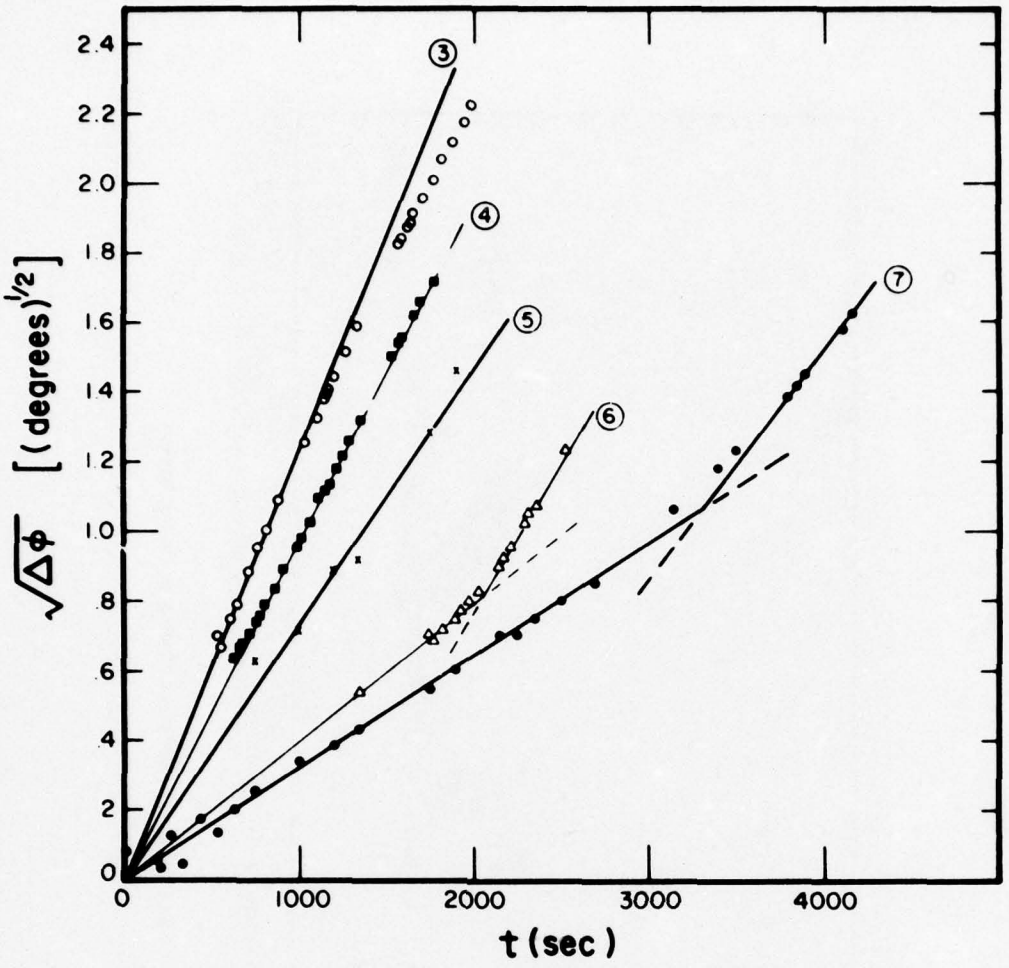

Figure 8: Square Root of Angular Distance of Density Structure From Initial Position as Function of Time Showing Linear Acceleration.

Figure 9: Spiral of Cs-Plasma Generated by Rotating Plasma Source in the Ionosphere (Sagdeev et al., 1976).

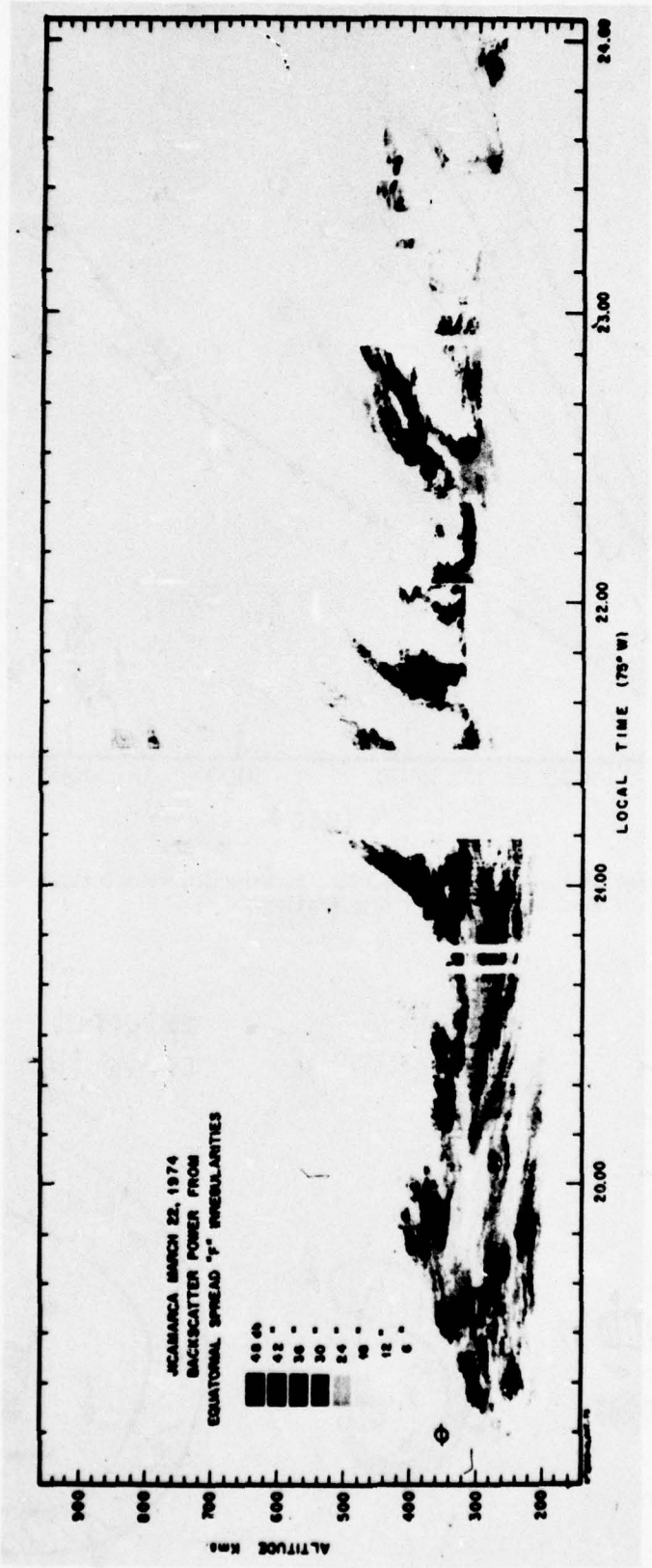

Figure 10: Radar Echos From Equatorial Spread-F Irregularities Showing a Rising Motion (Woodman and La Hoz, 1976).

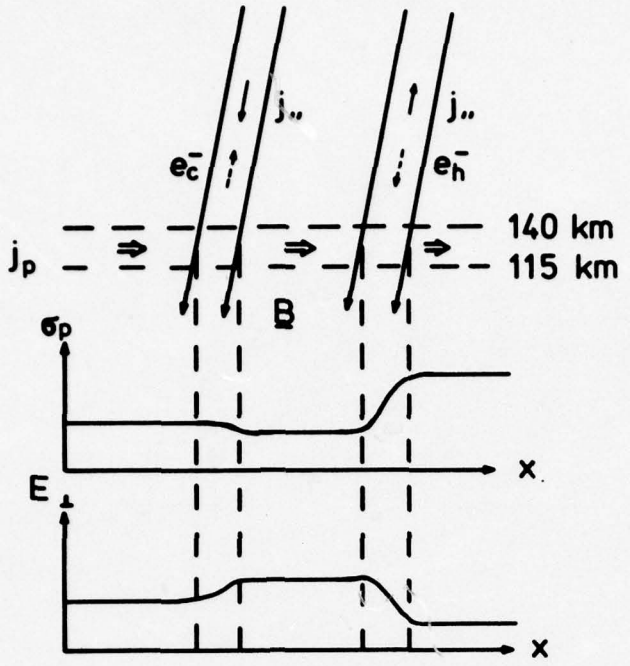

Figure 11: Image Clouds Formed Above and Below a Primary Ion Cloud Owing to Set up of Electric Polarization Fields (Lloyd and Haerendel, 1973).

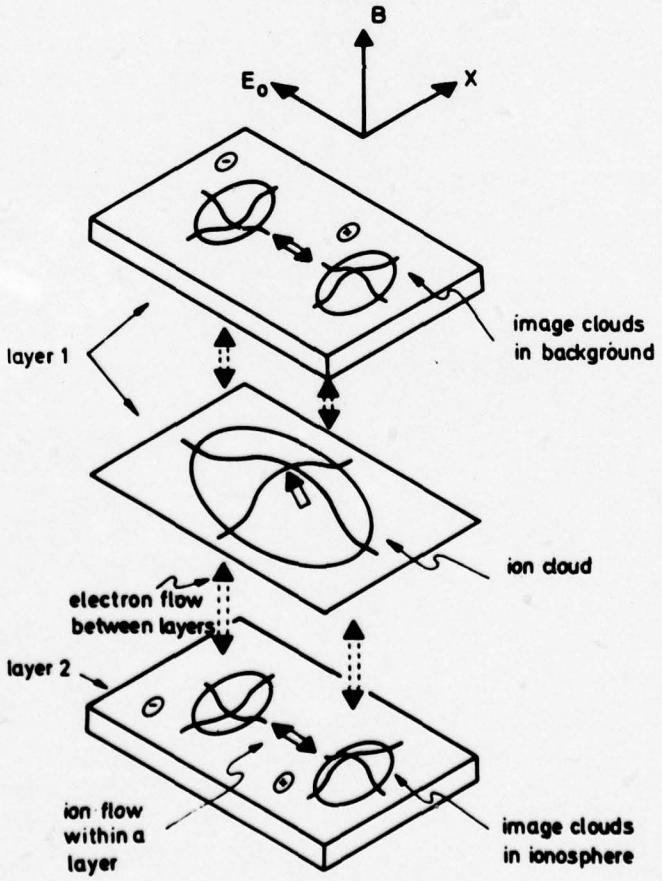

Figure 12: Modification of Ionosphere in Regions of Field-Aligned Currents Related to Auroral Arcs. The Metal Ion Density Should be Inversely Proportional to $E_{\perp}$ (Haerendel, 1976).

SPATIAL-TEMPORAL DEVELOPMENT OF MOLECULAR RELEASES CAPABLE OF CREATING LARGE-SCALE F-REGION HOLES

Michael Mendillo and Jeffrey Forbes
Department of Astronomy
Boston University
Boston, Massachusetts 02215 USA

SUMMARY

The discovery that the exhaust plume of the Saturn V rocket which launched NASA's Skylab Workshop caused a sudden and large-scale depletion of the ionospheric F-region total electron content has renewed interest in the creation of so-called "artificial ionospheric holes" by chemical release techniques (see Mendillo et al., 1975, for a published summary of the "Skylab Effect" and its related theory). A more detailed investigation of diffusion in an exponetial atmosphere, with and without chemical loss processes for the diffusing substance, and for a variety of possible release heights and solar cycle conditions is now under study. Since the amounts of material capable of injection into the F-region will, under most projected circumstances, be much less than the 1 ton/second of exhaust ejected by the Saturn V second stage engines during the Skylab launch, a thorough analysis of the diffusion process is vital for any prediction of the types of smaller holes which can be created. To a first approximation, the rate of decrease of electrons at any particular time and distance from the release point is proportional to the instantaneous concentration of the diffusing substance. Our initial results for diffusion of molecular hydrogen (one of the highly reactive molecules capable of creating F-region holes) shows that chemical loss by atomic oxygen severely affects the expansion of the released gas by creating a chemical sink in the lower thermosphere which competes with diffusion.

(Ref: "A Large-Scale Hole in the Ionosphere Caused by the Launch of Skylab", Mendillo, M., Hawkins, G.S., and J.A. Klobuchar, SCIENCE, 187, 343-346, 1975.)

1. INTRODUCTION

The dramatic "ionospheric hole" created by the exhaust of the Saturn V rocket which launched NASA's Skylab Workshop (MENDILLO, M., 1975a, 1975b) provided the impetus for a new look at large-scale ionospheric modifications. Rocket launches have long been known to provoke ionospheric disturbances (BOOKER, H.G., 1961, STONE, M.L. 1964, ARENDT, P.R., 1961, REINISCH, B.W., 1973), but these modifications were often small in magnitude, limited in geographical extent, and short-lived in duration. They were usually explained as being due to "ballistic interactions" between the physical structure of the rocket (or its exhaust) and the ambient atmosphere. It was felt that the rocket and/or its exhaust would, in essence, push-aside the neutral atmosphere and the ionized component embedded in it. For the "Skylab Effect", however, (MENDILLO, M., 1975a) suggested that the dominant mechanism responsible for creating the observed F-region hole was chemical. Specifically, the molecular content of the Saturn exhaust plume (H_2 and H_2O) caused the atomic-ion/electron plasma of the F-region (O^+ and e^-) to be rapidly transformed into a molecular ion/electron plasma (OH^+ or H_2O^+ and e^-) which rapidly recombined. The re-enactment of this process is the type of modification experiment we envision, and the calculations described below address this goal within a realistic experimental framework.

2. DETERMINING FACTORS FOR A SUCCESSFUL MOLECULAR RELEASE EXPERIMENT.

The aim of the present study is to investigate the most important aspect of any modification experiment by chemical releases, i.e., the exact temporal and spatial development of the substance released. It is anticipated that any future experiment could not realistically be expected to use the same enormous number of molecules ejected by the Saturn second stage engines. During that launch, several hundred tons of H_2O and H_2 were added to the F-region and consequently the horizontal region affected exceeded 1000 km in diameter. We envision rocket and/or Space Shuttle releases of perhaps only a ton ($\simeq 10^3$kg), and therefore one needs information as precise as possible concerning the expansion of the cloud into the ionospheric region it is due to modify. We see several specific factors to consider in the formulation of such a modification experiment:

1. The number of particles capable of being deposited in the ionosphere.
2. The height distribution of the source, e.g., a point source versus a gaussian or line source function.

3. The height or height range of the release.
4. The molecular weight and size of the released particles.
5. The reactivity of the released particles with the dominant constituents of the background atmosphere and ionsophere, taken to be O and O^+, respectively.
6. The state of the ambient atmosphere and ionosphere.
7. The extent and duration of the desired ionospheric hole.

The results of Mendillo (1975b) stressed that the temporal-spatial development of the expanding cloud of molecules was, to first approximation, a diffusion-dominated process. Since a truly enormous number of molecules were added to the upper atmosphere during that launch, depletion effects (whether photochemical or aeronomic) upon the diffusing substance were shown to be unimportant when accounting for the observed effects. To maintain this diffusion-dominated scenario for a much smaller release suggests that the main concern would only be that of not making the release from too high an altitude. The virtually explosive expansion of a molecular cloud into the topside ionsophere would simply argue for a release somewhat below the peak of the particular electron density profile to be modified. However, when dealing with a modest number of molecules, it is not possible to continue to ignore the chemical processes between the molecules and the ambient atmosphere the molecules are attempting to diffuse through. In particular, as the height of the release is lowered, the atmospheric chemistry which can destroy the molecules before they remove ion-electron pairs becomes more and more important, and eventually it dominates. To achieve maximum ionospheric effects, therefore, the height of the release must be a function of both the $N_e(h)$ profile and the state of the background atmosphere.

Concerning the molecular weight and size of the particles released, clearly the heavier and larger the molecules are, the slower is their diffusion. From simple kinetic theory, the diffusion coefficient (D) depends on the mean free path (λ) and average thermal velocity ($\bar{v}$), where λ varies inversely with molecular size and $\bar{v}$ inversely with the square root of mass.

The main thrust of our calculations is directed to topic (5), an assessment of the mechanism whereby the molecules are destroyed by atmospheric chemistry before they can begin to create an ionospheric hole. Within the framework of assessing topic (5), we also address topics (2), (3), and (6) to some extent. The case chosen for study is the release of molecular hydrogen. This seems the most appropriate one to consider because its light weight favors diffusion. Sections 3 and 4 give the physical assumptions and mathematical formulation for our model, and sections 5 and 6 present our results and associated discussion.

3. PHYSICAL ASSUMPTIONS AND BASIC DATA

To illustrate our technique, we have chosen to study the diffusion of an artificially-injected cloud of H_2 in the ionosphere for minimum (T = 800K) and maximum (T = 1400K) sunspot activity, thus providing a set of profiles which are representative of effects under most conditions. The released particles are assumed to be thermalized and dominated by mutual - rather than self-diffusion shortly (≈5 sec) after the release. Photo-dissociation and condensation of the released gas are not considered. While these latter two assumptions hold for H_2 (MENDILLO, M., 1975b), they might not be true for other possible release gases such as H_2O, CO_2, or NO_2.

In order to create the largest ionospheric hole, the optimum release height must lie somewhere in the bottomside F-region, permitting the H_2 gas to diffuse upward through the F-region peak as time progresses. We therefore assume the transport of H_2 to be governed by molecular diffusion combined with the chemical loss process

$$H_2 + O\ (^3P) \xrightarrow{\gamma_1} OH + H$$

Loss of H_2 by the ion-atom interchange reaction

$$H_2 + O^+ \xrightarrow{\gamma_2} OH^+ + H$$

is neglected. Our physical model can be justified by the following time-constant arguments. Consider the time constants (T) for the loss of H by chemical loss (1), ion deplection (2), and molecular diffusion to be defined by

$$\tau_c = e^z/\gamma_1 [O]_o \approx e^z/\beta_o$$

$$\tau_i = 1/\gamma_2 [O^+]$$

$$\tau_d = L^2\, e^{-z}/D_o$$

respectively, where z = distance in scale heights from the reference height h_o, L = characteristic scale length for diffusion, and subscript zero denotes values taken at h_o = 300 km. We will later find it convenient to think of T_d as a <u>diffusive residence time</u> over the characteristic length L. Values for relevant parameters adopted in the calculations are given in Table 1. Nighttime O^+ profiles are used to compute time constants since the proposed chemical releases are incapable of depleting the O_2^+ and NO^+ ions in the daytime F_1 layer, thus restricting the most dramatic ionospheric modifications to nighttime. Some daytime ionospheric data appear in Table 1 for comparison purposes. Taking L = 50 km. (appropriate during early stages of the release), one finds that $\tau_i \gtrsim 5\ \tau_d$ for T = 800K and T = 1400K at all heights, indicating that the diffusion of H_2 is, to a first approximation, decoupled from the ionospheric depletion process. In fact, these values of represent gross underestimates within the expanding cloud of H_2,

since the ambient ionosphere rapidly disappears during the initial stages of the release. Loss by O^+ would have significant effects if $[H] \sim [O^+]$, which occurs during the later stages of the release at the leading edge of the expanding H_2 cloud. The overall effects of including reaction (2) in the diffusion of H_2 were shown to be small by Bernhardt et. al., (1975) who considered diffusion alone. In section 6 we determine at what stage of the release H_2 depletion by O^+ can no longer be neglected when H_2 loss by reaction (1) is also included. On the other hand, $\tau_d > \tau_c$ below 300 km for 1400K and $\tau_d > \tau_c$ below 200 km for 800K, indicating that chemical loss by O cannot be neglected under all conditions. The effect of chemical loss appears to be relatively minor for T = 800K. However, it is found in Section 5 that the H_2 linear density profile descends with time, and the diffusive residence time lengthens, so that chemical loss eventually competes with molecular diffusion in this case also.

4. MATHEMATICAL FORMULATION

The diffusion of H_2 in O is governed by

$$\frac{\partial \eta}{\partial \tau} = -\beta\eta + D\left\{\frac{\partial^2 \eta}{\partial h^2} + \left(\frac{1}{H_o} + \frac{1}{H}\right)\frac{\partial \eta}{\partial h} + \frac{\eta}{H_o H}\right\} + D\left\{\frac{\partial^2 \eta}{\partial x^2} + \frac{\partial^2 \eta}{\partial y^2}\right\}$$

where

$\eta(\vec{r},t)$ = number density of H_2

$\beta(h)$ = chemical loss coefficient for H_2 to the ambient atomic oxygen atmosphere

$D(h)$ = mutual diffusion coefficient

H_0 = scale height for O

H = scale height for H_2

h = altitude

x,y = horizontal coordinates

The quantities β, D, H_0, and H are assumed to be independent of x and y. Moreover, we consider an isothermal background atmosphere consisting exclusively of atomic oxygen, thus limiting the validity of our results to regions above about 200 km. We wish to stress the mathematical formalism necessary to handle the case of diffusion with chemical loss, coupled with a representative set of illustrations which show the importance of the loss process. The final effect upon the ionosphere of the molecular release ultimately depends upon the total number of molecules available at any given height and time. We therefore integrate (3) over horizontal space, obtaining

$$\frac{\partial N}{\partial t} = -\beta N + D\left\{\frac{\partial^2 N}{\partial h^2} + \left(\frac{1}{H_o} + \frac{1}{H}\right)\frac{\partial N}{\partial h} + \frac{N}{H_o H}\right\}$$

where

$$N(h,t) = \int_{-\infty}^{\infty}\int_{-\infty}^{\infty} (\vec{r},t)\, dx\, dy,$$

which is the total number of injected particles at altitude h and time t. This quantity, which we refer to as the linear number density, proves useful in evaluating the relative effects of chemical loss and diffusion in a concise, one-dimensional way. Applying the method of separation of variables to (4) leads to an eigenfunction-eigenvalue problem with solutions in terms of generalized Laguerre polynomials. Yu and Klein (1964)determined a solution to (4) for the case $\beta = 0$. We will refer to these solutions as L-results, for diffusion with loss, and D-results, for diffusion only, respectively.

5. RESULTS

As stated above, the technique of using one-dimensional, horizontally integrated, vertical profiles is a particularly concise way of assessing the differences between the number of molecules available at any given height and time as given by the diffusion only (- D -) and diffusion with loss (- L -) results. Table 2 summarizes four sample cases chosen to illustrate different release heights and extreme exospheric temperatures. The CIRA-72 model was used to determine the atomic oxygen concentration at the release height, and the exponential atmosphere used in our calculations was keyed to that value.

In Table 2, case (2) represents diffusion with maximum loss and case (3) diffusion with minimum loss. To illustrate these cases in comparison to the diffusion-only formulation, consider figures 1 and 2. For these calculations, a gaussion source function with a half-peak thickness of 20 km was used. The source was normalized to unity, and thus the linear concentrations on the abcissa should be multiplied by the total number of particles released. Thus, for a release of 100 kg of molecular hydrogen (H_2), the profiles appearing in Figures 1 and 2 would have to be multiplied by 3×10^{28} molecules.

In Figure 1, the linear number density profiles for diffusion only (labelled with a D)

and diffusion with loss (labelled with an L) differ significantly for times of a minute and longer. During the first 10 seconds or so, loss has not yet become important, and thus the D and L results are similar. However, after 360 seconds the L-results show a 6-fold decrease in the number of molecules simple diffusion would predict. Clearly, one cannot count on the longevity of an artificial hole as a natural consequence of lingering molecules, at least not under these solar maximum, low release conditions. Moreover, the horizontal extent of the expanding cloud, and therefore the anticipated ionospheric hole, would certainly be much smaller when chemical loss is taken into account.

In Figure 2, where the minimum loss condition is presented (cases D_3 and L_3), one can see that after 60 seconds of expansion the L and D results are very similar. The loss-less diffusion curves diverge from the diffusion-with-loss profiles only at the topside heights.

The integral with height of the vertical profiles appearing in Figures 1 and 2 gives the total particle count as predicted by the diffusion only (d) and diffusion-with-loss (L) formalisms. To illustrate how significant the loss mechanism can be for late times, consider the results for particle counts presented in Figure 3. Using the four atmospheric cases described in Table 2, and a 20 km half-peak source thickness, the resultant D and L profiles have been integrated between height limits of 200 and 600 km, for times of 3 minutes to 30 minutes. For the diffusion-only conditions, the particle counts decrease with time due to diffusion into the regions below 200 km and above 600 km. The diffusion-with-loss curves (L_1 to L_4) naturally include this type of diffusive loss, as well as the chemical loss of H_2 to the atomic oxygen within the 200 to 600 km height range. This is a clear case of how the temporal/spatial availability of molecules, and therefore the possible duration and horizontal extent of an F-region hole, is very much dependent upon how the molecules react with the ambient atmosphere.

6. DISCUSSION

Figures 1-3 show that chemical loss can have a marked effect on the diffusion of an artificially-injected cloud of H_2 in the ionosphere. Some insight into the physics involved can be obtained by comparing the time constant for chemical loss, $\tau_c = e^z/\beta_o$, and the diffusive residence time, $\tau_d = L^2 e^{-z}/D_o$. Since we are considering a rather localized source funtion, the scale length L is initially small, and diffusive residence time of the molecules is very short; hence τ_c must be comparatively small in order for the chemical loss to effectively compete with diffusion in the early stages of the release. Considering the time constant arguments in Section 3 and the profiles in Figure 1, this is in fact the case for a release at 250 km in a background atmosphere corresponding to sunspot maximum conditions. Referring to Figure 1, after 10 minutes the D (diffusion-only) profile has lowered its peak from 250 km to 225 km. Such behavior is expected since the topside particles are diffusing away faster than the bottomside ones, thus forcing the peak of the profile to descend. On the other hand, the peak of the L profile has ascended to 290 km with a peak value about a factor of 10 less than the D profile. The profile does not descend in this case since the bottomside particles are continually lost to a chemical sink in the lower thermosphere.

Now consider a release centered at 300 km in the T = 800 K atmosphere (Figure 2). The introduction of chemical loss appears to have a different effect in this case. Here diffusion dominates in the early stages of the release, and both the D and L profiles descend. (The dominance of diffusion is due to the combined effect of the temperature dependence of the rate constant γ_1, and the greater height of the release.) After about 60 seconds, the length scale associated with the diffusion process increases, hence lengthening the diffusive residence time and allowing chemical loss to once again compete effectively with diffusion. However, the relative abundance of particles at altitudes above ~ 250 km represented by the D profiles is not so obviously explicable on these grounds. One is reminded that the curves in Figure 2 represent the total number of particles at a particular height and time, and cannot be associated with any point in x-y space. We can presume, nevertheless, that many of these particles have travelled a considerable horizontal distance from the point of the release, since those which initially chose to travel vertically have escaped from the F-region. Therefore, the diffusive residence time of these remaining particles is very long, and in the presence of the chemical loss process are removed long before they would have reached these points under the assumption of diffusion alone.

7. ACKNOWLEDGEMENTS

This work was supported in part by contract F19628-75-C-044-P00001 from the Air Force Cambridge Laboratories to Boston University.

J. M. Forbes is a Staff Scientist with the Space Data Analysis Laboratory, Boston College, Chestnut Hill, Massachusetts 02167.

8. REFERENCES

ABRAMOWITZ, M., AND STEGUN, I. (ed.), 1970, "Handbook of Mathematical Functions", U.S. Government Printing Office, Washington, D.C.

ARENDT, P.R., 1971, Ionospheric Undulations Following Apollo 14 Launching, Nature, 231, 438.

BERNHARDT, P.A., PARK, C.G., AND BANKS, P.M., 1975, Depletion of the F2 Region Ionosphere and the Protonosphere by the Release of Molecular Hydrogen, Geophys. Res. Let., 2,341.

BOOKER, H.G., 1961, A Local Reduction of F-region Ionization Due to Missile Transit, J. Geophys. Res., 66, 1073.

COSPAR International Reference Atmosphere, 1972, Akademie Verlag, Berlin.

CLYNE, M.A.A., AND THRUSH, B.A., 1963, Rates of Elementary Processes in the Chain Reaction Between Hydrogen and Oxygen. I. Reactions of Oxygen Atoms, Proc. Roy. Soc., A275, 544.

FERGUSON, E.E., 1973, Rate Constants of Thermal Energy Binary Ion-molecule Reactions of Aeronomic Interest, At. Data Nucl. Data Tables, 12, 159.

MENDILLO, M., HAWKINS, G.S., AND KLOBUCHAR, J.A., 1975a, A Large-Scale Hole in the Ionosphere Caused by the Launch of Skylab, Science, 187, 343.

MENDILLO, M., HAWKINS, G.S., AND KLOBUCHAR, J.A., 1975b, A Sudden Vanishing of the Ionospheric F-region Due to the Launch of Skylab, J. Geophys. Res., 80, 2217.

REINISCH, B.W., 1973, Burnt-out Rocket Punches Hole into Ionosphere, Space Research, Vol. XIII, Akademie-Verlag, Berlin, 503.

RISHBETH, H., AND GARRIOTT, O.K., 1969, "Introduction to Ionospheric Physics", Academic Press, New York.

STONE, M.L., BIRD, L.E., AND BALSER, M., 1964, A Faraday Rotation Measurement on the Ionospheric Perturbation Produced by a Burning Rocket, J. Geophys. Res., 69, 971.

WESTENBERG, A.A. AND DE HAAS, N., 1967, Atom-molecule Kinetics at Higl. Temperature Using ESR Detection. Technique and Results for $O+H_2$, $O+CH_4$, and $O+C_2H_6$, J. Chem. Phys., 46,490.

WONG, E.L., AND POTTER, A.E., 1965, Mass-spectrometric Investigation of the Reactions of O Atoms with H_2 and NH_3, J. Chem. Phys., 43, 3371.

YU, K., AND KLEIN, M.M., 1964, Diffusion of Small Particles in a Non-Uniform Atmosphere, Phys. Fluids, 7, 651.

DISCUSSION

F. H. Hibberd: Was it likely that substantial molecular hydrogen was present ?

M. Mendillo: Yes. Fuel was liquid H_2 and O_2 and ..... ?

P.A. Bernhardt: Was the loss coefficient variable in height ?

M. Mendillo: Yes. It had an exponential dependence - following the neutral oxygen model.

G. Haerendel: 1) Was the recovery of the ionospheric hole consistent with the H_2 cloud model and the enhanced recombination coefficient arising from this cloud ?
2) Could the rapid recovery of the hole be related to transportation effects of the neutral cloud or/and the plasma hole ?

M. Mendillo: 1) We have not tried to reproduce in detail the recovery of the F-region hole following the SKYLAB launch because of the very complex nature of source, i.e., the rocket exhaust had two constituents and, of course, the rocket was continually changing its geographic position. The recovery of the hole depends upon a plasmaspheric flux and solar production effects.

2) The hole would take part in any convection effects appropriate for the local time and latitude. Thus, relatively un-modified plasma might appear along the diagnostic ray path monitoring the ionosphere. The neutral cloud would also be expected to follow ambient neutral wind patterns.

P. Halley: Pensez vous que le défaut où le trou d'ionisation provoqué artificiellement dans la région F puisse avoir créé une onde de gravité ? La courbe de densité électronique en fonction du temps présente un dépassement de la situation normale après une remontée rapide.

M. Mendillo: We looked carefully for any evidence for gravity waves, at several stations, but saw none. I suspect that since we observed a plasma loss effect, the total mass involved was small, and therefore probably not sufficient to launch gravity waves.

TABLE 1. BASIC DATA

Temperature	$[O]$ at 300 km (cm^{-3}) (a)	D at 300 km (cm^2 sec^{-1}) (b)	Peak electron concentration (cm^{-3}) (c) noon	midnight	Height of F-region peak (km) (c) noon	mid.	γ_1 (cm^3 sec^{-1}) (d)	γ_2 (cm^3 sec^{-1}) (d)
800 K	0.42×10^{9}	0.25×10^{12}	4.0×10^{5}	1.0×10^{5}	240	320	0.1×10^{-12}	0.2×10^{-8}
1400 K	0.13×10^{10}	0.11×10^{12}	1.6×10^{6}	5.0×10^{5}	320	380	0.2×10^{-11}	0.2×10^{-8}

(a) CIRA (1972)

(b) Kinetic theory hard-sphere model

(c) Risbeth and Gariott (1969), their TABLE IV.

(d) Intermediate among those measured by Clyne and Thrush (1963), Wong and Potter (1965), and Westenberg and De Haas (1967).

(e) Ferguson (1973)

TABLE 2

Case	Release Height	Exospheric Temperature	Oxygen Concentration
1	250 km	800 K	$1.32 \times 10^{9}/cm^3$
2	250 km	1400 K	$2.70 \times 10^{9}/cm^3$
3	300 km	800 K	$4.20 \times 10^{8}/cm^3$
4	300 km	1400 K	$1.32 \times 10^{9}/cm^3$

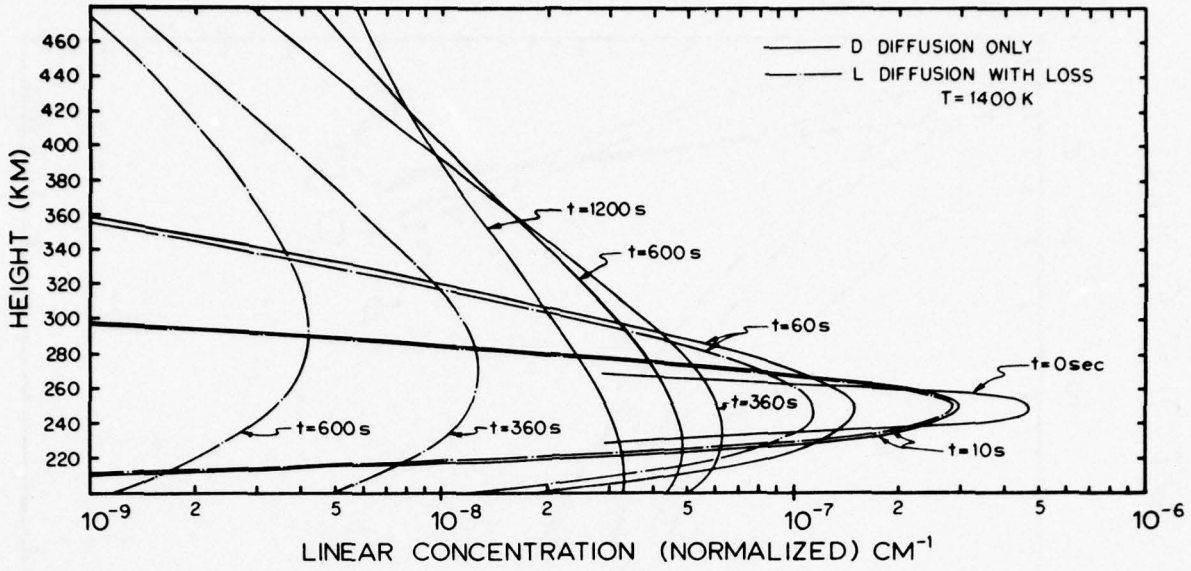

Figure 1:

Linear concentration profiles for diffusion-only (D) and diffusion with loss (L). The profiles are normalized by the total number of particles released. The source was taken as a gaussian distribution centered at 250 km and with a 20 km half-peak thickness. The background atmosphere is pure atomic oxygen at an exospheric temperature at 1400 K.

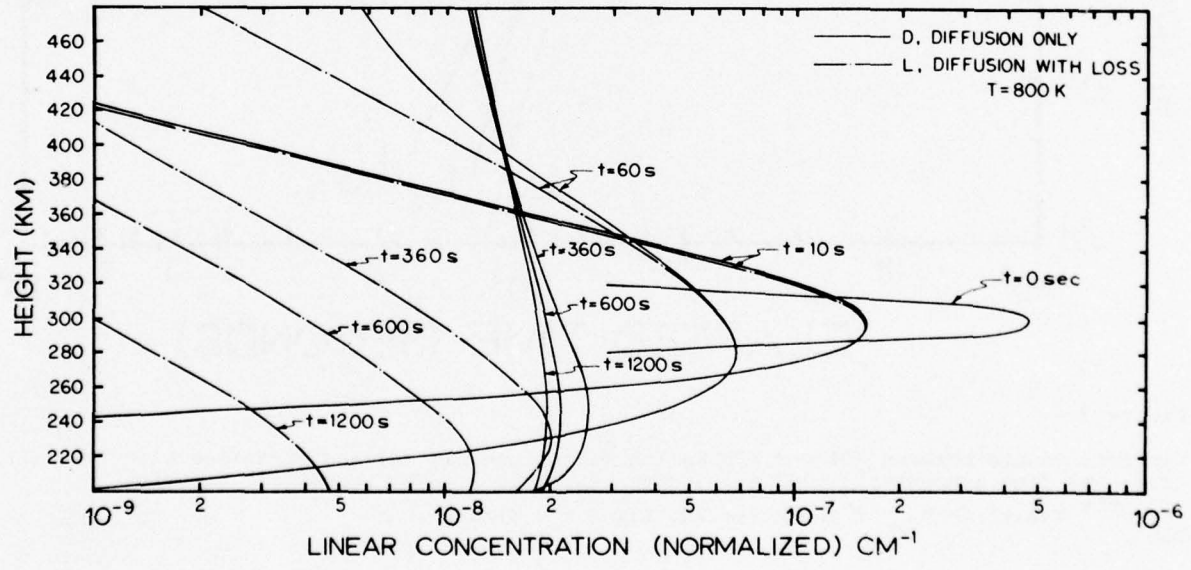

Figure 2:

Linear concentration profiles for diffusion-only (D) and diffusion with loss (L). The profiles are normalized by the total number of particles released. The source was taken as a gaussian distribution centered at 300 km and with a 20 km half-peak tnickness. The background atmosphere is pure atomic oxygen at an exospheric temperature of 800 K.

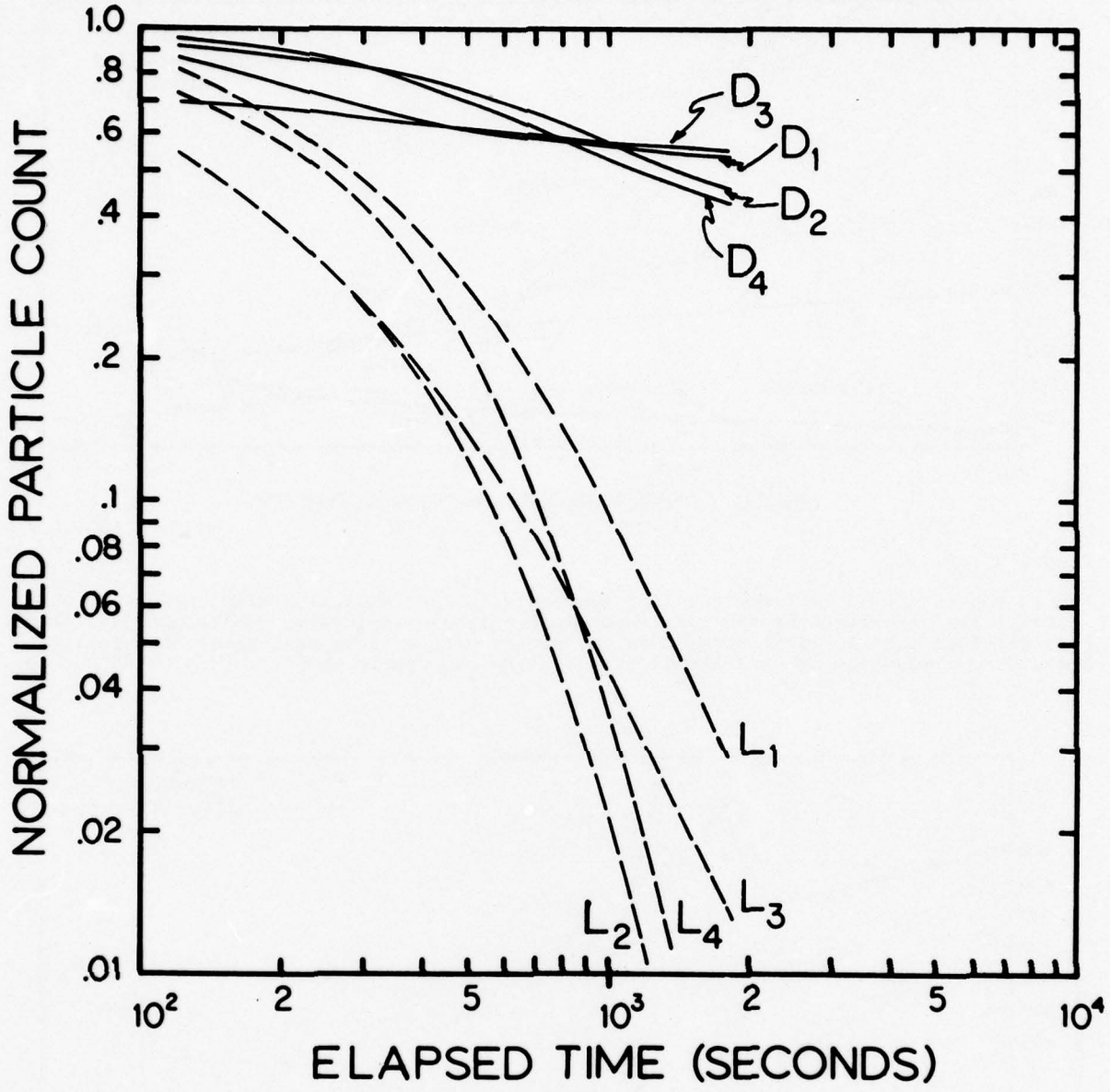

Figure 3:

Particle counts between 200 and 600 km for diffusion-only (D) and diffusion with loss (L), using the four atmospheric conditions given in Table 2. The normalized quantity $\int_{200}^{600} N(h,t)\, dh/N_{to}$ is shown for the times $t \geq 2$ minutes.

CHEMICAL DEPLETION OF THE IONOSPHERE

P.A. Bernhardt, A.V. da Rosa and C.G. Park
Radioscience Laboratory
Stanford University
Stanford, California 94305
U.S.A.

SUMMARY

An opening in the ionosphere may be created by the release of reactive chemicals that promote ion-electron recombination. The extent of the ionospheric modification partially depends on 1) the condensation, 2) the expansion rate, and 3) the chemical reaction rate of the injected gas. In the case of a diatomic hydrogen release, depression of the ionospheric O^+ and electron concentrations is governed by these reactions:

$$O^+ + H^2 \rightarrow OH^+ + H$$

$$OH^+ + e \rightarrow O + H$$

Side effects of chemically induced depletion of the ionosphere are increase of the electron temperature, decrease of the ion temperature, enhancement of airglow emissions and formation of depletion ducts extending into the magnetosphere. Radiowaves may be guided or focused as they propagate through the modified ionosphere or magnetosphere.

1. INTRODUCTION

Since the early 1960's it has been observed that the transit of rockets through the F-layer may produce observable reductions in the electron concentration. Early reports by Booker in 1961 and by Jackson, Whale, and Bauer in 1962 attribute this phenomenon to the displacement of the ionospheric plasma by the rocket exhaust gases. With a better understanding of the ionospheric chemistry, the question of the relative importance of the chemical versus the gas-dynamical effects of the rocket exhausts on the F-layer was raised. Observation of the large-scale depletion by the exhaust of a Saturn V rocket, as reported by Mendillo, et al. in 1975a, b, suggests that the chemical effects overshadow the plasma displacement effects within minutes after the injection of the exhaust into the ionosphere.

The first part of this paper is a discussion of a theoretical study of the chemical and gas dynamical processes resulting from the release of reactive gases into the daytime ionosphere. Only point releases, such as from an explosion or a pulsed jet, are considered. In the second part of the paper, some scientific uses of the artificial reduction of the ionospheric plasma are considered.

2. IONOSPHERIC MODIFICATION BY THE RELEASE OF POLYATOMIC NEUTRAL GASES

Figure 1 illustrates the various phenomena taking place between the time of gas release and the time of collisional mixing with the rarified F-region atmosphere. The coordinate axes in this figure are specific volume (reciprocal of mass density) and temperature. As a high temperature, high density gas cloud expands after release, its temperature rapidly drops and its volume increases as shown by the dark curve in the figure. If the gas does not condense, a low temperature is attained. The gas is then reheated by collisions with the background atmosphere. The whole process of cooling and reheating occurs in about ten seconds for a 100 kilogram release. Gases, such as water vapor, will partially condense upon release. The liberation of the heat of condensation tends to keep the vapor temperature elevated as shown by the dotted curve in the figure. Again, reheating of the molecules remaining in the vapor state is by collisions with the background atmosphere. In the example illustrated, 40% of the released gas has condensed. Thus, condensation may remove a significant portion of the gas molecules from the chemical process.

After thermalization with the background atmosphere, the remaining vapor molecules will expand diffusively. Figure 2 illustrates the diffusion of a gas ball into a nonuniform background atmosphere. The scale of the nonuniformity is characterized by the scale height H_a. When the ball expands over several scale heights, the ball becomes highly nonspherical. The calculation[a] of the diffusive expansion of a gas cloud into a nonuniform, chemically reactive atmosphere has been described by Bernhardt, Park and Banks [1975].

The gas cloud, during expansion, reacts with the ionospheric O^+. The average lifetime of an O^+ ion as a function of the neutral atmospheric composition is illustrated in Figure 3. The coordinate axes are 1) the ratio of released gas concentration to ambient nitrogen concentration and 2) the O^+ lifetime in seconds. Significant reduction in O^+ lifetime occurs for relatively small concentrations of water vapor, hydrogen, nitrogen dioxide, carbon dioxide, nitrous oxide, and diatomic oxygen. In the rest of this paper only H_2 depletion of the ionosphere is considered. H_2 was chosen because of its resistance to condensation and to photoionization[c], its low weight, and its high reaction rate with O^+.

The chemical reactions governing the ionospheric depletion are enumerated in Figure 4. In the normal, unperturbed F2-layer, the O^+ ion is removed by reaction with N_2 to produce NO^+. The NO^+ then reacts with an electron to produce N and O. The same sort of reactions occur[c] with the injection of H_2. Hydrogen undergoes ion-molecule charge exchange with O^+ to produce OH^+. The OH^+ then experiences rapid[c] dissociative recombination to produce O and H. A side effect of the release of H_2 is the production of excited states of O which leads to airglow emission.

Depletion of the ionosphere produces effects extending into the protonosphere. The field aligned geometry used in our simulation of the effects of H_2 release are shown in Figure 5. One hundred kilograms of H_2 are released into the F-layer at an altitude of 300 km. The field line at the point of release is L=3.

A block diagram of the Stanford plasmaspheric model is illustrated in Figure 6. The model is divided into three altitude regions corresponding to the ionosphere (less than 500 km), the $[O^+,H^+]$ charge exchange region (500 to 3000 km), and the protonosphere (above 3000 km). The blocks in the model are arranged into the neutral atmospheric model, the plasma model, and the thermal model. Two additional blocks, the H_2 continuity equation and the OH^+ continuity equation are needed to simulate the extraordinary processes resulting from H_2 release. The plasmaspheric model is described in detail in the report by Bernhardt [1976].

The density and temperature variations produced by the release of H_2 into the daytime F-region are examined in detail. Our simulation describes the effects of the release of 100 kg of H_2 at an altitude of 300 km and at a geographic latitude of 40°N. The field line through the release point is at L=3 with a dip angle of 70.5°. During the day, neutral winds are assumed to be zero.

Figure 7 shows a sequence of electron profiles for the daytime ionosphere with an overhead sun. The unperturbed profile at 0 seconds shows a large F2-layer above an F1-layer. One minute after the release of H_2, the F2 peak is reduced by an order of magnitude while the F1-layer is unaffected. The daytime increase in plasma temperature immediately after gas release produces a slight increase in the upward plasma flux. Eleven minutes after H_2 injection, the level of this flux has decreased below the unperturbed flux level because the F-region depletion has been communicated up the field line. After one-half hour, the shape of the F-layer has recovered but the peak density has not.

The daytime meridional plane contours of electron concentration in Figure 8 shows asymmetry and tilting resulting from the inclination of the geomagnetic field and nonuniformity of the neutral atmosphere. Because the H_2 cloud diffuses more rapidly upward into regions of lesser atmospheric density, its shape becomes nonspherical. The nonsphericity of the gas cloud coupled with the inclination of the magnetic flux tubes produces greater depletion to the north as compared with the depletion to the south of the release point. The daytime F-region is still recovering from the H_2 release after 4800 seconds.

The electron temperature rises dramatically during the day. This is a result of reduced cooling of electrons onto ions in the region where the plasma concentration has been depressed. Examination of the daytime electron temperature profiles along the field line through the point of H_2 injection (Figure 9) illustrates the effect of the lowered ion cooling. The local electron temperature minimum at the altitude of the F-layer concentration peak (300 km) rapidly disappears as high temperature electrons produced by thermalized photoelectrons enter the depletion region. The rise in the electron temperature produces a decrease in the downward thermal heat flux from the overlying protonosphere. The maximum electron temperature occurs about 10 minutes after H_2 release. At this time the temperature at 300 km has increased by 1500 K.

The spatial extent of the thermospheric modification is shown in Figure 10. Before the gas release, time 0 seconds, a slight meridional variation in the daytime electron temperature results from the latitudinal variation in the solar zenithal angle. One minute after H_2 release, a 100 km wide region of temperature enhancement (Figure 10) coincides with a similarly sized reduction in electron concentration (Figure 8). After ten minutes, the width of the supra-normal temperature region has increased to 250 km. Later, the electron contours relax toward the unperturbed state but even after 2 hours, significant thermospheric perturbation exists.

Coincident with a rise in the electron temperature is a decrease in the ion temperature. The heat source for the ions are the electrons. In the depleted ionosphere, the electron-to-ion heat transfer is reduced. After the reactive gas release, the ions are cooled by heat transfer to the neutral atmosphere.

The ion temperature reduction has a significant effect on the topside ionospheric H^+ concentration. The reduction in the F-region O^+ concentration produces a reduction in the H^+ concentration under conditions of isothermal chemical equilibrium because reaction of O^+ and H is the main mechanism for H^+ production in the F-region. However, comparison of the H^+ profiles before and after daytime H_2 injection reveals a decrease in H^+ only in the region at the bottom of the H^+ layer below 1100 km (Figure 11). Throughout most of the layer, the H^+ concentration increases. This is due to changes in H^+ loss and diffusion rates produced by ion temperature variations. The (H^+,O) reaction rate is proportional to the square root of the ion temperature. Thus, the reduction in ion temperature tends to produce an increase in H^+. The H^+ diffusion coefficient is proportional to the ion temperature to the 5/2 power [Schunk and Walker, 1970] resulting in a reduction in the diffusive transport of H^+ through the depletion region. These two effects produce a bulge in the H^+ profile in regions where production of H^+ by O^+ is not important.

The depletion of the F-layer produces a relative reduction in the protonospheric content above 3000 km. A temporal sequence in the formation of the daytime protonospheric depleted tube or trough is shown in Figure 12. The protonospheric content reduction is plotted against the meridional cross-field distance at the base of the tube relative to the field line passing through the point of release. The asymmetry in the trough is due to the magnetic field inclination.

As mentioned earlier, the release of H_2 into the F-layer will lead to the production of excited oxygen atoms. The region of 6300A airglow enhancements attributed to O (^1D) is illustrated in Figures 13 and 14. One minute after injection, a bright torus around the field line through the point of injection is formed. The intensity inside the ring is low because of the chemical depletion of the O^+ along the central magnetic field tube. The torus expands with the H_2 gas cloud producing a "smoke ring" effect.

The morphology of the expanding airglow ring is an indication of the electric fields and neutral winds in space surrounding the point of gas release. Without any externally imposed E-winds or fields the

ring will be circularly symmetric around the gas release point. A neutral wind will move the injected gas cloud toward one side of the depleted flux tube resulting in an elongated airglow ring with maximum brightness in the direction of the neutral wind. An electric field will move the partially depleted plasma tube toward the edge of the injected gas cloud. Thus, a neutral wind will move the optical portion of the ring away from the gas release point in the direction of the wind and in contrast, an electric field will move the hole in the ring away from the gas release point in the direction of the ExB tube drift. By measuring the variations in the structure of the airglow ring with respect to the point of gas injection, the magnitude and direction of neutral winds and electric fields deforming the airglow ring may be estimated.

The chain of events resulting from H_2 release into the ionosphere are summarized in Figure 15. Increased electron-ion recombination promoted by the diatomic hydrogen release produces airglow excitation and reduction of the F-layer plasma concentration. The ionospheric depletion is communicated up magnetic field lines causing a protonospheric depletion. In the depleted ionosphere, the cooling of electrons onto ions is reduced and the temperature of the electron gas increases. This produces a thermal expansion of the plasma resulting in a further reduction in electron and ion concentration. Collisions between neutral molecules and high temperature electrons produces additional enhancement in the airglow emissions.

3. EFFECTS OF THE DEPLETED IONOSPHERE ON RADIOWAVE PROPAGATION

The artificially depleted ionosphere and magnetosphere will produce variations in refractive index which affect the propagation of E-M radiation. Changes in radiowaves propagating through the modified plasmasphere are indicative of physical changes occurring in this region.

HF trajectories may be significantly affected in the vicinity of an ionospheric hole or trough. Generally, rays reflected from the sides of the trough are defocused. Focusing occurs for rays propagating through the depleted region (discussed later). Radiowaves with frequencies greater than the critical frequency at the trough center may escape through the ionospheric hole. Doppler frequency shifts in the returned HF waves indicate trough movement. Therefore, if an ionosonde is used to measure the structure of the chemically depleted ionosphere, angle-of-arrival and Doppler information may be necessary for proper interpretation of the ionosgrams. A theoretical study of reflection of high frequency ionospheric radiowaves in the vicinity of a trough has been presented by Helms and Thompson [1973].

Incoherent scatter radars are valuable tools for studying electron densities, electron and ion temperatures, and plasma drifts in the 200 to 800 km region. The power of radar signals scattered from the ionosphere is proportional to the electron density at the scattering point. The width of the received power spectrum is directly related to the electron-to-ion temperature ratio. The Doppler shift of the power spectrum is a measure of the plasma motion along the radar line-of-sight [Evans, 1969; Carpenter and Bowhill, 1971]. Thus, Thomson (incoherent) scatter radars may be used to determine density and temperature perturbations resulting from the injection of reactive gases.

A rarified plasma tube extending through the magnetosphere becomes a duct when it guides electromagnetic waves. In the guiding process, the raypaths are bent by the gradients of refractive index resulting from the variations of plasma density in the tube. A ray is said to be trapped if it tends to be bent toward the center of the tube when it is propagating parallel to the tube.

The guiding of a .9 MHz wave in a 60% depletion duct is illustrated in Figure 16. Reflection of the wave occurs at the topside ionosphere. (The depletion levels in Figures 16-18 are probably too large to be produced by ionospheric depletion. As such, these slides are only schematic illustrations of the guiding phenomena.)

The protonospheric trough may also be used to guide VLF waves. Figure 17 illustrates a magnetospherically reflected whistler trapped in a 40% depletion duct. The wave-normal angles are nearly perpendicular to the ray direction for trapped propagation below half the gyro frequency (Type 1 trapping).

Larger depletions are required for VLF trapping above half the gyro frequency than below this frequency. A 20 kHz whistler is guided by a 50% depletion duct (Figure 18). In the regions of Type 2 trapping, the wave frequency is above half the gyro frequency.

The ability to produce waveguides in the magnetosphere makes possible a number of experiments involving wave-particle interactions. For certain relationships between a charged particle velocity and electromagnetic wave frequency and phase velocity, strong interactions occur [Stix, 1962]. These interactions represent coupling between wave and particle energies. The energy exchange between streaming particles and waves has been suggested for the amplification and absorption of whistler signals (see, for example, Bernard [1973]). The collision-free magnetospheric plasma is not in a state of thermal equilibrium and, consequently, contains high energy trapped particles with a wide spectrum of pitch angles. Interaction between electromagnetic radiation and trapped particles may produce pitch angle scattering. Some of the scattered particles are no longer trapped and will precipitate along magnetic field lines to low altitudes where they will interact with the relatively dense D, E, and F-region atmosphere and may produce observable ionospheric phenomena such as enhanced airglow, heating or ionization. Observations at the base of the trough may indicate precipitation effects triggered by natural or manmade VLF propagation [Rosenberg et al., 1971].

Ground-based wave-particle interaction studies involving VLF transmission through the F-region into the magnetosphere have required signals with small wave-normal angles with respect to the magnetic field direction for penetration of the ionosphere and for guiding along natural, randomly placed enhancement ducts [Helliwell and Katsufrakis, 1974]. The excitation of VLF emissions by transmissions from spacecraft into the depletion ducts at known locations permits the study of wave-particle interactions with signals at all wave-normal angles under controlled conditions.

HF rays propagating through the hole in the ionosphere are focused. Figure 19 demonstrates the focusing property of the nighttime ionospheric hole 90 seconds after H_2 release. The frequency of the

radiowave is 10 MHz.

From ground-based measurements of the phase and amplitude perturbations produced in a plane wave propagating downward through the ionospheric hole, the reduction in ionospheric content and the width of the ionospheric hole may be estimated. The amplitude and phase changes produced in a 30 MHz signal are shown in the top two graphs in Figure 20. From these changes, the size of the ionospheric hole may be determined (bottom two graphs in Figure 20).

Use of the hole as an ionospheric lens in a radiotelescope is schematically illustrated in Figure 21. Calculations by Bernhardt and da Rosa [1976] indicate that a 5 mHz radiotelescope with a beamwidth less than .2 degree may be obtained by using the ionospheric lens resulting from the release of 100 kg of H_2 at that peak of the F-layer.

4. CONCLUSION

A number of experiments dealing with ionospheric modification by the release of reactive chemicals are suggested. The measurement of the recovery of the ionosphere from controlled depletion will give information about the mechanisms that maintain the ionosphere. Observations of airglow emission stimulated by the release of reactive gases contain information about electric fields and neutral winds exerting forces on the injected gas cloud and the ionospheric plasma. Radiowaves may be ducted by artificially produced troughs. The ducted waves may be used for interhemispheric propagation or controlled wave particle interaction experiments in the magnetosphere. Finally, the ionospheric hole may be used as a large lens for use in a high resolution radiotelescope.

ACKNOWLEDGMENTS

This work was supported by the National Aeronautics and Space Administration under grants NGR-05-020-001 and NAS 8-31769. The plasmaspheric calculations were made at the National Center for Atmospheric Research under the sponsorship of the National Science Foundation.

BIBLIOGRAPHY

Bernard, L.C., 1973, "Amplitude Variations of Whistler-mode Signals Caused by their Interaction with Energetic Electrons of the Magnetosphere," Technical Report No. 3465-2, Radioscience Laboratory, Stanford Electronics Laboratories, Stanford University, Stanford, Ca.

Bernhardt, P.A., C.G. Park, and P.M. Banks, 1975, "Depletion of the F2-Region Ionosphere and the Protonosphere by the Release of Molecular Hydrogen," Geophys. Res. Lett., 2, 341.

Bernhardt, P.A., 1976, "The Response of the Ionosphere to the Injection of Chemically Reactive Vapors," Technical Report No. 17, SU-SEL-76-009, Radioscience Laboratory, Stanford Electronics Laboratories, Stanford University, Stanford, Ca.

Bernhardt, P.A. and A.V. da Rosa, 1976, "A Refracting Radiotelescope," submitted to Radio Science.

Booker, Henry G., 1961, "A Local Reduction of F-Region Ionization due to Missile Transit," J. Geophys. Res., 66, 1079.

Carpenter, L.A. and S.A. Bowhill, 1971, "Investigation of the Physics of Dynamical Processes in the Top-side F-region," Aeronomy Report No. 44, University of Illinois.

Evans, J.V., 1969, "Theory and Practice of Ionospheric Study of Thomson Scatter Radar," Proc. IEEE, 57, 496, 1969.

Helliwell, R.A. and J.P. Katsufrakis, 1974, "VLF Wave Injection into the Magnetosphere from Siple Station, Antarctica," J. Geophys. Res., 79, 2511.

Helms, W.J. and A.D. Thompson, 1973, "Ray-Tracing Simulation of Ionization Trough Effects upon Radio Waves," Radio Science, 8, 1125.

Jackson, J.E., H.A. Whale, and S.J. Bauer, 1962, "Local Ionospheric Disturbance Created by a Burning Rocket," J. Geophys. Res., 67, 2059.

Mendillo, M., G.S. Hawkins, and J.A. Klobuchar, 1975a, "A Large-Scale Hole in the Ionosphere Caused by the Launch of Skylab," Science, 187, 343.

Mendillo, M., G.S. Hawkins, and J.A. Klobuchar, 1975b, "A Sudden Vanishing of the Ionosphere due to the Launch of Skylab," J. Geophys. Res., 80, 2217.

Rosenberg, T.J., R.A. Helliwell, and J. Katsufrakis, 1971, "Electron Precipitation Associated with Discrete Very Low Frequency Emissions," J. Geophys. Res., 76, 8445.

Schunk, R.W., and J.C.G. Walker, 1970, "Minor Ion Diffusion in the F2-Region of the Ionosphere," Planet. Space Sci., 18, 1319.

Stix, T.H., 1962, The Theory of Plasma Waves, McGraw-Hill Book Co., New York.

DISCUSSION

M. Mendillo: 1) If we have seen the movie, do we have to read the book ?
2) You discussed the possibility of a downward protonospheric flux, yet showed only a decrease in the upward flux. Would you please clarify this for me.

P. A. Bernhardt: 1) One always enjoys the book better after seeing the movie.
2) The flux shown was at 500 km during daytime. During night-time, the flux at 500 km is downward. After the release of H_2 into the ionosphere, the daytime upward-flux decreases and the night-time downward-flux increases. In these cases, the relative flow out of the protonosphere increases.

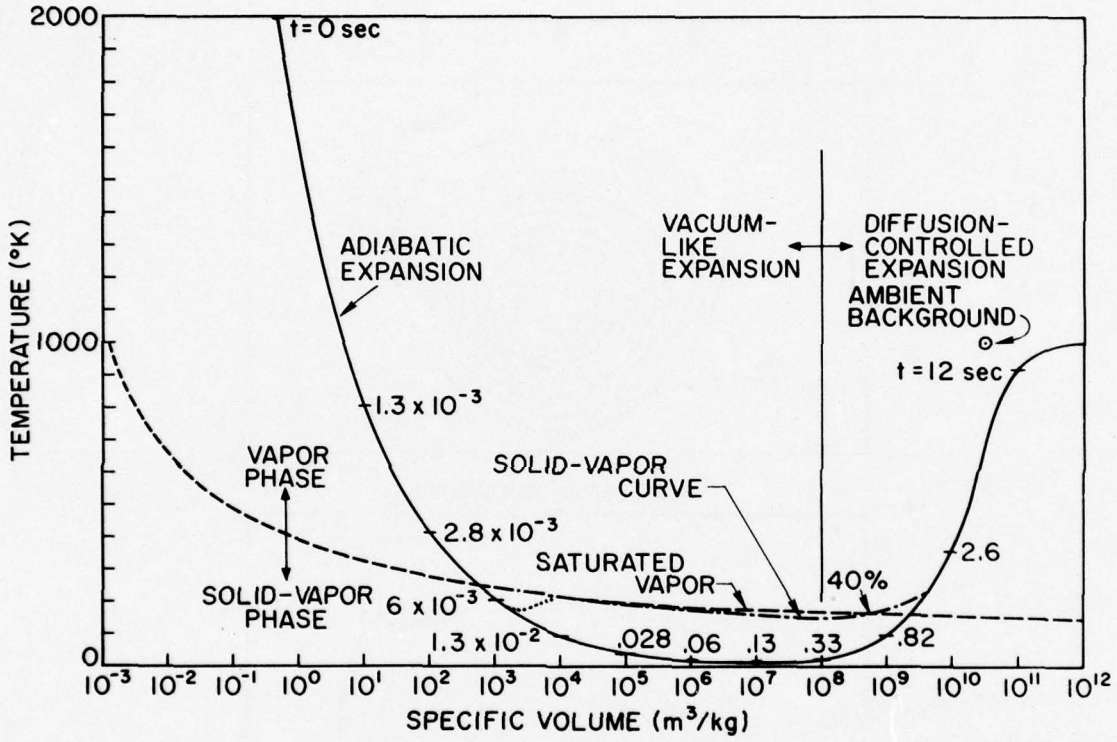

FIG. 1. Temporal variations in temperature and specific volume of expanding gas cloud. Solid line applies if no condensation occurs. Dash-dot curve applies for the condensation of H_2O.

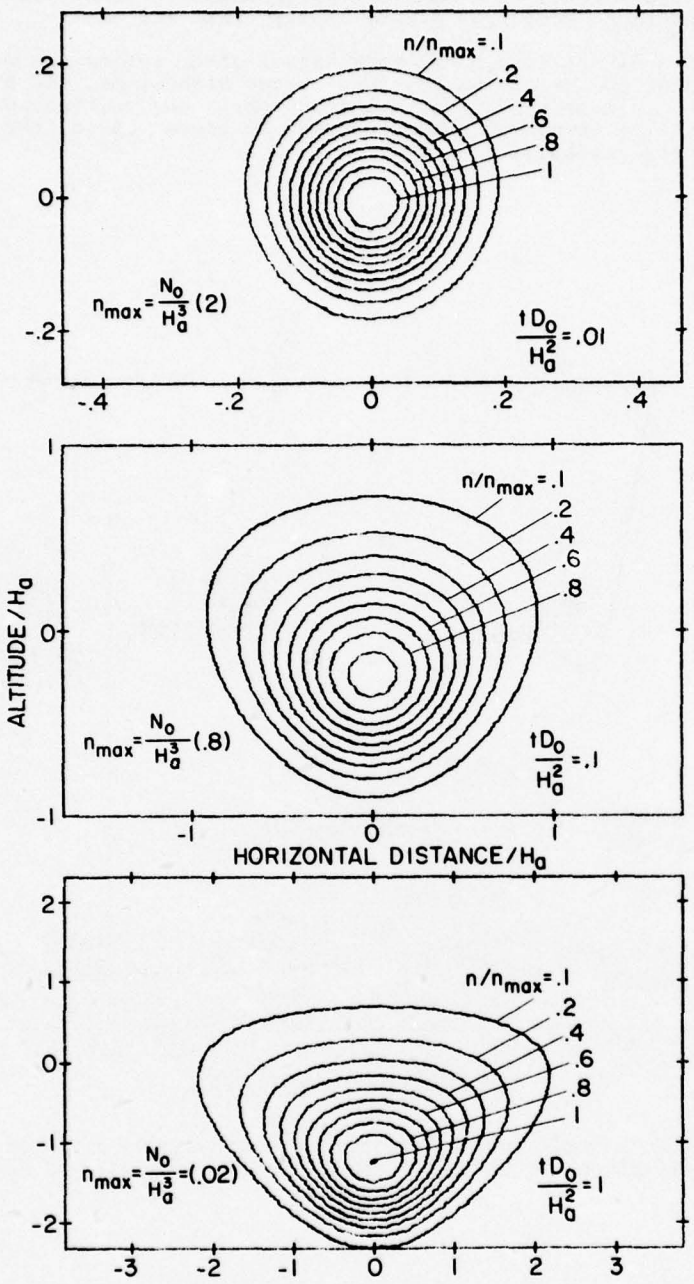

FIG. 2. Expansion of a gas cloud in a nonuniform atmosphere. The cloud becomes highly nonspherical after expanding over many scale heights. An expanding H_2 cloud containing N_0 molecules is released into an atmosphere with scale height H_a. The diffusion coefficient at the release point is D_0.

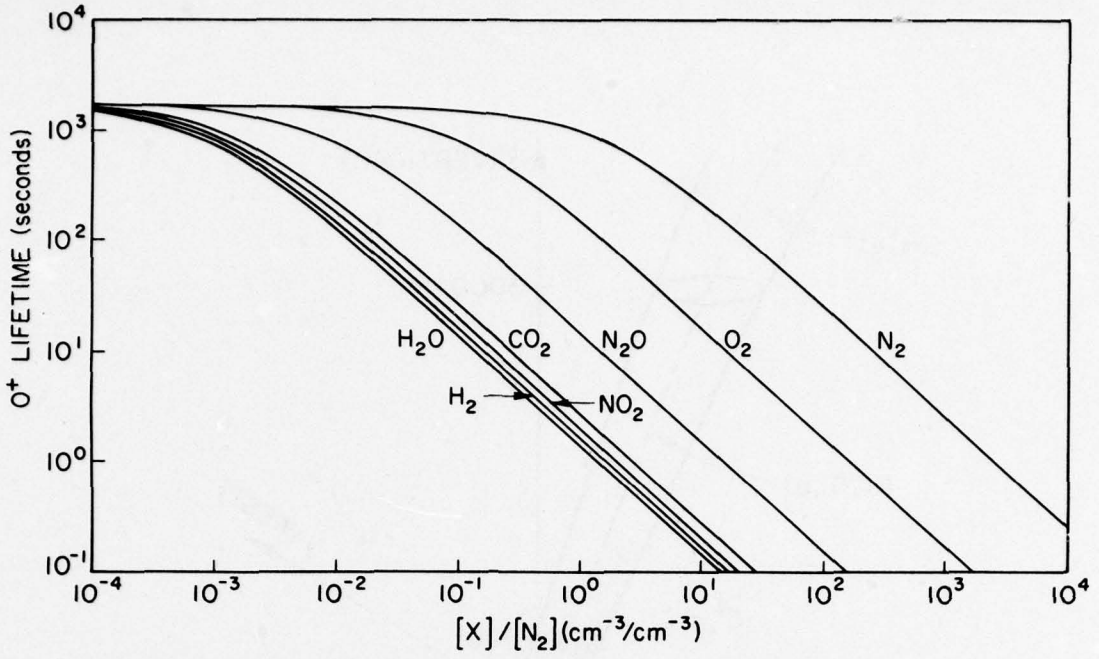

FIG. 3. Change in O^+ lifetime with the introduction of chemically reactive gases into the ionosphere. Ambient N_2 concentration is 3×10^8 cm^{-3}. O_2 concentration is 10^7 cm^{-3}. Undisturbed O^+ concentration is 2×10^5 cm^{-3}.

CHEMICAL REACTIONS

NORMAL F2-REGION DISSOCIATIVE RECOMBINATION

$$N_2 + O^+ \rightarrow NO^+(^1\Sigma^+) + N \qquad \text{RATE: } 1.3 \times 10^{-12} \text{ cm}^3 \text{ s}^{-1}$$

$$NO(^1\Sigma^+) + e^- \rightarrow N + O(^3P) \qquad \text{RATE: } 4.1 \times 10^{-7} \text{ cm}^3 \text{ s}^{-1}$$

ENHANCED RECOMBINATION

$$H_2 + O^+ \rightarrow OH^+(^3\Sigma^-) + H \qquad \text{RATE: } 2.0 \times 10^{-9} \text{ cm}^3 \text{ s}^{-1}$$

$$\left.\begin{aligned} OH^+(^3\Sigma^-) + e^- &\rightarrow H + O(^3P) \\ &\rightarrow H + O(^1D) \\ &\rightarrow H + O(^1S) \end{aligned}\right\} \qquad \text{RATE: } \cong 1 \times 10^{-7} \text{ cm}^3 \text{ s}^{-1}$$

QUENCHING OF $O(^1D)$

$$O(^1D) + N_2 \rightarrow O(^3P) + N_2 \qquad \text{RATE: } 7 \times 10^{-11} \text{ cm}^3 \text{ s}^{-1}$$

$$O(^1D) + H_2 \rightarrow OH + H + 1.9 \text{ eV} \qquad \text{RATE: } 1 \times 10^{-11} \text{ cm}^3 \text{ s}^{-1}$$

FIG. 4. Chemical reactions in the F-region with the introduction of H_2. The (O^+, N_2) reaction rate is three orders of magnitude less than the (O^+, H_2) reaction rate. Dissociative recombination of OH^+ may produce excited states of monatomic oxygen leading to airglow excitation. Quenching of the excited $O(^1D)$ atom occurs by reaction with both N_2 and H_2.

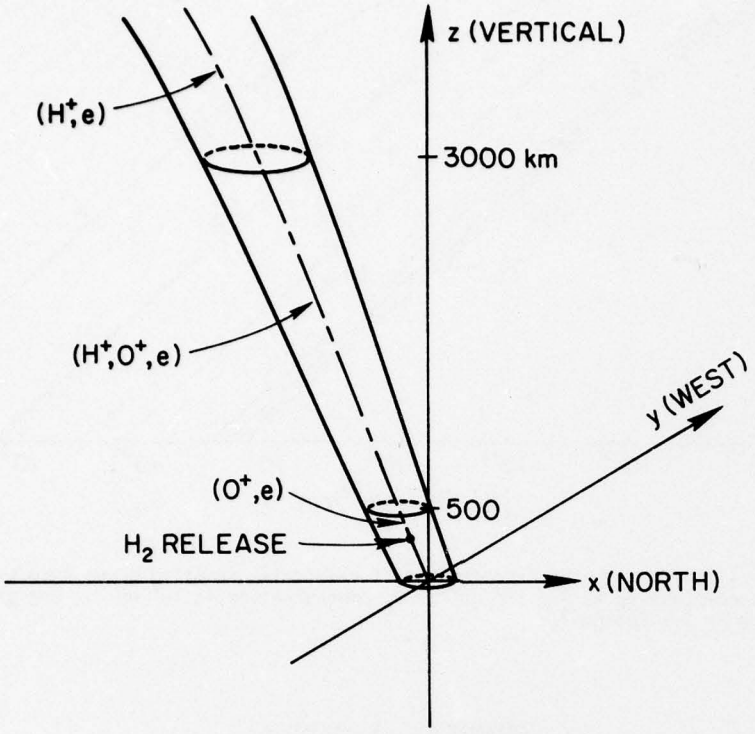

FIG. 5. Three dimensional coordinate system used in the plasmaspheric model.

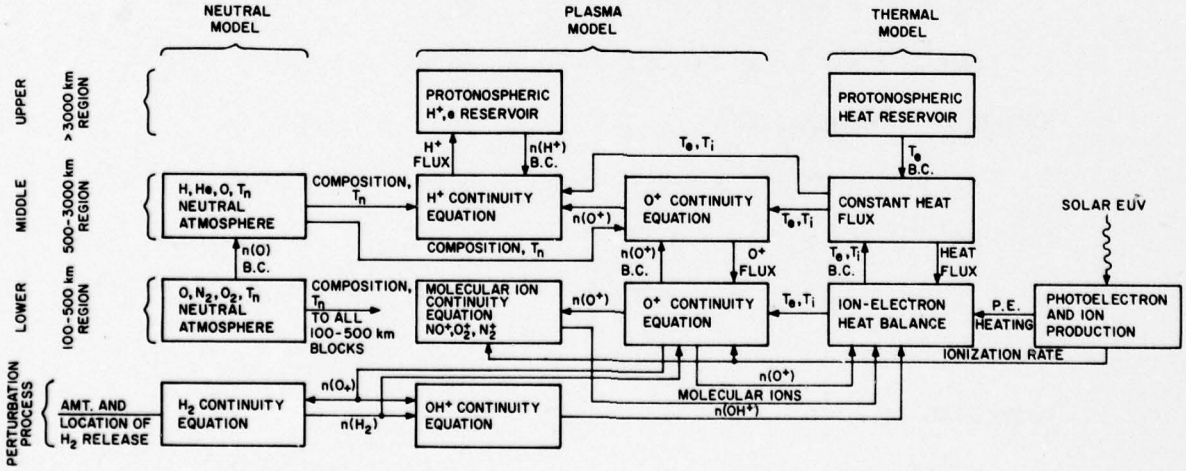

FIG. 6. Block diagram of the model of the mid-latitude ionosphere and protonosphere used in the simulation of the chemical modification experiment.

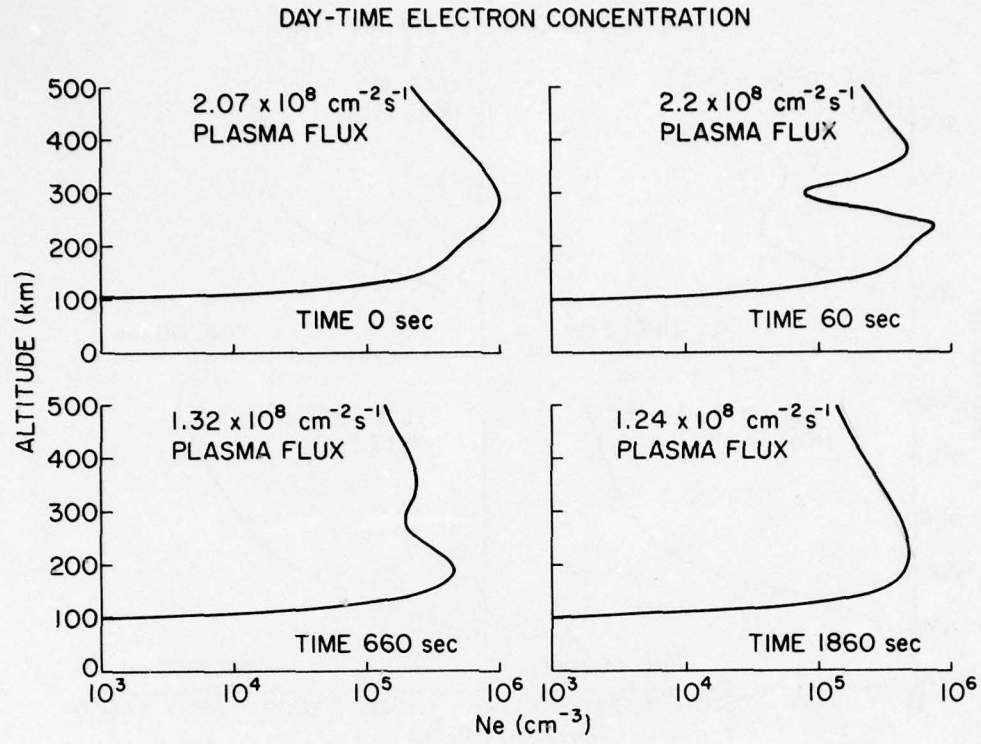

FIG. 7. Time sequence of daytime F-region profiles illustrating the effects of hydrogen injection.

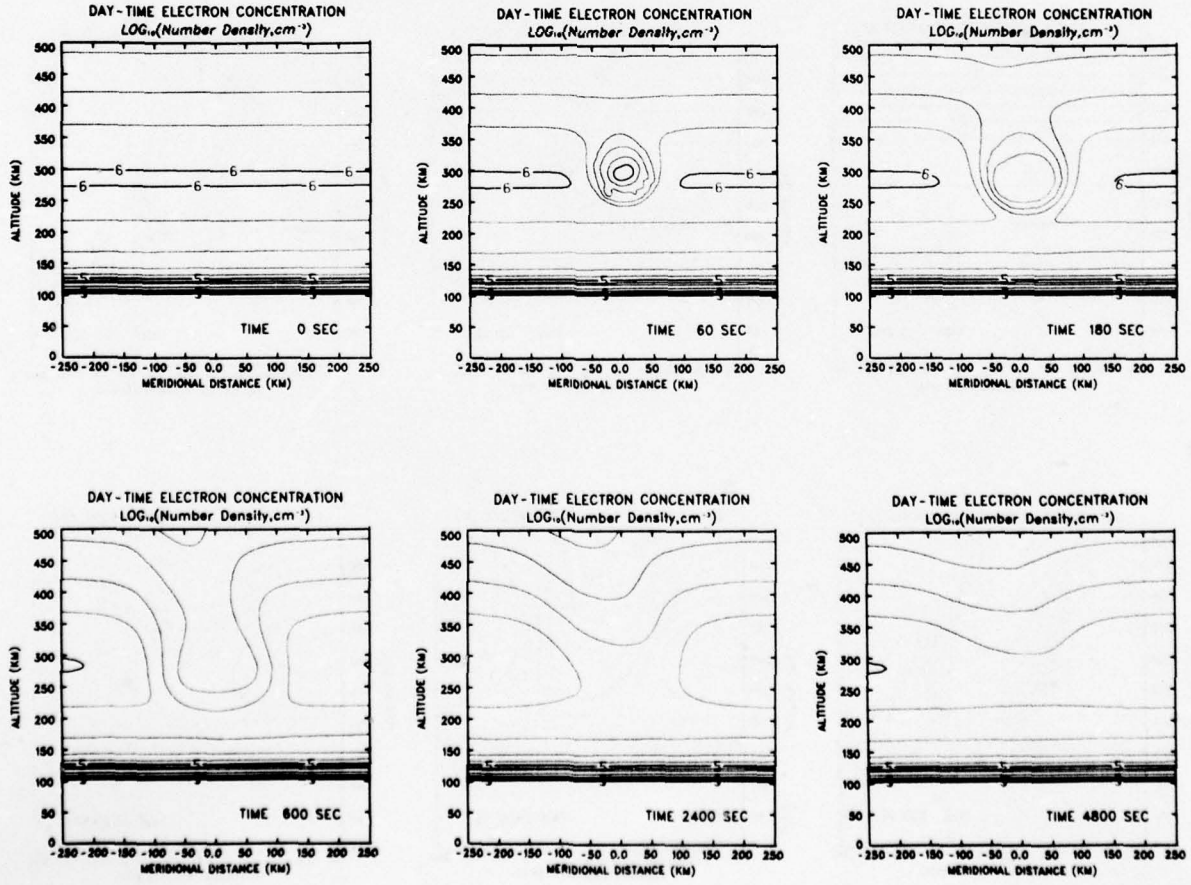

FIG. 8. Meridional plane variations in the daytime F-region electron concentration.

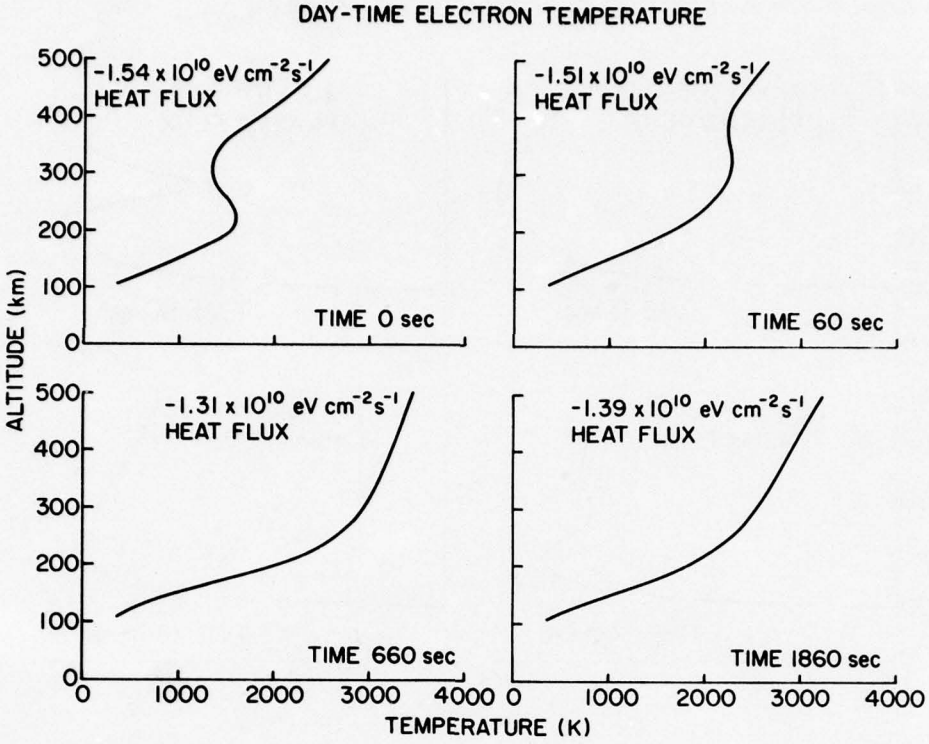

FIG. 9. Time sequence of daytime electron temperature profiles showing the large temperature increase.

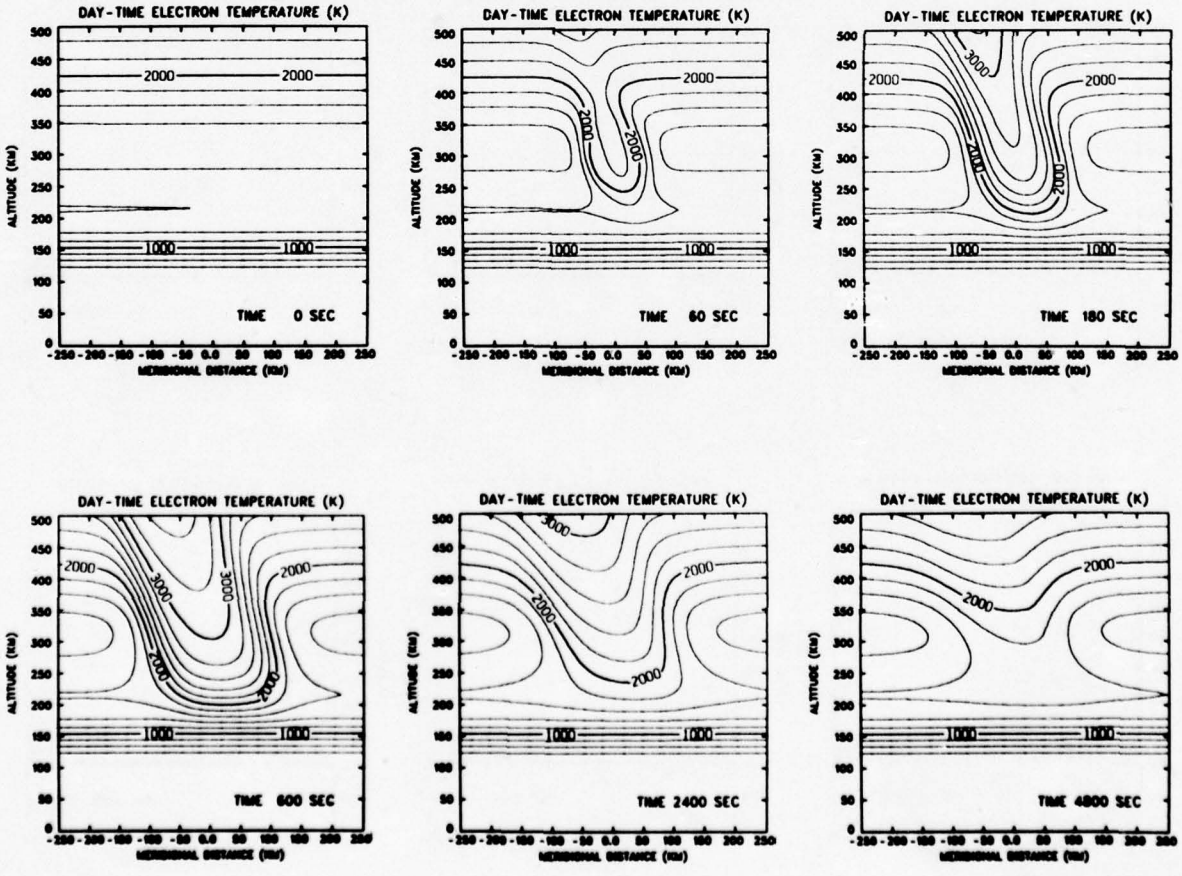

FIG. 10. Isothermal contour variations in the daytime ionosphere.

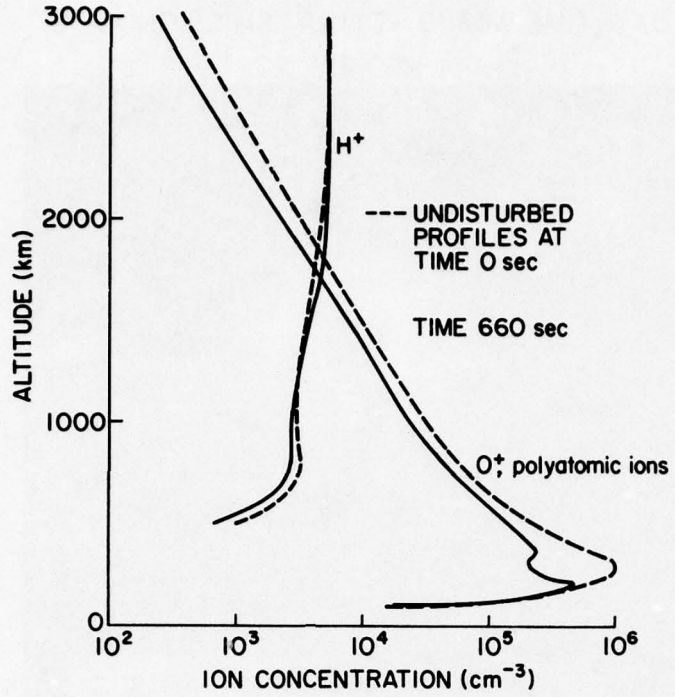

FIG. 11. Daytime H^+ and O^+ profiles along the field line through the point of H_2 release.

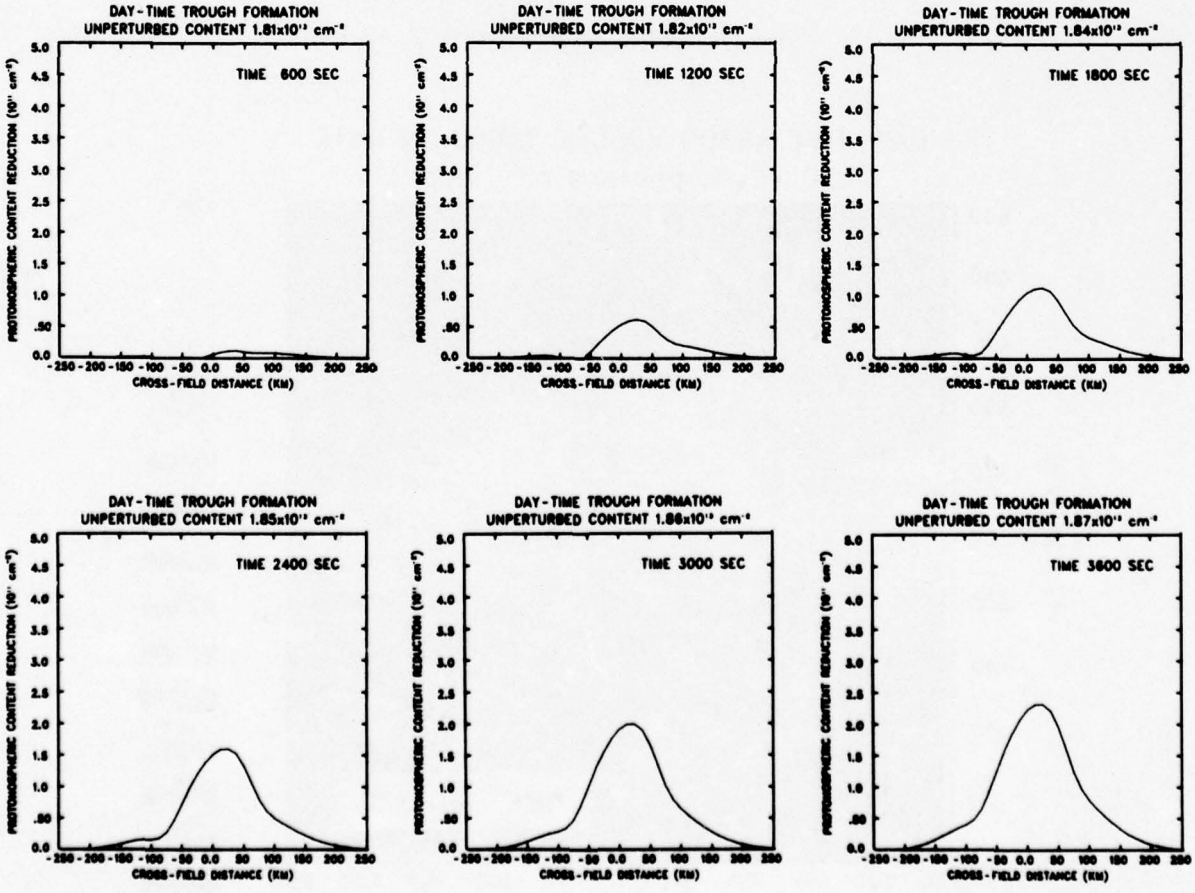

FIG. 12. Daytime depletion of the protonosphere. The reduction in protonospheric content from 3000 km to the equator is plotted against the distance between adjacent field lines in the meridional plane on the surface of the earth.

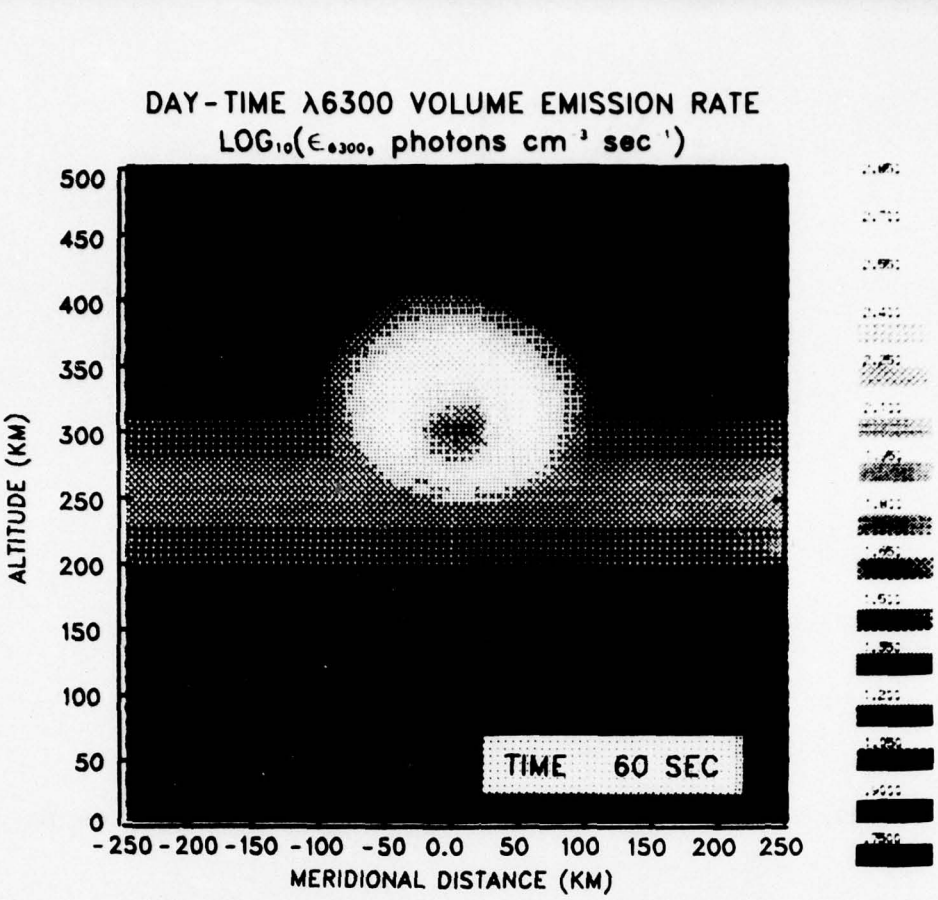

FIG. 13. Bright ring formed one minute after H_2 injection.

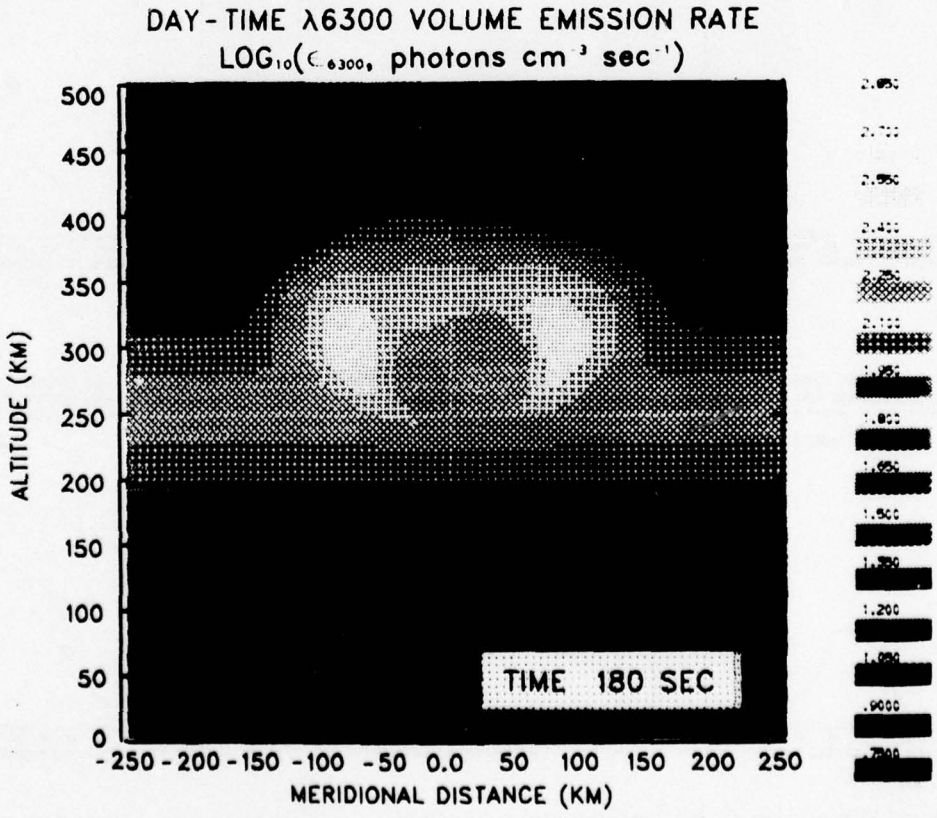

FIG. 14. Expanding λ6300 airglow ring.

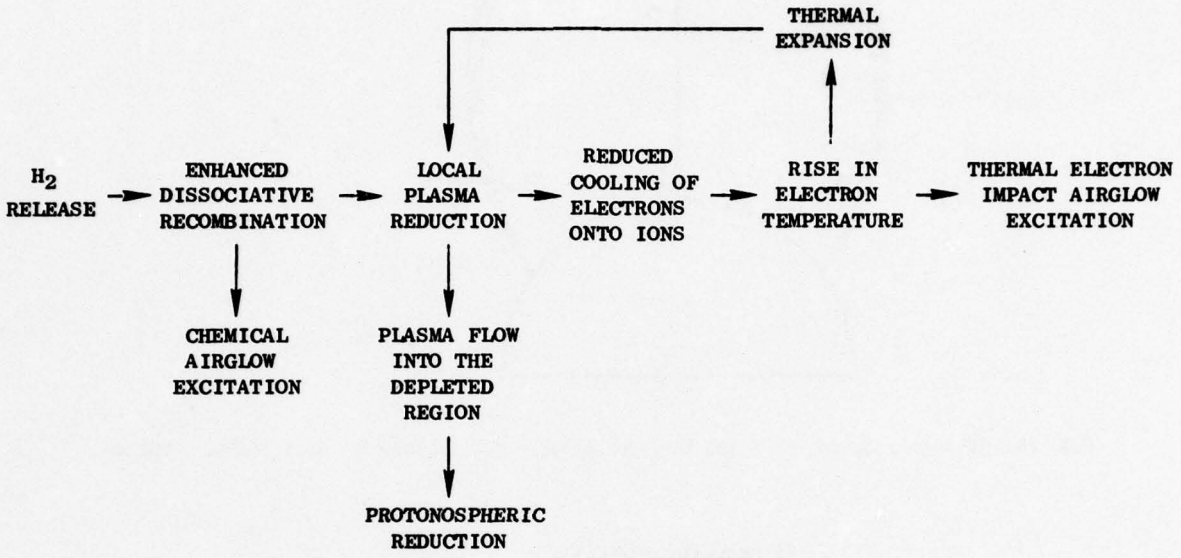

FIG. 15. Flow chart of physical phenomena resulting from the release of H_2 gas into the F-layer.

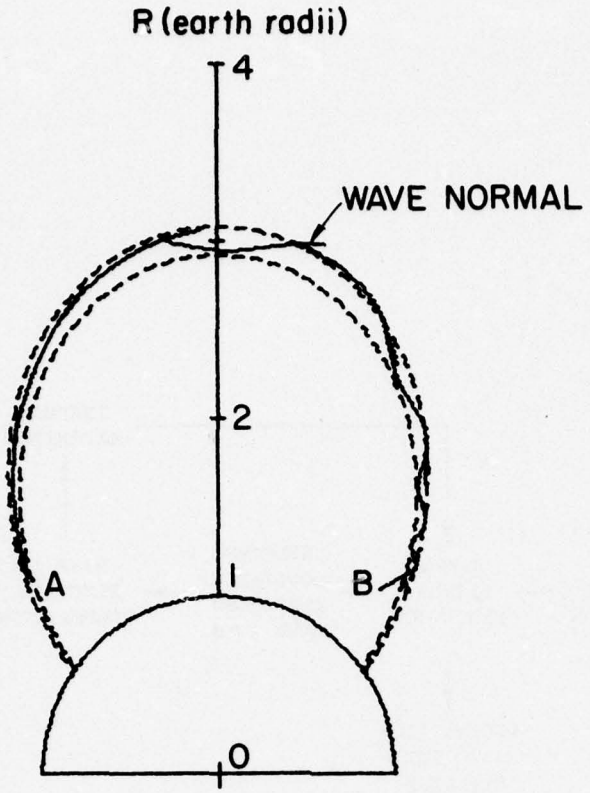

FIG. 16. HF ray trapping: f = 900 kHz, depletion = 60%, equatorial duct radius = 500 km.

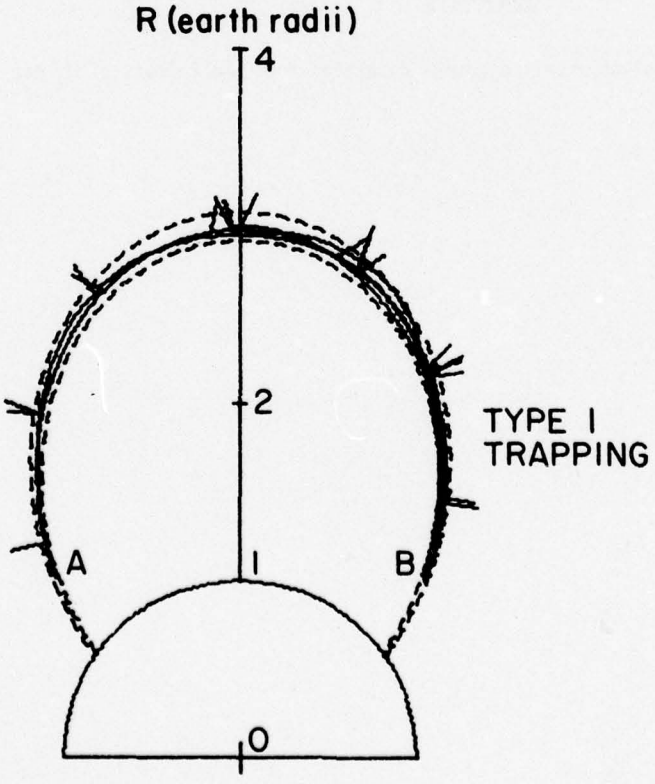

FIG. 17. Magnetospherically reflected whistler in a depletion duct: f = 7 kHz, depletion = 40%, equatorial duct radius = 500 km.

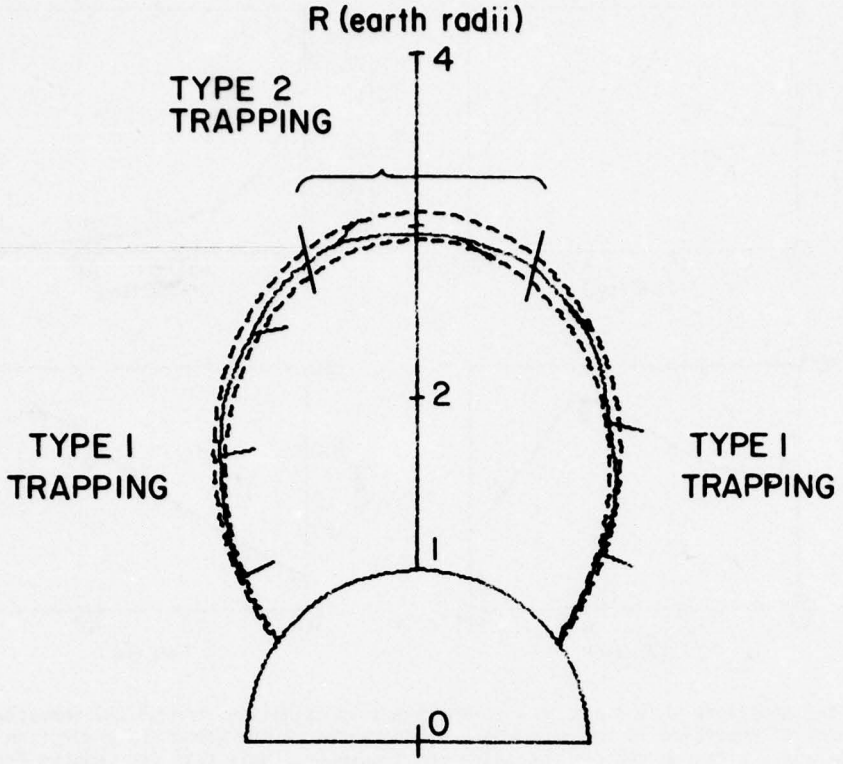

FIG. 18. VLF trapping for frequencies greater than half the equatorial gyro frequency: f = 20 kHz, depletion = 50%.

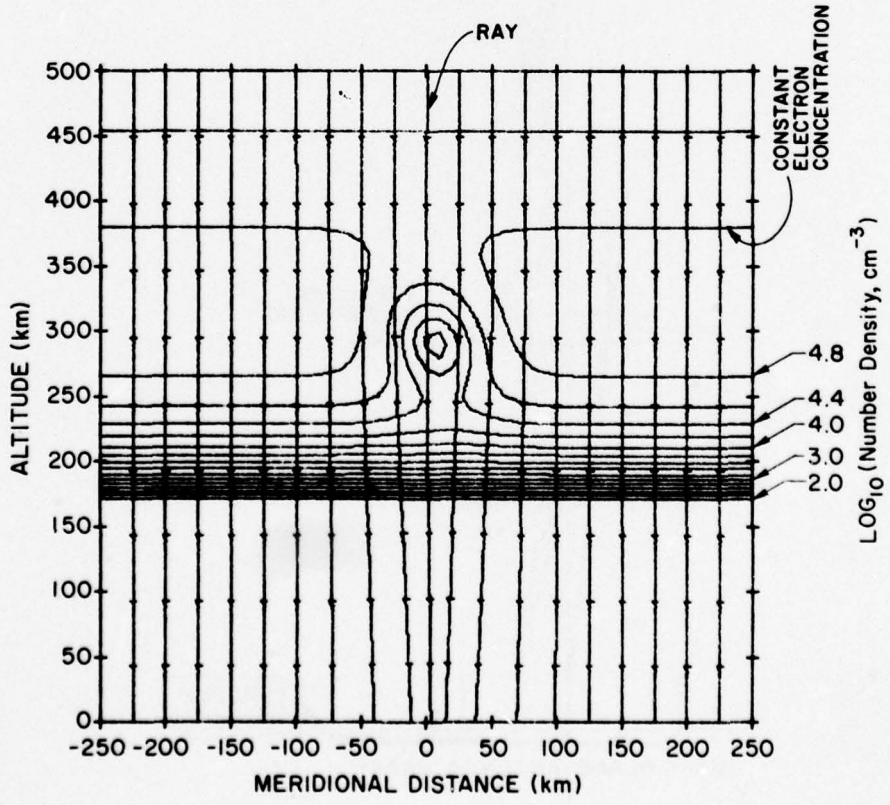

FIG. 19. Focusing of a vertically incident plane wave by the nighttime ionospheric depletion one minute after the release of 100 kg H_2. The downward propagating wave has a frequency of 10 MHz.

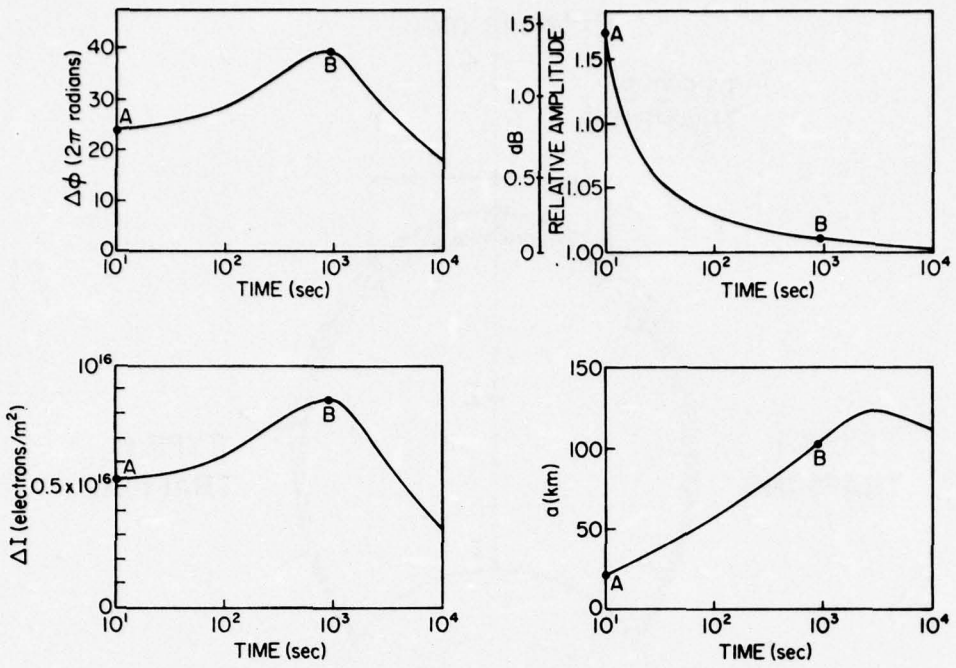

FIG. 20. Phase and amplitude variations in a 30 MHz signal propagating through the ionospheric lens. The point of reception is on the surface of the earth at the geometric projection of the center of the lens. Electron content reduction and ionospheric hole size are deduced from the variations.

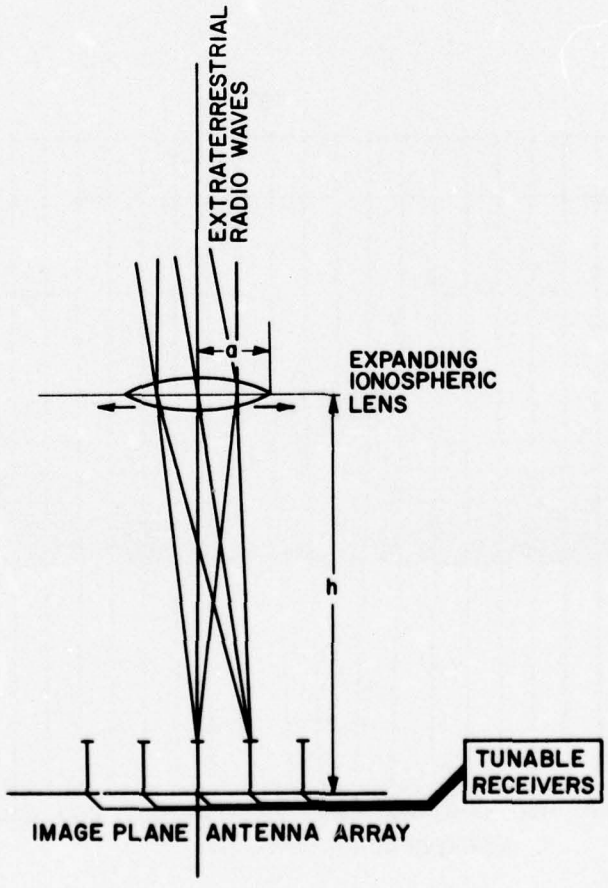

FIG. 21. The refracting radiotelescope.

SOME EFFECTS OF A HIGH ALTITUDE BARIUM RELEASE ON THE PROPAGATION CHARACTERISTICS OF HF RADIOWAVES

T.B. Jones and C.T. Spracklen
University of Leicester
England

1. INTRODUCTION

Local disturbances in the electron density of the ionosphere can be produced by releasing chemical mixtures into the upper atmosphere which ionize due to thermal or photon action. When release occurs at F-region heights an ionized cloud is formed together with its electrical image in the E-region. A detailed discussion of the behaviour of the ionized cloud has been given in the preceeding paper (Baxter, 1976).

The electron density changes produced by the release will affect the propagation of HF radiowaves and this paper describes some of the disturbances observed during the release of a Barium cloud at a height of 175 km over the South Uist range in the UK.

2. EXPERIMENTAL DETAILS

A change in the electron density-height distribution in the ionosphere will affect the propagation characteristics of radiowaves propagating through or reflected from that region. A technique well suited to the study of rapid transient changes in ionization density is the so-called "Doppler sounding" method in which the frequency of the reflected signal is measured as a function of time. Changes in electron density will change the phase path of the radiowave which, in turn, will produce a small frequency shift Δf in the reflected signal. The magnitude of the frequency shift can be expressed as

$$\Delta f = -\frac{1}{\lambda}\frac{dP}{dt} \qquad \ldots\ (1)$$

where λ is the free space wavelength and dP/dt the rate of change of phase path.

Observations of naturally occurring irregularities have demonstrated the suitability of the Doppler technique for studies of F-region disturbances. For E-region events, however, the rate of change of phase path is so small that the frequency shift is below the resolution of the measuring system. For this reason the phase of the signals reflected from the E-region has been measured directly. The phase observations have the disadvantage that at the time of the release the E-layer was moving upwards and so a continuous retardation in the phase was recorded. Any disturbance effects are thus superimposed onto this regular change.

Two frequency-stable transmitters were installed on the island of St Kilda, some 90 km north-west of the range head (see Fig. 1). The transmitters radiated CW signals at 3.502 and 1.615 MHz at powers of 50 and 20 Watts respectively and were stable to one part in 10^9. The Doppler receivers (3.502 MHz) were located at the range head and Lochboisdale and the phase of the 1.615 MHz transmission was recorded at the range head. In this way two reflection points in the F-region and one in the E-region situated to the north of the release were monitored.

3. RESULTS

3.1. F-region

The introduction of an overdense cloud of ionization in the F-region in the position shown in Fig. 1 was expected to produce significant Doppler shifts in the signals received from St Kilda. It seemed likely that direct reflection from the cloud would be received in addition to the normal F-region reflection (Wright, 1964) and that Doppler shifts would be produced as the cloud moved, their magnitude depending on the cloud velocity. Furthermore, the initial expansion of the cloud is likely to set up a shock wave which would perturb the reflection height of the 3.502 MHz signal as it propagated outwards from the release point (Jones and Spracklen, 1974). Finally, some of the overdense ionization from the cloud could possibly move into the propagation paths of the radiowaves and thus modify their propagation characteristics.

The results obtained are reproduced in Fig. 2 and are notable for their lack of any marked Doppler shift. No disturbance is evident at the time of release and this implies that if direct reflections were received from the cloud the rate of change of the phase path was very small after the initial expansion was over. There is, however, a significant difference between the Δf variations measured at the range head and Lochboisdale following the release. It would appear that some form of disturbance has propagated outwards from the cloud and affected the more southerly St Kilda-Lochboisdale path. The path length changes have been determined by integration of equation (1) and are shown in Fig. 3. The oscillatory nature of the St Kilda-Lochboisdale phase path could be interpreted as a wave-like perturbation moving outwards from the release point through the reflection point of this path. This disturbance is, however, of fairly small amplitude and is not evident on the more northerly (St Kilda-range head) path.

The effects of the release were small on both F-region paths monitored and no evidence of a large fast moving irregularity could be detected.

3.2. E-region Effects

Durion ion cloud releases at F-region heights, Stoffregen (1970) reported disturbances in the E-region and suggested that the ion cloud provides a trigger mechanism for precipitation of high energy magnetospheric particles into the lower ionosphere. These particles propagate down the lines of the geomagnetic field and produce ionization at about 110 km. In these experiments the E-region disturbances were detected optically as enhancements in the green (5577 Å) and violet (4275 Å) auroral emission starting a few seconds after release.

An alternative mechanism for the creation of E-region disturbances has been proposed by Haerendel, Lust and Rieger (1967). These authors suggest that electrons move from one end of the cloud along the geomagnetic field lines down to the E-layer and upwards along other field lines to the opposite part of the ion cloud. The reason for the current flow is that the electrons and ions in the cloud, under the action of the electric field, move with slightly different velocities so that a separation of the positive and negative charges develops. The current flow tends to neutralise the charge separation of the electric field. The current along the field lines is carried by electrons due to their higher mobility while the horizontal Pedersen current in the E-layer is carried largely by ions, as indicated in Fig. 4. There will be one region of the E-layer where downcoming electrons and the horizontal flow of ions will produce a local increase of electron and ion density and another region where a depletion occurs.

The area of the E-region likely to be affected by this process during the present experiment has been calculated (Baxter, 1976) and is shown in Fig. 5. The extent of the E-layer disturbance corresponds roughly to that of the ion cloud in the F-layer. The regions of enhanced and depleted electron densities at 120 km are marked + and - respectively in Fig. 5.

The phase recording of the E-region reflection is reproduced in Fig. 6. A very marked disturbance is observed at 19.17.13 UT, 2 mins after cloud release. The disturbances are so large that the phase tracking system failed to follow the signal. This could be interpreted as a very rapid change in phase or as a loss of signal amplitude, or that both phase and amplitude changes occurred. It would appear that the reflection properties of the E-region were completely disturbed for about $2\frac{1}{2}$ mins. At 19.19.52 UT the phase tracking is suddenly acquired again and the normal diurnal phase change is again evident.

The onset time of the phase disturbance corresponds exactly to the time at which instabilities (striations) in the cloud begin to develop. These features are indicative of instabilities in the cloud and correspond to large gradients in electron density. These are reflected in the E-region image and it is likely that steep gradients in electron density are also produced in the E-region at this time. Such gradients could provide multiple reflection points for the E-region signal which would produce rapid phase fluctuation at the receiver. It is less easy to explain the rapid recovery although once the phase-locked loop has acquired the signal it will track correctly irrespective the the signal amplitude provided this exceeds some critical value. The severity of the E-region disturbance was somewhat unexpected but clearly demonstrates that appreciable disturbances can occur in this layer as a consequence of the cloud release.

4. SUMMARY AND CONCLUSIONS

The disturbances produced by the ion cloud on the 3.502 MHz propagation paths were smaller than expected. The effects recorded indicate a wave-like disturbance passing through the reflection point of the St Kilda-Lochboisdale path. Marked E-region disturbances were observed which begin when structure is first observed in the released ion cloud. This suggests a current flow between the cloud and its image which redistributes the E-region ionization in a region located along the geomagnetic field line below the cloud. The exact mechanism which produces the phase anomally on the 1.6 MHz transmission is not fully understood but could involve multiple reflections from the disturbed region of the E-layer.

These preliminary experiments have established the usefulness of the radio Doppler and phase techniques for investigations of the ionospheric disturbances resulting from chemical releases at F-region heights.

ACKNOWLEDGEMENT

This work has been carried out with the support of Procurement Executive Ministry of Defence.

REFERENCES

BAXTER, A.J., 1976, Modification of the ionosphere by Barium ion clouds. AGARD Conf. Proc., this meeting.

BAXTER, A.J., 1976, Private Communication.

HAERENDEL, G., LUST, R. and RIEGER, E., 1967, Motion of artificial ion clouds in the upper atmosphere. Planet. Space Sci. 15, 1.

JONES, T.B. and SPRACKLEN, C.T., 1974, Ionospheric effects of the Flixborough explosion. Nature 250, 719.

STOFFREGEN, W., 1970, Electron density variations observed in the E-layer below an artificial barium cloud. J. Atmosph. Terr. Phys. 32, 171.

WRIGHT, W.J., 1964, Ionosonde studies of some chemical releases in the ionosphere. J. Res. Nat. Bur. Stand. 68D, 189.

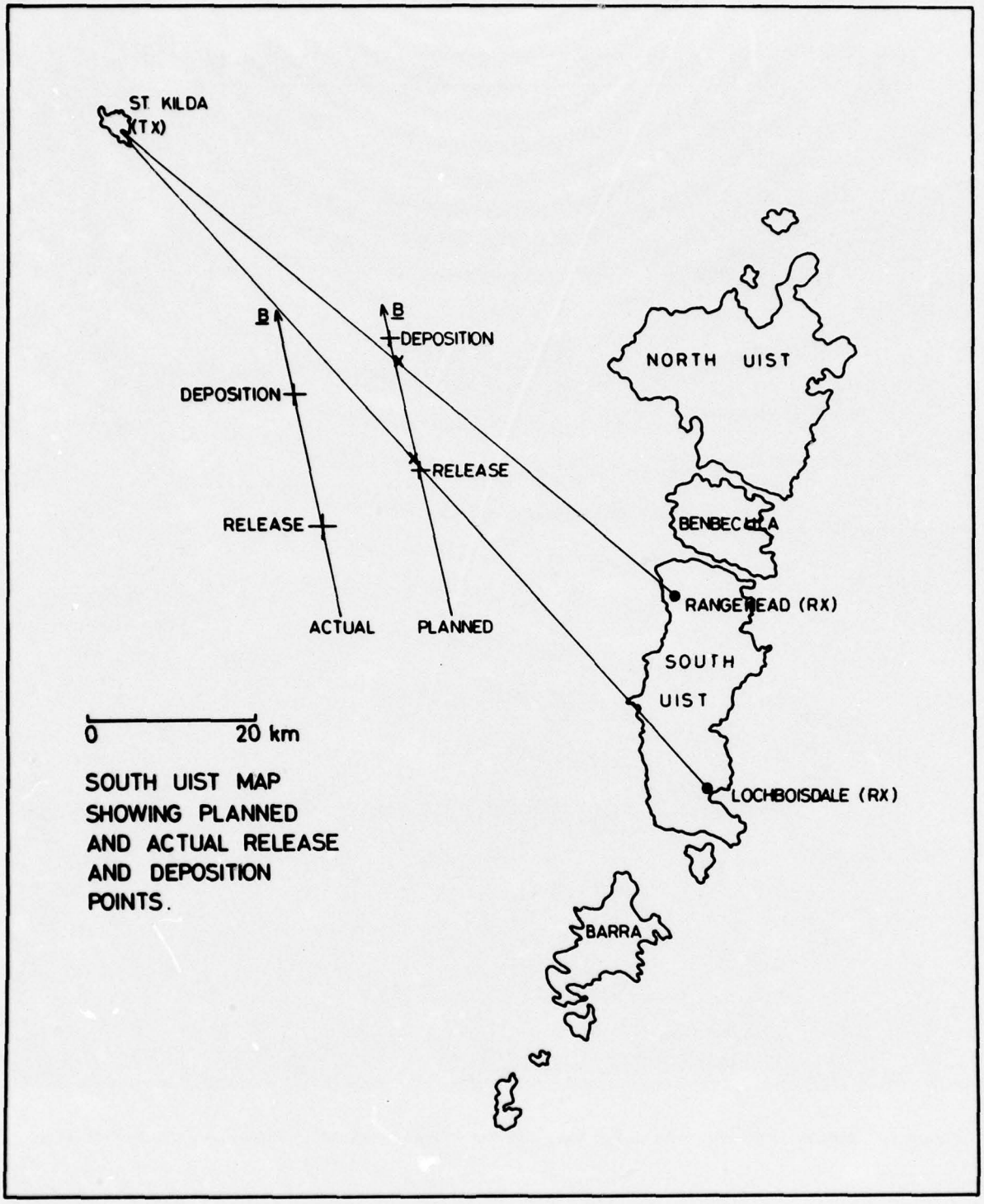

Figure 1. Location of transmitting and receiving sites. Initial Barium cloud position is indicated.

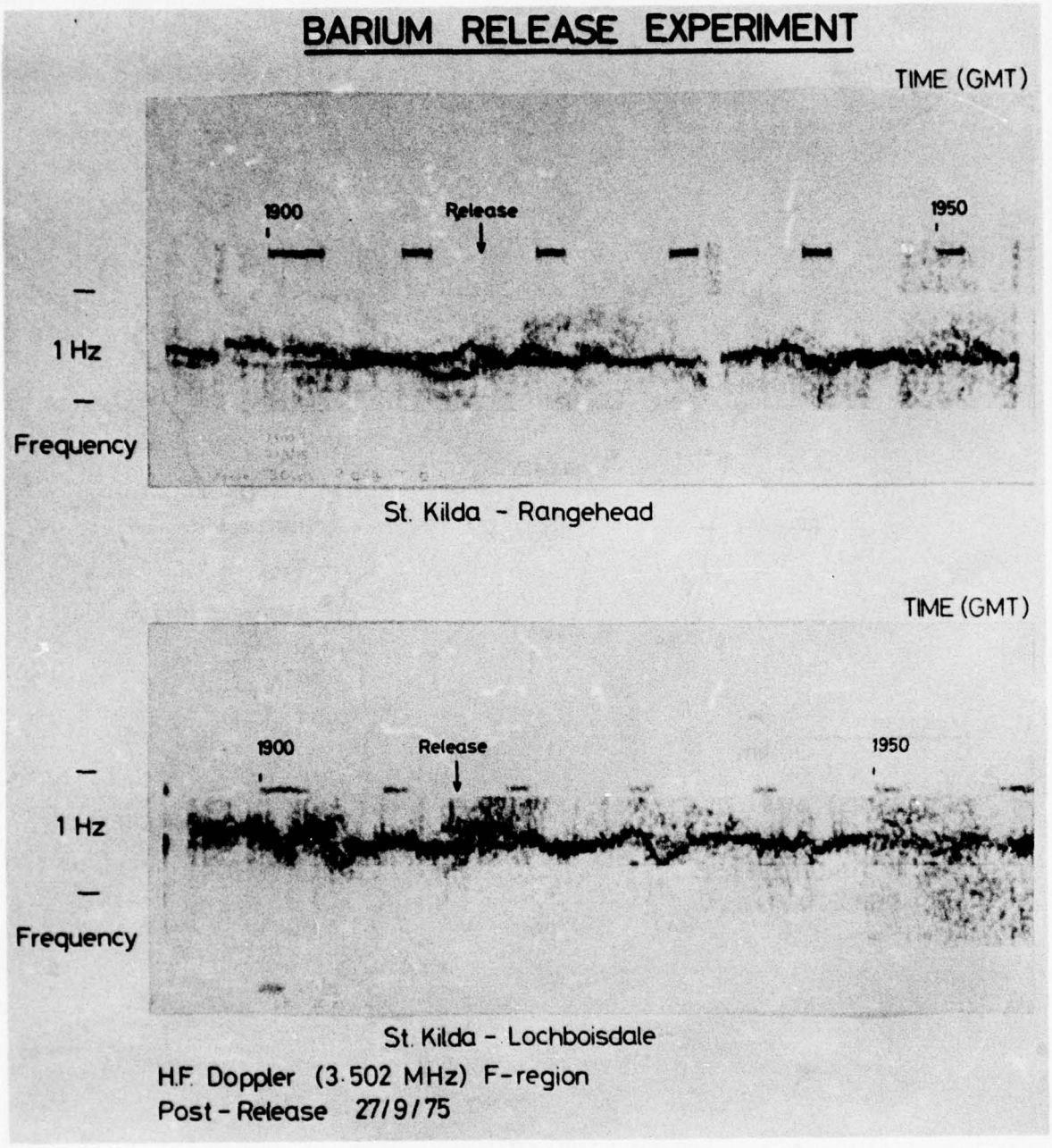

Figure 2. Doppler frequency records for the 3.502 MHz signal received at range head and Lochboisdale.

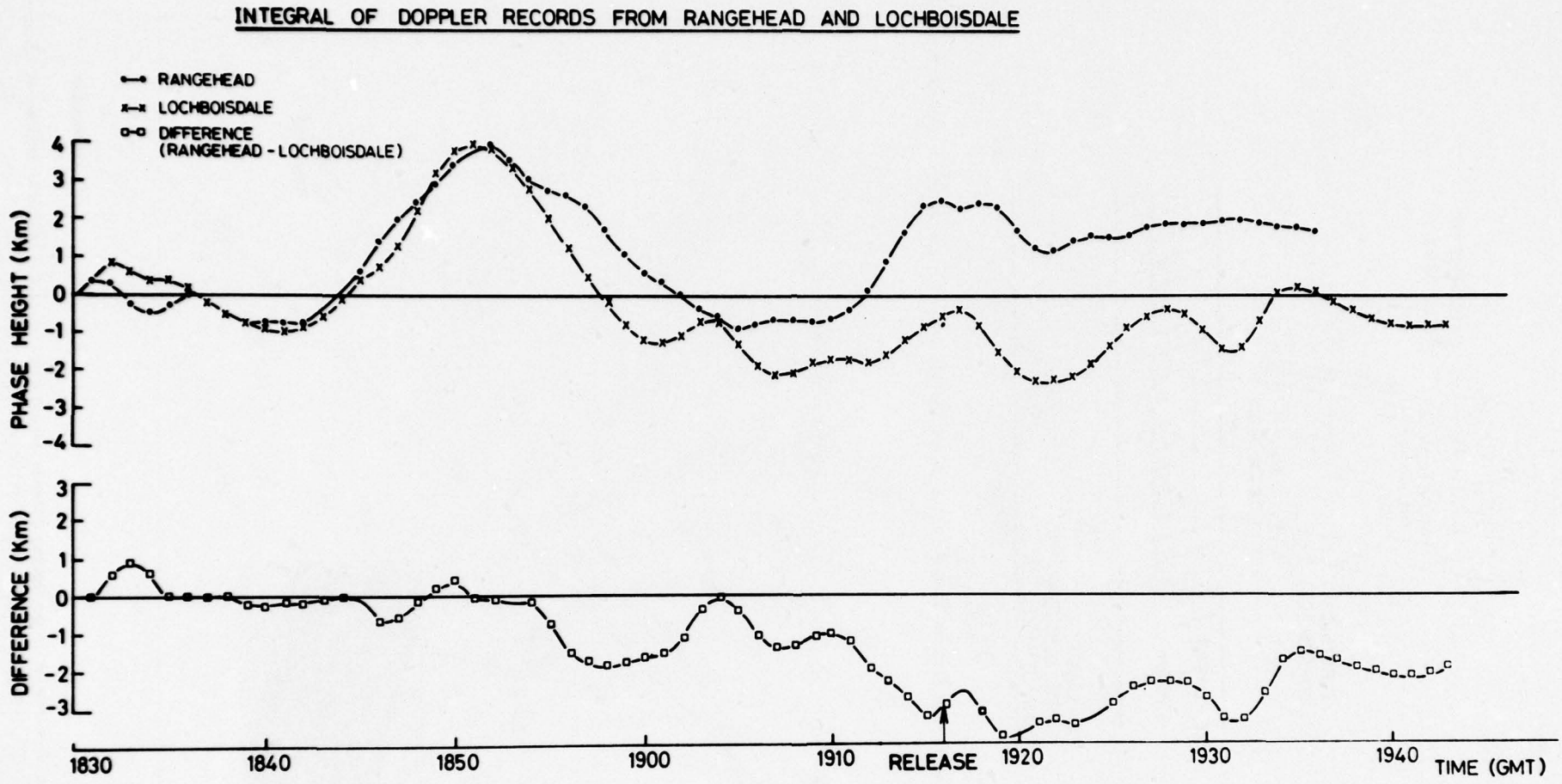

Figure 3. Phase path changes calculated from Doppler frequency records.

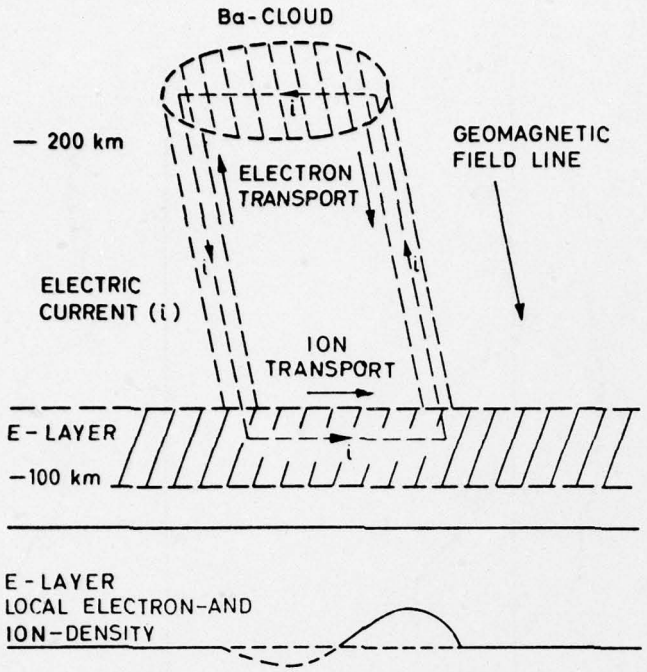

Figure 4. Possible current flow between F-region cloud and its image in the E-region (after Stoffregen, 1970).

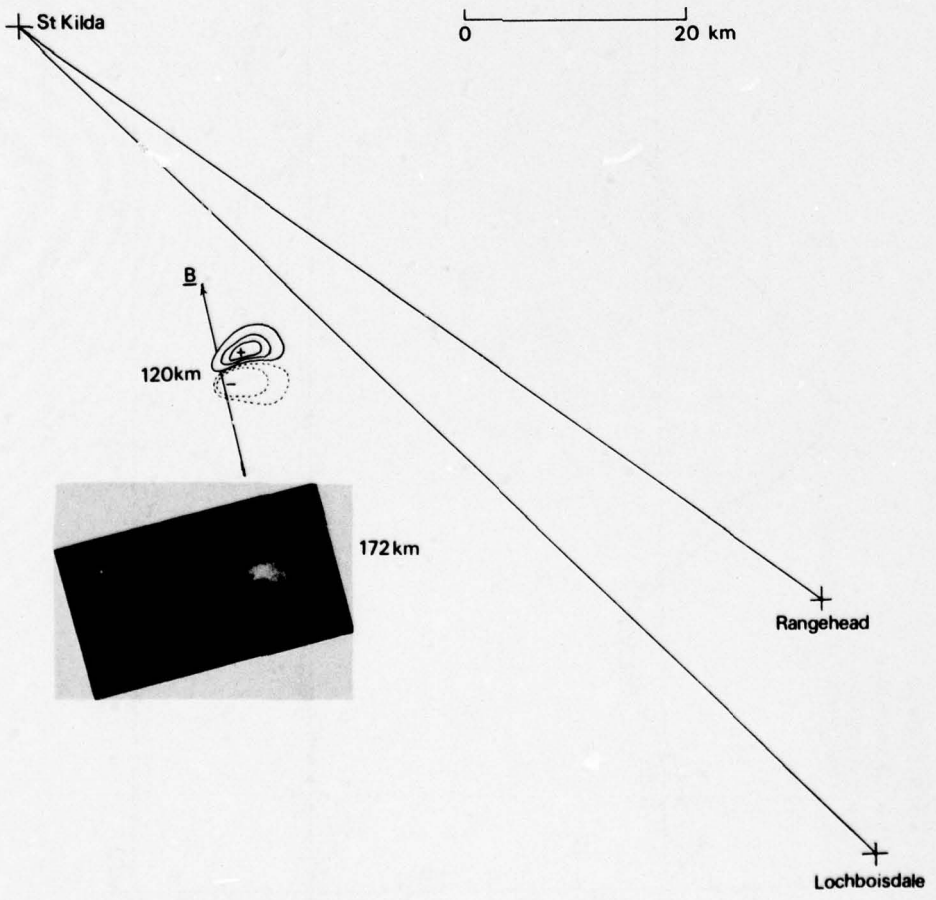

Figure 5. Location of E-region image during release experiment. + and - indicate regions of enhanced and depleted electron density respectively.

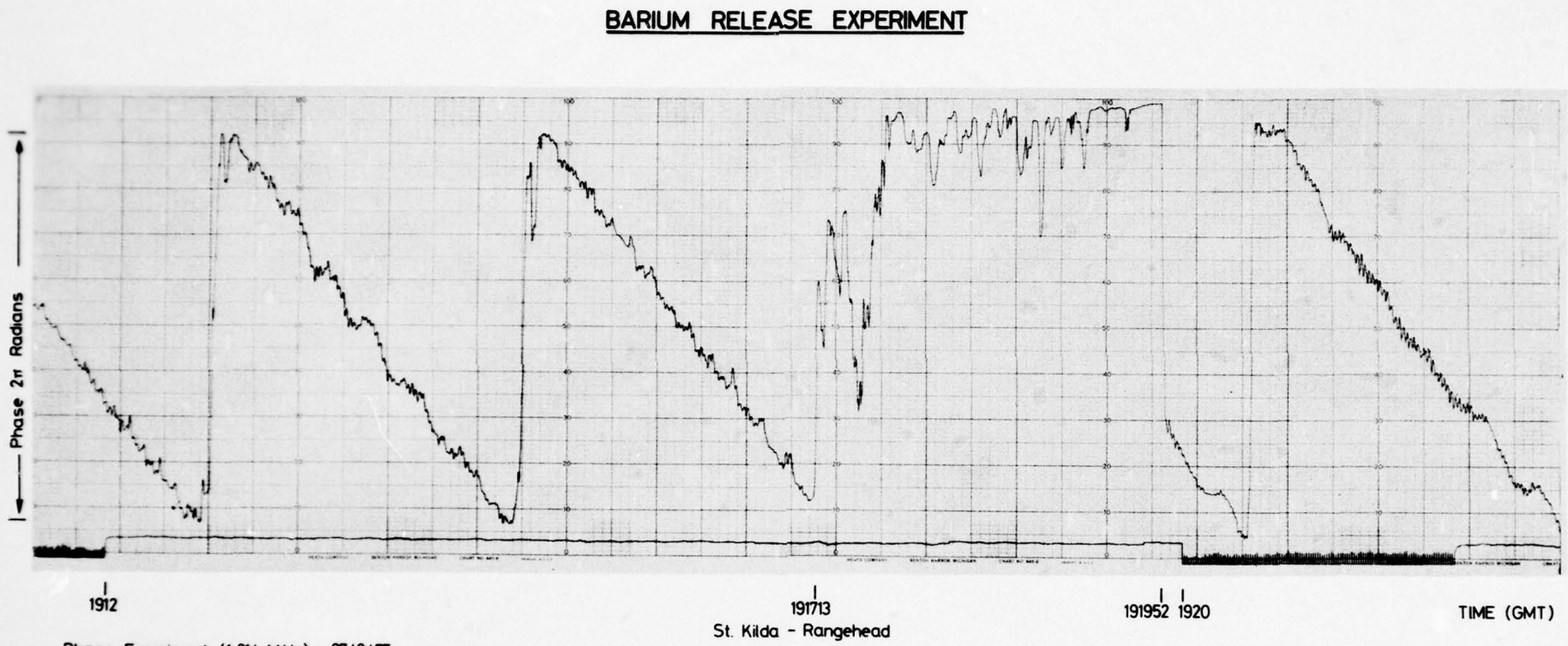

Figure 6. Phase disturbance on 1.615 MHz signal reflected from the E-region.

MODIFICATION OF THE IONOSPHERE BY BARIUM ION CLOUDS

A. J. Baxter
M.O.D. (P.E.) A.W.R.E.
Aldermaston, Reading, RG7 4PR, U.K.

SUMMARY

The release of barium clouds into the upper atmosphere gives an opportunity of observing the interaction processes of the ionospheric medium. The types of approximation used to model the development of ion clouds are discussed and reference is made to the ionospheric parameters that have been extracted from our experiments.

For a recent release experiment at South Uist conditions were particularly suited for viewing the ion cloud directly up the geomagnetic field lines. The characteristics of the ion cloud as it passes through its development phases are quite marked and an interruption to the propagation path of a subsidiary experiment (University of Leicester) was observed at the time of the onset of structure in the barium cloud. The optical observations are discussed and conclusions made on the form of ionospheric model that has been used to describe the phenomena.

1. INTRODUCTION.

The barium release technique (Haerendel et al 1967) has become an established method for disturbing the ambient ionosphere and providing a means of observing optically the interaction processes.

The theoretical interpretation of release phenomena (Lloyd and Haerendel, 1973, Perkins *et al*, 1973) is generally attempted by reducing the problem to two dimensions. The geomagnetic field lines are regarded as equi-potentials for the electrostatic field (excepting an ambipolar diffusion component) and the cloud and ionosphere are represented by transverse distribution functions having integrated the densities along the field. Observationally, the longitudinal diffusive elongation of clouds makes the extraction of transverse distortions difficult unless the cloud can be viewed with a line of sight near parallel to the field direction. Comparatively few observations have been reported where this is the case (Rosenberg, 1971, Davis *et al*, 1974, Lloyd and Haerendel, 1973).

At diminishing transverse scale sizes, such as to be found in ion cloud striations, the finite longitudinal resistivity limits the mapping of electrostatic fields to all levels of the ionosphere. The penetration of striations into the E-region has been discussed by Volk and Haerendel, (1971). Further, based on arguments on the observed elongation of clouds in the Hall direction, Lloyd and Haerendel, (1973) have suggested that the coupling between E and F layers is not very efficient.

In an earlier paper (Baxter, 1975), we attempted to account for the striation size distribution using an electrostatic field spreading model. The approach was unrealistic as it did not allow the ionosphere to distort in a self consistent manner. Where coupling is possible, the type of background ionospheric response in the E-(compressible) or the F-(incompressible) layers produces widely disparate growth rates at given striation sizes (Francis and Perkins, 1975).

For our latest release experiment, where we were fortunate to achieve field line viewing, we attempt to explore this contrary interpretation of perfect coupling to the E-layer. This approach seems to be supported by the point of formation of structure in the cloud. The difficulty of destabilisation at small sizes (Francis and Perkins, 1975) can be overcome in the cloud by a convective mechanism but this still leaves the details of structure in the coupled E-layer uncertain.

When we examine some of our earlier experiments, however, neglect of the E-layer seems more appropriate, providing we can enhance the F-region conductivities.

2. REDUCTION OF OBSERVATIONS.

The basic details of our releases are given in Table 1. Two features characterise this work; namely the sub-auroral location (L = 3.5) of the experiments and the comparatively low altitude of release where quite strong perturbing effects can be produced with modest payloads.

TABLE 1

RELEASE EXPERIMENT LAUNCH DETAILS

Designation	Date	Time UT	Payload kg		Altitude km
SP1	4.6.70	2302	5.9	1.8 Ba + CuO	158
SP2	7.9.71	2015	6.0		166
SP3	15.5.73	2208	5.8		158
SP4	16.5.73	2248	5.5	$Ba(N_3)_2$ + $6T_i$	159
SP5	27.9.75	1915	6.1		172

The 'routine' parameters that we attempt to establish optically from a release experiment are summarised in Table 2. One of the biggest uncertainties lies in the estimation of yield due to the correcting factors which have to be applied to get an absolute measure of cloud radiance. Should our quoted values appear low, the enhanced oxidation loss at these lower altitudes, as well as a less efficient payload in the two most recent experiments should be noted. A recent attempt (SP5) to confirm the yield reduction method using a radio beacon technique suggests there is scope for doubling the quoted values. This may only compound the difficulties with ionospheric magnitudes noted later. The determination of the gyro/collision frequency ratio, K, is also subject to error since we have to compensate for the projective situation of the cloud in measuring the longitudinal extension. The term steepening (Simon and Sleeper, 1972) refers to the enhancement in density gradient of the side of the ion cloud nearest the neutral material from which separation is occurring, a characteristic feature of release experiments.

TABLE 2

PRIMARY PARAMETERS ESTIMATED FROM OPTICAL MEASUREMENTS

Quantity	Method	Assumptions
$\underline{U}_n$ $\underline{U}_i$ drift velocities	Triangulation	
Q Ionised barium yield	Integrated radiance	Transmissions and oscillator strengths
R transverse scale radius	Densitometry	Cloud symmetry
K barium gyro/ collision/frequency	Densitometry longitudinal diffusion	Cloud geometry Ambipolar diffusion ion temperature
Rate of steepening S $\frac{d}{dt}\left[\left(\frac{1}{N}\left(\frac{\partial N}{\partial r}\right)_{\frac{1}{2}Nm}\right)^{-1}\right]$	Densitometry early convective changes	Cloud geometry

From these primary parameters we estimate the degree of peturbation of the cloud, expressed in terms of the integrated Pedersen conductivity ratio at the cloud centre to the coupled ionosphere λ. Using a simple analytic model, the steepening/drift rates, $S/|\underline{U}_i-\underline{U}_n|$, (ie a quantity we can measure) defines a unique value of λ. In addition this ratio also establishes the degree of screening to scale the ion-neutral drift speeds, either to calculate an effective shear velocity between coupled regions of the ionosphere U or to estimate the ambient electric field E. Finally, we can make a rough estimate of the coupled ionospheric conductivity Σ_{pi}:

$$\Sigma_{pi} = \frac{1}{\lambda}\,\frac{Q}{\pi R^2}\,\frac{e}{mB}\,\frac{K}{1+K^2}$$

All these quantities are summarised in Table 3.

TABLE 3

REDUCTION OF OBSERVATIONS FOR THE RELEASE EXPERIMENTS

Designation	Q gms	U_n(e)	U_n(n)	U_i(e)	U_i(n)	R km	K	S m s^{-1}
SP1	20	-171	+ 42	-153	+ 30	-	-	-
SP2	35	-226	- 80	-230	- 66	1.4	16	2.0
SP3	20	-203	-159	-306	-125	1.2	25	5.8
SP4	2	-102	- 42	- 1	- 53	1.0	15	4.1
SP5	5	-101	- 26	- 28	- 6	1.8	16	7.0

Designation	$S/\lvert\underline{U}_i-\underline{U}_n\rvert$	λ	U m s^{-1}	E(co-rot) mV m^{-1}	^{o}E of mag N	Σ_{ip} ohm^{-1}
SP2	0.14	1.4	22	11	27	5.4
SP3	0.05	0.3	126	16	- 8	2.7
SP4	0.04	0.3	114	2.5	270	0.6
SP5	0.09	0.7	98	0.3	13	0.5

We cannot claim a high degree of confidence in the absolute magnitude of these reduced quantities nor do four releases represent sufficient statistics to generalise any conclusions. They are reproduced to indicate the scheme of reduction and to point to trends in the interpretation.

3. MODELLING OF ION CLOUD DEVELOPMENT

Methods for modelling the development of ion clouds are detailed elsewhere (eg Lloyd and Haerendel, 1973). We assume a two layer model consisting of the cloud ($K_C \simeq 15$) coupled to the E-layer ($K_E = 1$), where K_C, K_E are the respective ion gyro/collision frequency ratios. We consider the field acting on the cloud to be local, ie result from the wind-shear between cloud and background levels such that the field is zero in a frame of reference moving with the E-layer neutrals.

In general, for ion and electron species, j, at each level, we establish a relation between the transverse velocities, $\underline{V}_j$, the applied field, $\underline{E}$, polarisation potential, ϕ, species density, N_j, gyro/collision frequency ratio, K_j, and temperature, T_j:

$$\underline{V}_j = F_j\ (\underline{E},\phi,\ N_j,K_j,T_j)$$

Hence if we use a computational cell fixed on the cloud-level neutral drift frame we may write:

$$\underline{V}_C = F_C(\underline{U} \times B,\phi,\ N_C,K_C,\ T_C) \quad \text{for species, C, at the cloud level}$$

and $$\underline{V}_E = F_E(O,\phi,\ N_E,K_E,T_E) - \underline{U} \quad \text{for species at the E-layer level}$$

where $\underline{U}$ is the wind-shear, the velocity of the cloud level neutrals with respect to the E-layer neutrals.

The polarisation potential is determined by solving

$$\sum_j \nabla \cdot (N_j\ e_j\ \underline{V}_j) = 0$$

and the solution can be advanced in time using the continuity equation.

$$\frac{\partial N}{\partial t} + \nabla \cdot (N\underline{V}) = 0$$

for the ions at each level independently since ion transfer between levels is assumed to be negligible. No allowance for recombination has been made.

For discussion we present results from the following simulations:-

(a) The development of a coupled ion cloud chosen with parameters, (λ,$\underline{U}$,K,R) approximating to the release conditions SP5 (Figure 1).

(b) To a slab model of ionisation with a 1% perturbation and scale length comparable to the spatial resolution of structure in barium cloud, 250 m (Figure 2(a)).

(c) To a model with conditions similar to (b) but with scale length close to the spacing observed in release SP5, 750 m (Figure 2(b)).

4. DISCUSSION OF RELEASE SP5

The development of release SP5 viewed along the magnetic field direction is shown in Figure 3. The ion-neutral separation vector was determined by fitting to the cloud positions over a 60-600 s interval and the error in aligning the photographs is claimed to be better than 5^o. The motions over this interval are steady and restriction to observations over 60-180 s would only change the angle by 2^o. In Figure 4 we present in greater detail the record 165 s from release a time when the structure is emerging clearly. The appearance of structure is abrupt and can be first noted optically about 140 s from release.

Based on the optical records alone we make the following observations:-

(a) The structure emerges as sheets inclined at an angle to the ion-neutral separation direction. At 165 s the angle is about 30^o which is contrary to the normal observation of sheets near parallel to this relative drift direction (Rosenberg, 1971). At later times (300 s) the cloud has taken on a more conventional $\underline{E} \times \underline{B}$ elongated appearance but further convective motions then complicate the interpretation.

(b) With this change in inclination, the structure is not all concentrated at the steepened edge. The condition for structure to form noted by Perkins and Doles, (1975) that the cloud develops to a point which is sufficiently one-dimensional with the density gradient parallel to the drift direction does not appear to have been met.

(c) Structure is also formed on the lower part of the cloud as seen in the 200 s record in Figure 3. There is some evidence that part of this structure is present soon after release and may have been due to delayed venting from the payload. However, the quantity of material is small and no anomalies were present in the steepening observations over the first 30-120 s after release.

(d) At late times the density gradient along the lower edge becomes distinct in contrast to the diffuse drift towards the upper right of the photographs.

We attempt to interpret these observations using the simulations in Figures 1 and 2. From the two-layer cylindrical cloud model we see that by the observed time of structure formation, the cloud has steepened in density not only on the edge nearest the point of origin but along the side passing between the image clouds. The images have developed to more than double and near depleted values of the ambient density. Two regions of greatest density gradient can be noted in the E-layer.

(i) On the edge of the negative image cloud remote from the positive image but tending towards the point of origin.

(ii) Along the line between the two image clouds.

These regions are probably the most likely areas to go unstable which may be in keeping with observations (b) and (c) above.

Also apparent in Figure 1 is the gradual superposition of the released cloud on the depleted image. This feature has been termed the 'exchange process' by Lloyd and Haerendel, (1973). The mechanism goes a long way to explain the distinct edge noted in (d) above. If we have reached a stage where the superposition has developed then the visual ion cloud no longer acts as a tracer for the perturbation which has progressed to the positive image cloud in the E-layer.

The occurrence of structure of comparable sizes in a wide variety of release experiments can be cited as evidence for a selective or preferential growth mechanism. The application of instability analyses to the striation problem has been criticised on the grounds that quite arbitrary initial values can produce widely disparate times of appearance of structure (Lloyd and Haerendel, 1973). The point to which a cloud will steepen before structure appears is a measure of the level of granularity the cloud or coupled ionosphere will support. However, we cannot ignore the predictions of analyses which are based on the same physical assumptions as the alternative descriptions.

In particular, we note the conclusion of Francis and Perkins, (1975) that clouds dominated by the E-region are destabilised at all wavelengths. In Figure 2 we reproduced some simulations of the slab-type instability problem. A numerical treatment is used in preference to an analytic approach in order to investigate the non-linear regime. A wind-shear origin has been assumed for the field and a 1% perturbation inserted at the cloud level. The disturbance soon transfers itself to the E-layer, 90^{o} out of phase (Volk and Haerendel, 1971) and the enhancement in growth rates noted by Francis and Perkins (1975) is reproduced at the unstable edge. However, quite marked differences are found with wavelength in the two examples presented in Figure 2. Whereas at 750 m wavelength the structure can move out and give a detached appearance, at 250 m it tends to merge back on itself at least at the cloud level. Such merging is similar to the velocity shear stabilisation noted by Perkins and Doles (1975) but more complex in nature since we have coupled regions of differing gyro/collision frequency ratios.

The differences in appearance relate to the choice of density gradient in the cloud. If we consider an inhomogeneity in electric field, $\delta E(y)$, along the unstable edge of gradient,

$$\frac{1}{n}\left(\frac{\partial n}{\partial x}\right) = -\frac{1}{d}$$

the change in density at the cloud, dn, and E-layer, dn', can be written as:

$$dn = -\delta v\left(\frac{\partial n}{\partial x}\right) dt = \frac{\delta E}{B}\frac{n}{d}\, dt$$

$$dn' = -\frac{n' K}{1+K^2}\frac{1}{B}\frac{\partial}{\partial y}\left(\delta E\right) \simeq \frac{\delta E}{B} k \frac{K}{1+K^2}\, n'\, dt$$

If we assume the phase relation between disturbances to be constructive (Volk and Haerendel, 1971), we expect the E-layer to distort more rapidly and dominate the situation as we approach the non-linear regime (provided $\lambda \simeq 1$) if:

$$\frac{dn'}{n'} > \frac{dn}{n}$$

ie

$$\frac{K}{1+K^2} k > \frac{1}{d}$$

For the numerical example in Figure 2, $k \simeq 2\pi/470\ m^{-1}$

Hence the above granularity argument may be taken further to state that we only expect structure to emerge at sizes comparable to the density gradients occurring at the unstable edge. The use of barium as a visual tracer for the fine structure is limited under these conditionsof perfect coupling and provided of course we have the optical resolution necessary for the observations.

5. CONCLUSIONS

The question of mapping of electrostatic fields to levels of the ionosphere is crucial to understanding the formation of structure in artificial clouds. Using a single experiment we have suggested that the development can be understood in terms of an E-layer coupled model with a local origin for the electric field. We reproduce Table 3 to indicate that from other experiments such an interpretation is not consistent since it would require E-region winds of impractical magnitude (eg SP3 >300 m s^{-1}).

Before we accept an external origin for the field at this sub-auroral location we note the predicted ionospheric conductivities are greater in the earlier experiments and speculate whether the enhanced Pedersen conductivity through electron-ion collisions in the F-layer used by Francis and Perkins (1975) can be accepted at times of greater solar activity. A local F-region origin could then be proposed for the field, which would correlate with auroral activity not directly through the propagation of fields southward from the auroral zone but indirectly by the neutral motions. We note that in an experiment (Rees et al, 1973) where an attempt was made to measure simultaneously the E-region parameters necessary to describe the drift motion of a barium cloud, a consistent interpretation was not achieved at twilight.

The onset of loss of signal during SP5 reported by Spracklen and Jones (1976), 110-140 s from release coincides with the period of gross changes within the E-layer at a time just prior to the appearance of structure in the ion cloud. The limitations to barium as a tracer are recognised and such effects may indicate much more extensive deformations than apparent as borne out by the numerical simulations.

REFERENCES

Baxter, A.J., 1975, Planet. Space Sci., 23, 973.

Davis, T.N., Romick, G.J., Wescott, E.M., Jeffries, R.A., Kerr, D.M., and Peek, H.M., 1974, Planet. Space Sci., 22, 67.

Francis, S.H., and Perkins, F.W., 1975, J.G.R., 80, 3111.

Haerendel, G., Lust, R., and Reiger, E., 1976, Planet. Space Sci., 15, 1.

Lloyd, K.H., and Haerendel, G., 1973, J.G.R., 78, 7389.

Perkins, F.W. and Doles III, J.H., 1975, J.G.R., 80, 211.

Perkins, F.W., Zabusky, N.J. and Doles III, J.H., 1973, J.G.R., 78, 697.

Rees, D., Haerendel, G., Felgate, D.G., Lloyd, K.H. and Low, C.H., 1973, Planet. Space Sci., 21, 1237.

Rosenberg, N.W., 1971, J.G.R., 76, 6856.

Simon, A. and Sleeper, A.M., 1972, J.G.R., 77, 2353.

Spracklen, C.T. and Jones, T.B., 1976, These proceedings.

Volk, H.J. and Haerendel, G., 1971, J.G.R., 76, 4541.

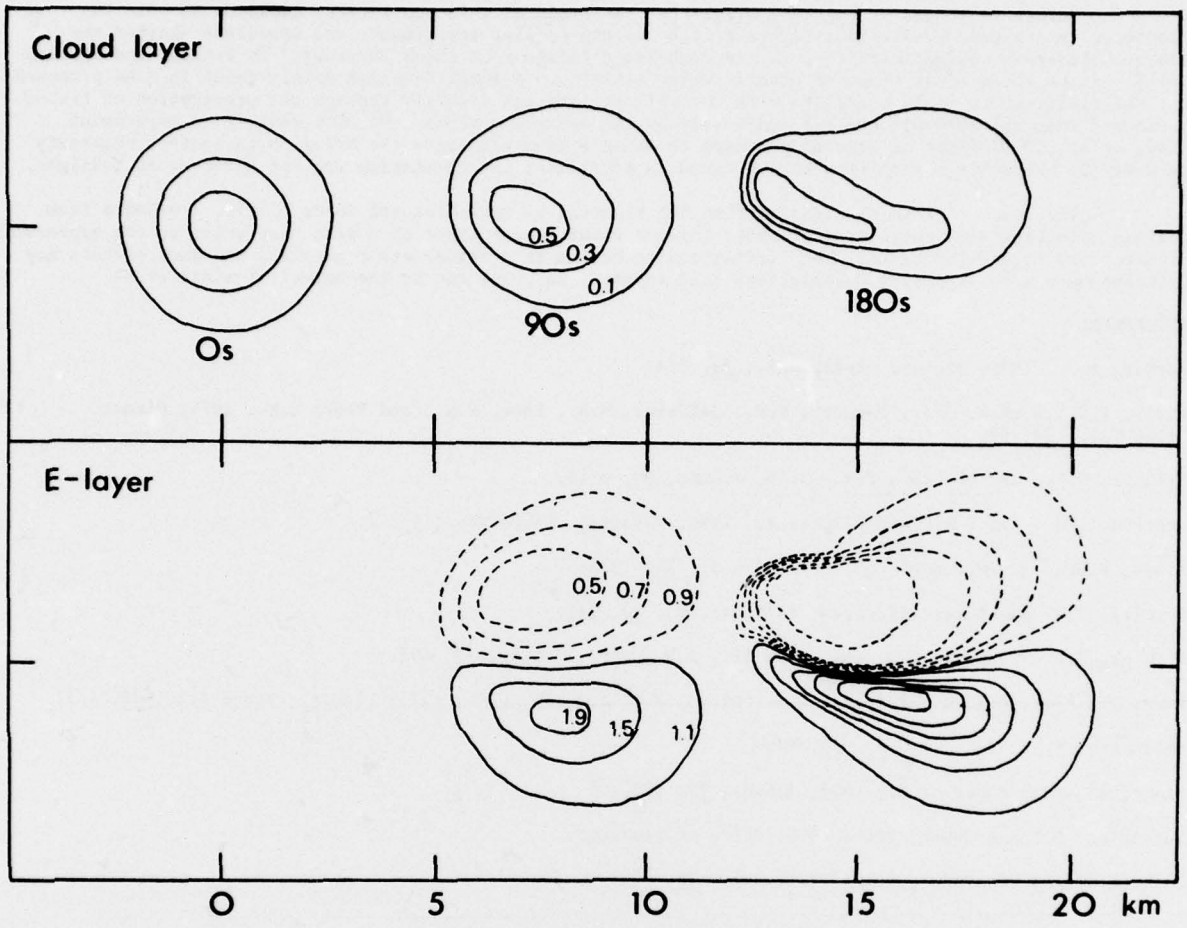

FIGURE 1

The development of a two layer model of the barium cloud situation. The initial cloud distribution is given by $N_c = 0.6 \exp(-R^2/1.85^2)$ where N_c is the cloud Pedersen conductivity with respect to an ionospheric value of unity, and R is the radial distance in km. The grid is presented in the neutral frame of reference at the cloud level with the E-region neutrals moving at 100 m s^{-1} in a horizontal sense towards the right of the figure. Perfect coupling between layers is assumed with no ambient electric field present in the ionospheric level rest frame. Values of 15, 1 and 725, 300^{o}K are used for the gyro/collision frequency ratio and temperature of the cloud and ionospheric levels respectively.

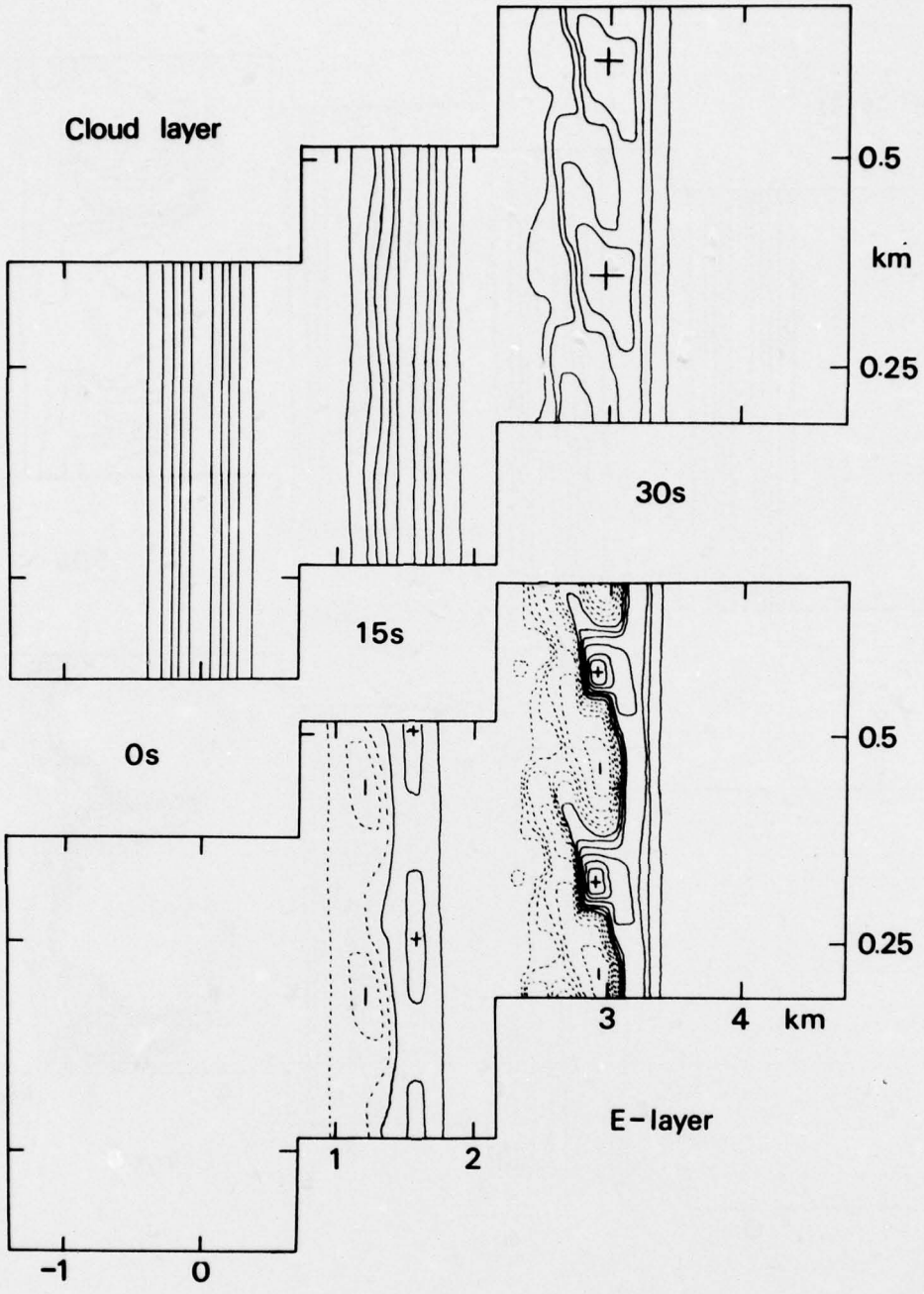

FIGURE 2(a)

The development of structure in a two-layer slab model of ionisation. The starting distribution is given by

$$N_c = 1.0 \exp\left(-\left(\frac{x}{250}\right)^2\right)\left(1. + 0.01 \cos\left(\frac{2\pi y}{250}\right)\right)$$

The grid is presented in the neutral frame of the slab cloud with the ionospheric level moving with a (100, 10) m s^{-1} wind shear. Contours are indicated at N = 0.1, 0.3, 0.5 ... etc with the signs indicating the extrema. Values of 10, 1 and 725, 300°K are used for the gyro/collision frequency ratio and temperature at the slab and ionospheric levels respectively.

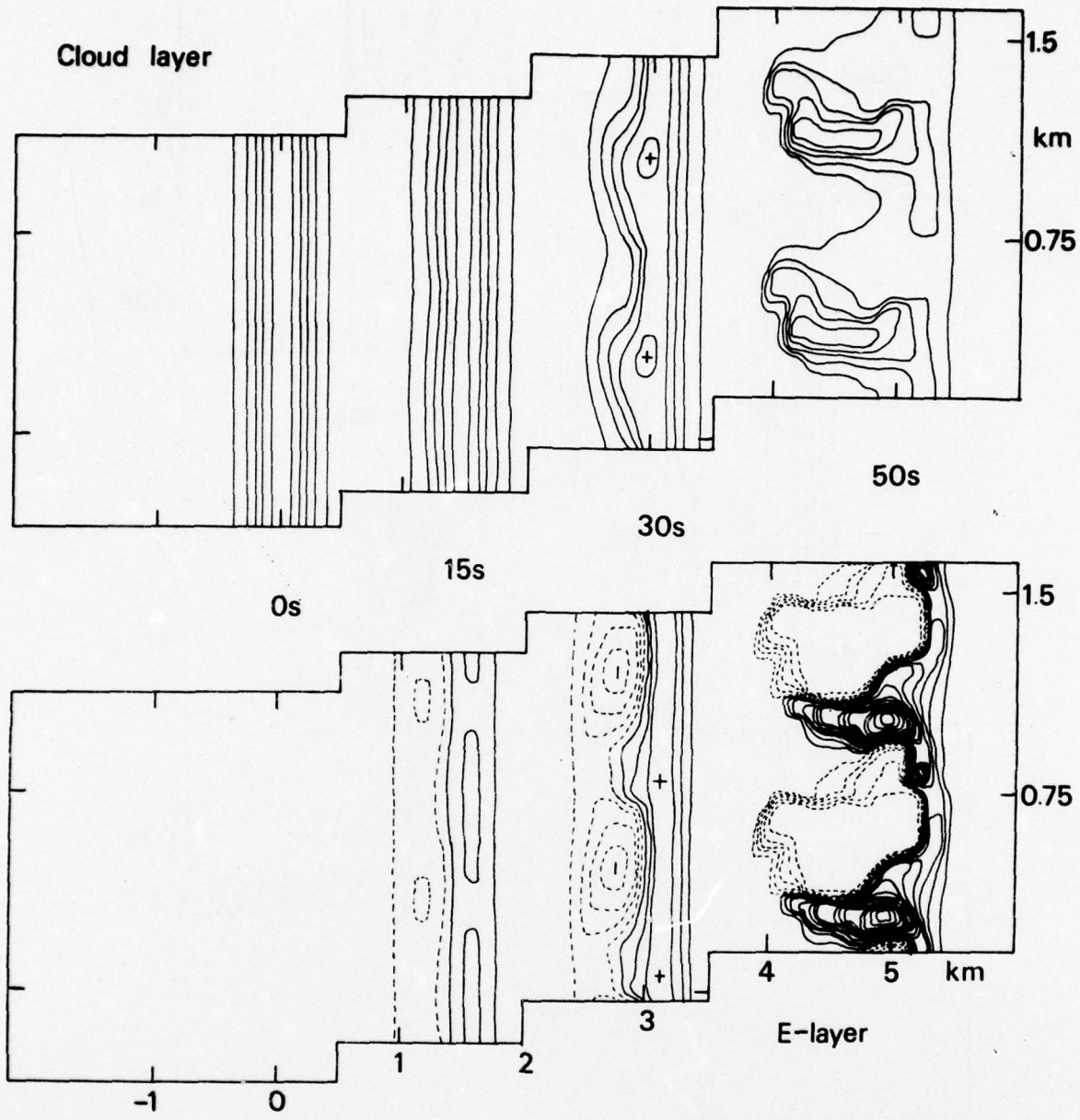

FIGURE 2(b)

Repeat calculation to Figure 2(a) with a 750 m perturbing wavelength. Note the Y-axes are different in the two figures.

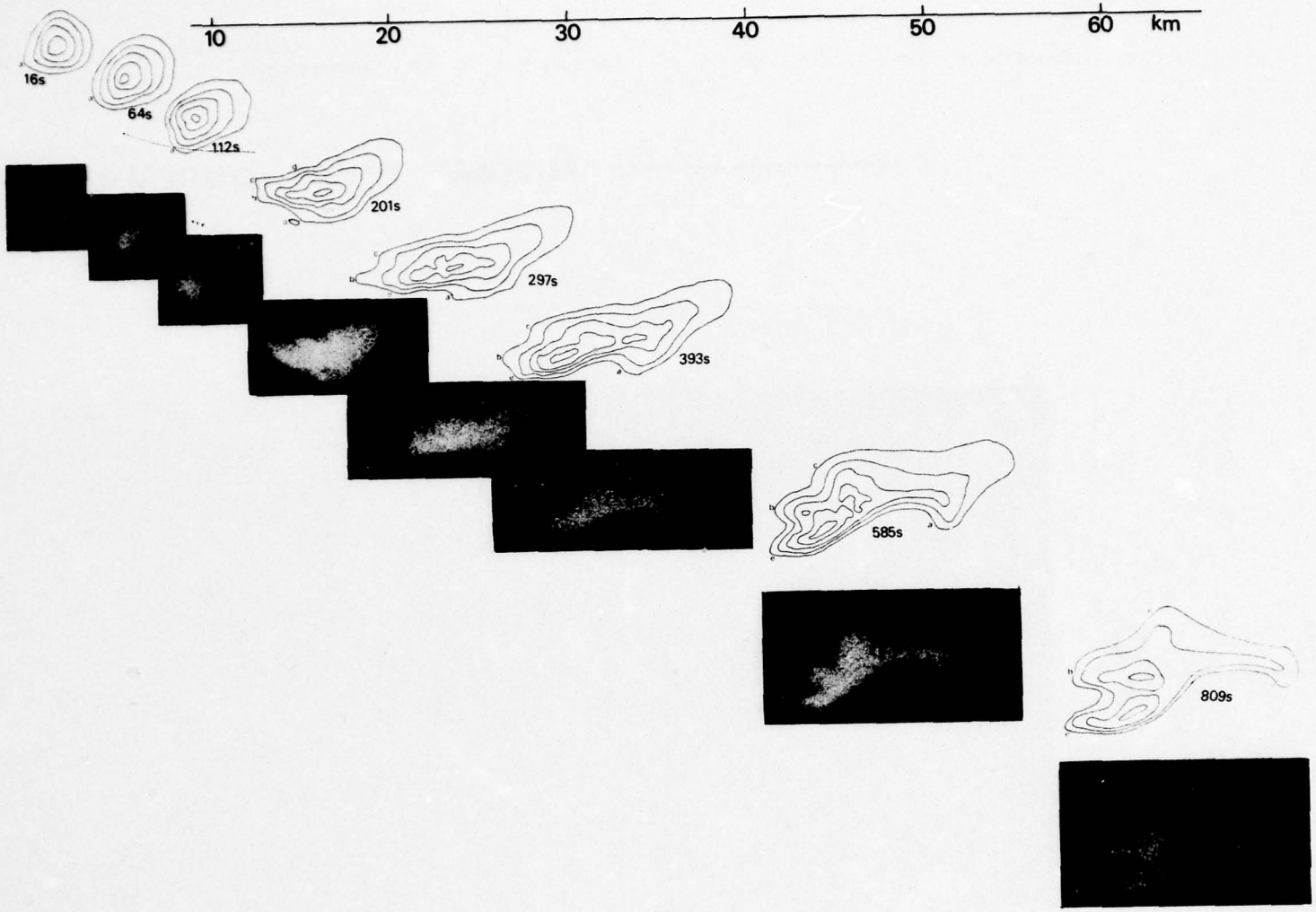

FIGURE 3

The development of barium ion cloud SP5. The photographs have been aligned such that the horizontal axis is parallel to the projection of the ion-neutral cloud separation vector ($\underline{U}_i$-$\underline{U}_n$). The angle between the photographic normal and the magnetic field direction at the cloud decreases from 7 to 2° over this period.

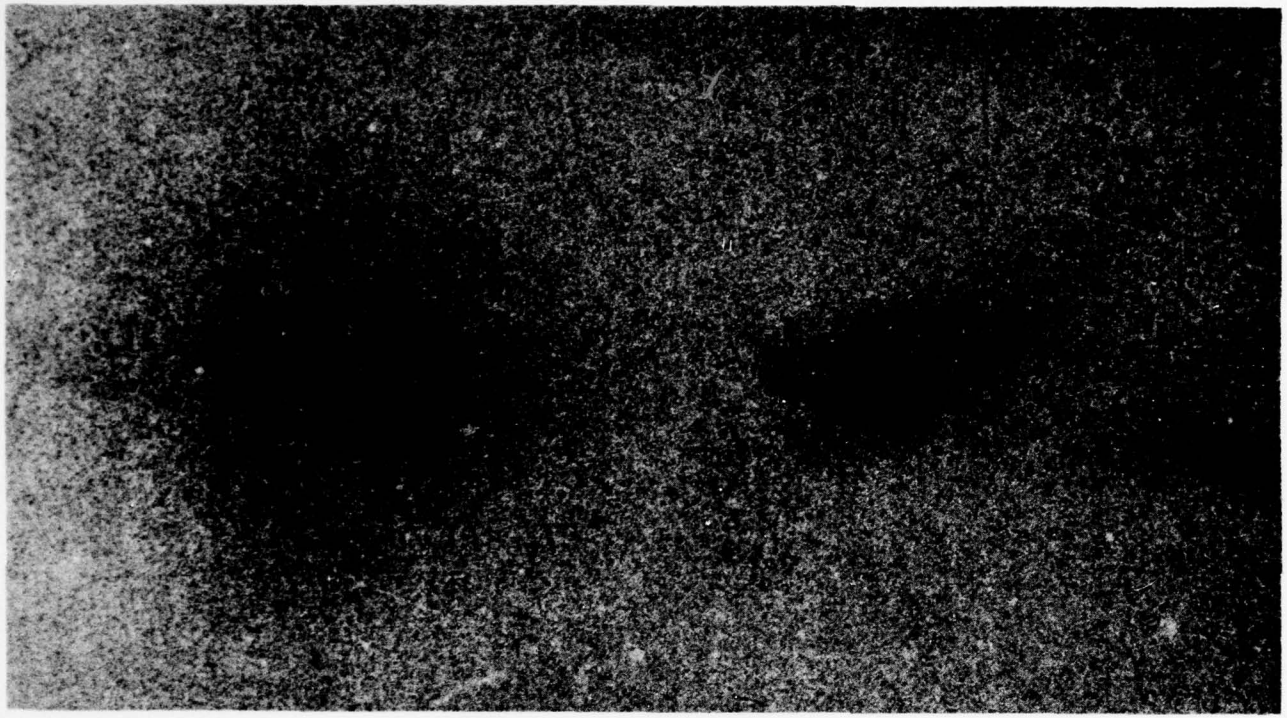

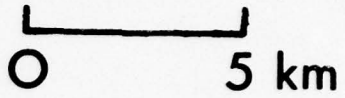

Ion-neutral cloud velocity ⟶

FIGURE 4

The formation of structure in barium ion cloud SP5, 165 s from release. The alignment conditions of Figure 3 apply.

SESSION III, ROUND-TABLE DISCUSSION

MODIFICATION OF IONIZED MEDIA BY CHEMICAL SUBSTANCES

Participants at Round Table: J. Belrose (Chairman)
A. J. Baxter
P. A. Bernhardt
G. Haerendel
M. Mendillo
C. T. Spracklen

(This substitute summary had to be compiled by the editor at short notice in order to meet the final deadline for publication. A tape-recording had to be used as the sole basis; apologies are offered to speakers who could not be identified.)

In summarizing the objectives of this round-table discussion, its chairman, J. Belrose, presented a list of subjects which could be considered representative of the entire field of modifications of ionized media by chemical substances. They may be subdivided into three main categories, viz., the Understanding of the Use of Chemical Releases, the Effects upon Communications, and Other Effects. Questions like the creation of ionospheric instabilities and the generation of waves and plasmas are examples of the first-mentioned group, whereas the communication effects may be subdivided into those due to ionization increases and others related to ionization decreases. The third category referred to the discussion of additional effects.

In introducing the subjects for discussion, J. Belrose pointed out that chemical releases could be utilized to provide traces and thus contribute to an understanding of natural visible processes in the upper atmosphere. As examples, he mentioned the measurement of winds, wind shear, and drift in the E- and F-regions of the atmosphere. With regard to the creation of ionospheric instabilities, reference was made to the importance of understanding the unstable nature of the ionosphere and of the study of magnetic field perturbations as well as changes in the conductivity. Turning to the generation of waves and plasmas, gravity waves and electromagnetic waves were mentioned, also micropulsations and related subjects, such as duct conditions for whistler propagation.

J. Belrose referred to the communication effects as being of main importance for the work conducted by the AGARD-Panel sponsoring this Specialists' Meeting. Two categories were identified, effects due to ionization increases and others due to decreases. With regard to the first topic, a general comment was made concerning the generation of ionization as well as to the increase of the abundance of ionizable constituents in the D-region. With ionization decreases, communication effects may be visualized as being particularly effective during a polar-cap-absorption event, for instance, with the consequent extreme difficulty of maintaining HF-communications between two points on the earth's surface. The creation of a hole in the D-region could yield a positive effect on communications. His comments referred to hydrogen effects observed in the F-region, e.g. the rocket exhaust of a Saturn V during the launch of SKYLAB.

For the subject of other effects, J. Belrose used the comparison of the earth's atmosphere to a large laboratory which may serve to understand the use of chemical releases in studying natural processes.

For the first part of the round-table discussion, on the subject of understanding the use of chemical releases, layer recovery and the use of such data to determine the mechanism responsible for maintaining the layer were the initial topics, followed by the question of parallel electric fields. G. Haerendel reported on experiments which had been conducted with this objective. Doubts exist as to the existence of such fields in the F-region altitudes where the plasma density is high, yet he referred to increasing evidence for their existence at higher altitudes, e.g., above 1000 or 2000 km, where the plasma density is low; reference was made to actual results at 2500 and 7500 km. A. Egeland agreed on the parallel electric fields being weak and transient in the polar ionosphere and also commented on the restriction in time which limits the observation of parameters useful for the understanding of the natural physical processes based on chemical releases. Supporting this opinion, G. Haerendel pointed out that, however, there have been experiments under all types of conditions, from very quiet to extremely disturbed ones.

In a discussion on more experimental work, G. Haerendel commented on the particular suitability of the equatorial area, the zone around the magnetic equator, where the region of the disturbance may be separated horizontally from the region of the return current in the lower F- or E-region. He then suggested an experiment involving 100 or less, say 20 kg of hydrogen, and not the exhaust of a Saturn V rocket, to be released at an altitude of about 250 km after sunset in the equatorial ionosphere at the equator. A large depletion in a certain volume could be expected to result and, due to the instability at the equator, this hole would rise; it would be carried out of the region where it was created, towards higher altitudes. However, the increasingly lower recombination

coefficients would increase its lifetime; perhaps even hours would then be available for observations. The only problem may be the separation of natural effects from the perturbation caused artificially.

With regard to the amount necessary, J. Mendillo again referred to the papers contributed by himself and P.A. Bernhardt which indicated that much less than the exhaust of rockets like Saturn V, indeed 100 kg or less, should provoke very localized but very interesting effects.

In the course of the following discussion, reference was made to the occurrence of small scale irregularities suddenly appearing and being noticed by a 50MHz-radar observation, together with the ionospheric perturbation, which may be of a scale of 20 km or so. It was felt that these effects are not fully explored at this stage and that carefully chosen modification experiments could supplement the theoretical work.

In summing up the discussion on the topic of understanding the use of chemical releases as a means of artificial modification of the ionosphere, J. Belrose particularly referred to the paper by C. T. Spracklen and T. B. Jones in emphasizing the importance of appropriate diagnostic means, an example being incoherent scatter radar.

Introducing the subject of communications within this round-table discussion, J. Belrose summarized ideal objectives such as the creation of an intense amount of ionization in the lower ionosphere for purposes of disrupting communication or the creation of a hole in the D-region, perhaps by firing a rocket into the desired volume, with the possible advantage of enabling communication, particularly up in the north, on high frequencies on some circuit. However, he underlined the questionability of such possibilities and opened the discussion on this topic.

In supporting the desirability of the above-mentioned chances of influencing the ionosphere, E. Thrane commented on the difficulty presented by the fact that a gas, which is, for instance, introduced in the D-layer, would expand very rapidly but still rather locally for an area of the order of several hundred meters until pressure equilibrium would be established; a further expansion would then take hours by which time the volume affected may have been carried away by the wind.

Reference was also made to the description of very relevant experiments in the paper contributed by T. B. Jones and C. T. Spracklen ; supplementary comments concerned the slight drift experienced by ion cloud releases, its direction being westwards.

With regard to the final topic of this round-table discussion, entitled "Other Effects", J. Belrose referred to the use of the earth's atmosphere as a large observatory, a laboratory without walls.

As an example of such an application, G. Haerendel described the injection experiment conducted by France and the Soviet Union. A strong electron beam with an energy of the order of 20 KeV was injected at the Kerguelen Islands in the South-Indian Ocean in order to investigate its effects in the ionosphere at the conjugate point north of Moscow. Television cameras covered the sky in an attempt to detect optical radiation. However, no optical effects were noticed, although previous localized experiments had been successful, with an electron gun pointing downwards from the rocket altitude. Nevertheless, the electron beam arrived at the conjugate ionosphere, as confirmed by radar back-scatter detected by means of radar equipment installed on the ground. It may be concluded that the strong electron beam had lost the major part of its energy on the path, perhaps degraded down to a few KeV. On the other hand, aurora is known to be caused by a few KeV pointing down into the atmosphere. More investigations seem to be required.

Concluding this summary it may be pointed out that the round-table discussion of this session supplemented the exchange of information on the subject of artificial modification of ionized propagation media by chemical substances. In addition, promising areas for future research were indicated.

REPORT DOCUMENTATION PAGE			
1. Recipient's Reference	**2. Originator's Reference** AGARD-CP-192	**3. Further Reference** ISBN 92-835-1234-1	**4. Security Classification of Document** UNCLASSIFIED

5. Originator Advisory Group for Aerospace Research and Development
North Atlantic Treaty Organization
7 rue Ancelle, 92200 Neuilly sur Seine, France

6. Title

ARTIFICIAL MODIFICATION OF PROPAGATION MEDIA

7. Presented at the Electromagnetic Wave Propagation Panel Specialists' Meeting held in Brussels, 26–29 April 1976.

8. Author(s)	**9. Date**
Various Edited by H.J.Albrecht	January 1977
10. Author's Address	**11. Pages**
Various	204

12. Distribution Statement This document is distributed in accordance with AGARD policies and regulations, which are outlined on the Outside Back Covers of all AGARD publications.

13. Keywords/Descriptors

Wave propagation
Electromagnetic wave transmission
Weather modification
Atmospheric composition
Ionosphere
Chemical composition

14. Abstract

Communication systems are affected by characteristics of different propagation media depending on frequency range and distances to be covered. An artificial modification of the propagation media may improve system reliability or even establish the propagation conditions basically required.

A Specialists' Meeting was particularly concerned with recognition and definition of limiting propagation criteria, optimum methods of modification, and efficiency of changing propagation media as a function of means employed. It represented an early, if not the first scientific meeting actually addressing, with its main topic, the anthropogeneous changes to the earth's atmosphere as a propagation medium. The entire subject was subdivided into three sections, viz. modification of non-ionized media, of ionized media by e.m. waves, and of ionized media by chemical substances.

In addition to the recognition of the state of the art and the predominant directions of progress, the stimulation of propagation-oriented modification projects may be mentioned as a major achievement of the meeting; it also indicated promising areas of future research.

Papers and discussion material in this publication were presented at the Specialists' Meeting of the AGARD Electromagnetic Wave Propagation Panel on "Artificial Modification of Propagation Media" held in Brussels, Belgium, from 26th to 29th April 1976.

AD-A036 355 ADVISORY GROUP FOR AEROSPACE RESEARCH AND DEVELOPMENT--ETC F/G 20/14
ARTIFICIAL MODIFICATION OF PROPAGATION MEDIA.(U)
JAN 77 H J ALBRECHT

UNCLASSIFIED AGARD-CP-192 NL

3 OF 3
ADA036355

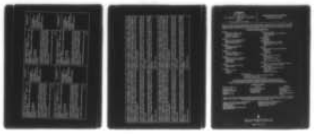

END

DATE
FILMED
3 - 77

AGARD Conference Proceedings No.192 Advisory Group for Aerospace Research and Development, NATO ARTIFICIAL MODIFICATION OF PROPAGATION MEDIA Edited by H.J.Albrecht Published January 1977 204 pages Communication systems are affected by characteristics of different propagation media depending on frequency range and distances to be covered. An artificial modification of the propagation media may improve system reliability or even establish the propagation conditions basically required. A Specialists' Meeting was particularly concerned with P.T.O.	AGARD-CP-192 Wave propagation Electromagnetic wave transmission Weather modification Atmospheric composition Ionosphere Chemical composition	AGARD Conference Proceedings No.192 Advisory Group for Aerospace Research and Development, NATO ARTIFICIAL MODIFICATION OF PROPAGATION MEDIA Edited by H.J.Albrecht Published January 1977 204 pages Communication systems are affected by characteristics of different propagation media depending on frequency range and distances to be covered. An artificial modification of the propagation media may improve system reliability or even establish the propagation conditions basically required. A Specialists' Meeting was particularly concerned with P.T.O.	AGARD-CP-192 Wave propagation Electromagnetic wave transmission Weather modification Atmospheric composition Ionosphere Chemical composition
AGARD Conference Proceedings No.192 Advisory Group for Aerospace Research and Development, NATO ARTIFICIAL MODIFICATION OF PROPAGATION MEDIA Edited by H.J.Albrecht Published January 1977 204 pages Communication systems are affected by characteristics of different propagation media depending on frequency range and distances to be covered. An artificial modification of the propagation media may improve system reliability or even establish the propagation conditions basically required. A Specialists' Meeting was particularly concerned with P.T.O.	AGARD-CP-192 Wave propagation Electromagnetic wave transmission Weather modification Atmospheric composition Ionosphere Chemical composition	AGARD Conference Proceedings No.192 Advisory Group for Aerospace Research and Development, NATO ARTIFICIAL MODIFICATION OF PROPAGATION MEDIA Edited by H.J.Albrecht Published January 1977 204 pages Communication systems are affected by characteristics of different propagation media depending on frequency range and distances to be covered. An artificial modification of the propagation media may improve system reliability or even establish the propagation conditions basically required. A Specialists' Meeting was particularly concerned with P.T.O.	AGARD-CP-192 Wave propagation Electromagnetic wave transmission Weather modification Atmospheric composition Ionosphere Chemical composition

recognition and definition of limiting propagation criteria, optimum methods of modification, and efficiency of changing propagation media as a function of means employed. It represented an early, if not the first scientific meeting actually addressing, with its main topic, the anthropogeneous changes to the earth's atmosphere as a propagation medium. The entire subject was subdivided into three sections, viz. modification of non-ionized media, of ionized media by e.m. waves, and of ionized media by chemical substances.

In addition to the recognition of the state of the art and the predominant directions of progress, the stimulation of propagation-oriented modification projects may be mentioned as a major achievement of the meeting; it also indicated promising areas of future research.

Papers and discussion material in this publication were presented at the Specialists' Meeting of the AGARD Electromagnetic Wave Propagation Panel on "Artificial Modification of Propagation Media" held in Brussels, Belgium, from 26th to 29th April 1976.

ISBN 92-835-1234-1

recognition and definition of limiting propagation criteria, optimum methods of modification, and efficiency of changing propagation media as a function of means employed. It represented an early, if not the first scientific meeting actually addressing, with its main topic, the anthropogeneous changes to the earth's atmosphere as a propagation medium. The entire subject was subdivided into three sections, viz. modification of non-ionized media, of ionized media by e.m. waves, and of ionized media by chemical substances.

In addition to the recognition of the state of the art and the predominant directions of progress, the stimulation of propagation-oriented modification projects may be mentioned as a major achievement of the meeting; it also indicated promising areas of future research.

Papers and discussion material in this publication were presented at the Specialists' Meeting of the AGARD Electromagnetic Wave Propagation Panel on "Artificial Modification of Propagation Media" held in Brussels, Belgium, from 26th to 29th April 1976.

ISBN 92-835-1234-1

recognition and definition of limiting propagation criteria, optimum methods of modification, and efficiency of changing propagation media as a function of means employed. It represented an early, if not the first scientific meeting actually addressing, with its main topic, the anthropogeneous changes to the earth's atmosphere as a propagation medium. The entire subject was subdivided into three sections, viz. modification of non-ionized media, of ionized media by e.m. waves, and of ionized media by chemical substances.

In addition to the recognition of the state of the art and the predominant directions of progress, the stimulation of propagation-oriented modification projects may be mentioned as a major achievement of the meeting; it also indicated promising areas of future research.

Papers and discussion material in this publication were presented at the Specialists' Meeting of the AGARD Electromagnetic Wave Propagation Panel on "Artificial Modification of Propagation Media" held in Brussels, Belgium, from 26th to 29th April 1976.

ISBN 92-835-1234-1

recognition and definition of limiting propagation criteria, optimum methods of modification, and efficiency of changing propagation media as a function of means employed. It represented an early, if not the first scientific meeting actually addressing, with its main topic, the anthropogeneous changes to the earth's atmosphere as a propagation medium. The entire subject was subdivided into three sections, viz. modification of non-ionized media, of ionized media by e.m. waves, and of ionized media by chemical substances.

In addition to the recognition of the state of the art and the predominant directions of progress, the stimulation of propagation-oriented modification projects may be mentioned as a major achievement of the meeting; it also indicated promising areas of future research.

Papers and discussion material in this publication were presented at the Specialists' Meeting of the AGARD Electromagnetic Wave Propagation Panel on "Artificial Modification of Propagation Media" held in Brussels, Belgium, from 26th to 29th April 1976.

ISBN 92-835-1234-1

AGARD

NATO OTAN

7 RUE ANCELLE · 92200 NEUILLY-SUR-SEINE

FRANCE

Telephone 745.08.10 · Telex 610176

DISTRIBUTION OF UNCLASSIFIED AGARD PUBLICATIONS

AGARD does NOT hold stocks of AGARD publications at the above address for general distribution. Initial distribution of AGARD publications is made to AGARD Member Nations through the following National Distribution Centres. Further copies are sometimes available from these Centres, but if not may be purchased in Microfiche or Photocopy form from the Purchase Agencies listed below.

NATIONAL DISTRIBUTION CENTRES

BELGIUM
Coordonnateur AGARD – VSL
Etat-Major de la Force Aérienne
Caserne Prince Baudouin
Place Dailly, 1030 Bruxelles

CANADA
Defence Scientific Information Service
Department of National Defence
Ottawa, Ontario K1A OZ2

DENMARK
Danish Defence Research Board
Østerbrogades Kaserne
Copenhagen Ø

FRANCE
O.N.E.R.A. (Direction)
29 Avenue de la Division Leclerc
92 Châtillon sous Bagneux

GERMANY
Zentralstelle für Luft- und Raumfahrt-
dokumentation und -information
Postfach 860880
D-8 München 86

GREECE
Hellenic Armed Forces Command
D Branch, Athens

ICELAND
Director of Aviation
c/o Flugrad
Reykjavik

ITALY
Aeronautica Militare
Ufficio del Delegato Nazionale all'AGARD
3, Piazzale Adenauer
Roma/EUR

LUXEMBOURG
See Belgium

NETHERLANDS
Netherlands Delegation to AGARD
National Aerospace Laboratory, NLR
P.O. Box 126
Delft

NORWAY
Norwegian Defence Research Establishment
Main Library
P.O. Box 25
N-2007 Kjeller

PORTUGAL
Direccao do Servico de Material
da Forca Aerea
Rua de Escola Politecnica 42
Lisboa
Attn: AGARD National Delegate

TURKEY
Department of Research and Development (ARGE)
Ministry of National Defence, Ankara

UNITED KINGDOM
Defence Research Information Centre
Station Square House
St. Mary Cray
Orpington, Kent BR5 3RE

UNITED STATES
National Aeronautics and Space Administration (NASA),
Langley Field, Virginia 23365
Attn: Report Distribution and Storage Unit

THE UNITED STATES NATIONAL DISTRIBUTION CENTRE (NASA) DOES NOT HOLD STOCKS OF AGARD PUBLICATIONS, AND APPLICATIONS FOR COPIES SHOULD BE MADE DIRECT TO THE NATIONAL TECHNICAL INFORMATION SERVICE (NTIS) AT THE ADDRESS BELOW.

PURCHASE AGENCIES

Microfiche or Photocopy

National Technical
Information Service (NTIS)
5285 Port Royal Road
Springfield
Virginia 22151, USA

Microfiche

Space Documentation Service
European Space Agency
10, rue Mario Nikis
75015 Paris, France

Microfiche

Technology Reports
Centre (DTI)
Station Square House
St. Mary Cray
Orpington, Kent BR5 3RF
England

Requests for microfiche or photocopies of AGARD documents should include the AGARD serial number, title, author or editor, and publication date. Requests to NTIS should include the NASA accession report number. Full bibliographical references and abstracts of AGARD publications are given in the following journals:

Scientific and Technical Aerospace Reports (STAR),
published by NASA Scientific and Technical
Information Facility
Post Office Box 8757
Baltimore/Washington International Airport
Maryland 21240, USA

Government Reports Announcements (GRA),
published by the National Technical
Information Services, Springfield
Virginia 22151, USA

Printed by Technical Editing and Reproduction Ltd
Harford House, 7–9 Charlotte St, London W1P 1HD

ISBN 92-835-1234-1